

Lawrence Berkeley Laboratory

UNIVERSITY OF CALIFORNIA

CHEMICAL BIODYNAMICS DIVISION

IN SITU ELECTRON MICROSCOPY OF CELL MONOLAYERS:
APPLICATION TO THE STUDY OF THE INTERACTIONS BETWEEN
BALB 3T3 FIBROBLASTS

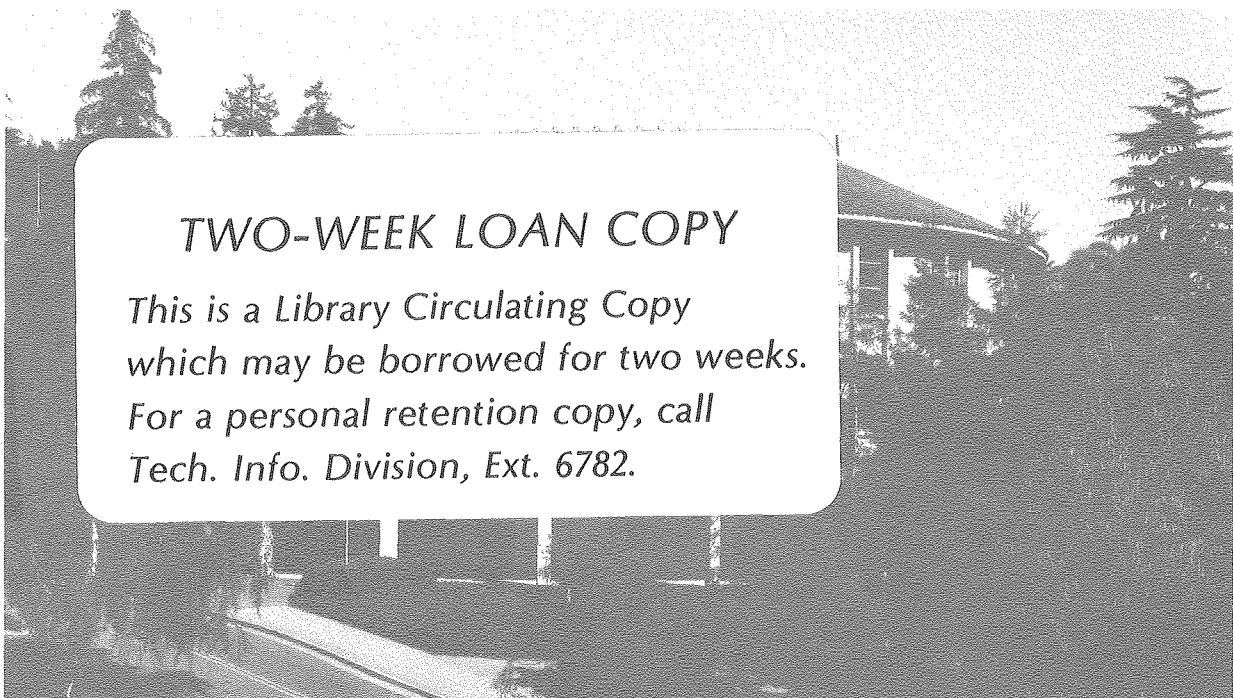
Terryl Rand Collins
(Ph.D. thesis)

November 1979

RECEIVED
LAWRENCE
BERKELEY LABORATORY

FEB 25 1980

LIBRARY AND
DOCUMENTS SECTION



TWO-WEEK LOAN COPY

*This is a Library Circulating Copy
which may be borrowed for two weeks.
For a personal retention copy, call
Tech. Info. Division, Ext. 6782.*

LBL-10106 d.2

DISCLAIMER

This document was prepared as an account of work sponsored by the United States Government. While this document is believed to contain correct information, neither the United States Government nor any agency thereof, nor the Regents of the University of California, nor any of their employees, makes any warranty, express or implied, or assumes any legal responsibility for the accuracy, completeness, or usefulness of any information, apparatus, product, or process disclosed, or represents that its use would not infringe privately owned rights. Reference herein to any specific commercial product, process, or service by its trade name, trademark, manufacturer, or otherwise, does not necessarily constitute or imply its endorsement, recommendation, or favoring by the United States Government or any agency thereof, or the Regents of the University of California. The views and opinions of authors expressed herein do not necessarily state or reflect those of the United States Government or any agency thereof or the Regents of the University of California.

In Situ Electron Microscopy of Cell Monolayers:
Application to the Study of the Interactions Between
Balb 3T3 Fibroblasts

By

Terryl Rand Collins
Lawrence Berkeley Laboratory, University of California
Berkeley, California 94720
Abstract

The present study was undertaken to determine whether freeze-fracture could be used to detect possible changes in the properties of Balb 3T3 cell membranes resulting from density-dependent inhibition of growth. Preliminary results with conventional methods of preparing cell cultures for freeze-fracture indicated that these techniques caused gross changes in the native morphology of the monolayer. An in situ technique for freeze-fracture of monolayer cultures was therefore perfected and was found to increase greatly the yield of information available from replicas of cultured cells. Since it was necessary to avoid changes in the properties of cultures which might result from variations in the growth conditions used for different experimental techniques, silicon monoxide was evaluated as a substratum for growing cells during all biochemical and morphological experiments. This material can be readily vacuum-deposited on both culture dishes and specimen carriers for electron microscopy. Thin films of silicon monoxide prepared in this way exhibited excellent optical, chemical, and heat-conducting properties and proved to be good substrata for growth of a variety of fibroblastic and epithelial cell lines. Existing techniques for high resolution scanning electron

microscopy (HRSEM) and thin sectioning were therefore modified for use with silicon monoxide. These technical advances allowed examination of the biochemical properties and native morphology of cultured fibroblasts growing under the same conditions. Morphological studies showed that cellular interactions between Balb 3T3 fibroblasts could be divided into four classes: simple overlap, edge-to-edge contacts, interdigitation, and filopodial interactions. Localized areas of close apposition of the membranes of neighboring cells occurred at frequent intervals around the cell periphery and may represent sites of intermediate junction formation. Freeze-fracture studies showed that neither the density nor the distribution of intramembranous particles appeared to be changed by cell contact, suggesting that if the membrane properties of cultured fibroblasts change as a result of density-dependent inhibition of growth, the changes may be reflected in an alteration of the mobility rather than the distribution of the IMP. Therefore, initial experiments were carried out using incubation in glycerol solutions as a means of inducing redistribution of the intramembranous particles. The results of these preliminary experiments are described and suggestions are made for future studies on glycerinated cultures.

Acknowledgements

I am deeply grateful for the friendship and support which I received from my associates at the Berkeley campus and the Lawrence Berkeley Laboratory during the course of this study. I would like especially to thank my advisor, Professor Melvin Calvin, for his faith and encouragement throughout this project and for giving me the invaluable opportunity manage the electron microscopy facility at the Laboratory of Chemical Biodynamics. Professor Dorothy Pitelka was always available to advise and answer questions. Her sensitivity, warmth, and willingness to help on many fronts eased many difficult times. Professor Peter Satir spent a great deal of time discussing results with me; his encouragement and insights contributed greatly to the development of this thesis. Dr. Jim Bartholomew worked closely with me on almost every phase of this work, and my job would have been much more difficult without his participation. Carroll Hatie, Priscilla Ross, and Hisao Yokota of the cell culture laboratory were always ready with technical assistance and advice.

I would like to give special thanks to my friend Jack Murchio of the School of Public Health. Besides teaching me electron microscopy, Jack suggested the use of silicon monoxide as a culture substratum, and shared many of the ups and downs of the project with me. Dr. Karl Pfenninger of Yale University generously shared his experience with in situ freeze fracture. I had many profitable discussions with Dr. Scott McNutt of the San Francisco Veterans Administration Hospital and Dr. Daniel Friend of the UCSF Medical Center. Dr.

McNutt kindly lent the micrograph shown in Fig. 30.

Jack Harvey and Dick Wolgast of the Lawrence Radiation Laboratory Vacuum Division gave unselfishly of their experience with design and maintenance of vacuum equipment. Pete Dowling of the Donner Laboratory machine shop turned his expert attention to the construction of many gadgets, including the hats used for in situ freeze-fracture. Carolyn Schooley and the staff of the Electron Microscope Laboratory trained me in freeze-fracture. My association with them has always been rewarding and enjoyable. Many thanks also to Mike Nemanic for teaching me high resolution scanning electron microscopy.

During my first two years at the University of Chicago, Professor Jane Overton was kind enough to supervise chapters of this work, and Dr. Paul Meyer advised me on the statistical analyses.

Finally, I owe my greatest debt to my wife, Janie, who in addition to typing the first draft of this work, shared all of the triumphs and misfortunes of our five years in Berkeley. Her courage and faith in me often gave me strength to attempt and master tasks which I might never have considered.

This work was supported by the U. S. Department of Energy under Contract number W-7405-ENG-48.

Table of Contents

Chapter	Page
1 Introduction	1
2 Preliminary Studies	24
Materials and Methods	24
Results	28
Discussion	48
3 Comparison of Cell Growth on Silicon Monoxide and Conventional Substrata	51
Materials and Methods	52
Results	55
Discussion	72
4 Morphology of Balb 3T3 Monolayers: Studies with High Resolution Scanning Electron Microscopy	74
Materials and Methods	74
Results	81
Discussion	116
5 <u>In Situ</u> Freeze-Fracture Studies on Balb 3T3 Monolayers . .	129
Materials and Methods	130
Results	137
Discussion	162
6 <u>In Situ</u> Thin Sectioning with Balb 3T3 Monolayers	165
Materials and Methods	165
Results and Discussion	168
7 Effect of Glycerol on Balb 3T3 Cell Membranes: Preliminary Results	177

Chapter	Page
Materials and Methods	177
Results	179
Discussion	233
8 Conclusions and Suggestions for Future Studies	237
References	242

List of Figures

Figure	Page
1. Swiss 3T3 4A cells prepared for freeze-fracture without prior fixation	30
2. P faces of Swiss 3T3 4A cell membranes showing the three characteristic distributions of IMP	33
3. Typical E faces of Swiss 3T3 4A cell membranes	37
4. A typical Swiss 3T3 4A RK2 cell fixed with paraformaldehyde-glutaraldehyde before glycerination	41
5. Typical P and E fracture faces of fixed Swiss 3T3 4A RK2 cells	44
6. Area of overlap between the peripheral regions of three fixed Swiss 3T3 4A RK2 cells	47
7. Cell growth on Falcon plastic and silicon monoxide	58
8. Growth of Swiss 3T3 4A RK2 cells on uncoated and silicon monoxide-coated areas of a fragment from a Lab-Tek plastic culture dish	61
9. Growth of sparse and dense Swiss 3T3 4A RK2 cells on Balzers specimen carriers and silicon monoxide	63
10. Growth curve of Swiss 3T3 4A RK2 cells on silicon monoxide and Falcon plastic	66
11. Balb 3T3 cells on Falcon plastic and silicon monoxide after 15 min. in 0.1% trypsin	68
12. Growth curve of Balb 3T3 cells on silicon monoxide and Falcon plastic	71
13. Apparatus for critical point drying of cell monolayers	79
14. Confluent culture of Balb 3T3 cells growing on a Balzers carrier coated with silicon monoxide	83
15. Surface of Balzers flat-topped specimen carrier after grinding with 800 mesh boron carbide followed by 6 μ m and 1 μ m diamond paste	85
16. Scanning electron micrograph of a typical cell from a confluent culture of Balb 3T3 cells growing on a flat-ground, silicon monoxide-coated Balzers specimen carrier	88
17. Higher magnification view of Fig. 16, showing the area of	

Figure	Page
interaction between three cells	90
18. Low magnification scanning electron micrograph of a confluent culture of Balb 3T3 cells growing on a silicon monoxide-coated glass coverslip	93
19. Higher magnification view of Fig. 18, showing a typical Balb 3T3 cell and its interactions with neighboring cells	95
20. Higher magnification view of Fig. 19, showing a region of complex filopodial interaction	97
21. Higher magnification view of Fig. 19, showing interactions between cells 1, 5, and 6	99
22. Higher magnification view of Fig. 19, showing the region of interdigitation between the edges of Cell 1 and Cell 6	101
23. Plasma membrane interactions in the region of interdigitation between Cells 1 and 6	104
24. Area of overlap between two cells	107
25. Filopodial interactions between four cells	109
26. Higher magnification view of Fig. 25	111
27. Area of interaction between two cells, showing filamentous bundles	113
28. Higher magnification view of Fig. 27	115
29. Appearance of surface filaments in a region of interdigitation between two cells	118
30. Balb 3T3 A31 cells sectioned parallel to and just above the substratum, showing strands of filamentous material in the extracellular space	120
31. Copper hats with a Balzers flat-topped specimen carrier	134
32. Replica of one entire Balb 3T3 cell fractured <u>in situ</u> using the copper hats	139
33. Higher magnification view of Fig. 32, showing parts of the region of interdigitation between P ₆ and P ₈	142
34. Photographic enlargement of Fig. 33, showing two presumptive intermediate junctions	144

Figure	Page
35. Replica of a Balb 3T3 monolayer, showing overlap	146
36. Higher magnification view of Fig. 35	148
37. Higher magnification view of Fig. 35	150
38. Montage from an area adjacent to that seen in Fig. 35	152
39. Higher magnification view of Fig. 38, showing area of close apposition between E ₂₆ and P ₂₅	154
40. Freeze-fracture replica of a region of filopodial interaction	156
41. Thick section cut from a confluent monolayer of Balb 3T3 A31 cells fixed and imbedded <u>in situ</u>	170
42. Electron micrograph of a confluent monolayer of Balb 3T3 A31 cells, showing parts of three cells and numerous small pro- cesses from other cells	172
43. Appearance of the cytoplasm of a typical Balb 3T3 A31 cell . .	174
44. Changes in the pH and the fraction of cells detached from the dish during incubation of FNE cells with isotonic tris buffer	182
45. Changes in the pH and the fraction of cells detached from the dish during incubation of FNE cells with saline G	184
46. Changes in the pH and the fraction of cells detached from the dish during incubation of FNE cells with DME	186
47. Changes in the pH and the fraction of cells detached from the dish during incubation of FNE cells with DME containing 25 mM HEPES but minus Phenol Red	188
48. Changes in the pH and the fraction of cells detached from the dish during incubation of FNE cells with DME containing 25 mM HEPES but minus Phenol Red and vitamins	190
49. Changes in the pH and the fraction of cells detached from the dish during incubation of FNE cells with DME containing 100 mM HEPES but minus Phenol Red, vitamins, and bicarbonate . .	192
50. Changes in the pH and the fraction of cells detached from the dish during incubation of Balb 3T3 cells with isotonic tris buffer	195
51. Changes in the pH and the fraction of cells detached from the dish during incubation of Balb 3T3 cells with DME	197

Figure	Page
52. Changes in the pH and the fraction of cells detached from the dish during incubation of Balb 3T3 cells with DME containing 100 mM HEPES but minus Phenol Red, vitamins, and bicarbonate	199
53. Balb 3T3 fibroblasts photographed during incubation at 37° with HEPES-DME and glycerol/HEPES-DME	201
54. Scanning electron micrograph of Balb 3T3 cells after 45 min. incubation in HEPES-DME	204
55. Typical fully rounded cell from a preparation incubated 45 min. in HEPES-DME	206
56. Typical flattened cell from a preparation incubated 45 min. in HEPES-DME	208
57. Balb 3T3 cells after incubation for 45 min. in glycerol/HEPES-DME	211
58. Higher magnification view of Fig. 57, showing a typical flattened cell from a culture incubated 45 min. in glycerol/HEPES-DME	213
59. Higher magnification view of Fig. 57, showing a typical rounded cell	215
60. Higher magnification view of area 2 of Fig. 58	217
61. Higher magnification view of area 1 of Fig. 58	219
62. Freeze-fracture replica of a confluent monolayer of Balb 3T3 cells incubated for 45 min. in glycerol/HEPES-DME	222
63. Low magnification and high magnification views of a cell which developed numerous blebs after incubation with glycerol/HEPES-DME	224
64. (a) Appearance of a typical P face from a cell incubated 45 min. at 37°C with glycerol/HEPES-DME. (b) Appearance of an E face where lines of IMP formed in a specific area on the underside of the cell	226
65. Higher magnification view of Fig. 62	229
66. Photographic enlargement of Fig. 65	231

Chapter 1

Introduction

Fibroblasts cultured at low density on a plane surface move about over the substratum, preceded by a thin sheet of ruffled membrane usually referred to as the leading lamella (Abercrombie and Ambröse, 1958; Abercrombie, 1961 and 1970; Abercrombie et al., 1970 and 1971). Collision of the leading lamellae of two fibroblasts results in intercellular adhesion, paralysis of ruffling, contraction of the lamellae, and cessation of cell movement. The latter effect is referred to as contact inhibition of movement (Abercrombie and Heaysman, 1954).

If a sparse population of cells from certain lines such as 3T3 (Todaro and Green, 1963) is maintained in culture for several days, the cell number will increase until a characteristic density (referred to as the saturation density) is reached, at which time the culture will cease to grow. At saturation density, the majority of cells are arrested in the G_1 phase of the cell cycle, piled up behind an as yet unexplained growth blockade (Nilausen and Green, 1965; Prescott, 1968). This restriction of growth in dense culture is referred to as density dependent inhibition of growth (Stoker and Rubin, 1967). Cultures exhibiting these two phenomena have been used by many workers as in vitro model systems mimicking some of the behavior of tumors (Dulbecco, 1969), since density dependent inhibition of growth can be abolished by transformation with tumor viruses such as SV40 (Stoker, 1972), and cells derived from sarcomas have been observed to be deficient in con-

tact inhibition of movement (Abercrombie et al., 1957).

The mechanisms responsible for density dependent inhibition of growth and, to a lesser extent, contact inhibition of movement, have been the subject of a great deal of research, as well as an intense controversy between those who attribute these effects to long-range factors involving diffusible substances, and those who favor a short-range mechanism dependent on the local topography and interrelationships of the cells concerned.

The literature relating to this debate has been the subject of several reviews (Abercrombie, 1970; Martz and Steinberg, 1972 and 1973a; Pardee, 1975; Stoker, 1972) and is much too extensive to be described here in its entirety. In the case of contact inhibition of movement, the available evidence suggests that some aspects of this effect are truly mediated via cell contact (Martz and Steinberg, 1973a and 1973b). However, the technical problems associated with studies on moving cells have hampered direct investigation of the mechanisms concerned, and the majority of research in this area has been carried out on density dependent inhibition of growth. It is now clear that inhibition of growth in dense cultures is strongly influenced by the depletion of serum factors and other nutrients in the culture medium (see, for example, Holley and Kierman, 1968; Kruse and Miedema, 1965). Some authors have, in fact, concluded that density dependent inhibition of growth in cultured fibroblasts is determined solely by the availability of certain components of the culture medium (Dulbecco and Elkington, 1973), whose access to the cell surface is influenced by effects such as the formation of diffusion boundary layers in dense culture (Stoker,

1973). However, although these long-range effects represent one important mechanism for the control of cell multiplication in culture, there is also a large body of recent evidence which suggests that the control of both growth and movement in cultured cells may in part be dependent on alterations in the dynamic properties of the cell membrane. The present study is aimed at using electron microscopy to search for membrane structural changes which might be associated with density dependent inhibition of growth in culture. Since freeze-etching can reveal both the surface and internal structure of the membrane (Branton, 1971), this technique offers a promising approach to the study of membrane alterations during cell interaction. Consequently, much of the work reported here will be focused on the application of freeze-etching to the study of the interactions between cultured cells. The evidence which links alterations in membrane structure with the control of cell growth and movement will be described in the present chapter, followed in subsequent chapters by the results of electron microscope observations on 3T3 mouse fibroblast cultures.

Much of the evidence linking membrane changes with the control of cell growth has come from studies using lectins, multivalent plant proteins which bind to specific carbohydrate groups on the cell surface [reviewed by Sharon and Lis (1972)]. Extensive use has been made of two of these proteins, wheat germ agglutinin (WGA) which binds preferentially to N-acetyl-D-glucosaminides (Burger and Goldberg, 1967; Liske and Franks, 1968), and concanavalin A (Con A) which binds to α -D-mannopyranosides and α -D-glucopyranosides (Edelman et al., 1972). One of the primary results of these studies has been the discovery that

both Con A and WGA agglutinate a variety of tumor and DNA virus-transformed cells at concentrations that do not cause agglutination of untransformed cells (Aub et al., 1963 and 1975; Burger, 1969; Benjamin and Burger, 1970; Inbar and Sachs, 1969; Sharon and Lis, 1972). Cells transformed by RNA tumor viruses will also display enhanced agglutinability if they are pretreated with hyaluronidase (Burger and Martin, 1972; Moore and Temin, 1971). These data indicate that the loss of growth control resulting from viral transformation is accompanied by an increase in agglutinability by Con A and WGA. Conversely, revertants of transformed 3T3 cells selected for resistance to Con A toxicity have been found to have reduced agglutinability and lower saturation densities than the parent cell line (Culp and Black, 1972; Ozanne and Sambrook, 1971a; Wright, 1973). There is even some evidence for a quantitative relationship between agglutinability and density dependent inhibition of growth; two independent studies have demonstrated that the saturation densities of a number of cell lines are closely correlated with the concentration of Con A or WGA required for half-maximal agglutination (Burger, 1971; Pollack and Burger, 1969; Weber, 1973). Mild pretreatment of untransformed cells with proteolytic enzymes increases their agglutinability to approximately the level shown by untreated transformed cells (Burger, 1969 and 1971; Inbar and Sachs, 1969; Pollack and Burger, 1969).

Clues to the mechanisms by which lectins agglutinate transformed and protease-treated cells have come from electron microscope studies of the distribution of Con A binding sites (CABS) on the cell surface. Despite initial claims to the contrary, present evidence suggests that

untransformed and transformed cells bind similar amounts of Con A and WGA, and that there is no correlation between agglutinability and the number of available lectin receptor sites (Cline and Livingstone, 1971; Kraemer et al., 1973; Ozanne and Sambrook, 1971b). In fact, trypsin treatment has been shown to enhance agglutinability while actually decreasing the number of available CABS on the cell surface (Kraemer et al., 1973). When untransformed, transformed, or protease-treated fibroblasts are fixed before being exposed to Con A, the distribution of CABS is found to be uniform in all three cases, as predicted by the fluid mosaic model (Singer and Nicolson, 1972). However, when Con A is bound to the cell surface before fixation, CABS on transformed cells are found to be gathered into clusters, while CABS on the surface of untransformed fibroblasts remain distributed uniformly over the cell surface (Nicolson, 1971; Rosenblith et al., 1973; Ukena et al., 1974). Mild pretreatment of the cells with proteolytic enzymes also allows clustering of CABS to occur (Nicolson, 1972; Rosenblith et al., 1973). If cells are kept in the cold after treatment with Con A, clustering of CABS is not observed (Nicolson, 1973c; Noonan and Burger, 1973; Rosenblith et al., 1973). The present interpretation of these data is that the inherent distribution of CABS on the surface of untransformed, transformed, or protease-treated cells is uniform, and that transformation or proteolysis enhances the mobility of lectin receptors within the plane of the membrane, permitting the multivalent lectins to crosslink these sites into patches. The original uniform distribution can be preserved either by fixation with reagents which crosslink membrane proteins, or by using low temperatures to slow the lateral movement of CABS by reducing the fluidi-

ty of the lipid bilayer (Edidin and Fambrough, 1973; Frye and Edidin, 1970).

On the basis of these results, it has been suggested that enhanced agglutinability by lectins results from an increased mobility of receptors within the plane of the membrane, with cell-cell binding being due to the formation of lectin crossbridges between receptors on neighboring cells (Nicolson, 1972; Noonan and Burger, 1973). Originally, it was believed that receptor clustering was required for agglutination. However, recent studies by Rutishauser and Sachs (1974, 1975a and 1975b) have shown that receptor clustering is not a prerequisite for cell-cell binding. Rather, the enhanced mobility of receptors on the surfaces of transformed and protease-treated cells permits short-range lateral movement and alignment of lectin binding sites on adjacent cell surfaces, followed by the formation of multi-point lectin bridges between two cells. Taken as a whole, the results of these studies of fibroblast agglutination suggest that in vitro transformation enhances the lateral mobility of certain surface lectin binding sites, and that these changes in mobility may be linked either directly or indirectly to alterations in the cells' sensitivity to density-dependent inhibition of growth.

Transformation also induces a variety of other changes in the surface properties of fibroblasts, including alterations in glycolipids (Hakamori, 1975), galactosyltransferases (Roth and White, 1972; Roth et al., 1974; Webb and Roth, 1974), and a variety of surface proteins (Hynes, 1976). It is possible that these surface moieties may also be involved in growth control mechanisms, though exactly how all of the various cell surface factors might interact is not clear at present.

Whereas experiments using fibroblasts suggest that cultures deficient in growth control show alterations in the dynamic properties of the cell membrane, a large number of studies with cultured lymphocytes have demonstrated that the converse is also true, i.e. that altering the distribution of certain receptor sites on the cell surface results in stimulation of cell division. Binding of a variety of divalent or multivalent ligands (lectins, anti-immunoglobulins, or anti-theta antibodies) to the surfaces of lymphocytes has been found to induce redistribution of these sites into patches, followed by aggregation of the patches into a cap over the Golgi pole of the cell. These events are followed by transformation into blast cells and, finally, by cell division (Comoglio and Guglielmone, 1972; Fanger et al., 1970; Greaves and Janossy, 1972; Inbar et al., 1973; Karnovsky et al., 1972; Karnovsky and Unanue, 1973; Novogrodsky and Katchalski, 1971; Powell and Leon, 1970; Raff and de Petris, 1973; Stackpole et al., 1974; Taylor et al., 1971; Unanue et al., 1972). Monomeric ligands such as Fab fragments bind to the cell surface but are ineffective in inducing patching or subsequent events (Fanger et al., 1970; Greaves and Janossy, 1972; Raff and de Petris, 1973; Taylor et al., 1971; Unanue et al., 1972). However, cross-linking of these monomers with anti-Fab antibody causes receptor redistribution and cell proliferation. These results suggest that a certain degree of cross-linking and redistribution of surface receptors is required for lymphocyte stimulation in vitro. Patching has been found to be a passive phenomenon which does not require a metabolically active cell, while capping has been shown to be an energy-requiring process that is inhibited by metabolic inhibitors (Karnovsky and Unanue, 1973; Raff and de Petris,

1973; Taylor et al., 1971; Unanue et al., 1973). The exact point at which cell proliferation is triggered has not been determined as yet; however, since capping is only observed after fairly extensive cross-linking of the cell surface (Karnovsky and Unanue, 1973; Unanue et al., 1972) and since triggering of cell growth and capping can occur independently, it is likely that stimulation of cell division occurs sometime during the initial redistribution of receptors into patches (Raff and de Petris, 1973). Similar mechanisms may also be involved in the stimulation of lymphocytes by antigens during the immune response. It is now believed that cross-linkage of surface immunoglobulin by antigen is required for stimulation of B lymphocytes in vivo, and it may be that the role of helper T cells involves presentation of antigen to B cells in a multivalent array (Greaves and Janossy, 1972; Raff and de Petris, 1973).

Evidence is accumulating which suggests that receptor cross-linking may play an important role in the stimulation of a variety of active processes in cells other than lymphocytes. Patching and capping induced by lectins or antibodies against surface antigens have been observed in fibroblasts, polymorphonuclear leukocytes, and macrophages (Edidin and Weiss, 1972; Romeo et al, 1973; Ryan et al., 1974; Weller, 1974). This treatment resulted in stimulation of oxidative metabolism in leukocytes and macrophages (Romeo et al, 1973). Exposure of fibroblasts to pokeweed mitogen caused cell proliferation at a concentration ten times smaller than that required to stimulate lymphocytes (Vaheri et al., 1973). Crosslinking of surface IgE is required for release of histamine by mast cells (Ishizaka and Ishizaka, 1969 and 1970). Finally,

human epithelial breast tumor cells have been shown to respond to treatment with antibodies from breast cancer patients by patching, capping, and shedding of surface antigens (Nordquist et al., 1977). This may be an important tumor survival mechanism, since the shed antigen effectively blocks host cytotoxicity.

In addition, a number of studies have demonstrated that chemical modification of the cell surface can initiate cell division. Cell proliferation has been shown to occur after mild proteolysis of fibroblasts (Blumberg and Robbins, 1975; Burger, 1970) and after treatment of lymphocytes with periodate (Novogrodsky and Katchalski, 1972; Parker et al., 1973 and 1974) or neuraminidase followed by galactose oxidase (Novogrodsky and Katchalski, 1973). Stimulation of cells by proteolysis does not seem to be related to the effect of proteolytic enzymes on CABS mobility and agglutination (Glynn et al., 1973). The mechanisms underlying stimulation by these agents are not understood, but it has been suggested that, at least in some cases, chemically modified surface moieties may undergo spontaneous cross-linking reactions (Novogrodsky and Katchalski, 1973).

All of the studies cited so far have been concerned with density-dependent inhibition of growth. However, there is some evidence that contact inhibition of movement may also involve changes in the cell membrane. Heaysman and Pegrum (1973a) employed time-lapse cinematography and thin sectioning to examine regions of contact between colliding chick heart fibroblast cells. Within twenty seconds after collision, they observed regions where the opposing cell membranes were separated by only 50 - 100 Å. At these points of close approach, electron-dense

areas appeared just below the plasma membrane in both cells, and the intercellular cleft frequently contained dense amorphous material. By sixty seconds after collision, these specialized regions were associated with microfilament bundles and could be identified as typical intermediate junctions (see Chapter 4). Similar studies were carried out with mouse sarcoma S180 cells which do not show contact inhibition of movement when they collide with each other or with chick heart fibroblasts (Heaysman and Pegrum, 1973b). In this case, contact regions of S180 cells showed no evidence of junction formation even after thirty minutes of contact. In collisions between sarcoma cells and fibroblasts, the fibroblasts showed some signs of junction development and microfilament alignment, but there was no corresponding specialization of the opposing regions of S180 cells. It appears that there may be a correlation between sensitivity to contact inhibition of movement and the capacity for formation of intermediate junctions after cell contact. It is not clear how such rapid and localized junction formation occurs, or in what fashion junction formation might influence subsequent cell locomotion. However, it is possible that contact induces a change in the cell surface which is propagated across the membrane, inducing junction formation and condensation of cytoplasmic microfilaments. Contraction of this microfilament network might then cause retraction of the leading lamella and cessation of cell movement.

The data presented here point to the existence of pathways for two-way communication between the cell surface and the cytoplasm. By means of these pathways, events such as viral transformation occurring within the cell might be expressed as changes in the dynamic properties of the cell membrane, and perturbations at the cell surface could be propagated

inward to influence cell growth and movement.

If such pathways do in fact exist, there must be some mechanism whereby information can be transmitted across the plasma membrane. In recent years, some clues to the possible nature of this process have come from research on the structure of the erythrocyte membrane.¹ Most of the protein on the erythrocyte surface is accounted for by two glycoproteins, PAS-1 (also known as the major glycoprotein or glycophorin), and band 3 (also called component a). PAS-1 has a molecular weight of 50-55,000, of which approximately sixty percent is carbohydrate. This molecule accounts for eighty percent of the carbohydrate and over ninety percent of the sialic acid on the cell surface; included in the carbohydrate region are the AB and MN blood group antigens, as well as receptors for influenza virus, phytohemagglutinin, and WGA (Marchesi et al., 1974). The carbohydrate is restricted to the N-terminal portion of the polypeptide chain, which protrudes from the cell surface, while the C-terminal region is exposed at the cytoplasmic side of the membrane. These two hydrophilic domains are connected by a roughly 30-residue hydrophobic segment which spans the apolar core of the membrane.

Band 3 has been less well characterized, but it is thought to be a dimer of molecular weight about 180,000, containing approximately seven percent carbohydrate and contributing roughly ten percent of the total carbohydrate on the cell surface. Present evidence suggests that band

¹ Since Bretscher (1973) and Steck (1974) have prepared excellent reviews of this field, references to specific research studies will be given in most cases only when they are not adequately summarized in one of these two publications. Membrane proteins are denoted here by the nomenclature of Steck.

3 also spans the membrane. Unlike PAS-1, which has negligible Con-A binding activity, band 3 appears to be the major Con A receptor on the erythrocyte surface (Findlay, 1974; Fukuda and Osawa, 1973).

There is now some reasonably good evidence which identifies both of these glycoproteins with the intramembranous particles (IMP) seen by freeze-fracture. It was thought for some time that the IMP were at least partially composed of protein (Branton and Deamer, 1972; Engstrom, 1970), and in addition, it was known that PAS-1, band 3, and the IMP were present in approximately equal numbers in the erythrocyte membrane. More recently, surface labelling studies have shown that AB antigens (Pinto da Silva and Branton, 1972), anionic sites (presumably sialic acid; see Nicolson, 1973a; also Pinto da Silva et al., 1973) and receptors for influenza virus and phytohemagglutinin (Marchesi et al., 1972; Tillack et al., 1972) as well as CABS (Pinto da Silva and Nicolson, 1974) are exclusively associated with the IMP. In view of the binding specificities of PAS-1 and band 3, this result has been interpreted as evidence that the IMP are oligomeric structures containing at least one molecule of PAS-1 and a molecule of band 3.

It is also likely that PAS-1 and band 3 (and hence the IMP) interact with structures at the cytoplasmic surfaces of the membrane. Approximately thirty percent of the erythrocyte membrane protein is present as two species, referred to as band 1 and band 2, having molecular weights of approximately 240,000 and 220,000 respectively. These two species are probably associated into dimers to form the fibrous protein spectrin (also referred to as Tektin A), which is thought to form a meshwork on the inner membrane surface (Elgsaeter and Branton, 1974; Nicolson et

al., 1971). Nicolson (1973b) and Nicolson and Painter (1973) have shown that cross-linking spectrin with anti-spectrin antibodies results in aggregation of anionic sites on the outer surface of the membrane. Also, Elgsaeter and Branton (1974) found that exposure of erythrocytes to a variety of conditions which result in a release of spectrin from the membrane allows translational redistribution of the IMP to occur more readily. These data suggest that some interaction occurs between spectrin and the PAS-1/band 3 complex at the cytoplasmic surfaces of the cell membrane, though there is presently no information as to the nature of this association.

It is apparent that the erythrocyte membrane as it is now understood represents a simple model system with all of the elements necessary for transmembrane communication, i.e., specific receptor sites on the cell surface linked to membrane-spanning proteins which are associated with cytoplasmic elements. This system becomes even more interesting when one considers that, although PAS-1 has no known functions other than those of providing membrane rigidity and bearing the negatively charged sialic acid groups, band 3 has been implicated in the facilitated diffusion of Cl^- , $\text{SO}_4^{=}$, and D-glucose. In addition, there is evidence that in the membrane, band 3 is bound to two polypeptides designated band 4.2 and band 6. The function of band 4.2 is not known, but band 6 has been shown to be the monomer of a tetrameric glyceraldehyde-3-phosphate dehydrogenase. In view of this evidence, it does not seem unreasonable to suggest that, in a system of this type, alterations in cell surface receptor sites might induce changes in transport rates or in the activity of enzymes bound to the cytoplasmic surface of the membrane, with subsequent effects on the behavior of the cell

concerned. It is important to stress at this point that the mammalian erythrocyte, lacking a nucleus and cytoplasmic organelles, is not a true cell and is therefore not really a good model for the phenomena described in the first part of this chapter; however, the presence of transmembrane linkages in erythrocytes does at least set a precedent for their existence in the more complex and less well understood membranes of metabolically active cells.

That conclusions derived from the study of isolated erythrocyte hosts cannot be freely extrapolated to live eukaryotic cells is apparent from a number of recent reports. In contrast to studies on erythrocyte ghosts, where aggregation of the surface receptor sites described above is always accompanied by corresponding aggregation of the IMP, independent movement of IMP and surface receptors has been observed in both normal and transformed mouse 3T3 fibroblasts (Pinto da Silva and Martinez-Palomo, 1975), mouse lymphocytes (Karnovsky and Unanue, 1973), and human platelets (Feagler et al., 1974). Similar results have been reported for Entamoeba histolytica (Pinto da Silva and Martinez-Palomo, 1974; Pinto da Silva et al., 1975) and Trypanosoma cruzi (Martinez-Palomo et al., 1976). The surface sites involved in these studies included anionic sites, immunoglobulin, and H-2 antigens, as well as receptors for Con A, phytohemagglutinin, and antilymphocyte globulin. Clearly, if transmembrane linkages to these sites exist, they probably do not involve the IMP.

Models for transmembrane communication which are more relevant to living eukaryotic cells have been proposed by Berlin et al. (1974) and Edelman (Edelman et al., 1973; Edelman, 1976). Berlin's group

measured the number of carrier proteins for different transport systems in phagocytosing polymorphonuclear leukocytes or alveolar macrophages and were able to show that no transport carriers are removed from the membrane even after 35-50% of the membrane has been internalized (Tsan and Berlin, 1971). After pretreatment with colchicine, however, phagocytosis results in a decrease in transport rate which parallels the degree of membrane internalization (Ukena and Berlin, 1972). On the other hand, receptors for Con A and Ricinus communis agglutinin (RCA) are selectively removed from the cell surface, apparently by concentration in regions undergoing internalization (Oliver et al., 1974). Colchicine reduces this specific removal of lectin binding sites. Berlin et al. (1974) postulated that cell surface proteins are anchored to an intracellular array of colchicine binding proteins (CBP), which are required for directed movement of surface elements. Thus the CBP assembly would be responsible for movement of lectin binding sites into, and transport sites out of, regions of membrane internalized by phagocytosis. Colchicine presumably abolishes the attachment of membrane proteins to the CBP, allowing these sites to move at random over the cell surface. The CBP assembly probably represents some component of the cytoplasmic assembly of microtubules. It is interesting that binding sites specific for both Con A and RCA were removed from the surfaces of polymorphonuclear leukocytes during phagocytosis, leaving behind receptors specific for only one lectin. This result suggests that only certain defined populations of surface proteins are anchored to the CBP. The CBP also appear to be involved in the process of capping in fibroblasts (Ukena et al., 1974) and polymorphonuclear leukocytes (Ryan et al., 1974), but colchicine seems to act differently in each

of these two systems.

Edelman's research team has discovered that high concentrations of Con A inhibit both cap formation and mitogenesis in lymphocytes treated with either Con A alone or with antibodies directed against other lymphocyte surface antigens (Rutishauser et al., 1974; Yahara and Edelman, 1972 and 1973). Treatment of cells with colchicine or vinblastine greatly reduces these inhibitory effects (Edelman et al., 1973). Succinylated Con A, which is dimeric rather than tetrameric, is mitogenic even at high concentrations but neither induces cap formation nor inhibits the mobility of Con A or immunoglobulin surface sites (Gunther et al., 1973). Both activities can be restored by the addition of antibodies against Con A to cells that have bound succinylated Con A. These results suggest that lymphocytes, like the other cell types discussed above, may have CABS and other cell surface receptors bound to a cytoplasmic array of CBP. Furthermore, the fact that Con A can inhibit cap formation and mitogenesis by its own or other receptors implies that aggregation of CABS on the cell surface by Con A may decrease the mobility, or alter the association-dissociation equilibria, of the CBP. These alterations in the CBP could in turn inhibit the mobility of other surface receptors. Succinylated Con A would presumably not provide sufficient aggregation of CABS to immobilize the CBP assembly, but addition of anti-Con A would restore the inhibitory effects by cross-linking the bound succinyl-Con A molecules. Colchicine might abolish the attachment of some membrane proteins to the CBP assembly, resulting in increased lateral mobility, followed by cap and patch formation and mitogenesis. There is also reason to believe that microfilaments play an essential role in the functions of the CBP

assembly (de Petris, 1974; Taylor et al., 1971; Ukena et al., 1974), possibly by linking surface receptors to the CBP (Edelman, 1976). Edelman et al. (1973) have postulated that mitogenic stimulation by lectins or antibodies may result from the cross-linking of surface receptors into micropatches with subsequent alterations of the CBP assembly. This process would be inhibited by high, CBP-immobilizing concentrations of Con A, but not by succinylated Con A, the latter substance presumably being incapable of immobilizing the CBP assembly. Recent evidence indicates that cross-linking occurring on only a small portion of the surface can result in restriction of the movement of receptors over the whole plasma membrane (Yahara and Edelman, 1975), suggesting that localized events at the cell surface can be propagated via the CBP over the whole cell. On the basis of studies such as these, Edelman (1976) has proposed that modulation of the CBP may play an important general role in the control of cell movement, recognition, and growth. According to this theory, the CBP would be involved in the regulation of the early biochemical signals that induce a cell to mature, divide, and move; loss of one of these regulatory functions due to defects in the microtubular-microfibrillar array might then lead to some of the altered properties of transformed cells (Edelman and Yahara, 1976). This system of CBP and associated surface receptors appears to be quite separate from the IMP, since aggregation of the IMP by incubation with glycerol (McIntyre et al., 1974) does not affect the distribution of the CABS (G. M. Edelman, personal communication).

Several laboratories have recently published data which are consistent with the model proposed by these two groups. Fluorescence

energy-transfer techniques have provided evidence for the existence of specific colchicine-sensitive associations between membranes and polymerized tubulin (Becker et al., 1975), and associations between microfilaments and membranes have also been demonstrated (see Chapter 4). The distribution and mobility of surface sites on spermatozoa has been found to vary between different regions of the plasma membrane, a result which is suggestive of the existence of transmembrane restraints (Nicolson and Yanagimachi, 1974). Phagocytosis in macrophages is accompanied by the formation of a complex network of microfilaments and microtubules in the cytoplasm adjacent to the region of internalizing membrane (Reaven and Axline, 1973), and inhibition of phagocytosis by cytochalasin B is correlated with disorganization of microfilament bundles in the portion of this network that is situated directly beneath the plasma membrane (Axline and Reaven, 1974). Local anesthetics, which alter agglutinability and receptor mobility in Balb 3T3 cells, have also been found to cause changes in cytoplasmic microfilaments and microtubules (Nicolson et al., 1976). Especially interesting is the observation by Albertini and Clark (1975) that Con A-induced capping of ovarian granulosa cells results in an accumulation directly under the cap of numerous microtubules oriented perpendicular to the membrane. This represents the first direct evidence that perturbation of the cell surface can modify the cytoplasmic distribution of microtubules. Finally, Edelman and Yahara (1976) have found that temperature sensitive mutants of transformed chick embryo fibroblasts, which lack ordered arrays of microfilaments and microtubules at the permissive temperature (37°C), also exhibit much less inhibition of receptor mo-

bility by Con A at 37°C than at the restrictive temperature (41°C). The reduced effect of Con A on the mobility of other surface receptors at 37°C was attributed to a transformation-induced defect in the CBP array. This defect may be due to inadequate polymerization of tubulin as a result of the lower levels of cyclic nucleotides (Brinkley et al., 1975) or higher concentrations of Ca^{++} (Fuller et al., 1976; Kiehart and Inoue, 1976; Schliwa, 1976) found in transformed fibroblasts.

These data suggest that the control of cell growth and mobility is a complex process which is mediated at least in part via alterations in a subplasmalemmal array of microfilaments and microtubules. This cytoplasmic array may in turn be modulated by changes in the topography of certain surface receptor sites and by fluctuations in the levels of intracellular messengers such as Ca^{++} and cyclic AMP. The fact that freeze-fracture permits examination of large areas of both the cell surface and the hydrophobic inner membrane region at high resolution suggested that this technique might be a very useful tool for investigation of the possible role of these membrane changes in the control of cell growth. However, very little data is available on the structure and function of the IMP in eukaryotic cells, and it is not known at present whether the IMP play any role in the growth-regulating mechanisms just described. The fact that the IMP do not comigrate with the various surface receptors of the cell types investigated in these studies indicates that in these cells such receptor molecules are not part of the IMP as they appear to be in the erythrocyte. Also, there is some evidence that connections between the IMP and cytoplasmic structures may exist in protozoa (Martinez-Palomo et al., 1976), but

similar connections have not yet been observed in mammalian cells. With the exception of cell junctions (McNutt and Weinstein, 1973), IMP in mammalian cell membranes appear to be sprinkled in a relatively uniform fashion over the fracture face, and this native distribution of IMP does not seem to be altered by density dependent inhibition of growth at high cell density or by viral transformation with its accompanying loss of growth control (Gilula et al., 1975; Pinto da Silva and Martinez-Palomo, 1975).

However, an extremely interesting approach to using freeze-etching in the study of the possible relationships between membrane alterations and growth control has recently been reported by McIntyre et al. (1973 and 1974), who showed that treatment with glycerol or dimethylsulfoxide induced the formation of particle aggregates on the fracture faces of unfixed lymphoid cells. Treatment of untransformed Balb 3T3 mouse embryo fibroblasts or chick embryo fibroblasts with glycerol also caused redistribution of IMP into aggregates (Gilula et al., 1975). Glycerol-induced particle redistribution was fully reversible, occurred independently of temperature and cell density, and had little effect on cell viability. The most intriguing result, however, was the discovery that transformed fibroblasts exhibited only a marginal degree of particle aggregation after exposure to glycerol. Apparently, glycerol acts as a membrane-perturbing agent, revealing differences in IMP mobility between untransformed and transformed cells which are not apparent in untreated cells. Glycerol pretreatment was also accompanied by a marked decrease in the overall density of IMP. Cultures that had been fixed before glycerination showed no signs of

particle redistribution or loss. Mild proteolysis also reduced the degree of particle aggregation shown by untransformed cells. Experiments using temperature-sensitive mutants established that the changes in IMP mobility were definitely related to viral transformation rather than simply being the result of virus infection itself.

These results are difficult to interpret at present. The effect of glycerol is opposite to that of lectins and other cross-linking agents, i.e., where lectins reveal an increased mobility of surface sites on transformed cells, glycerol causes much less redistribution of IMP in transformed than in untransformed fibroblasts. The effect of proteolysis on the redistribution of lectin receptors and IMP is similar, however, in that proteolytic enzymes cause untransformed cells to act more like transformed cells in both cases. The fact that IMP redistribution can be eliminated by fixation suggests that the IMP may be associated with some sort of proteinaceous network to which they can be covalently bound by chemical fixatives.

Although the mechanisms responsible for these differences in IMP redistribution by glycerol are not understood, some other recent evidence suggests that there may be some degree of correlation between the control of cell growth and the mobility and distribution of the IMP. Using statistical analysis, Weinstein (R. S. Weinstein, personal communication; Weinstein, 1974) showed that the seemingly random native distribution of IMP is, in fact, a nonrandom arrangement; furthermore, changes in the degree of ordering were found to occur during neoplastic transformation in vivo. More recently, Barkla and Tutton (1976) found that IMP in the membranes of malignant rat colonic epithelial cells were more heterogeneous in size and showed a more

aggregated distribution than IMP on the fracture faces of nonmalignant cells. Changes in IMP density also accompany transformation in vitro and in vivo, although the direction of the trend is not always the same; Barkla and Tutton (1976) found that malignant colonic cells had fewer IMP than their nonmalignant counterparts, while Gonzalez-Robles et al. (1976) and Torpier et al. (1975) found increased IMP densities in leukemic cells and virally transformed fibroblasts, respectively. The existence of a significant degree of ordering in the distribution of IMP in untransformed cells is consistent with the idea that particles may be associated with cytoskeletal elements. Furthermore, the fact that modification of the mobility, ordering, and density of IMP occurs in cells transformed in vitro and in vivo suggests that transformation may cause insertion of IMP into, or removal of IMP from, the plasma membrane and, in addition, that transformation may alter the association between IMP and the cytoskeleton.

In order to further investigate this hypothesis, experiments were begun which were aimed at comparing the density and distribution of IMP on the membranes of untransformed and transformed 3T3 mouse embryo fibroblasts before and after treatment with glycerol. A special effort was made to examine as large a portion of the cell membrane as possible in order to determine whether cell contact modified the distribution or mobility of the IMP. After preliminary studies (Chapter 2), it became apparent that available techniques for examining cultured cells by electron microscopy were inadequate for the needs of this project, and it was therefore necessary to develop the required methodology before any meaningful data could be obtained. For this reason, much of this

report is devoted to the description of improved techniques for electron microscopy of cultured cells. This improved methodology was then used to carry out a detailed examination of cell interactions and membrane structure in cultured Balb 3T3 mouse embryo fibroblasts. In addition, preliminary results of studies with glycerinated Balb 3T3 cells are described in Chapter 7.

Chapter 2

Preliminary Studies

The initial freeze-fracture experiments were carried out on Swiss 3T3 mouse embryo fibroblasts cultured under a variety of conditions. These preparations included confluent nontransformed and SV40-transformed cultures, logarithmically growing cultures, and three samples from an experiment in which cells were synchronized by serum starvation. These cultures were prepared for freeze-fracture without fixation. In addition, one confluent culture was fixed in paraformaldehyde-glutaraldehyde before glycerination. Fracturing was carried out using the conventional technique of slicing the frozen sample with a razor blade mounted on the microtome arm of a Balzers freeze-fracture apparatus. Although these preliminary studies yielded considerable morphological information, it became obvious that a profitable examination of cell interactions in culture required more sophisticated techniques which would allow cell monolayers to be fractured in situ.

Materials and Methods

Preparation of unfixed cells for freeze-fracture. 3T3 clone 4A Swiss mouse embryo fibroblasts (Swiss 3T3 4A cells) obtained from Robert Holley of the Salk Institute, and SV40-transformed clone 56 cells (SV3T3 cells), derived from Swiss 3T3 and provided by Renato Dulbecco, were grown in 100 mm Falcon plastic culture dishes (Falcon Plastics, Oxnard, Ca.) in Vogt and Dulbecco's modification of Eagle's medium (DME, Grand Island Biological Company, Grand Island, N. Y.; Vogt and Dulbecco,

1963) supplemented with 10% newborn calf serum (GIBCO). Cultures were incubated at 37°C in a 10% CO₂ atmosphere. The Swiss 3T3 4A cells were recloned after the freeze-fracture studies on unfixed cultures and cells of the clone RK2 (Swiss 3T3 4A RK2 cells) were used for all subsequent experiments.

During the first phase of the preliminary study (Experiments 1-9),² cells were prepared for freeze-fracture by the following procedure (Method I). After removal of all but 1-2 ml of culture medium, the cells were scraped off the dishes with a rubber policeman and centrifuged at 1000-2000 RPM for 1-2 min in an International IEC HNS centrifuge. The pellet was resuspended in DME containing 10% serum and 20% glycerol (Baker Analyzed Reagent grade) and left for 20-30 min. The cells were then pelleted as before and the supernatant removed. This procedure was carried out at room temperature. Small droplets of the pelleted cells were placed on 3 mm cardboard disks and rapidly frozen in the liquid phase of partially solidified Freon 22 (E.I. duPont de Nemours and Co., Wilmington, Del.) cooled by liquid nitrogen.

Method I was abandoned after it was found that the DME-glycerol-serum mixture became progressively more basic (up to pH 8.5) as a result of the loss of dissolved CO₂ when stored or exposed to air. Cells were subsequently (Experiments 10-15) prepared using the following procedure (Method II). The medium was removed from the dish, and the monolayer rinsed three times with cold (6-10°C) saline GM, a 2.0 mM phosphate buffer, pH 7.2 - 7.4, containing 6.1 mM glucose, 0.14 M NaCl,

² In this study each freeze-fracture run was called an "experiment" and given a number. The freeze-fracture data in this thesis were obtained in a total of forty-five such experiments.

and 5.4 mM KCl. Three ml of saline GM were added to each 100 mm dish and the monolayer was gently scraped off the dish with a rubber policeman. The cell suspension was removed, 3 ml of 20% glycerol in saline GM were added, and the pellet was resuspended. The cell suspension was left for thirty minutes and then recentrifuged as before. The supernatant was removed and the cells were frozen. By the time freezing was completed, the cells had been in 20% glycerol for 1/2 - 2 hr. The culture dishes and tubes containing the cell suspensions were kept on ice whenever possible.

Preparation of fixed cells for freeze-fracture. Confluent cultures of Swiss 3T3 4A RK2 cells were prepared by a procedure (Method III) similar to that of Pfenninger and Bunge (1974). Cells were fixed in the dish for 15 min in 4% paraformaldehyde (Matheson, Coleman, and Bell Reagent grade) and 0.5% glutaraldehyde (Electron Microscopy Sciences, Port Washington, Pa.) containing 0.1 M phosphate buffer and 0.14 mM $\text{CaCl}_2 \cdot 2\text{H}_2\text{O}$. Cultures were then fixed 45 min in 4% glutaraldehyde containing 0.15 M phosphate buffer and 0.14 mM $\text{CaCl}_2 \cdot 2\text{H}_2\text{O}$, and incubated for 45 min - 2 hr in cold 30% glycerol in 0.1 M phosphate buffer. All solutions had a pH of 7.0 - 7.4 at the temperature employed. Culture dishes were floated on the surface of a 37°C water bath during fixation and were transferred to an ice-water slush during washing and glycerination. Each solution was gradually replaced by the next one to minimize the osmotic shock to the cells. Osmotic concentrations of these solutions, measured with a Fiske osmometer, were approximately as follows: paraformaldehyde-glutaraldehyde, 1500 mosmol/kg; glutaraldehyde, 770 mosmol/kg; and 0.2 M buffer, 430 mosmol/kg. After glycerina-

tion, the monolayer was carefully scraped off the dish with a rubber policeman, then pelleted gently. The pelleted cells were pipetted onto Balzers 3 mm flat-topped gold specimen carriers (Balzers High Vacuum Corporation, Santa Ana, Ca.) and frozen as before.

Freeze-fracture. Droplets of pelleted cells were fractured at -115°C , then shadowed with platinum-carbon followed by carbon in a Balzers BA 360M freeze-etching apparatus. The fractured specimens were thawed and the cellular material was digested away from the replica by chlorine bleach (5.25% sodium hypochlorite, 30 min) followed by two 10 min washes with distilled water. Replicas were picked up on flamed 300 or 75 x 300 mesh copper grids, examined in a Siemens Elmiskop I electron microscope at an accelerating voltage of 80 or 100 kV, and photographed on Kodak Electron Image Plates (Eastman Kodak Co., Rochester, N. Y.). Shadows are white, and shadow direction is indicated by an arrow on each figure. Particle diameters were measured perpendicular to the shadow direction.

Cell synchronization. The Swiss 3T3 4A RK2 cells used in this experiment were synchronized by the serum starvation technique. Cultures were blocked in G_1 by growth to saturation density in medium containing 10% calf serum. The cells were then removed from the dishes and seeded at 1×10^6 cells per 10 mm plastic dish in medium containing either 0.8% or 20% serum. At various times after seeding, cells were prepared for freeze-fracture and for cell cycle analysis by autoradiography (Bartholomew et al., 1976) and flow microfluorometry (Trujillo and Van Dilla, 1972). Cells plated into 0.8% serum attached to the dish but remained blocked in G_1 , while those plated into 20% serum passed into S and G_2 +M. Cells in 20% serum remained in G_1 for approximately 14 hr., then traversed the cell cycle synchronously and were once again growing

randomly by 24 hr.

Results

Unfixed preparations. The characteristic appearance of Swiss 3T3 4A cells frozen and fractured without prior fixation is shown in Fig. 1. Scraping off and suspending the monolayer caused cells to round up and lose contact with their neighbors, though some cells could be seen which had retained contact with another cell (Fig. 1, arrow). Regions of intercellular contact seldom involved large portions of the membrane. Cell shape varied from spherical (Cell 2) to highly convoluted (Cell 1). Cells were approximately 20 μm in diameter. Identifiable organelles included the outer and inner nuclear membranes, nuclear pores, Golgi apparatus, endoplasmic reticulum, mitochondria, microvilli, and vesicles which appeared to be in the process of budding from or fusing with the plasma membrane. Preservation of the cytoplasm in unfixed cultures was variable. While some cells retained the elongated mitochondria and laminar endoplasmic reticulum and Golgi apparatus seen in Fig. 1, others showed varying degrees of vesiculation of these organelles, an artifact which has been attributed to the effect of high concentrations of glycerol (Moor, 1971). The plasma membrane varied from smooth (Cell 2) to highly convoluted with numerous microvilli, blebs, and larger protrusions (Cell 1). Wrinkling of the plasma and nuclear membranes may have been due to the rapid addition of glycerol to the cell suspension (Reith and Oftebro, 1971). These morphological observations were consistent with the results of other freeze-fracture studies on unfixed cultures (Bererhi and Malkani, 1969, 1970; Kouri et al., 1971; McIntyre et al., 1974; Malkani and Bererhi, 1970; Reith and Oftebro, 1971).

Figure 1. Swiss 3T3 4A cells prepared for freeze-fracture without prior fixation (Method II, Experiment 15). The larger cell (#1), which has fractured through the cytoplasm, still retains an attachment (arrow) to its neighbor (#2). N, nuclear membrane with numerous pores; er, endoplasmic reticulum; G, Golgi apparatus; Mv, microvilli; V, vesicles budding from or fusing with the plasma membrane. 7800X.

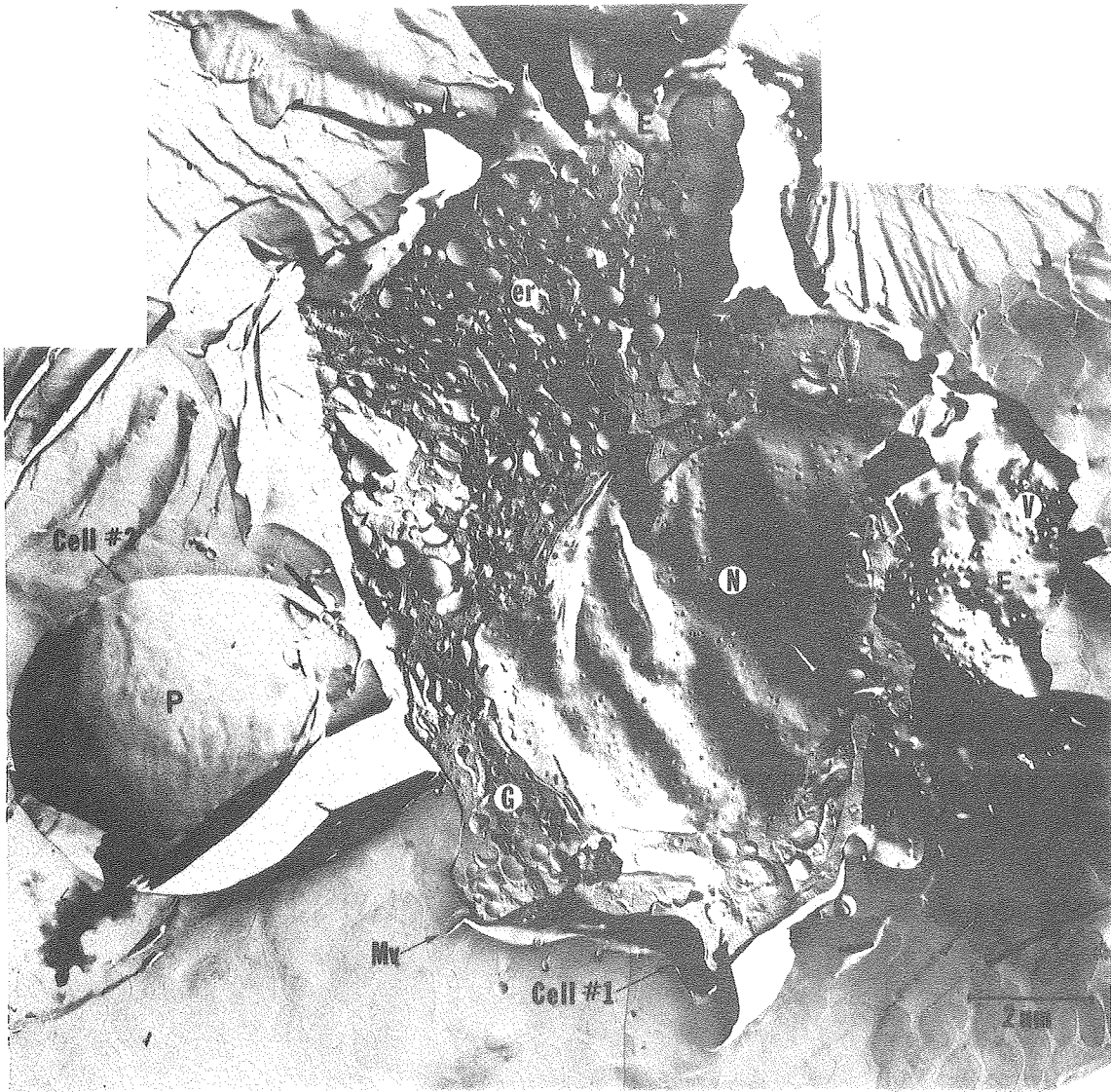


Fig. 1

XBB766 5238

Freeze-fracture of Swiss 3T3 4A and SV3T3 cell membranes revealed two distinctly different fracture faces, the protoplasmic (P) face and the extracellular (E) face (Branton et al., 1975). Each fracture face was photographed at low (5000X) and high (20,000X) magnification. Combining information regarding shadow angle, membrane curvature, and cell shape from both low and high magnification micrographs usually permitted identification of each fracture face as a P or E face. Those fracture faces which could not be classified definitely were not used here. The P face appeared as a smooth region of cell membrane, punctuated by numerous IMP, 91 Å in diameter ($N = 125$, standard deviation = 19 Å). Both P and E faces exhibited various degrees of aggregation of the IMP. Particle aggregation was presumably induced by the glycerol cryoprotectant (Gilula et al., 1975; McIntyre et al., 1973 and 1974). The majority of the IMP distributions seen on the P faces of 3T3 and SV3T3 cells could be classified into one of three patterns: "uniform," "patched," and "clumped." The uniform distribution of IMP is shown in Fig. 2a. A P face was defined as "patched" if it bore one or more large particle clusters with a diameter greater than 0.1 μm (Fig. 2b). P faces were defined as having the "clumped" particle configuration if particles aggregated into small clusters less than 0.1 μm in diameter. In every example of the latter type of particle distribution, the small particle clusters were distributed uniformly over the fracture face (Fig. 2c).

The background of the E face had a roughened, stringy appearance unlike that of the P face, and many of the particles were elongated as if they had been partially pulled out of the membrane during cleavage and allowed to fall back onto the fracture face. The shape of these particles was reminiscent of the appearance of freeze-fractured poly-

Figure 2. P faces of Swiss 3T3 4A cell membranes prepared by Method II, showing the three characteristic distributions of IMP: Uniform (a), patched (b), and clumped (c). Bar represents 0.1 μm . 80,000X.

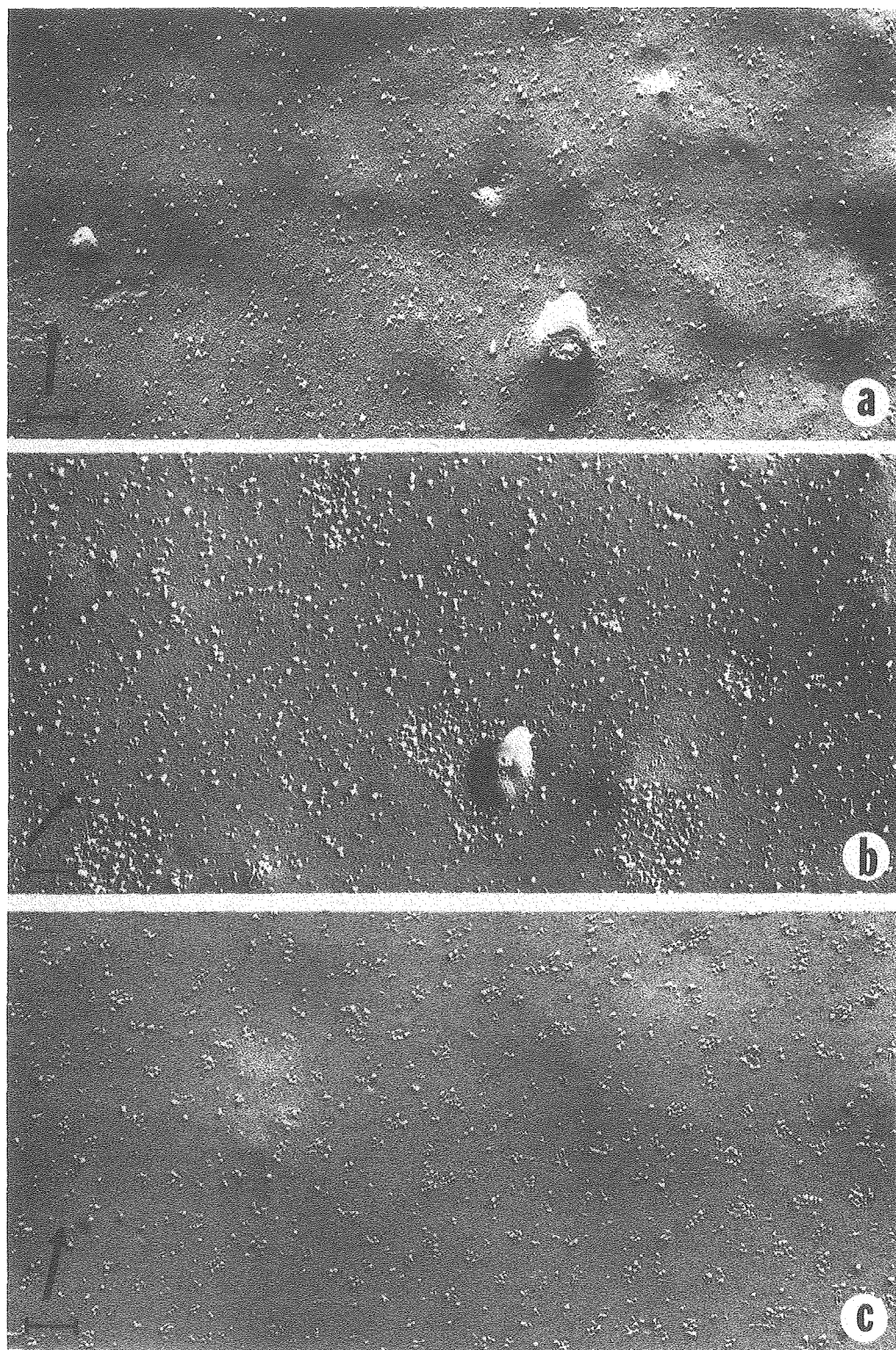


Fig. 2

XBB766 5245

styrene spheres, which stretch and pull away from the membrane during fracturing (Clark and Branton, 1968).

Changes in the distribution of IMP on the E face were difficult to differentiate, but it was possible to classify most E faces as having a uniform or non-uniform particle distribution. Representative samples of these two types of membrane topography are shown in Figs. 3a and 3b, respectively. In the unfixed cultures examined, twelve cells were found where both the P and E faces were exposed on the same cell. In all such cases, the IMP distributions (9 uniform, 3 non-uniform) were the same on both fracture faces.

It is interesting to note that the characteristic difference between the "clumped" and "patched" distributions has been observed in other studies with unfixed material. After preparing lymphocytes by procedures similar to Method II, both Mandel (1972) and McIntyre et al. (1974) noted the presence of two types of particle aggregates, and classified fracture faces accordingly. The similarity in IMP distributions is readily apparent if the micrographs of "monogranular," "small polygranular," and "large polygranular" lymphocytes (Mandel, 1972) and cells with "mono-dispersed particles," "small clusters," and "large clusters" (McIntyre et al., 1974) are compared with the "uniform," "clumped," and "patched" distributions, respectively. Further research should reveal whether the clumped and patched distributions result from intrinsic differences in plasma membrane structure, or whether they are merely successive steps in a time-dependent aggregation process.

In some cases, numerous small filamentous objects appeared to protrude from the cytoplasmic fracture plane along the edge of the E

face (Fig. 3a, arrows). These may be IMP which have stretched during cleavage and fallen onto the cytoplasm; alternatively, they may represent sites where microfilaments are attached to the plasma membrane. The latter view is supported by the fact that filaments similar to these have been observed at the intercalated disc of cardiac muscle cells where actin filaments insert into the fascia adherens (McNutt, 1970 and 1975), and in the intestinal microvillus, where short filamentous cross-bridges are known to attach microfilaments to the membrane (McNutt et al., 1977). These filamentous objects disappear when cytoplasmic actin filaments are depolymerized in 0.6 M KI (McNutt, 1976; McNutt et al., 1977). There is also an interesting resemblance between these filaments and the short filamentous bridges which are believed to attach the IMP-rich plaques in the membranes of the urinary bladder epithelium (Stachelin, 1972). The filamentous objects were seen only in unfixed preparations.

The results of the freeze-fracture studies on unfixed 3T3 cells are summarized in Table I. The sample size in the early experiments (5, 7, 9, and 11) was small because of problems with replica preparation and handling. In all, a total of 145 cells were photographed, including 92 P faces and 68 E faces. A number of fracture faces had IMP distributions which could not be classified definitely into any of the five categories. For the purpose of summarizing the data for all of the cells examined, these fracture faces were classified as "uncertain."

The data shown in Table I did not reveal any consistent effect of the growth state of the culture on the distribution of IMP. Since changes in pH have been found to alter IMP distribution (Pinto da

Figure 3. Typical E faces of Swiss 3T3 4A cell membranes, showing the uniform (a) and non-uniform (b) distribution of IMP. Note filamentous objects (arrows) at the juncture of the E face and the cytoplasm (cyt). Bar represents 0.1 μm . 80,000X.

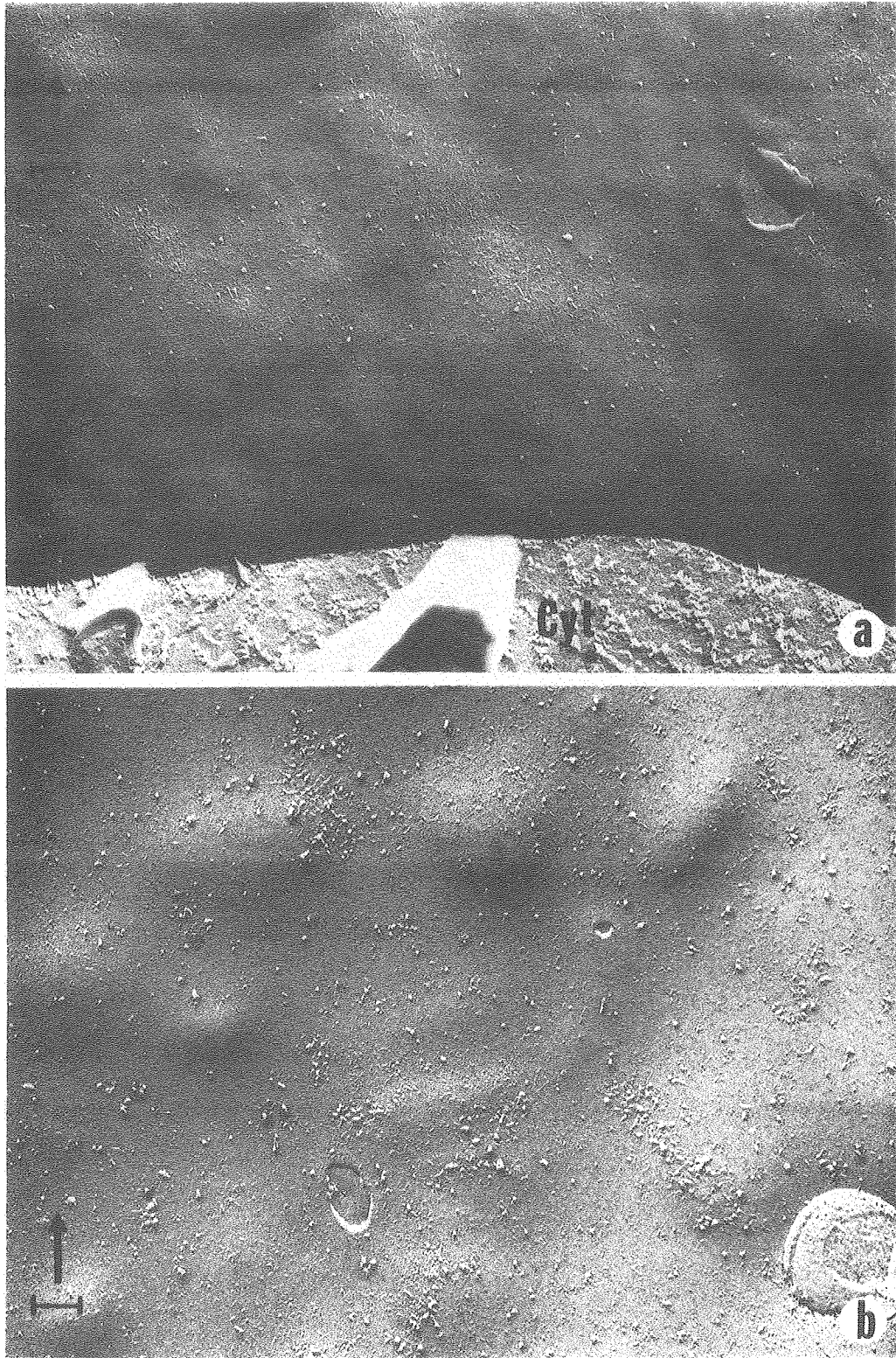


Fig. 3

XBB766 5246

Silva, 1972), the results of experiments 5, 7, 9, and 11 should be viewed with caution, as the basicity of the DME could have affected the particle distribution. However, in comparing data from these first experiments with the results obtained using Method II, it is interesting to note that the clumped configuration was only observed with cells prepared in the cold. This might represent an effect of temperature on glycerol-induced particle aggregation.

In experiments 12 through 15, both SV40-transformed and synchronized 3T3 cells showed a significant incidence of both uniform and non-uniform particle distributions. Although cells in G_2 and M were not included in the samples examined by freeze-fracture, the data obtained using synchronized cells (experiments 12, 14, and 15) did not show any consistent relationship between the fraction of cells in a given phase of the cell cycle and the incidence of a particular type of IMP distribution. Also, there did not appear to be any correlation between cell shape and particle distribution. The results of experiments 7 and 13 differ from those of Gilula et al. (1975) in that in a considerable fraction (approximately 50%) of the fracture faces of SV3T3 cells exhibited particle aggregates.

Fixed preparations. Swiss 3T3 4A RK2 cell cultures prepared by Method III were similar in appearance to sectioned fibroblasts (Abercrombie et al., 1971, Cherny et al., 1975; Lucky et al., 1957; McNutt et al., 1971). In almost all cases, cells fractured in cross section appeared flattened, with a thicker portion (3-4 μm) over the nucleus sloping gently to thin peripheral sheets of cytoplasm which often extended for several micrometers (Fig. 4). These peripheral sheets were as thin as 0.06 - 0.07 μm in places, contained few membrane-bound

Table I. Results of Freeze-Fracture Studies on Unfixed Cultures.

Expt. Number	Cell type	Preparation method	Uniform	Number of P faces			Number of E faces		
				Patched	Clumped	Uncertain	Uniform	Non-uniform	Uncertain
5	Confluent 3T3	I	$\frac{3}{5}$	$\frac{0}{5}$	$\frac{0}{5}$	$\frac{2}{5}$	$\frac{1}{1}$	$\frac{0}{1}$	$\frac{0}{1}$
7	Confluent SV3T3	I	$\frac{3}{7}$	$\frac{3}{7}$	$\frac{0}{7}$	$\frac{1}{7}$	$\frac{2}{2}$	$\frac{0}{2}$	$\frac{0}{2}$
9	Log Phase 3T3	I	$\frac{7}{9}$	$\frac{0}{9}$	$\frac{0}{9}$	$\frac{2}{9}$	$\frac{5}{7}$	$\frac{0}{7}$	$\frac{2}{7}$
11	Log Phase 3T3, impregnated with glycerol at 0°C	I	$\frac{0}{2}$	$\frac{0}{2}$	$\frac{2}{2}$	$\frac{0}{2}$	$\frac{0}{0}$	$\frac{0}{0}$	$\frac{0}{0}$
12	24 hr., 20% serum sample from cell synchronization expt. 13% G ₁ , 87% S.	II	$\frac{1}{12}$	$\frac{4}{12}$	$\frac{2}{12}$	$\frac{5}{12}$	$\frac{4}{6}$	$\frac{1}{6}$	$\frac{1}{6}$
13	Confluent SV3T3	II	$\frac{1}{6}$	$\frac{0}{6}$	$\frac{3}{6}$	$\frac{2}{6}$	$\frac{4}{7}$	$\frac{3}{7}$	$\frac{0}{7}$
14	20 hr., 0.8% serum sample from cell synchronization expt. 95% G ₁ , 5% S.	II	$\frac{1}{17}$	$\frac{8}{17}$	$\frac{3}{17}$	$\frac{5}{17}$	$\frac{3}{18}$	$\frac{7}{18}$	$\frac{8}{18}$
15	20 hr., 20% serum sample from cell synchronization expt. 29%G ₁ , 71% S.	II	$\frac{12}{36}$	$\frac{15}{36}$	$\frac{4}{36}$	$\frac{5}{36}$	$\frac{12}{27}$	$\frac{7}{27}$	$\frac{8}{27}$

Figure 4. A typical Swiss 3T3 4A RK2 cell fixed with paraformaldehyde-glutaraldehyde before glycerination. Organelles are restricted to the central portion of the cell, with few organelles in the thin peripheral regions (upper part of this cell). Numerous mycoplasma (arrowheads) adhere to the right hand side of the cell, which presumably was the upper surface in the monolayer. N, nuclear membrane. 5500X.

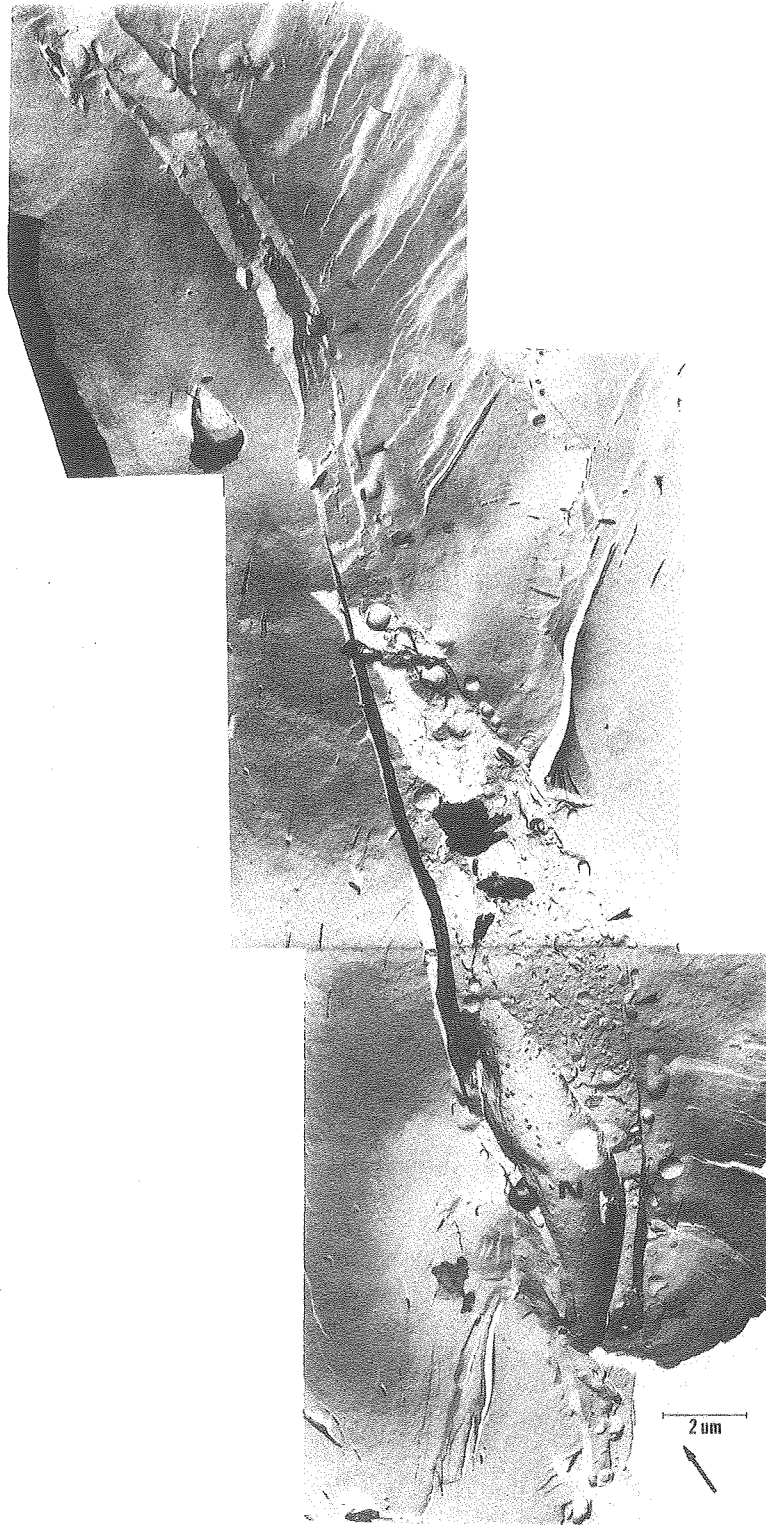


Fig. 4

XBB766 5237

organelles, and showed extensive overlap with similar regions on neighboring cells. There was no special protrusion of the membrane over the nucleus. The plasma membrane exhibited few microvilli and none of the blebs and larger protrusions characteristic of unfixed cells. Mitochondria were more elongated than in unfixed cells. These observations were based on photographs of portions of 20 cells, including both cross-fractured cells and extensive areas of the plasma membranes of cells which had fractured parallel to the cell surface.

The interpretation of replicas of fixed, pelleted monolayers was complicated by the fact that, in most cases, it was impossible to determine which fracture face represented the upper surface of the cell. However, some of the cultures used in the preliminary experiments on fixed and unfixed material had become contaminated with mycoplasma, which could be recognized by their characteristic size and shape (Brown et al., 1974) both in freeze-fractured preparations and by scanning electron microscopy. In cases where mycoplasma adhered primarily to one surface of the cell (Fig. 4), it seemed likely that this surface was uppermost in the original monolayer.

Typical P and E fracture faces of fixed Swiss 3T3 4A RK2 cells are shown in Fig. 5. IMP diameter on the P face was 88 Å (N= 140, standard deviation = 17 Å). In all cases, distribution of IMP on both faces was uniform with no evidence of particle aggregation, indicating that aldehyde fixation had prevented glycerol-induced clustering of the IMP (Gilula et al, 1975; McIntyre et al., 1973 and 1974; Pinto da Silva and Martinez-Palomo, 1974 and 1975).

In areas where the peripheral regions of neighboring cells overlapped, localized regions could be observed where the plasma membranes

Figure 5. Typical P (a) and E (b) fracture faces of fixed Swiss 3T3 4A RK2 cells. (b) includes both faces and was taken from the peripheral region of a cross-fractured cell. Vesicular stomata (arrowheads) were common on both P and E faces. Continuity of the plasma and vesicular membranes at the stomata was apparent in favorable fractures (*). I, II, and III probably represent successive stages in pinocytosis or exocytosis. Cyt, cytoplasm. Bar represents 0.1 μ m. 80,000X.

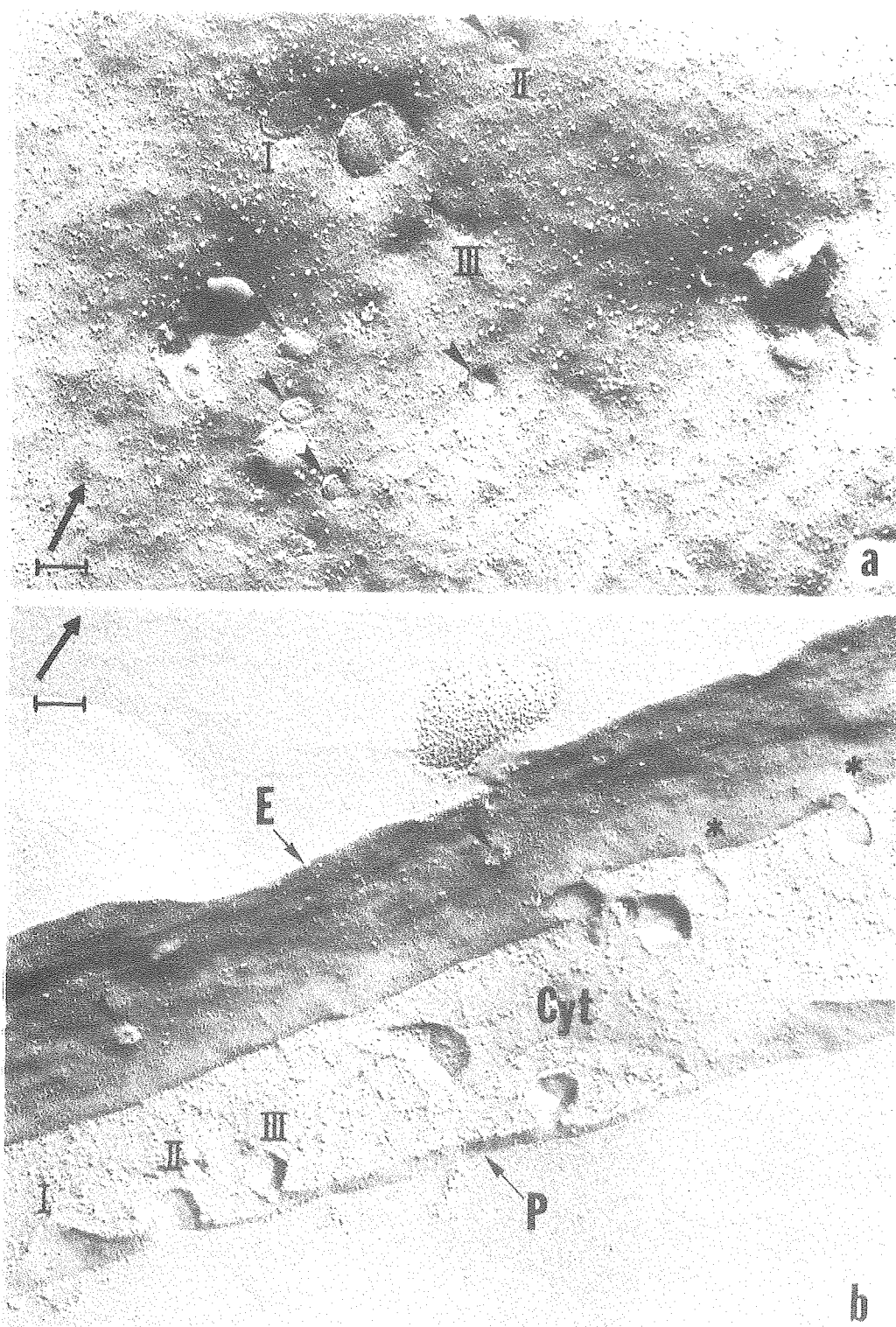


Fig. 5.

XBB766 5244

of two cells came into very close apposition (Fig. 6). Although the tilt of the fracture face usually made it difficult to examine membrane structure in these areas, there did not appear to be any specialization of the membrane at such regions. Gap junctions, observed in Chinese hamster fibroblasts (Gilula et al., 1972), chick embryo fibroblasts (Pinto da Silva and Gilula, 1972), and baby hamster kidney fibroblasts (Revel et al., 1971), were almost never seen in either fixed or unfixed Swiss 3T3 cell cultures.

The background matrix of both P and E faces exhibited a fine particulate substructure which seemed more pronounced on the E face. The presence of these "subparticles" has been noted in other studies. Their existence as real entities within the plasma membrane is suggested by the fact that particles and subparticles can be induced to coaggregate, leaving behind smooth regions of plasma membrane (Pinto da Silva and Martinez-Palomo, 1974 and 1975).

One prominent aspect of the membranes of fixed 3T3 cells was the numerous vesicular stomata which appeared on both the P and E faces (Fig. 5). On the P faces, the stomata appeared as shallow depressions 0.012 to 0.12 μ m in diameter. Continuity of the vesicular membrane with the plasma membrane was apparent in regions where the fracture plane had followed the vesicle membrane through its neck to the fracture face of the plasma membrane (asterisks, Fig. 5b). There was no evidence of the specialized annulus of IMP around the stomata observed in intestinal smooth muscle (Orci and Perrelet, 1973) and Tetrahymena (Satir et al., 1972 and 1973). In fact, the membrane in the region of the vesicular stomata did not appear to be significantly different from

Figure 6. Area of overlap between the peripheral regions of three fixed Swiss 3T3 4A RK2 cells. The surfaces of cells 2 and 3 are in close apposition, but only small portions of the fracture faces (P_2 and E_3) are exposed in this region. Furthermore, the tilt of the fracture plane often results in insufficient shadowing (arrowheads) or overly heavy shadowing (double arrowheads). Inadequate shadowing and the lack of extensive fracture faces resulted in the loss of much of the information potentially available from fractures through these regions of cellular interaction. Cyt, cytoplasm. 42,000X.

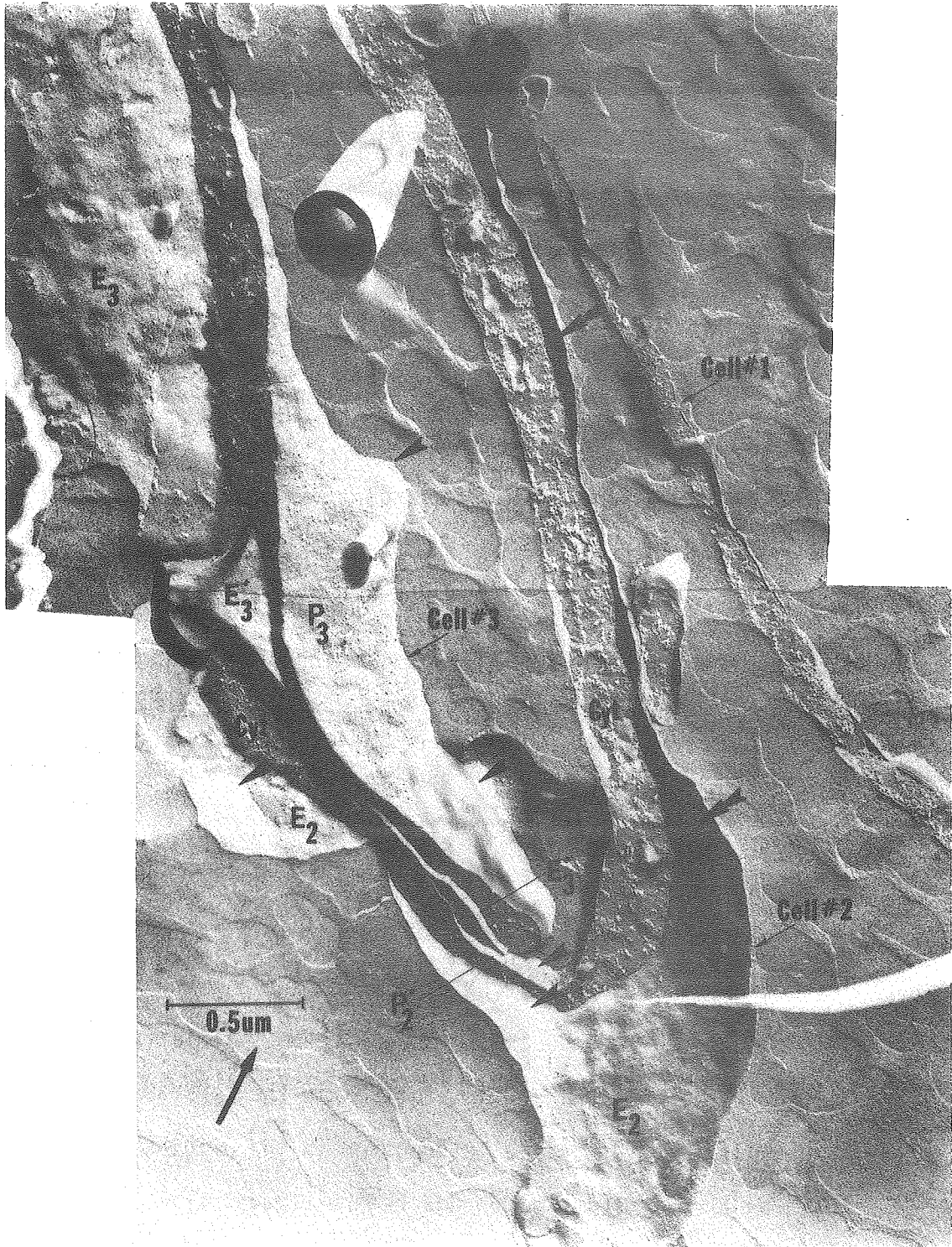


Fig. 6

XBB766 5239

nearby nonvesiculated membrane, a characteristic which this preparation appeared to share with cells of the adrenal medulla (Smith et al., 1973), the islets of Langerhans (Orci et al., 1973), and mammary adipose tissue (Elias et al., 1973, and D. R. Pitelka, personal communication). The variation in the size and morphology of the stomata and vesicles probably represented various stages in pinocytosis or exocytosis (Fig. 5, I, II, and III). Palade and Bruns (1968) have described this process in detail.

Discussion

Until recently, the customary method of preparing cultures for freeze-fracture has involved gently scraping fixed or unfixed cell layers off the culture dish, centrifuging the resulting suspension, and freezing portions of the pelleted cell layer. The results of the preliminary studies described here indicate that this method is inadequate for the study of cell interactions in culture. After suspension and glycerination of unfixed cultures, the majority of cells undergo drastic morphological alterations, and most regions of cellular interaction are disrupted. Although the glycerol-induced particle aggregation shown in Figs. 2 and 3 may be useful in examining regional differences in membrane structure, the morphological changes occurring with unfixed cultures using existing methods are so extensive that it is virtually impossible to relate regional specializations in the membranes of unfixed, fractured cells to any specific interaction in the original culture.

Cultures prefixed with aldehydes before removal from the culture dish yield somewhat more information, since fixed cells retain their original shape and cytoplasmic morphology. However, removal of the

fixed monolayer from its substratum still results in the unavoidable loss of a great deal of information regarding morphology in situ and inter-cellular relationships. Although the cell sheet usually retains its integrity during preparation, scraping and pelleting cause extensive folding and crumpling of the monolayer (Fig. 6). Consequently, it is usually very difficult to ascertain which are the upper and lower surfaces of the cell, and whether a given cell is overlapping or being overlapped by its neighbors. Tilting of the fracture face often results in excessive or insufficient platinum shadowing (Fig. 6) and makes estimation of the particle density extremely difficult, since determination of the angle of inclination of the face requires complex reconstructive analysis (Hirschauer and Prioul, 1969). Furthermore, cross-fractured cells (figs. 4 and 6) frequently do not expose large enough fracture faces to yield much information about membrane topography. Finally, even when large fracture faces do occur, pelleted cells are sufficiently contorted that in most cases, only a portion of the cell surface is exposed by the fracture plane.

Experience with these problems made it clear that examination of cell interactions in monolayer cultures could not be carried out profitably with existing freeze-fracture techniques. For this reason, methods were developed which allowed cell cultures to be prepared in situ for scanning, thin section, and freeze-fracture electron microscopy as well as for the standard techniques of cell culture analysis. It was felt that these methods would allow a more complete analysis of regional differences in both the ultrastructure of the plasma membrane and its sensitivity to glycerol-induced aggregation of the IMP. The subsequent chapters of this study are therefore devoted to a description of such methods and their use with native and glycerinated monolayers of mouse

embryo fibroblast cells.

Chapter III

Comparison of Cell Growth on Silicon Monoxide and Conventional Substrata³

Studies with both the light microscope (Taylor, 1961; Weiss and Garber, 1952) and electron microscope (Westbrook et al., 1975) have demonstrated clearly that the morphology of cultured cells can change when cells are grown on different surfaces. It follows that if cell morphology is partially determined by the nature of the substratum, then other growth properties such as cell cycle parameters may also be influenced by the surface upon which the culture is grown. For this reason, particular attention was paid to developing a method which would allow comparison of the biochemical properties and ultrastructure of cells grown on the same material in all cases.

The choice of a substratum was severely restricted by the physical requirements of the freeze-fracture technique (Chapter V), which dictated that the substratum must be deposited onto the surface of Balzers specimen carriers in a thin, heat-conducting film. The material chosen for this purpose was silicon monoxide, which can be readily vacuum-evaporated as a thin, amorphous, silicate film (J. Murchio, personal communication). Collagen layers have also been used for this purpose (Pfenninger and Rinderer, 1975). However, use of collagen necessitates biochemical isolation procedures with their attendant risk of bacterial contamination, and collagen itself may not always be the ideal substratum

³Portions of the material described in this chapter have been published previously (Collins et al., 1974 and 1975).

for some lines of cells. This chapter describes the evaluation of the suitability of silicon monoxide as a substratum for the growth of cultured cells. These results include a comparison of the morphology of a number of different cell lines grown on silicon monoxide and Falcon plastic, as well as a careful evaluation of the effect of silicon monoxide on the growth parameters of Swiss 3T3 4A RK2 and Balb 3T3 A31 HYF cells, the two cell lines used for electron microscopy.

Materials and Methods

Cell culture. Swiss 3T3 4A RK2 cells were cultured as described in Chapter II. TC-7 African green monkey kidney cells (obtained from Dr. Helene Smith, Naval Biomedical Laboratories, Oakland, California), WI-38 human diploid lung fibroblasts (obtained from Dr. Leonard Hayflick of Stanford University at passage level 15; used at passage level 27), and NMuLi mouse liver epithelial cells (obtained from Dr. Robert Owens, Naval Biomedical Laboratories; Owens, 1974) were used without cloning. Balb/c 3T3 clone A31 mouse embryo fibroblasts were obtained from Dr. Helene Smith and cloned prior to use to give Balb 3T3 A31 HYF (hereafter referred to as Balb 3T3), the clone used in both light and electron microscopy experiments. The continuous line of MSV/MLV Balb 3T3 A31 HYF (hereafter referred to as MSV/MLV Balb 3T3) was obtained by infecting Balb 3T3 A31 HYF cells with the Moloney strain of murine sarcoma virus (MSV/MLV), obtained from Dr. Adeline Hackett of the Naval Biomedical Laboratories. Stocks of Balb 3T3 and MSV/MLV Balb 3T3 cells were frozen after cloning, and cells from each frozen vial were carried a maximum of two months after thawing. TC-7, WI-38, Balb 3T3, and MSV/MLV Balb 3T3 cells were grown in DME (GIBCO) containing 10% newborn calf

serum (GIBCO). NMuLi cultures were grown in minimal Eagle's medium (GIBCO; Eagle, 1959), containing 10% fetal calf serum (GIBCO) and 10 $\mu\text{g/ml}$ insulin (Schwartz-Mann, Orangeburg, New York). These cells were carried in 100 mm Falcon plastic dishes and were incubated at 37°C in a 10% CO₂ atmosphere. Cultures were judged free of mycoplasma by incorporation of ³H-thymidine (20.1 C/mM; New England Nuclear, Boston, Massachusetts) into the nucleus of cells but not the cytoplasm. Balb 3T3 cultures were also shown to be free of mycoplasma by scanning electron microscopy (Brown et al., 1974).

Secondary cultures of chick embryo fibroblasts (CEF) and CEF transformed with the Schmidt-Ruppin strain of Rous Sarcoma Virus (RSV-CEF) were prepared by the method of Bissell et al. (1974). Primary cultures of C3H murine mammary tumor epithelial cells (kindly prepared by S. Hamamoto, Cancer Research Laboratory, U. C. Berkeley) were grown in Waymouth's medium (Waymouth, 1959) containing 15% fetal calf serum (GIBCO), penicillin (Nutritional Biochemical Co., Cleveland, Ohio, 100 units/ml), streptomycin (NBC, 100 $\mu\text{g/ml}$), insulin (Sigma Chemical Co., St. Louis, Missouri, 10 $\mu\text{g/ml}$), and hydrocortisone (NBC, 5 $\mu\text{g/ml}$). Cells were incubated at 37°C in a 5% CO₂ atmosphere, fixed in Karnovsky's fixative (Karnovsky, 1965) and photographed in 0.1 M sodium cacodylate buffer, pH 7.3.

The growth curve of Swiss 3T3 4A RK2 cells on clean or silicon monoxide-coated dishes was determined by seeding 5×10^4 cells per 35 mm dish. Each day four coated and four uncoated dishes were removed and the number of cells per dish was determined by washing the culture with cold saline GM, incubating the monolayer for 10-15 minutes at 35°C with 2.0 ml of 0.01% trypsin (DIFCO) in isotonic Tris buffer (25 mM Tris

buffer, pH 7.4, containing 0.14 M NaCl, 5 mM KCl, and 0.7 mM Na₂HPO₄) and aspirating off the cells with a pipette. The suspended cells were then transferred to a test tube, 8.0 ml Isoton (Coulter Diagnostic Inc., Hialeah, Florida) were added to each sample, and 0.5 ml of the suspension was counted in a model Fn Coulter counter. The life cycle parameters of cells at their saturation density on coated and uncoated dishes were analyzed by flow microfluometry (Trujillo and Van Dilla, 1972). The growth of Balb 3T3 cells was determined using the same technique, except that cells were plated at 2×10^4 cells per 35 mm dish and were removed with 0.1% trypsin (GIBCO) in saline GM containing 0.5 mM EDTA. Doubling times were calculated from a computer least squares fit of the linear portion of the growth curve.

Vacuum coating. Vacuum coating with silicon monoxide was carried out in a Varian model VE-10 vacuum evaporator fitted with a 10 RPM rotating table and a liquid nitrogen trap. An automatic liquid nitrogen filling device was employed to keep the liquid nitrogen trap partially full at all times during operation, thus minimizing contamination from back-streaming diffusion pump oil. Small pieces of silicon monoxide (Ladd Research Industries, Burlington, Vermont) were placed in a tungsten wire basket situated 9 cm from the specimen. Evaporation was carried out for 20 seconds at a current of 18-20 amp and a vacuum less than 1.0×10^{-4} torr. Use of thinner coatings resulted in cracking and detachment of the coating after a few days in culture. A small square of tungsten cut from a tungsten boat was clipped over the top of the basket to prevent the hot silicon monoxide from flying out during evaporation. Balzers flat-topped specimen carriers were sonicated in acetone followed by absolute ethanol and petroleum ether before coating. For

photography of cells growing on Falcon plastic and silicon monoxide, a portion of each culture dish was masked during evaporation to provide an uncoated region, allowing comparison of cell growth on both substrata within the same dish. The brownish-yellow color of the silicon monoxide allowed the boundary of the coated area to be distinguished using phase contrast or conventional optics.

Light microscopy of cells grown on silicon monoxide coated substrata.

Swiss 3T3 4A RK2 cells were grown on coated and uncoated Balzers specimen carriers in 35 or 60 mm Falcon culture dishes. These cultures were prepared for microscopy either by fixation in cold trichloroacetic acid followed by a standard Giemsa stain, or by simultaneous fixation and staining in 1% Crystal Violet in 25% ethanol. Cells were photographed on Kodachrome II Professional Type A film using a Leitz Orthomat camera on an Ortholux microscope fitted with a 22X objective and a Leitz Ultrapac vertical illuminator system. Cells growing on transparent substrata (Falcon culture dishes, glass coverslips, and fragments from a bacterial culture dish [Lab-Tek Products, Westmont, Illinois]) were photographed without fixation or staining on Tri-X film using either a Nikon or a Zeiss inverted tissue culture microscope equipped with phase contrast optics. The results described in this section were based on 330 photographs of fixed and living cultures. Cultures were seeded, allowed to grow, and photographed at least twice, with the exception of MSV/MLV Balb 3T3, RSV-CEF, and the mammary tumor cells, which were grown and photographed only once.

Results

In order to evaluate the suitability of silicon monoxide as a sub-

stratum for cell culture, a comparison was made of the morphology of different cell lines growing on coated and uncoated areas of Falcon plastic culture dishes (Fig. 7). There was no visible difference in the density or morphology of Swiss 3T3 4A RK2 (Fig. 7, a and b), TC-7 (Fig. 7, c and d), WI-38 (Fig. 7, e and f), RSV-CEF (Fig. 7, k and l) or MSV/MLV Balb 3T3 cells (Fig. 7, o and p) growing on coated and uncoated areas of Falcon dishes. Cultures of Swiss 3T3 4A RK2 cells seeded at low and high density onto coated and uncoated glass coverslips (not shown) also appeared identical to those grown on Falcon plastic. NMuLi cells (Fig. 7, g and h) exhibited the same growth pattern on Falcon plastic and silicon monoxide, although the morphology on either substrate tended to vary between different areas of the same dish. Chick embryo fibroblasts (Fig. 7, i and j) exhibited a more criss-crossed growth pattern, a higher frequency of cell vacuoles, and more bare patches in the monolayer on silicon monoxide; however, cell density seemed to be roughly comparable on the two substrates. Murine mammary tumor cells (Fig. 7, m and n) appeared to grow to similar cell densities on either substrate, but exhibited more variability, less close packing, more spindle-shaped cells, and fewer domes (Pickett et al., 1975) on silicon monoxide. The morphology of Balb 3T3 cells (Fig. 7, q and r) was the same on both Falcon plastic and silicon monoxide. However, confluent cultures of Balb 3T3 cells growing on Falcon plastic produced large quantities of floating vesicular material (Fig. 7a, white refractile objects) while cultures of this cell line grown to confluency on silicon monoxide (Fig. 74) rarely produced much of this material.

In order to determine that cells were actually growing on the oxide

Figure 7. Cell growth on Falcon plastic (a,c,e,g,i,k,m,o,q) and silicon monoxide (b,d,f,h,j,l,n,p,r). a and b, Swiss 3T3 4A RK2 cells; c and d, TC-7 cells; e and f, WI-38 cells; g and h, NMuLi cells; i and j, secondary chick embryo fibroblasts; k and l, RSV-transformed chick embryo fibroblasts; m and n, primary mammary tumor cells; o and p, MSV/MLV transformed Balb 3T3 cells; q and r, Balb 3T3 cells. 100X.

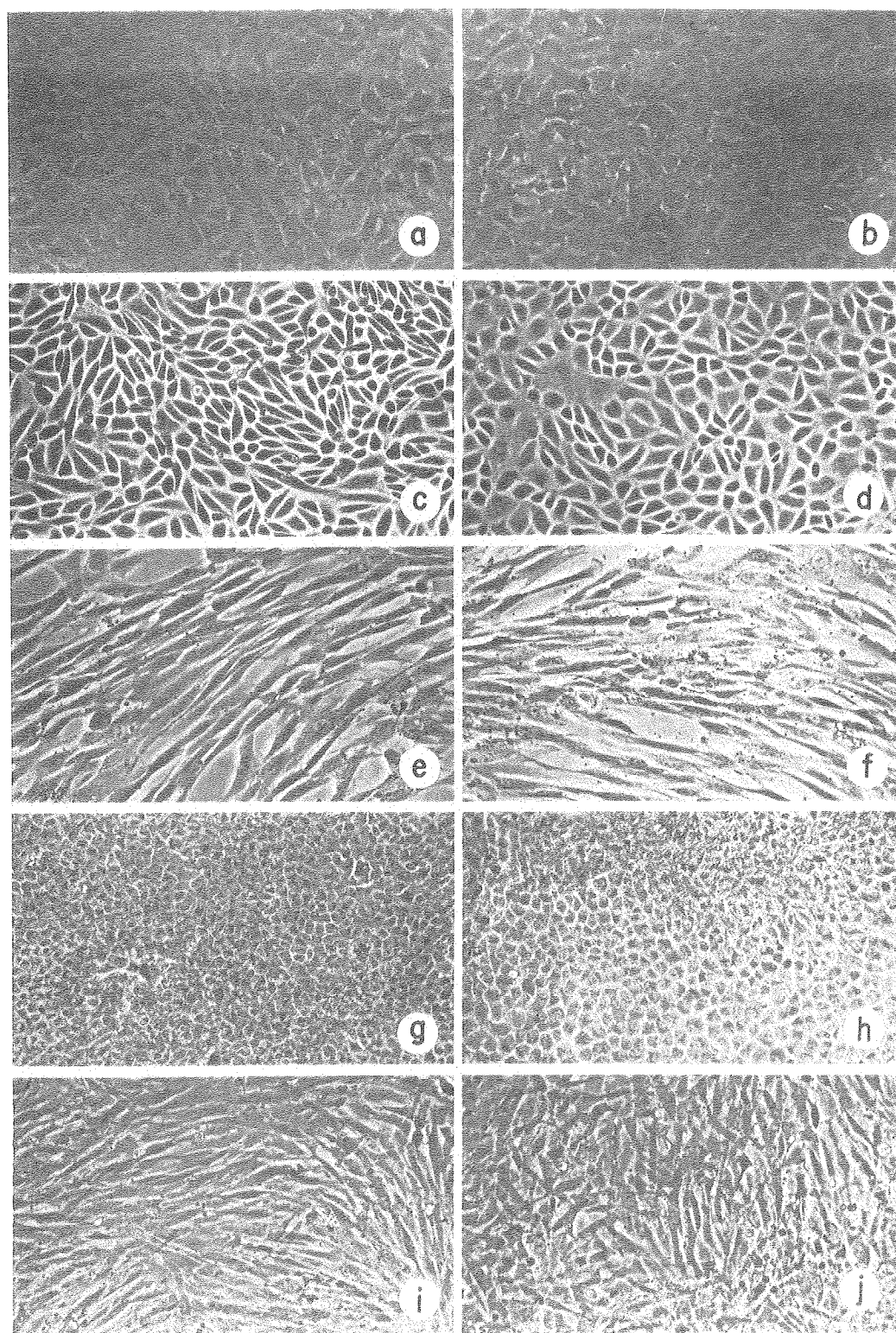


Fig. 7

XBB757 5027

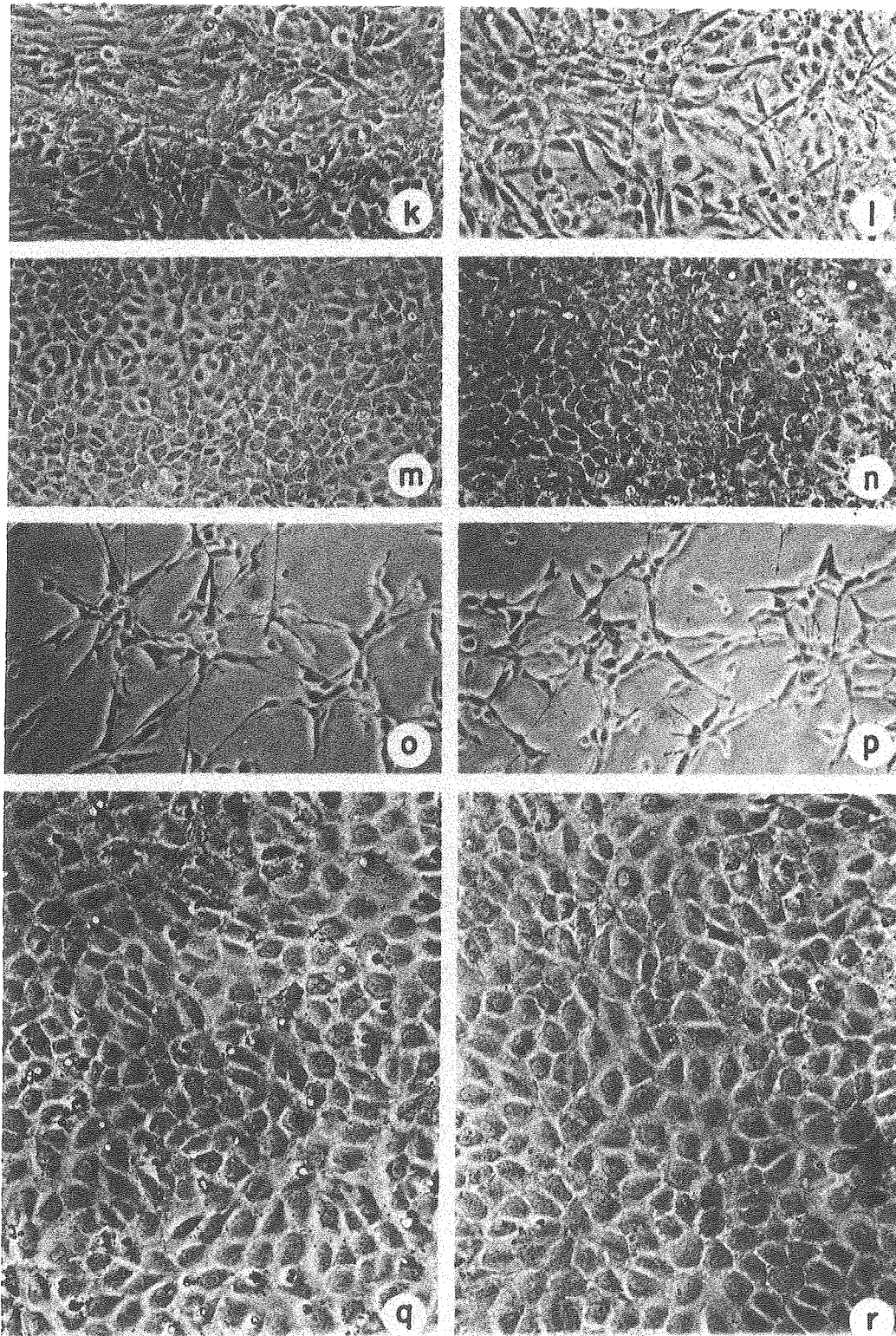


Fig. 7

XBB766 5241

coating, rather than on areas where the culture dish might be accessible through microscopic cracks or bare patches, Swiss 3T3 4A RK2 cells were grown on fragments from a Lab-Tek bacterial culture dish, a substratum which cannot support the growth of this line of cells (Fig. 8). While the cell layer on the coated areas of these fragments appeared normal, cells in uncoated areas were sparse and tended to grow in clumps. A sharp boundary could usually be seen between the coated and uncoated areas. Gentle agitation of the plastic fragment caused the cell layer in the clear patches to detach and roll up to the edge of the coated area. This result suggested that the Swiss 3T3 4A RK2 cells were weakly attached to this type of plastic, but had no difficulty in adhering to, and growing on, the silicon monoxide coating.

In similar experiments with coated and uncoated Balzers specimen carriers, Swiss 3T3 4A RK2 cells grew to confluency on both the silicon monoxide coat and the clean metal surface (Fig. 9). Although it was not possible to observe fine details of cell morphology with the vertical illumination system, both sparse and dense cultures growing on coated and uncoated specimen carriers appeared to have the same size and shape as those on Falcon plastic. Apparently, it might be possible to eliminate the silicon monoxide coating when using cell lines such as Swiss 3T3 4A RK2 which can be grown on metal. However, in experiments with cell lines which do not grow well on metal, or when it is necessary to compare results obtained using different ultrastructural and biochemical techniques, use of a coating such as silicon monoxide would be highly desirable.

To test whether the growth parameters of Swiss 3T3 4A RK2 cells on

Figure 8. Growth of Swiss 3T3 4A RK2 cells on uncoated and silicon monoxide-coated areas of a fragment from a Lab-Tek plastic culture dish. The fragment was masked during coating to produce a 3 mm circle of uncoated plastic. Note the dramatic change in the morphology of the cell layer at the boundary of the coated area. Cells formed a confluent sheet on the coated regions, but grew sparsely and tended to form clumps on the uncoated plastic. This culture was fixed and stained with 1% Crystal Violet in 25% ethanol. 115X.

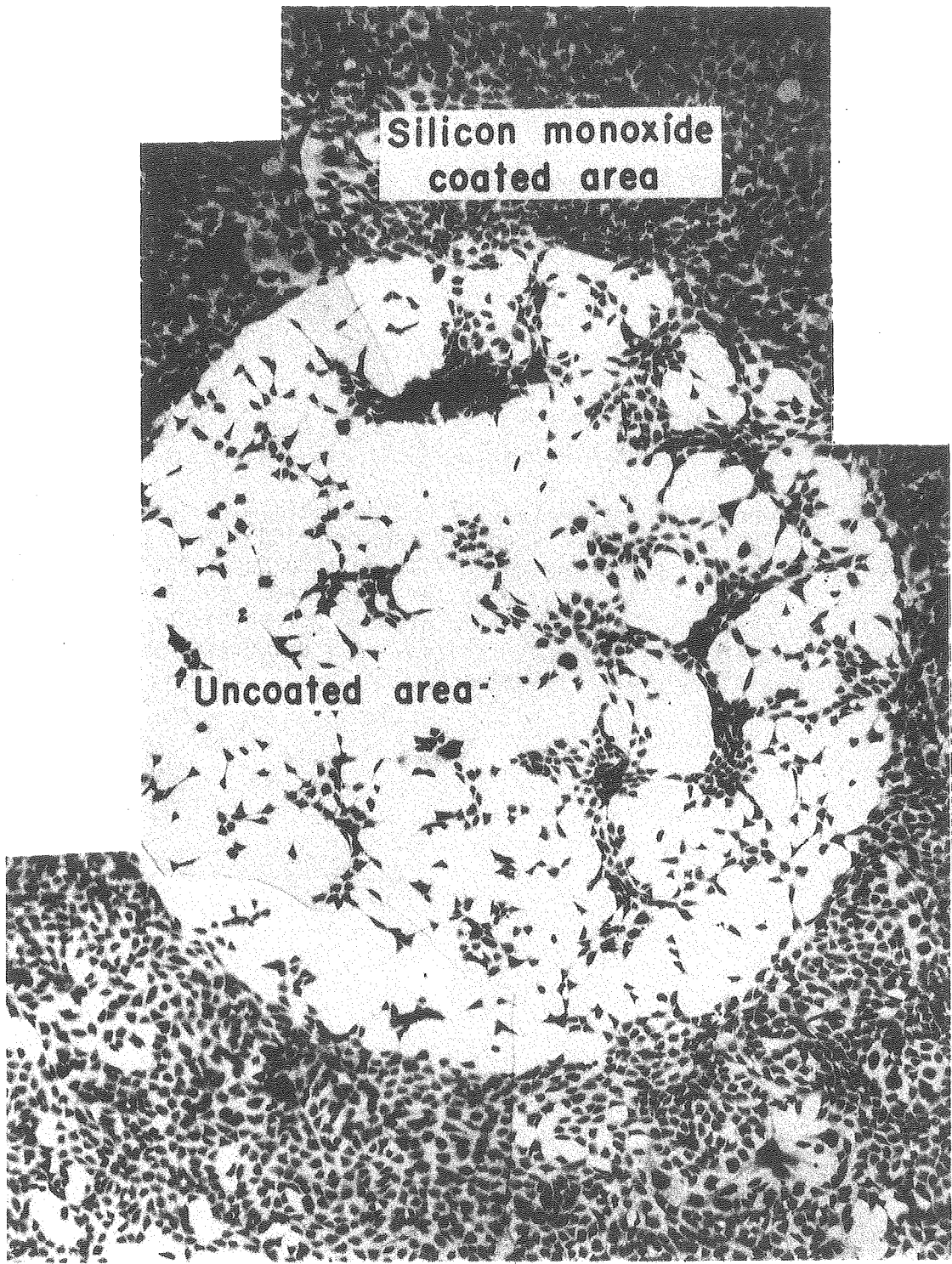


Fig. 8

XBB766 5240

Figure 9. Growth of sparse (a,b,c) and dense (d,e,f) Swiss 3T3 4A RK2 cells on Balzers specimen carriers and Falcon plastic. a and d, cells growing on silicon monoxide-coated carriers; b and e, cells growing on the clean metal surface of uncoated carriers; c and f, cells growing on the Falcon plastic dishes holding the carriers. All cultures were fixed and stained with 1% Crystal Violet in 25% ethanol. 130X.

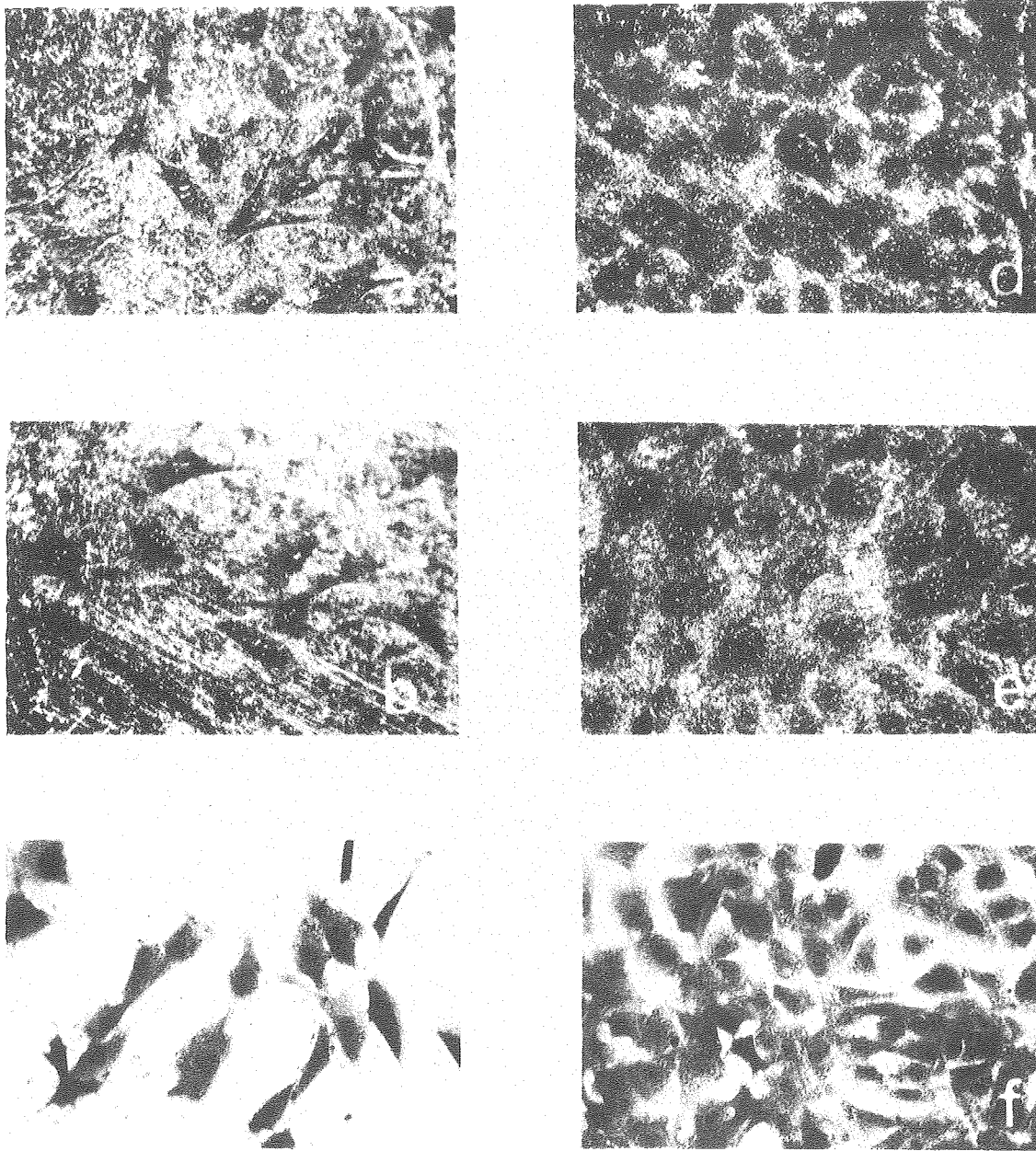


Fig. 9

XBB766 4859

silicon monoxide were any different from those of cells grown on standard Falcon dishes, the growth curve (Fig. 10), doubling time, and saturation density of Swiss 3T3 4A RK2 cells were determined as described in Materials and Methods. This cell line had a doubling time of 15 ± 2 hr. and a saturation density of 6.2×10^4 cells/cm² growing on both Falcon plastic and the silicon monoxide coating. At their saturation density, 95% of Swiss 3T3 4A RK2 cells grown on both coated and uncoated dishes had a DNA content equivalent to cells in the G₁ part of their life cycle. The increased scatter in the growth curve on silicon monoxide reflects the fact that in some cases these cells adhered so tightly to the silicon monoxide substrate that they were difficult to hose off the dish even after extensive (60 min.) trypsinization. Adhesion of the cells was a particular problem with the dishes counted at 48 hr. and probably caused the low cell density recorded at that time.

The strong attachment of 3T3 cells to silicon monoxide was particularly striking in the case of Balb 3T3 cultures. This clone, selected for its flatness and low cell density, adhered so strongly to silicon monoxide that the standard 15 min. trypsin treatment left most cells still firmly anchored to silicon monoxide, while causing extensive rounding up and detachment of cells grown on uncoated Falcon dishes (Fig. 11). Removal of Balb 3T3 cultures from silicon monoxide required extensive trypsinization, vigorous pipetting, or scraping of the dish with a rubber policeman. Furthermore, the silicon monoxide coating under dense Balb 3T3 cultures frequently began to crack and flake off after several days in culture. Flaking of the silicon monoxide was also noted with NMuLi cultures, but only occurred with thin (10 sec.)

Figure 10. Growth curve of Swiss 3T3 4A RK2 cells on silicon monoxide (. — . — .) and Falcon plastic (o — o — o). Error bars represent one standard deviation.

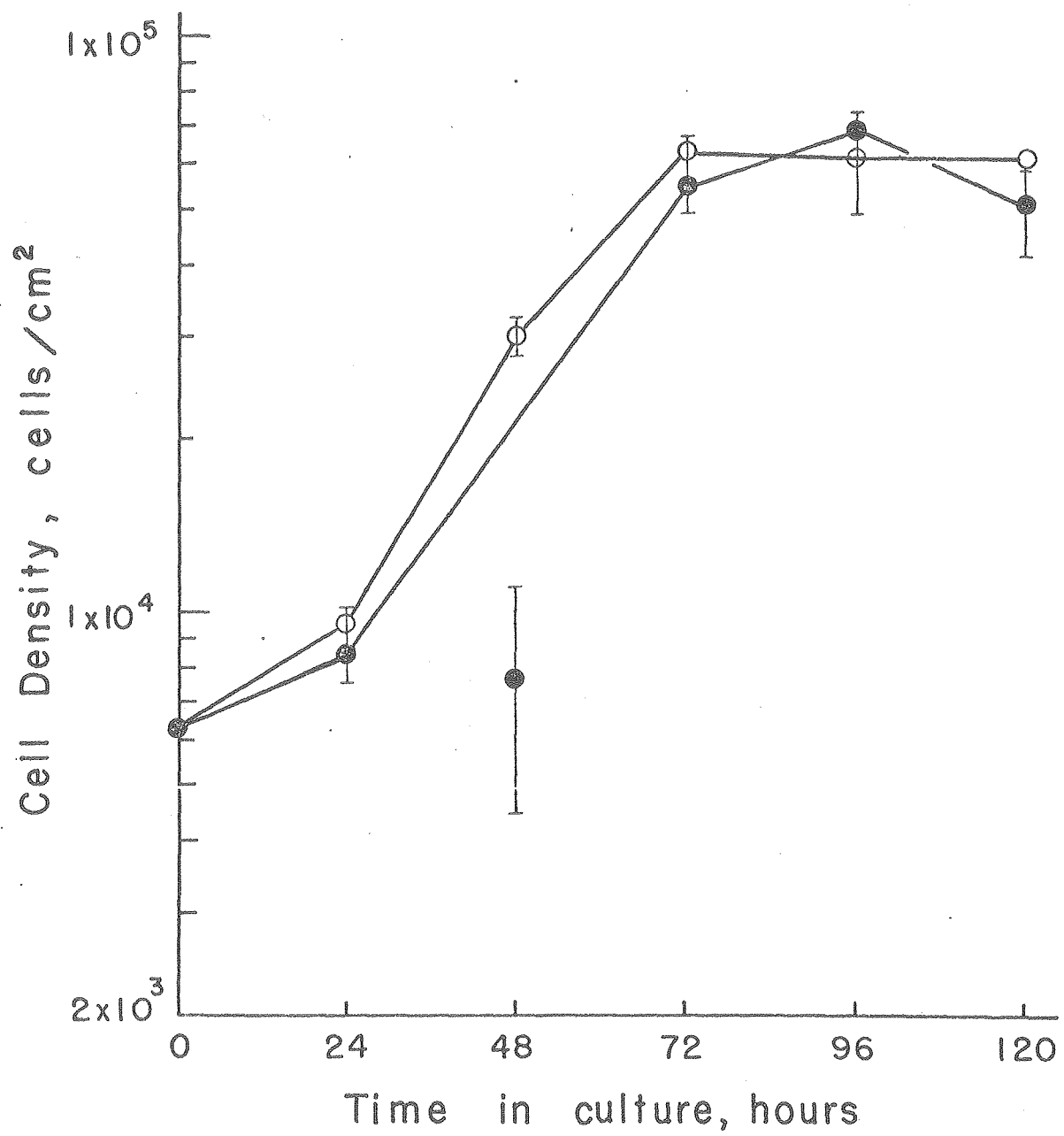


Figure 11. Balb 3T3 cells on Falcon plastic (a) and silicon monoxide (b) after 15 min. in 0.1% trypsin. In the uncoated dish, most of the cells have rounded up, and many have floated off into the medium. Cells growing on silicon monoxide, however, are only partially rounded, and remain anchored to the substratum by numerous filopodia. 130X.

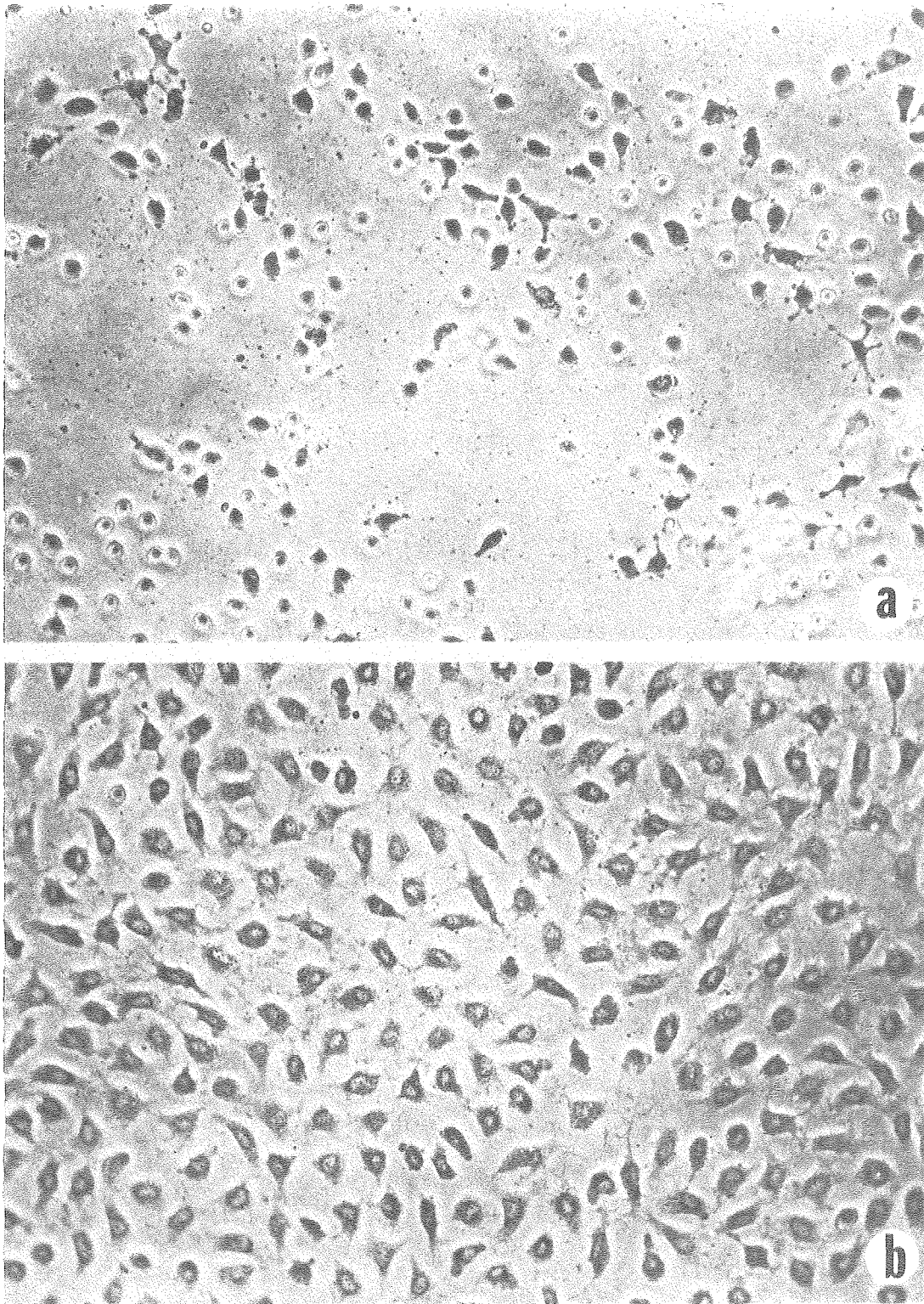


Fig. 11

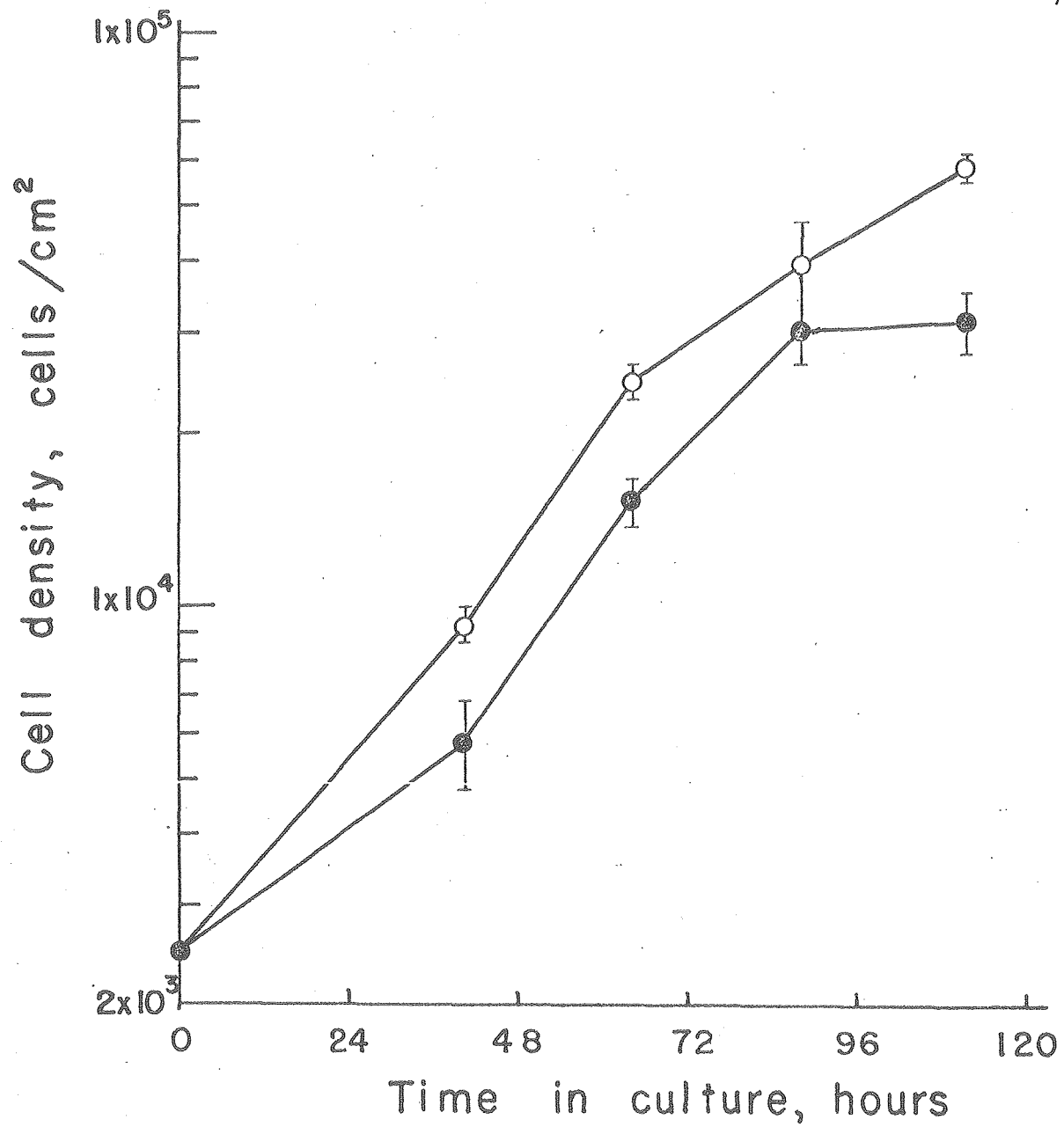
XBB766 5242

coatings and was not a problem when the standard 20 sec. coating was used. Since this problem was encountered only with Balb 3T3 and NMuLi cells, it seems likely that flaking occurred because these cells attached so strongly to silicon monoxide that the mechanical force exerted by the monolayer was sufficient to detach the coating from the underlying plastic. Presumably, thinner coatings would have less mechanical stability and could be peeled off more readily.

The adhesiveness of Balb 3T3 cells to silicon monoxide made determination of the growth curve (Fig. 12) extremely difficult. Removal of cells with a rubber policeman broke up the loose silicon monoxide into small fragments which were sucked through the aperture of the Coulter counter, resulting in very high apparent cell counts. For the growth curve, cells were therefore removed using a 60 min. trypsin treatment followed by vigorous pipetting. However, this treatment apparently caused cell lysis in older cultures, since the number of cells per sample decreased progressively with time in cultures more than 120 hr. old, even though such cultures appeared confluent and morphologically normal. In spite of these complications, the usable cell counts suggested that there was no significant difference between the doubling time of Balb 3T3 on Falcon plastic (23 ± 5 hr.) and silicon monoxide (20 ± 2 hr.).

Although reliable cell densities could only be obtained up to the point where cultures had just reached confluency, the data in Fig. 12 suggested that the saturation density of Balb 3T3 cells was significantly lower on silicon monoxide than on Falcon plastic. In order to confirm this result, the saturation density was determined in three further experiments. Although flaking of the silicon monoxide coating

Figure 12. Growth curve of Balb 3T3 cells on silicon monoxide (. — . — .) and Falcon plastic (o — o — o). Error bars represent one standard deviation.



caused problems with all of these determinations, it appeared that the saturation density of Balb 3T3 cultures grown on silicon monoxide was approximately half that obtained using Falcon plastic dishes. Since this difference in saturation density was probably due to the adhesiveness of Balb 3T3 to the coating rather than to any toxic effect of silicon monoxide itself, it should not influence results obtained with this cell line as long as the coating is employed in all experimental studies.

Discussion

The results presented here indicate that vacuum-deposited silicon monoxide is a useful substratum for the growth of a number of different types of fibroblastic and epithelial cells. The majority of these cultures (Swiss 3T3, TC-7, WI-38, NMuLi, RSV-CEF, and MSV/MLV Balb 3T3) showed no alteration in cell morphology at the light microscope level as a result of growth on silicon monoxide. Furthermore, the saturation density, doubling time, and fraction of G₁-blocked cells at confluency for Swiss 3T3 4A RK2 cultures grown on silicon monoxide were identical to those for cultures grown in Falcon plastic dishes. These data suggest that silicon monoxide and Falcon plastic have an equivalent effect on this line of cells. Those cultures that showed some alteration in morphology or growth properties (CEF, murine mammary tumor cultures, and Balb 3T3 cells) still appeared to grow well on the coating. The fact that morphological changes did occur when cultures were grown on different surfaces emphasizes the importance of using the same substratum whenever results from different techniques are to be compared.

The main problem encountered with this coating was that of the flaking which occurred with strongly-adhering cell lines. It may be

possible to minimize this problem by using thicker coatings than those employed in this study; alternatively, a different substratum may have to be used with such cultures.

The silicon monoxide coating itself has several advantages. After coating, petri dishes, carriers, and coverslips can be sterilized by ultraviolet light or by heating to 132°C without any apparent change in the oxide layer. The coating has excellent optical properties, and is unaffected by any of the reagents or procedures employed in preparing tissues for freeze-fracture, thin sectioning, or scanning electron microscopy (see Chapters IV-VI). There was no evidence of toxicity from the silicon monoxide with any of the cell lines used. These results suggest that the ability to coat culture vessels routinely with silicon monoxide should allow comparison of the biochemical properties and ultrastructure of cells grown under identical conditions.

Chapter 4

Morphology of Balb 3T3 Monolayers: Studies with High Resolution Scanning Electron Microscopy

Since freeze-cleavage often produces a complex arrangement of membrane fracture faces, interpretation of the results of in situ freeze-fracture studies required an understanding of the morphology of 3T3 cells growing on silicon monoxide. For this reason, monolayers of Balb 3T3 cells were examined using a high resolution scanning electron microscope, with special emphasis being given to the study of cellular interactions. The increased resolution of high resolution scanning electron microscopy (HRSEM) allowed the structure of cell interactions to be studied at high magnification. Previous studies on cultured fibroblasts (Boyde et al., 1972; Porter et al., 1973) have employed conventional scanning electron microscopy (SEM) and therefore have been limited to examination of gross surface structures such as blebs, microvilli, and ruffles.

Materials and Methods

Preparation of cultures for critical point drying. 3T3 cell cultures were grown to confluency as described in Chapter 3 either on Balzers specimen carriers or on 15 mm diameter #2 coverslips coated with silicon monoxide and placed in the bottom of Falcon plastic dishes. Preliminary observations were carried out with Swiss 3T3 4A RK2 cells, but this cell line was found to be contaminated by mycoplasma (Brown et al., 1974) and was discarded in favor of the Balb 3T3 cell line.

In the initial preparations, cultures were fixed with paraformaldehyde-glutaraldehyde (Chapter 2) and heavily impregnated with osmium

using the thiocarbohydrazide technique of Kelley et al. (1973). Osmicated cultures were then dehydrated and critical point dried. However, use of fixatives with a high osmolality has been shown to cause shrinkage of both retinal tissue (Rasmussen, 1974) and cultured fibroblasts (Boyde and Vesely, 1972). The optimum fixative appears to be one in which a vehicle (defined as the buffer plus added metal ions and/or sucrose) isotonic with the culture medium is combined with a moderate concentration of glutaraldehyde (Boyde and Vesely, 1972; Brunk et al., 1975; Rasmussen, 1974). For this reason, the use of the paraformaldehyde-glutaraldehyde fixative was discontinued. Heavy osmication with thiocarbohydrazide was also abandoned, as this technique proved to be time-consuming and did not prevent charging at high accelerating voltages.

The procedure used to prepare Balb 3T3 cells for morphological studies involved first washing the monolayers three times with HEPES-DME (DME without bicarbonate, phenol Red, or vitamins, but with 100 mM HEPES buffer [Sigma] added to maintain pH; see Chapter 7). Cells were then fixed for 60 min. in 2% glutaraldehyde (Polysciences Inc., Warrington, Pennsylvania) containing 0.1 M phosphate buffer, 12 mM sucrose, and 0.14 mM $\text{CaCl}_2 \cdot 2\text{H}_2\text{O}$. Use of this fixative was suggested by Dr. K. H. Pfenninger. Culture dishes and solutions were maintained at 37°C in a water bath during washing and fixation. Each dish was washed three times at room temperature in 0.15 M phosphate buffer containing 0.14 mM $\text{CaCl}_2 \cdot 2\text{H}_2\text{O}$, and postfixed for 60 min. at room temperature in 1% osmium tetroxide (Fisher Scientific Co., Fairlawn, New Jersey) containing 0.1 M phosphate buffer. The fixed monolayers were then washed three times in glass-distilled water at room temperature and dehydrated for critical point drying.

Each solution was gradually replaced by the next one to minimize osmotic shock to the cells. The HEPES-DME, 2% glutaraldehyde, and 0.15 M phosphate buffer had a pH of 7.0 - 7.3 at the temperature employed. Osmotic concentrations of these solutions were as follows: HEPES-DME, approximately 300 mosmol/kg; glutaraldehyde, 560 mosmol/kg; fixative vehicle (buffer + sucrose + CaCl_2), 340 mosmol/kg; 0.15 M buffer, 320 mosmol/kg.

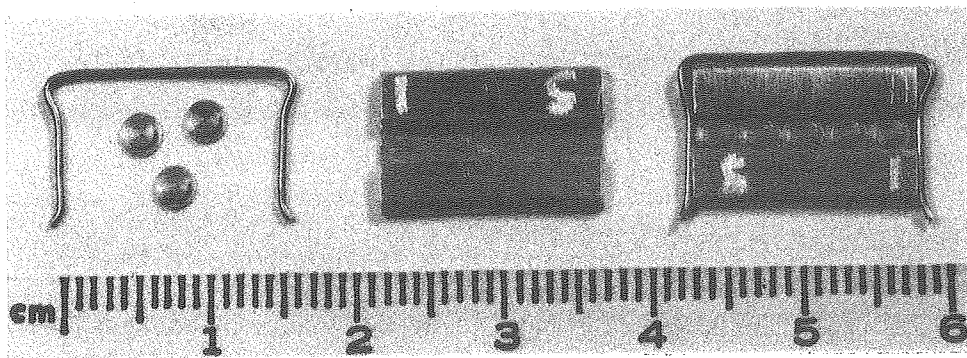
Critical point drying and scanning electron microscopy. Monolayers of Balb 3T3 cells proved difficult to critical point dry without air drying artifacts. Initially, all specimens were dehydrated through a graded ethanol series (5 min. each in 25%, 50%, 70%, and 95% ethanol in distilled water, followed by two 5 min. immersions in 100% ethanol) and then through a series of solutions of Freon TC (E.I. duPont de Nemours Co., Wilmington, Delaware) in ethanol (5 min. each in 25%, 50%, and 75% Freon TC, followed by two 5 min. immersions in 100% Freon TC). Specimens were then transferred from Freon TC to a critical point drying chamber of the type described by Cohen et al. (1968) and critical point dried from Freon 13.

Serious difficulties were encountered in all attempts to use this method in preparing cultures grown on Balzers specimen carriers. Cells were invariably flattened by air drying which occurred between removal of the specimens from Freon TC and the time when the chamber could be closed and filled with Freon 13. Also, the carriers were often blown about during filling, resulting in severe damage to the cell layer. Several small aluminum clips were constructed, each holding five carriers; these kept the specimens from blowing about but did not prevent air drying.

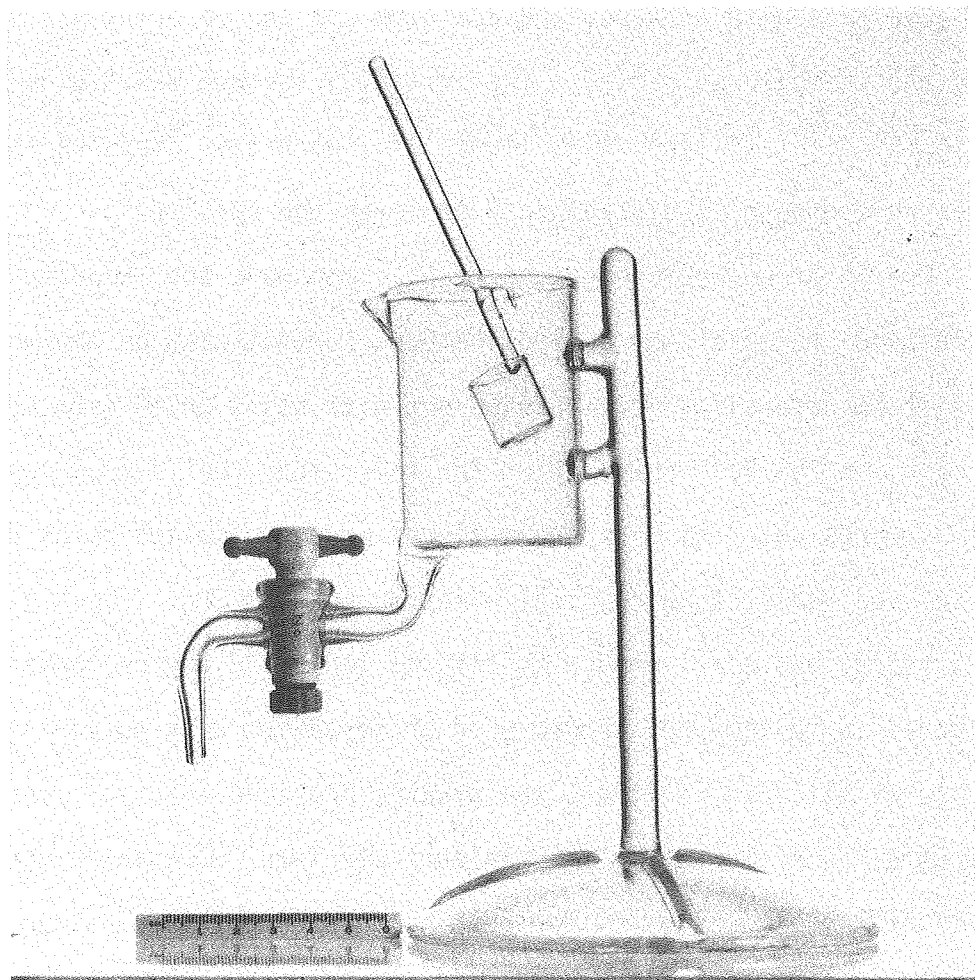
Cultures grown on round glass coverslips proved somewhat easier to dry. The coverslips were held in a stack approximately 1 mm apart by inserting them into a small stainless steel spring; this stack of coverslips was then processed through the dehydration and drying steps (M. K. Nemanic, personal communication). Evaporation of Freon TC during transfer could be minimized by using liquid nitrogen to cool the beaker containing the specimens until the Freon began to solidify, and by insuring that the drying chamber was as cold as possible before specimen transfer (Lewis and Nemanic, 1973). Cells dried in this manner showed some collapse of the microvilli, but were usable for morphological studies. Apparently, enough Freon was held between the stacked coverslips to prevent air drying during transfer.

Good preservation of cell monolayers on Balzers specimen carriers was finally achieved by use of a technique which completely eliminated any exposure of the specimens to air during dehydration, transfer, and filling of the chamber. Carriers were placed into small aluminum clips (Fig. 13a) and dehydrated through a graded acetone series (5 min. each in 50%, 70%, 80%, 90%, and 95% acetone in distilled water followed by two 5 min. immersions in 100% acetone). Solution exchanges were made in a small glass vessel with a drain at the bottom (Fig. 13b). Using this apparatus, solutions were changed by draining off one step in the series, leaving only enough liquid to cover the specimens, and then pouring the next step gently down the side of the vessel. Dehydrated specimens were then placed into a small glass ladle (Fig. 13b) inserted under the surface of the liquid, and transferred in the ladle to the drying chamber.

Figure 13. Apparatus for critical point drying of cell monolayers. Cultures growing on Balzers specimen carriers were held in small aluminum clips (a) which were then placed in the bottom of the dehydration vessel (b). Specimens remained immersed in liquid until dehydration was completed, then were transferred to the drying bomb using the glass ladle. In this way, specimens could be dehydrated and critical point dried without risk of drying artifacts resulting from exposure to air.



a



b

Fig. 13

XBB766 5442

Critical point drying from CO_2 was carried out in a Polaron critical point drying chamber (Polaron Instruments Corp., Line Lexington, Pennsylvania). Unlike the device used for critical point drying from Freon, this apparatus was equipped with a drain at the bottom and a viewing port in the side of the chamber. These features made it possible to observe the liquid level while draining the chamber, so that specimens could be transferred by filling the apparatus with acetone, immersing the ladle bearing the specimens under the surface of the liquid, removing the specimens with forceps, and draining off the majority of the liquid once the chamber was closed. The remaining acetone was flushed out before drying by eight fillings with liquid CO_2 , each time draining the chamber until only enough liquid remained to cover the specimens.

The 15 mm coverslips proved fragile and were too large to sit on the curved bottom of the drying chamber, so that most of the morphological studies on coverslips were carried out with cells dried from Freon 13. However, in the last preparation for this study, cells grown on coated 1 cm squares cut from microscope slides were dehydrated using the glass vessel and ladle, then critical point dried from CO_2 . The glass squares were sturdy and small enough to fit the ladle and drying chamber. Cells prepared in this manner showed good preservation with no apparent collapse of microvilli. In addition, the squares provided a larger specimen area and were easier to handle than Balzers carriers. Combining the use of small coated glass squares for cell culture with the techniques described here for dehydration and drying from CO_2 probably represents the most satisfactory method of preparing critical point dried cell monolayers for scanning electron microscopy.

After critical point drying, specimens were mounted on aluminum stubs and vacuum coated with platinum-carbon using a standard Balzers electrode with 10 cm of 0.1 mm platinum wire. Specimens were observed in a Coates and Welter model 100 field emission scanning electron microscope equipped with a high resolution photography monitor, and photographed on 4 x 5 in Tri-X or Ilford type FP4 film. Ilford film had a greater latitude and proved to be superior for recording SEM images. The morphological studies described in this chapter were made using two preparations of Balb 3T3 cells. Conclusions regarding gross cell morphology were derived from photographs at intermediate magnification (2500X - 6000X on the print) of 35 individual cells. Representative regions of cellular interaction were selected and photographed at high magnification (20,000X - 120,000X). In all, high magnification photographs of such regions included portions of the edges of 32 cells. The data also included numerous photographs taken at various magnifications on Polaroid type 52 film.

Results

Cell growth on Balzers specimen carriers. HRSEM observations at low magnification confirmed that Balb 3T3 cells grew to confluency on the surface of silicon monoxide-coated Balzers carriers (Fig. 14). However, because of the requirements of the freeze-fracture technique (Chapter 5), carriers used for growth of Balb 3T3 cultures had their upper surfaces ground flat with boron carbide/diamond or aluminum oxide optical grinding compounds. This treatment left the surface quite rough (Fig. 15), and secondary electron emission from this surface passed up through the monolayer, producing a mottled background pattern which ob-

Figure 14. Confluent culture of Balb 3T3 cells growing on a Balzers carrier coated with silicon monoxide. 100X.

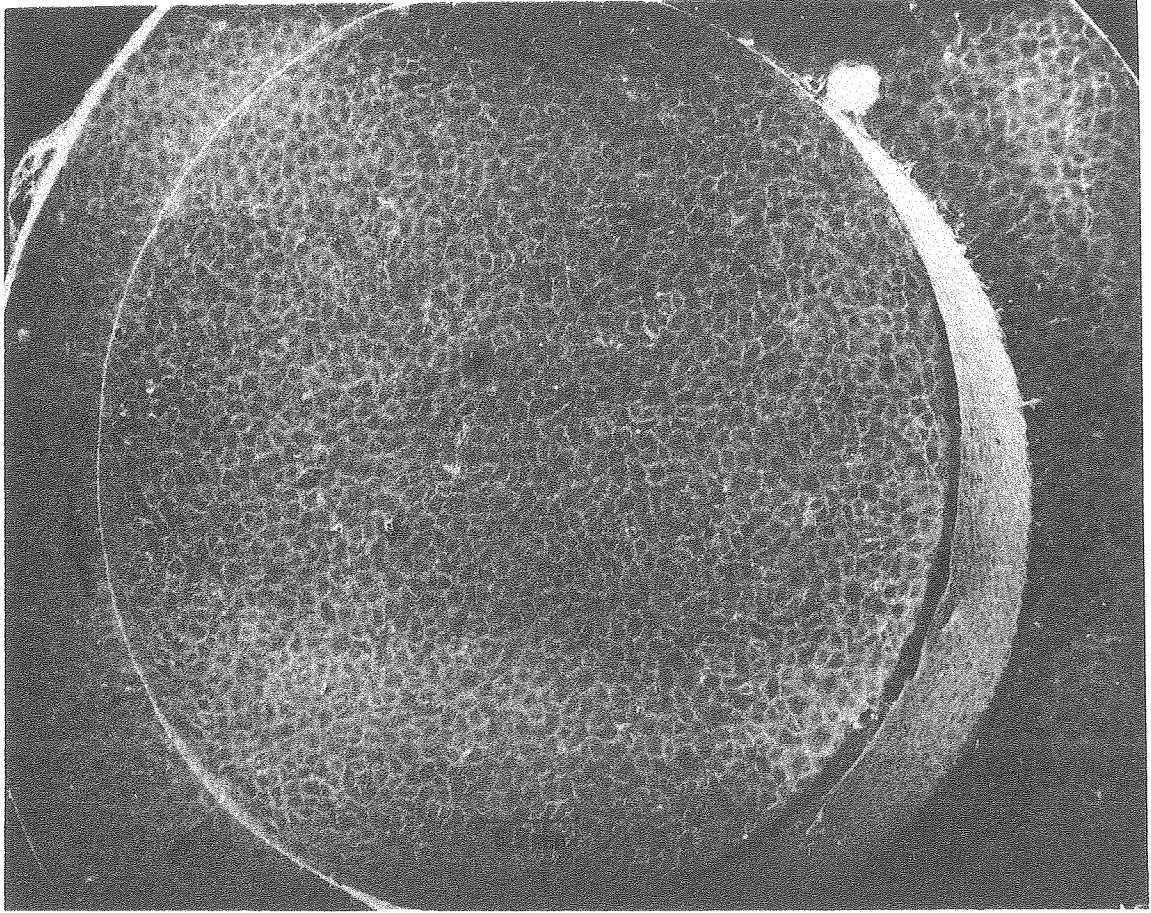


Fig. 14

XBB767 6498

Figure 15. Surface of Balzers flat-topped specimen carrier after grinding with 800 mesh boron carbide followed by 6 μm and 1 μm diamond paste. 5400X.

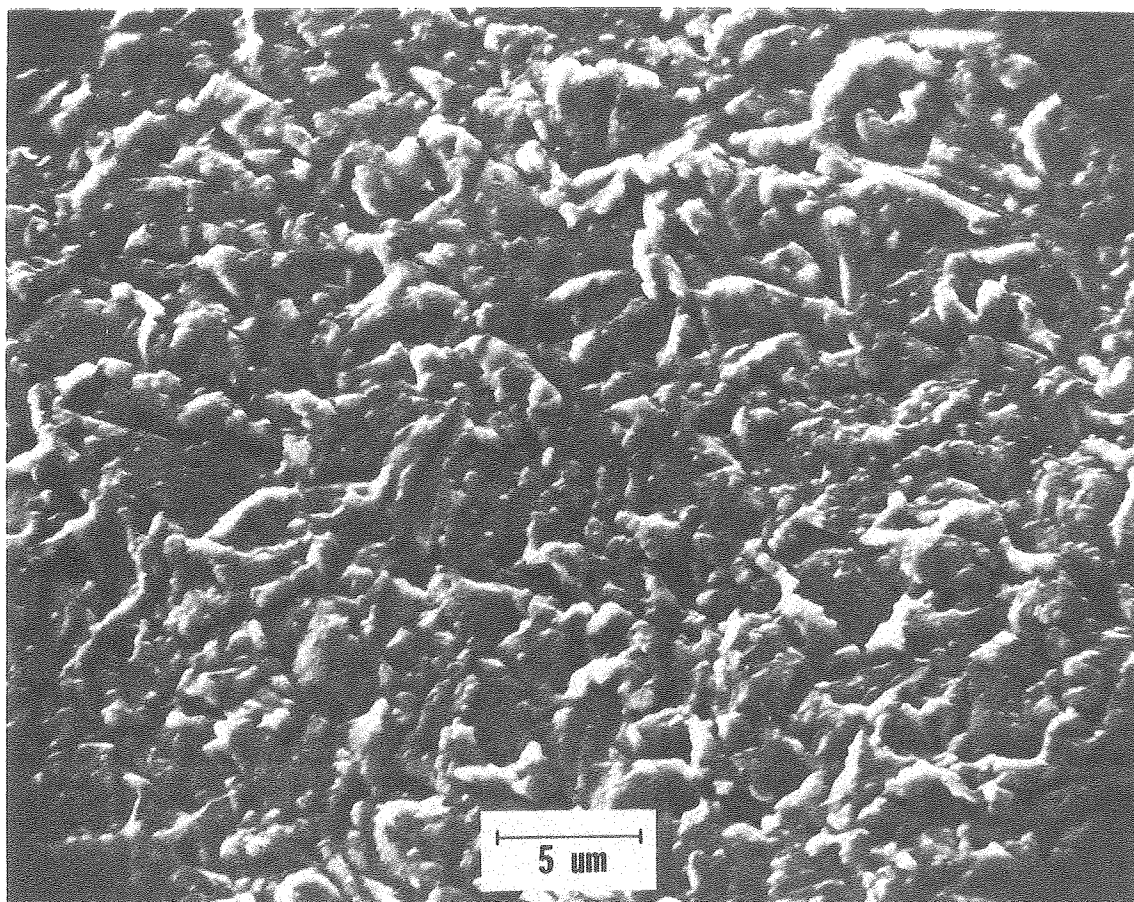


Fig. 15

XBB767 6518

scured many cellular details. Background interference was particularly troublesome at the magnifications used for examination of single cells (Fig. 16); however, it was possible to obtain some morphological information from such preparations.

Balb 3T3 cells in confluent culture appeared as flattened polygons approximately 40 μm in diameter, with varying numbers of microvilli 0.1 μm in diameter on the upper cell surface. The peripheral regions of these cells produced large numbers of filopodia measuring 0.05 - 0.1 μm in diameter, and up to 20 μm in length. In general, short processes arising from the upper surface of the cell were described as microvilli, while longer processes extending out of the edge of the cell were classed as filopodia. However, these two groups were not mutually exclusive, and near the cell periphery there were some processes which could have been put in either class. Filopodia frequently extended over the upper surface of neighboring cells, where they came in contact with microvilli, other filopodia, and the cell surface itself. Each cell appeared to interact with its neighbors around the whole cell periphery, but the nature of these associations was difficult to determine because of background interference. At magnifications above 10,000X (measured on the final print), the background pattern was less noticeable, and it became apparent that, in addition to filopodial contacts, there was considerable overlap between the thin peripheral regions of neighboring cells (Fig. 17). These observations were in agreement with the studies of Porter et al. (1973) on clone A31 of Balb 3T3, except that the cells used here seemed to have fewer surface microvilli than those used by Porter et al. In view of the difficulties presented by background interference, the majority of the morphological studies on Balb 3T3 were

Figure 16. Scanning electron micrograph of a typical cell from a confluent culture of Balb 3T3 cells growing on a flat-ground, silicon monoxide-coated Balzers specimen carrier. The area within the rectangle is shown at higher magnification in Fig. 17. Fil, filopodia; Mv, microvilli. 2700X.

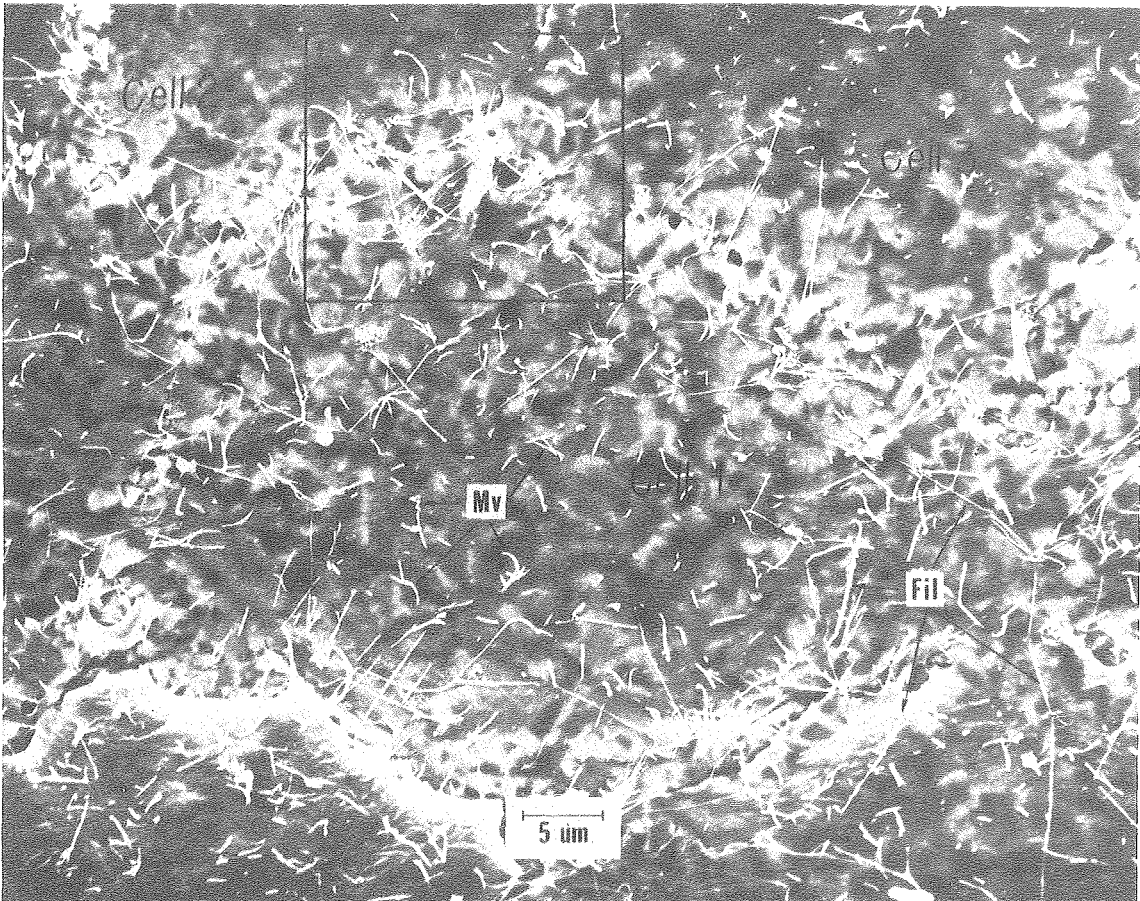


Fig. 16

XBB767 6497

Figure 17. Higher magnification view of Fig. 16, showing the area of interaction between three cells. At this magnification, the mottling effect of electron emission from the uneven substratum is less noticeable, and the details of cellular interaction become apparent. Cell 3 overlaps both Cell 1 and Cell 2, and the filopodia of Cell 2 interact with those of Cell 3 (arrowheads). Fil, filopodia; Mv, microvilli. 12,000X.

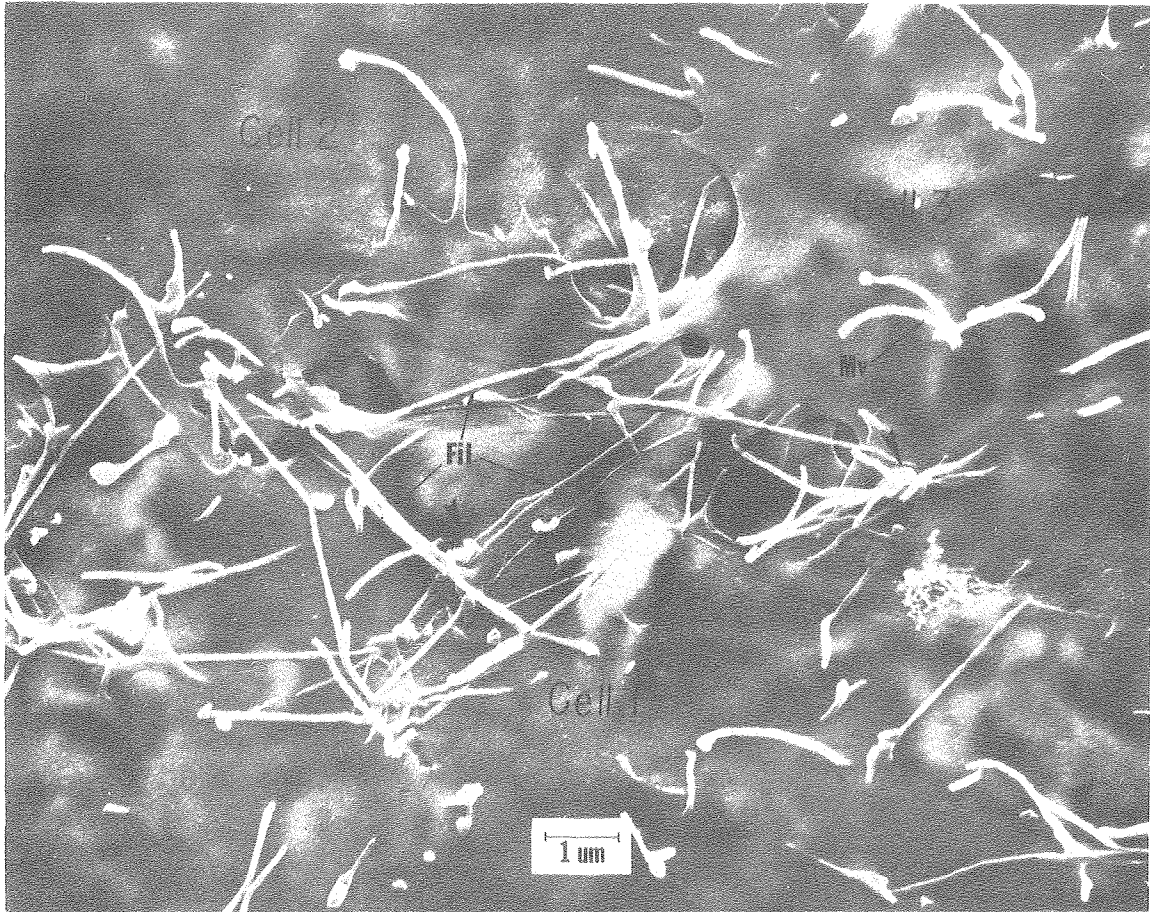


Fig. 17

XBB767 6496

carried out using monolayers grown on coverslips. The problems associated with grinding Balzers carriers are discussed further in Chapter 5.

Cell growth on coated glass coverslips. The appearance of typical Balb 3T3 cells grown on silicon monoxide-coated glass coverslips and critical point dried from Freon 13 is shown in Figs. 18 and 19. Cells were similar in size and shape to those grown on Balzers carriers. The cell nucleus could be seen as a slightly depressed central area 15 - 20 μm in diameter. Within each nuclear region appeared the outlines of several rounded structures approximately 1.7 μm in diameter; such structures were presumed to represent nucleoli. The majority of organelles were located in the central portion of the cell, leaving a peripheral zone which has been shown to contain mostly microfilaments and free ribosomes (Cherny et al., 1975). The majority of cell interactions seemed to occur within this peripheral region.

Cell interactions could be grouped into four general classes: interactions involving filopodia, edge-to-edge contacts, simple overlap, and interdigitation (Figs. 18-22). The morphology of interactions involving filopodia was highly variable, ranging from the simple contact of a filopodium on one cell with the surface of a neighboring cell to complex tangles where it was often impossible to determine the point of origin of a given filopodium (Fig. 20). Edge-to-edge contacts (Figs. 18 and 21) occurred where the edges of cells approached and adhered to each other but did not overlap to any significant extent. Simple overlapping of one cell by its neighbors (Figs. 18, 19, and 21) occurred extensively and probably involved more of the cellular surface area than any of the other interactions (see Chapter 6). Finally, cells were described as interdigitating when two opposing cell edges put forth short

Figure 18. Low-magnification scanning electron micrograph of a confluent culture of Balb 3T3 cells growing on a silicon monoxide-coated coverslip. The majority of organelles appear to be restricted to the central area around the nucleus (N), leaving an organelle-free peripheral zone (P). Cellular interactions vary from simple overlap (O) or edge-to-edge contacts (E) to complex tangles of filopodia (F). The spherical bodies within the nucleus are presumed to be nucleoli (Ni). The area within the rectangle is shown at higher magnification in Fig. 19. 1000X.

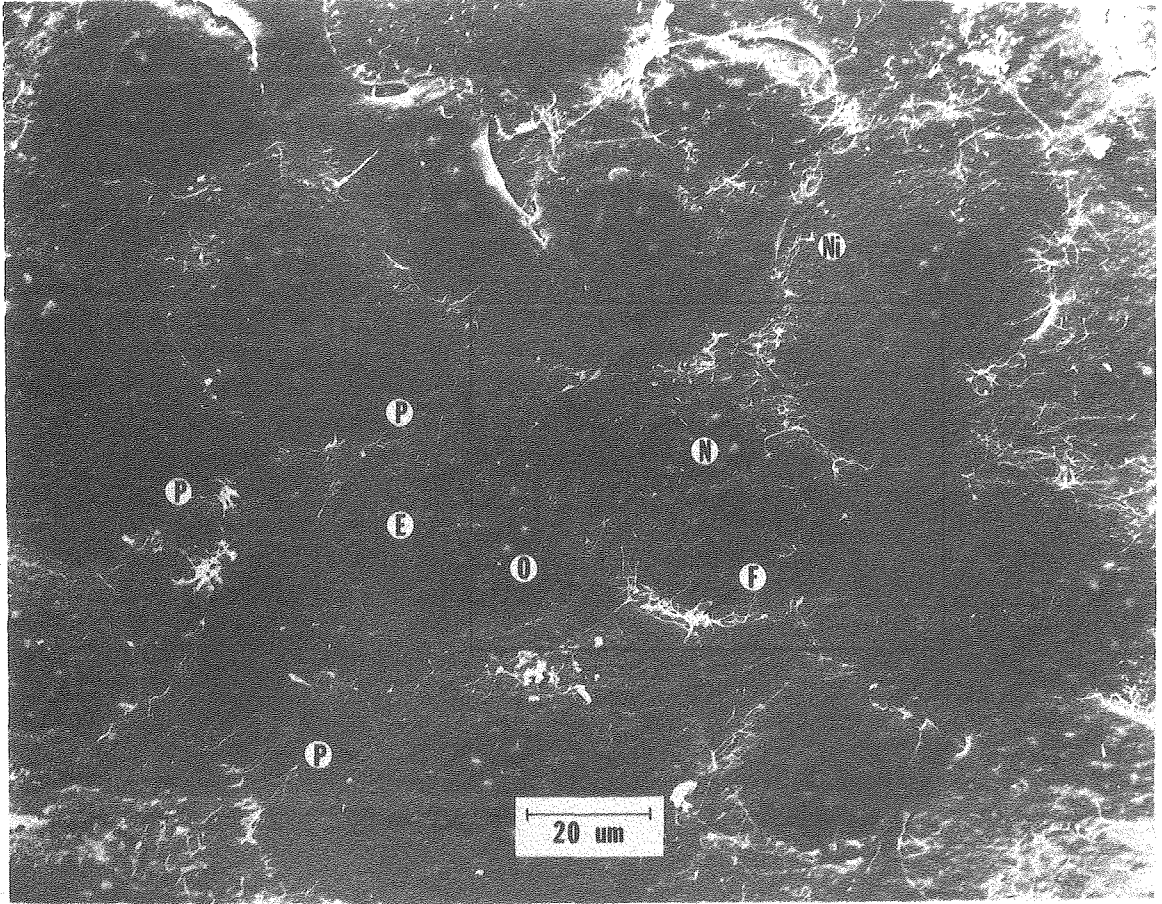


Fig. 18

XBB767 6506

Figure 19. Higher magnification view of Fig. 18, showing a typical Balb 3T3 cell (Cell 1) and its interactions with neighboring cells (Cells 2-6). Simple overlap (O) occurs between Cell 5 and Cell 6, Cell 4 and Cell 1, and Cell 4 and Cell 3. A region of interdigitation (I) can be seen where the edges of Cell 1 and Cell 6 come into contact. Complex filopodial interactions (F) occur between Cell 1 and Cells 3 and 5. The areas marked 1, 2, and 3 are shown at higher magnification in Figs. 20, 21, and 22, respectively. N, nucleus; Ni, nucleoli. 3000X.

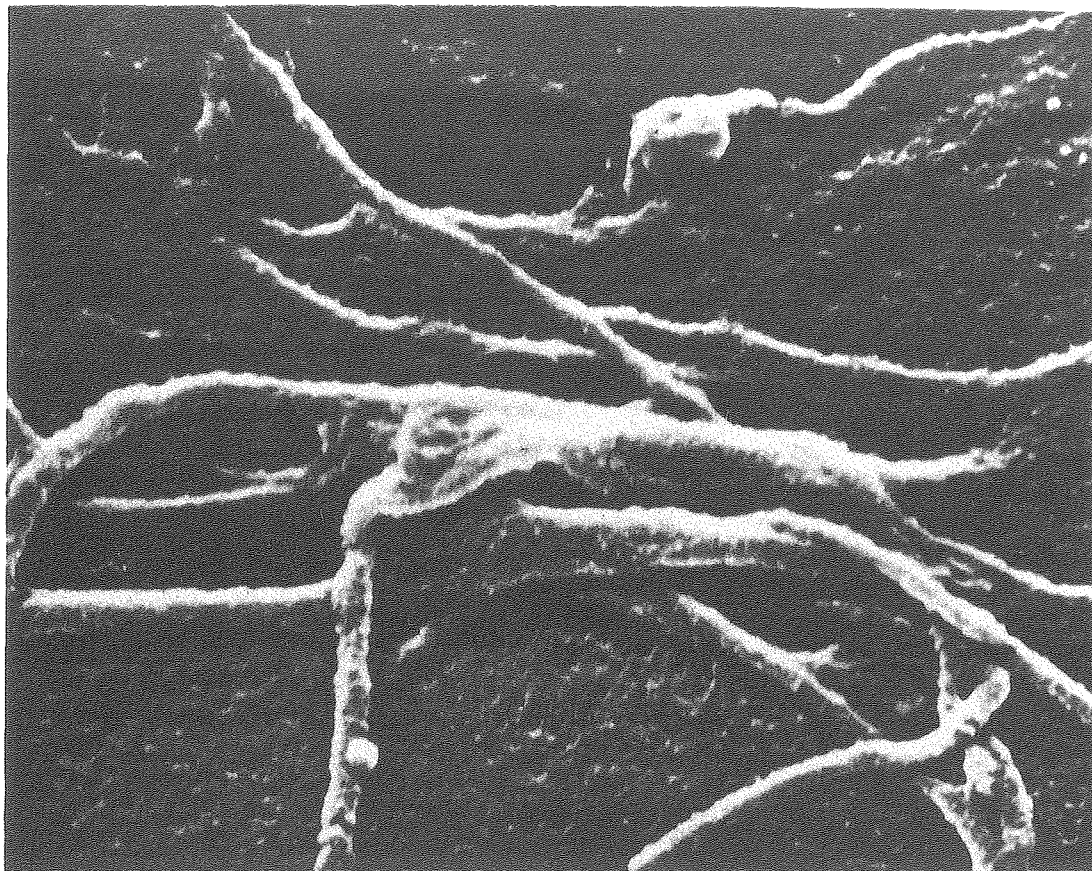


Fig. 19

XBB767 6516

Figure 20. Higher magnification view of Fig. 19, showing a region of complex filopodial interaction between Cell 1 and Cell 5. V, vesicular stomata. 12,000X.

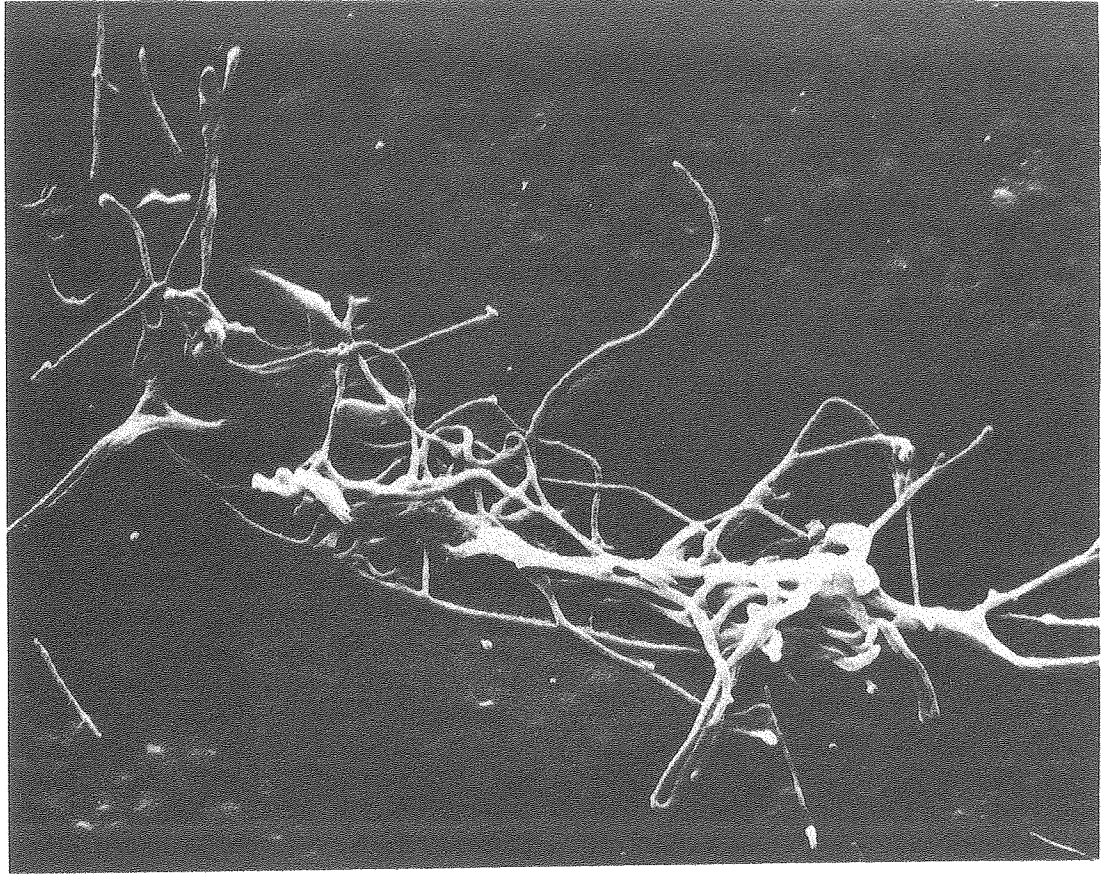


Fig. 20

XBB767 6513

Figure 21. Higher magnification view of Fig. 19, showing interactions between Cells 1, 5, and 6. Cell 5 has extended a process (arrow) which overlaps the edge of Cell 6. Numerous small adhesions (arrowheads) appear to bind the surfaces of the two cells together in this region. Two edge-to-edge contacts (E) occur between Cells 1 and 5. Part of a complex tangle of filopodia (F) is also visible in this micrograph. Mv, microvilli; SM, silicon monoxide substratum; V, vesicular stomata. 12,000X.

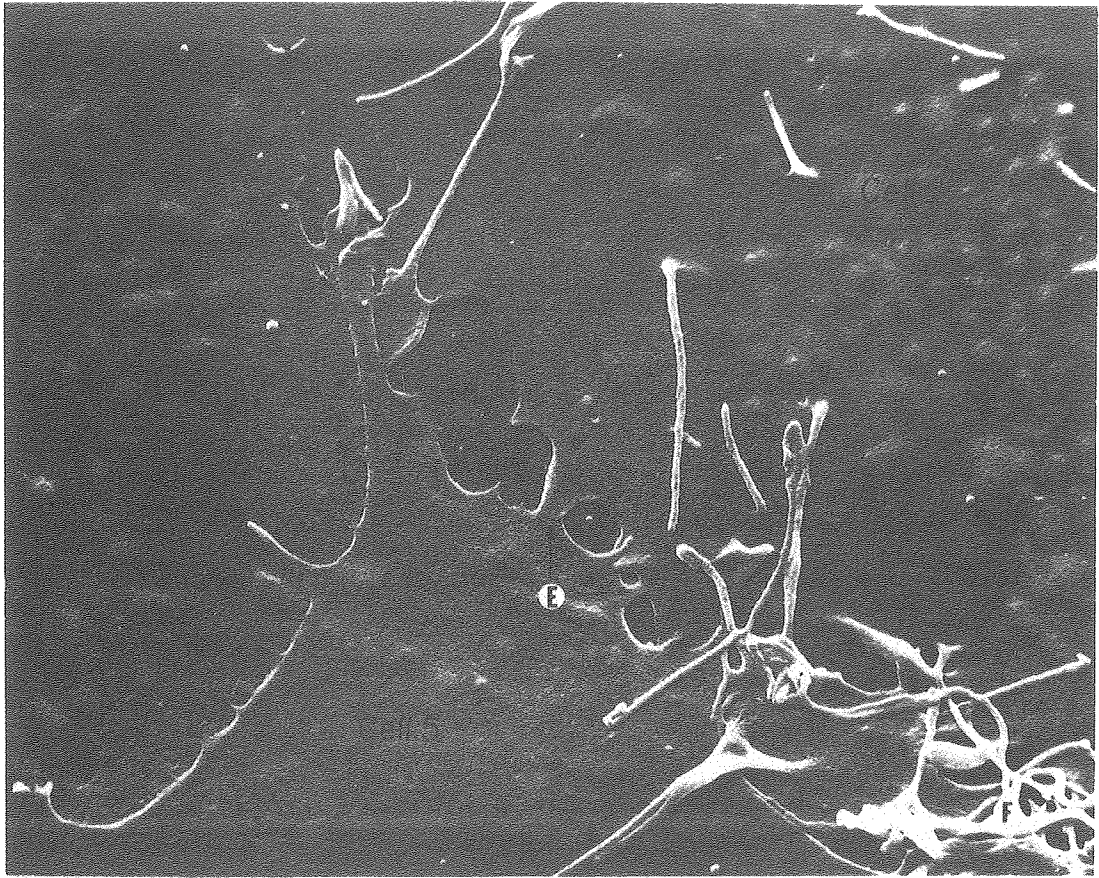


Fig. 21

XBB767 6514

Figure 22. Higher magnification view of Fig. 19, showing the region of interdigitation between the edges of Cell 1 and Cell 6. The area within the rectangle is shown at higher magnification in Fig. 23. Fil, filopodia; My, microvilli; N, nucleus; Ni, nucleoli; SM, silicon monoxide substratum; V, vesicular stomata. 9,000X.

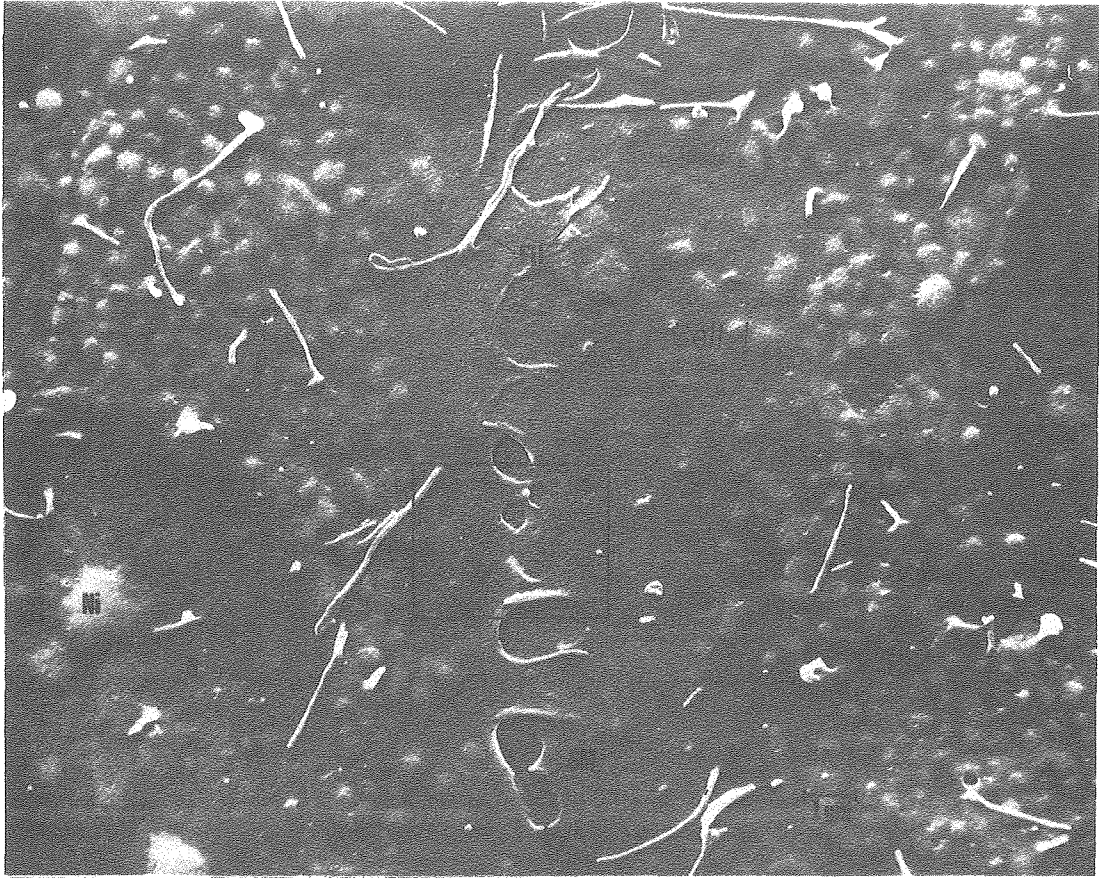


Fig. 22

XBB767 6512

finger-like projections which interlocked like the fingers of two joined hands (Figs. 19 and 22). This type of interaction could also be viewed as a series of alternating microoverlaps. This classification scheme represents at best only a rough grouping of the observed interactions and certainly should not be construed as implying any necessary functional differentiation between classes of interactions; however, it should serve as a useful descriptive tool in studies involving monolayer cultures of fibroblasts. The majority of cells exhibited all of the four types of interaction at various points around their peripheries, and there did not seem to be any localization of an interaction type to a specific region of the cell.

A distinct cell edge could be clearly distinguished around most of the cell's periphery; i.e., it was usually possible to determine in a region of interaction where one cell ended and the next began. However, in certain localized regions, the surfaces of neighboring cells appeared to adhere so closely that HRSEM revealed only a smooth fusion of the edges of the two cells with no discernible intercellular boundary being visible. These adhesions ranged in width from 0.1 to 1.0 μm , and were observed in regions of edge-to-edge contact (Fig. 21), simple overlap (Fig. 21), and interdigitation (Figs. 22 and 23). Although the complexity of interactions at the cell periphery made it difficult to determine the number of these structures accurately, the average spacing between adhesions was estimated to be approximately 1.6 μm . Approximating the cell by a circle of diameter 40 μm and circumference 125 μm suggests that there should be an average of 80 adhesions around the edges of a typical cell. Since the irregular shape of the cell would tend to increase its perimeter, this quantity probably represents an underestimation

Figure 23. Plasma membrane interactions in the region of interdigitation between Cells 1 and 6. In the areas delimited by the arrows, the surfaces of the two cells adhere so closely that no clear intercellular boundary can be seen. Small fibrous elements (arrowheads) are frequently observed to connect the two cell surfaces in these regions of intercellular adhesion. Fil, filopodium. 67,000X.



Fig. 23

XBB767 6511

of the average number of adhesions per cell. Furthermore, if adhesions formed below the cell (where they would not be seen by HRSEM) as well as at the periphery, the total number of adhesions per cell could be several times greater than this estimate.

One curious feature of the intercellular adhesions was the frequent presence of small fibers 100 - 250 Å in diameter and 300 - 900 Å long which appeared to connect the opposing cell surfaces (Fig. 23). These fibers were primarily observed in or adjacent to regions of intercellular adhesion, but also appeared in other areas where cell membranes were closely opposed (Fig. 24). In a few cases, these fibers were observed to bind the basal portions of filopodia to the surface of neighboring cells (Figs. 25, 26, and 28).

In two cases, bundles of filaments were observed to converge on regions of intercellular adhesion (Figs. 27 and 28). The individual elements of these filament bundles were both thicker (approximately 280 Å in diameter) and much longer than the short intercellular fibers. Rather than symmetrically connecting two cell surfaces as did the short fibers, the filament bundles appeared to originate within the cytoplasm of one cell and terminate at a point of adhesion between the cell and one of its neighbors (Fig. 28).

Blister- or wart-like structures surrounded by roughened membrane (Figs. 25 and 27) were often observed at the cell periphery in regions of cell interaction. Freeze-fracture of such structures (Chapter V) revealed that they were filled with numerous small smooth-membraned vesicles. Similar membrane protuberances have been observed by other workers; their nature is uncertain at present, and they have been variously described as secondary lysosomes (D. S. Friend, personal

Figure 24. Area of overlap between two cells (7 and 8), showing numerous short fibers (arrowheads) connecting the surface of Cell 7 with that of its underlying neighbor, Cell 8. In the region between the arrows, it appears that numerous fine fibers radiate from a blunt process on Cell 7. SM, silicon monoxide substratum. 62,000X.

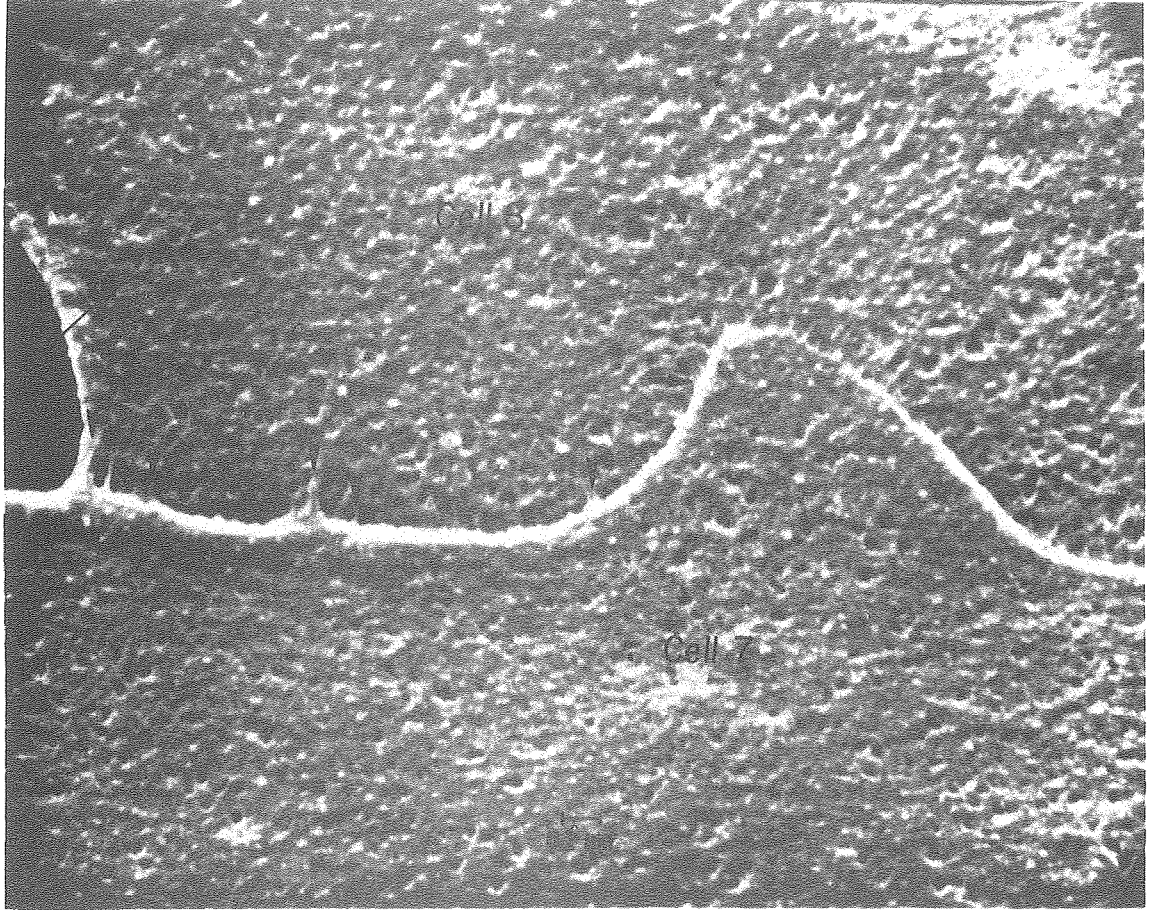


Fig. 24

XBB767 6510

Figure 25. Filopodial interactions between four cells (13-16). In this case, both cell processes and the basal portions of the filopodia seem to be held together by numerous small fibers (regions between arrowheads). The area within the rectangle is shown at higher magnification in Fig. 26. A patch of roughened membrane (RM) similar to that seen near blister-like structures (Fig. 27) is present where Cell 14 overlaps Cell 13. SM, silicon monoxide substratum. 26,000X.

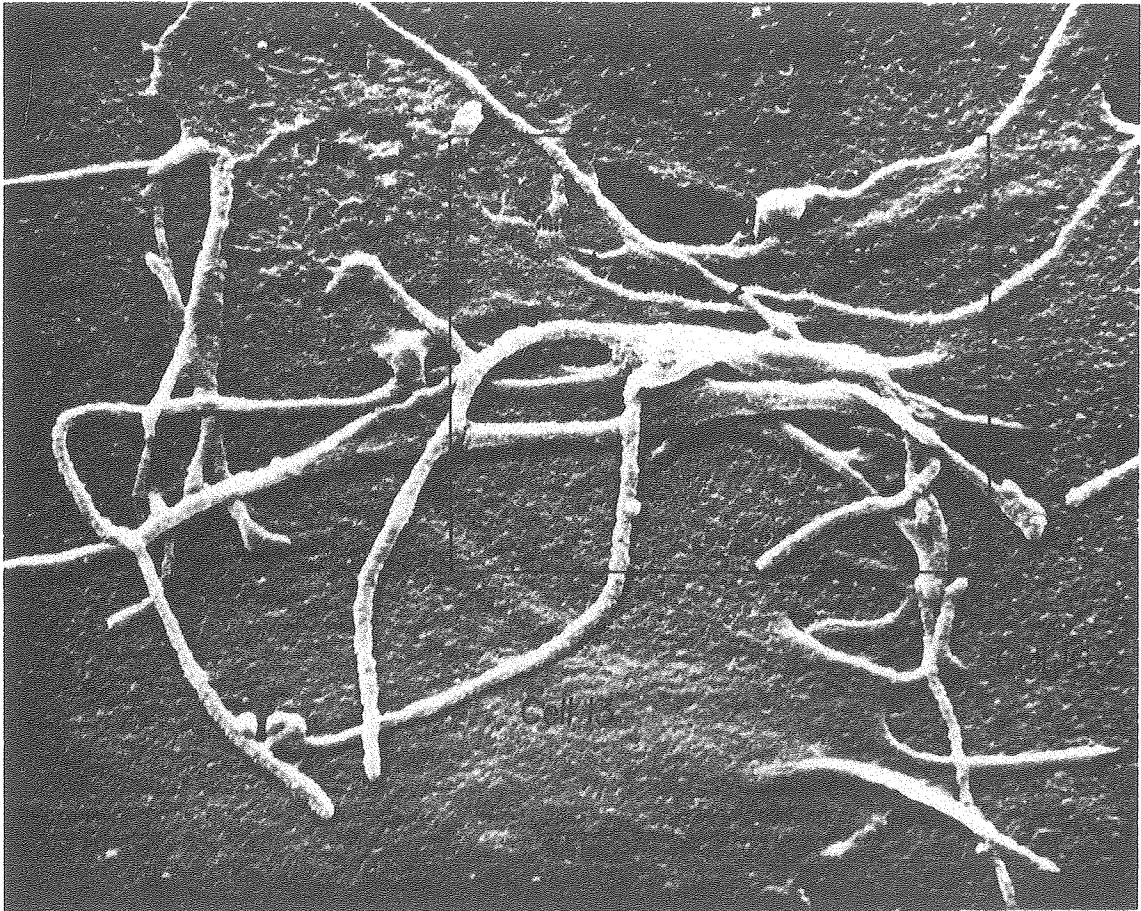


Fig. 25

XBB767 6507

Figure 26. Higher magnification view of Fig. 25. In addition to the fibers which occur between cell edges (e.g., between 13 and 15, 15 and 16) this micrograph includes regions where fibers are present between a cell surface and the basal portion of a filopodium (arrowheads). The arrows indicate an area where these fibers are particularly apparent. SM, silicon monoxide substratum. 55,000X.

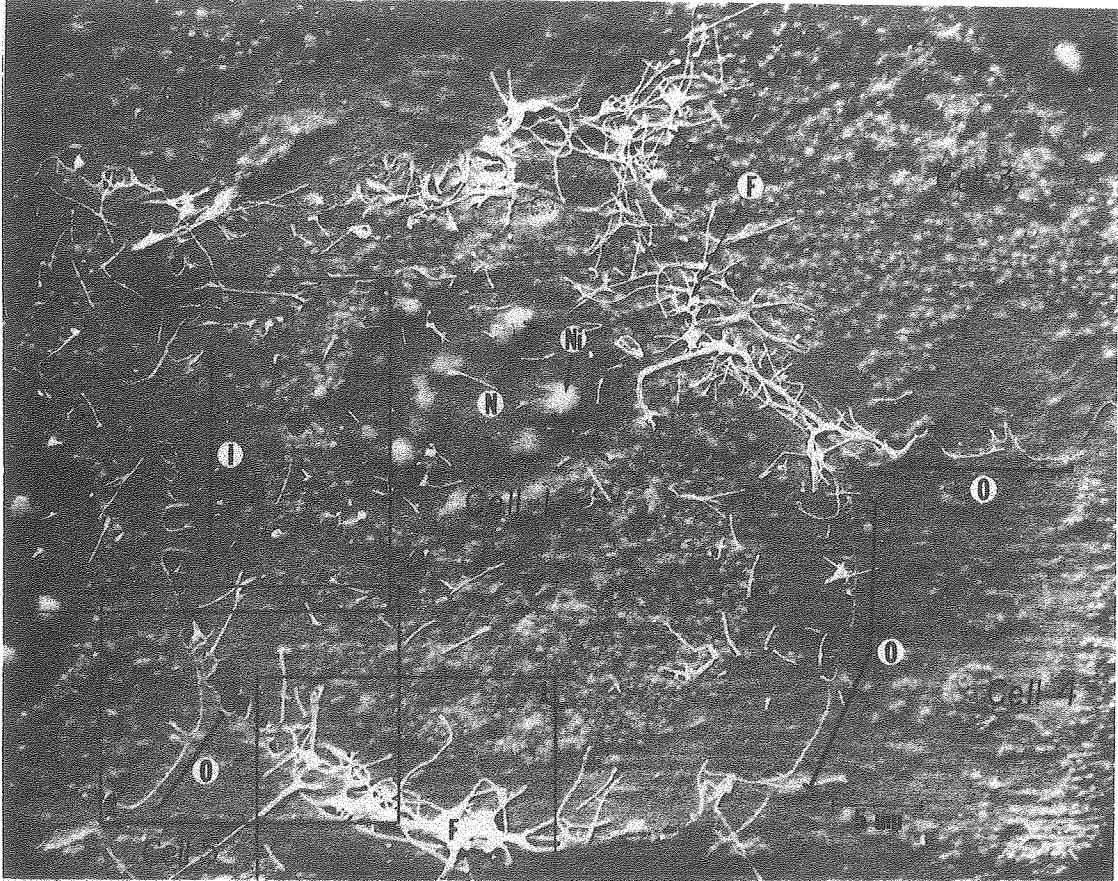


Fig. 26

XBB767 6515

Figure 27. Area of interaction between two cells (9 and 10), showing filamentous bundles (arrows) which appear to originate in the cytoplasm of Cell 10 and attach at the adhesions between Cells 9 and 10. Also shown are a few surface filaments (SF) which may be composed of some type of collagen. A small process (P), probably from Cell 10, is attached to Cell 9 by small adhesions (arrowheads). Blisterlike structures similar to the one shown in this micrograph (circled) were common in regions of cell interaction. The area enclosed by the rectangle is shown at higher magnification in Fig. 28. V, vesicular stomata. 12,000X.

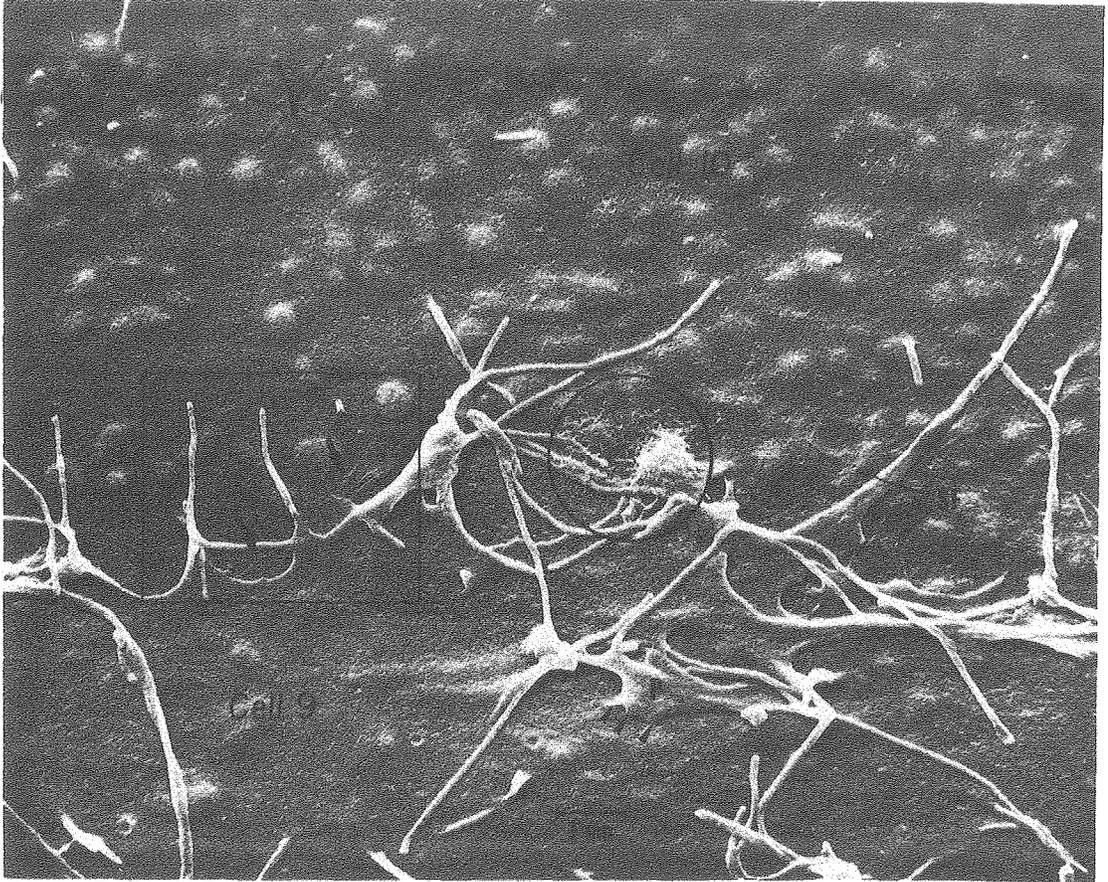


Fig. 27

XBB767 6509

Figure 28. Higher magnification view of Fig. 27, showing filament bundles (arrows) and their points of attachment at the edge of Cell 9 (arrowheads). The circle encloses three short fibers which connect the base of a filopodium (Fil) on Cell 9 to the surface of Cell 10. 50,000X.

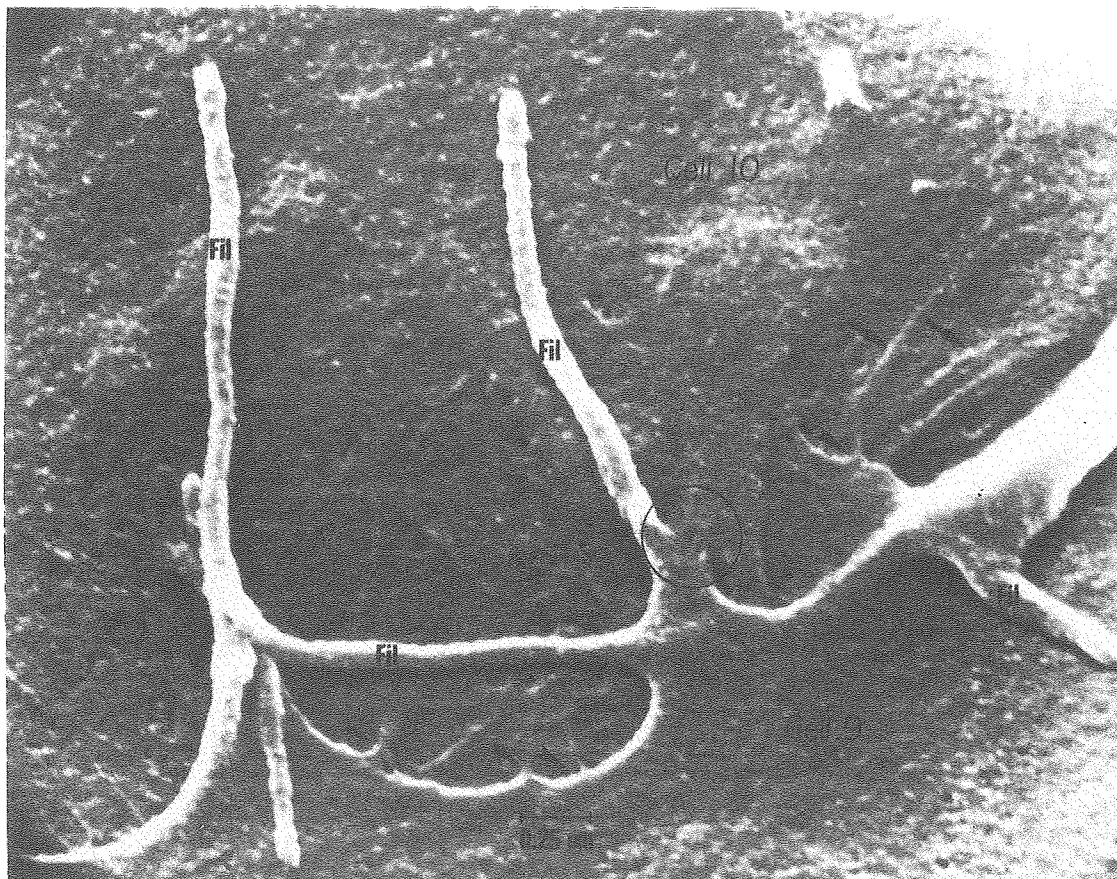


Fig. 28

XBB767 6585

communication) or regions where new membrane is being added (N. S. McNutt, personal communication).

Examination of the filament bundles and short fibers was somewhat complicated by the presence of long strands of filamentous material on the cell surface (Figs. 27 and 29). Surface filaments were 170 - 280 Å in diameter, extended for several microns over the cell surface and formed dense mats in a few localized areas. In most cases, this material was simply draped over the upper surface and edges of the cells, and could clearly be identified as extracellular. Filaments similar to these have been observed in Balb 3T3 A31 cells by McNutt (N. S. McNutt, personal communication; see also McNutt et al., 1971 and 1973) using both thin section and surface replication techniques (Fig. 30), and in secondary cultures of C3H mouse fibroblasts by Cherny et al. (1975). This material may be composed of collagen, since it is absent in cultures treated with hyaluronidase and collagenase (Cherny et al., 1975).

Discussion

One of the main points of interest arising from the results presented here is that of the nature and functional significance of the structures described as "adhesions." It is unlikely that these structures are either tight junctions or desmosomes, since no evidence of these junctional types has been found either in the Balb 3T3 cells used in this study (Chapter V) or in other types of fibroblasts (Pinto da Silva and Gilula, 1972; Revel et al., 1971). Since Balb 3T3 cells (Chapter V) and other fibroblastic cell lines (Cherny et al., 1975; Gilula et al., 1972; Pinto da Silva and Gilula, 1972; Revel et al., 1971; Cherny et al., 1975) form gap junctions, it is possible that

Figure 29. Appearance of surface filaments (SF) in a region of interdigitation between two cells (11 and 12). In this case, it is apparent that the surface filaments are merely draped over the edge of Cell 12 (arrows) and are not involved in cell-to-cell adhesion. The filaments at the upper left appear to be extending under Cell 12. V, vesicles. 36,000X.



Fig. 29

XBB767 6508

Figure 30. Balb 3T3 A31 cells sectioned parallel to, and just above, the substratum, showing strands of filamentous material (F) in the extracellular space (ECS). 60-80 Å microfilaments (Mf_{α}) are arranged in bundles in the cytoplasm of the cell periphery, and appear to attach to the plasma membrane at small dense regions (arrowheads). In this micrograph, the filamentous material has adhered to the plasma membrane and gives the impression of connecting two dense regions in the area between the arrowheads. Mf_{β} , 100 Å microfilaments, Mt, microtubules. Micrograph kindly provided by Dr. N. S. McNutt. 48,000X.

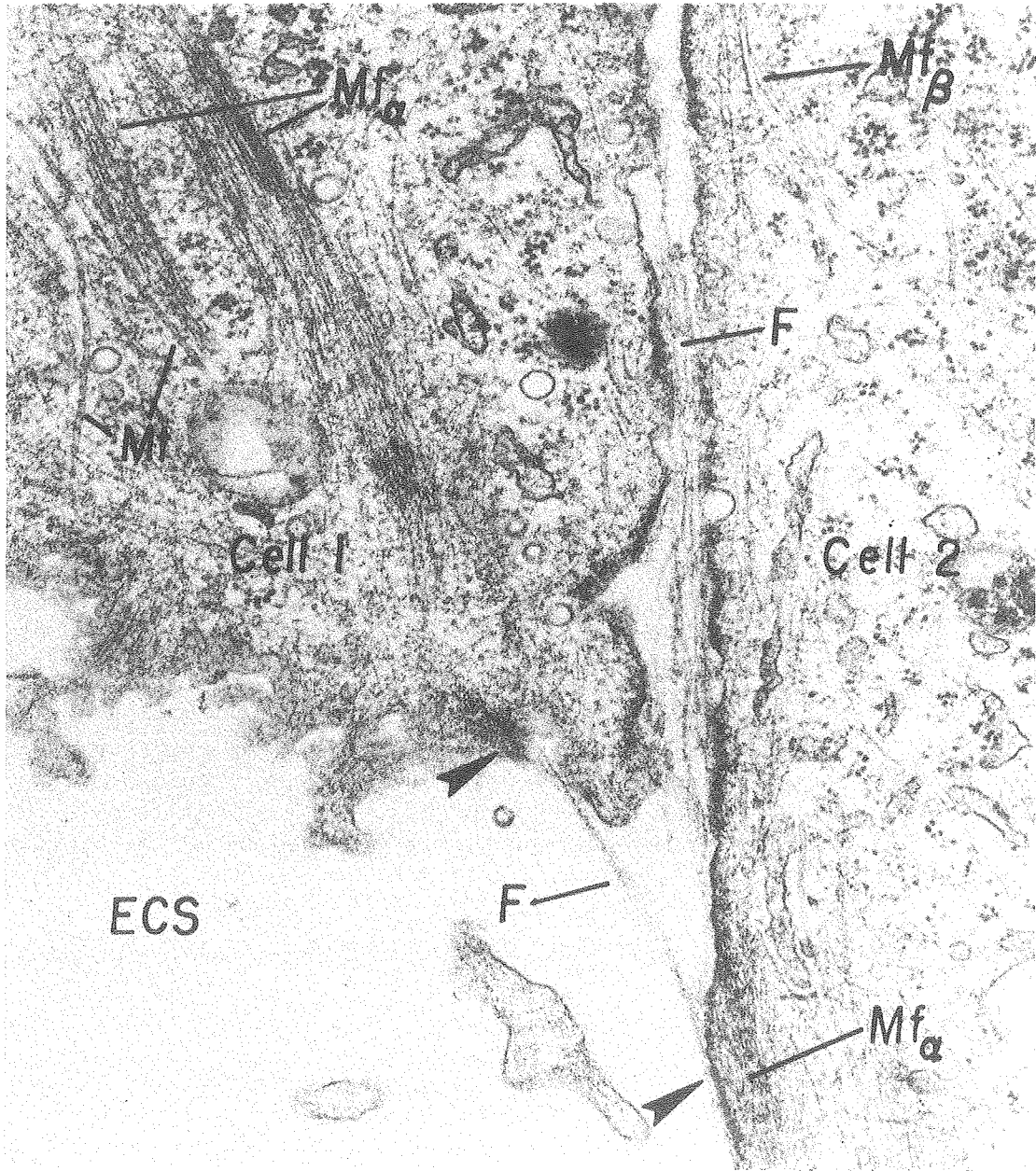


Fig. 30

XBB767 6517

some of the adhesions may represent sites of gap junction formation; however, the number of adhesions per cell suggested by HRSEM observations is much greater than the number of gap junctions estimated from freeze-fracture replicas (Chapter V). Also, examination of replicas of regions analogous to the adhesions did not show any of the morphology characteristic of freeze-fractured gap junctions (see McNutt and Weinstein, 1970 and 1973). In fact, membrane fracture faces in such regions did not appear significantly different from the rest of the cell membrane. The lack of internal specialization of the membrane at these sites suggests that they may represent intermediate or adherens junctions⁴ of the type originally described by Farquhar and Palade (1963). These junctions, which have been described in many tissues (see review by McNutt and Weinstein, 1973), are formed by two parallel plasma membranes separated by a 150 - 250 Å interspace. The interspace frequently has a condensa-

⁴ According to the most widely accepted classification scheme (Farquhar and Palade, 1963; McNutt and Weinstein, 1973), both the desmosome and the intermediate junction are classed as adherens junctions even though they are structurally unrelated. This scheme works well for adult mammalian tissues, where the desmosome forms a small disc-shaped junction or macula adherens, while the intermediate junction forms a band (zonula adherens) or large patch (fascia adherens). In tissue culture, however, both the desmosome and the intermediate junction form small localized junctions which would be classed as maculae adherentes. McNutt and Weinstein (1973) have proposed the terms "100F-macular adherens" for the desmosome and "70F-macula adherens" for the intermediate junction, but this terminology is awkward and could still be taken as implying some degree of structural relationship. In order to avoid this source of confusion, the term "intermediate junction" originally proposed by Farquhar and Palade (1963) will be used exclusively here to describe the structures formed by cultured cells. It should also be noted that Satir and Gilula (1973) have proposed a classification scheme in which all adherens junctions (i.e., both desmosomes and intermediate junctions) would be classed as cell contacts rather than true junctions.

sation of material which has been variously described as being amorphous (Farquhar and Palade, 1963; McNutt, 1975), having a central dense substratum (Farquhar and Palade, 1963; McNutt, 1970), or being finely fibrillar (Farquhar and Palade, 1963; McNutt, 1970). The cytoplasmic surface of the junctional membrane shows a condensation of electron-dense, finely fibrillar material termed the filamentous mat (McNutt, 1970). There is no specialization of the fracture face at intermediate junctions (McNutt and Weinstein, 1973).

The junctions of this type which have been described in cultured fibroblasts (Heaysman and Pegrum, 1973a; McNutt et al., 1971 and 1973; Ross and Greenlee, 1966) appear to have the same morphology as those in epithelia and other tissues except that in fibroblasts, they typically appear as small isolated spot junctions unlike the band (zonula adherens) or large patch (fascia adherens) junctions found in epithelia. Unfortunately, the lack of specialization of the fracture face at the intermediate junction has hampered efforts to examine the structure of this type of junction in the way that the tight, gap, and septate junctions have now been studied (McNutt and Weinstein, 1973). For this reason, use of the term "intermediate junction" in reference to cultured fibroblasts should not be construed as implying that these junctions are exactly homologous to those found in other tissues, even though present evidence suggests that they are morphologically and functionally very similar.

It is also necessary to consider the possibility that the adhesions do not represent cell junctions, but are merely sites where the outer surfaces of neighboring cells have stuck to one another. This possibility seems less likely in light of the fact that McNutt et al. (1971 and

1973), using Balb 3T3 A31 cells, have clearly identified numerous intermediate junctions in the same peripheral location where adhesions were seen by HRSEM (compare, for example, the adhesion in the region of edge-to-edge interaction in Fig. 21 with the cell processes joined by intermediate junctions in Fig. 3 of McNutt et al. [1973]). Identification of the adhesions as intermediate junctions is further supported by the fact that Ross and Greenlee (1966) found intermediate junctions to be the predominant type of junction occurring between fibroblasts in vivo. Interpretation of the adhesions as intermediate junctions therefore seems to offer the best explanation of the HRSEM data, and they will be referred to hereafter as "presumptive intermediate junctions." Since intermediate junctions have a characteristic appearance in thin sections, this question could probably be resolved conclusively if areas where adhesions were observed by HRSEM could be re-embedded, sectioned and examined by transmission electron microscopy.

With the exception of in situ thin sectioning techniques such as those employed by McNutt et al. (1971 and 1973), convenient methods of evaluating the overall distribution of the junctions occurring in a single cell have not been available to date. Although HRSEM does not permit identification of the type of junction occurring in a given region of intercellular adhesion, this technique does seem to be very useful for determining the distribution of adhesive regions at the cell periphery, since it combines the capacity to examine whole-cell morphology with resolution sufficient to permit ultrastructural studies to be carried out at high magnification. The data presented here suggest that the presumptive intermediate junctions may be the predominant type of adhesive cell junction occurring in mouse embryo and fibroblast cultures,

and may therefore be expected to contribute significantly to the maintenance of the integrity of the cell sheet. In addition to this strictly adhesive function, recent evidence suggests that intermediate junctions have a more important role as integral elements of the contractile cytoskeleton. Since it may now be possible to observe these structures with HRSEM, their role in cell motility will be discussed here in further detail.

The structure of this contractile apparatus has been shown by immunofluorescence studies (Goldman et al., 1975; Lazarides and Weber, 1974) to consist of a cytoplasmic array of actin-containing fibers which correspond to the bundles of 70 Å microfilaments seen by electron microscopy (Goldman et al., 1975; McNutt et al., 1971 and 1973). In addition to cytoplasmic fibers, a cortical layer of microfilaments is also often observed to occur just under the plasma membrane (Abercrombie et al., 1971; Lauweryns et al., 1976; McNutt et al., 1971 and 1973; Pollack et al., 1975; Reaven and Axline, 1973). Although actin is probably their primary component, the microfilament bundles have also been found to contain tropomyosin (Lazarides, 1975 and 1976), α -actinin (Lazarides, 1976), and probably myosin (Pollack et al., 1975; Weber and Groeschel-Stewart, 1975). There is now reasonably good evidence that this filamentous contractile system is responsible for cell motility (Huxley, 1973) and plasma membrane translocation (Reaven and Axline, 1973).

Several lines of evidence suggest that intermediate junctions function as discrete sites at which the contractile actin filaments are attached to the plasma membrane. The most carefully studied example of this interaction occurs in the intercalated disc of cardiac muscle cells (Fawcett and McNutt, 1969; McNutt, 1970 and 1975), where the thin actin

filaments of the I band are inserted exclusively into the filamentous mat of the fascia adherens, a large intermediate-type junction. Insertion of cytoplasmic actin filaments into intermediate junctions also occurs in the terminal web of the intestinal brush border (Farquhar and Palade, 1963; Rodewald et al., 1976), where actin filaments connect the membranes of the microvilli with the zonula adherens region of the terminal web. In this system, contraction is observed to occur between these two sites upon addition of ATP and Mg^{++} . In tissue culture, McNutt et al. (1973) have demonstrated that microfilament bundles converge on the intermediate junctions which form in regions of cell-cell contact. Heaysman and Pegrum (1973a) have shown that filament condensation and attachment is a rapid process which can occur within 60 sec after junction formation. Also, Abercrombie et al. (1971) and Pegrum and Maroudas (1975) have shown that adhesion plaques resembling half of an intermediate junction serve as attachment sites between the cell and its substratum; these sites also have microfilament bundles associated with them. In addition to the morphological data, there is considerable biochemical evidence for the association of actin with plasma membranes (Gruenstein et al., 1975; Pollard and Korn, 1973).

These studies suggest that intermediate junctions (and their related structures, the adhesion plaques) represent discrete regions of adhesion at which the force generated by the contractile system can be transmitted to the substratum or its neighboring cells. By means of these attachment sites, the cell is able to use its contractile apparatus to spread itself, move about over the substratum, and eventually form a cell sheet which has a measurable internal tension (Abercrombie, 1970). In view of the importance of intermediate junctions in cell motility, use of techniques

capable of revealing their distribution around the cell periphery may potentially advance present knowledge of cell locomotion. For this reason, HRSEM studies of the type described here are well worth pursuing.

The kind of association between microfilaments and intermediate junctions described here may also provide an explanation for the filament bundles which were seen to converge onto a region of cell interaction (Figs. 27 and 28). It seems likely that the appearance of these filament bundles is a drying artifact caused by collapse of the plasma membrane onto bundles of cytoplasmic microfilaments near a region where they were converging onto an intermediate junction. Deliberate collapse of the plasma membrane during air drying has, in fact, been used by McNutt (1973) to reveal bundles of cytoplasmic filaments.

Having found a reasonable interpretation for the adhesions, it is now necessary to explain the short fibers frequently associated with them (Figs. 23-26 and 28). Most workers agree that there is material in the intercellular cleft of the intermediate junction, although its appearance varies between different tissues (see above). Although this material has been described in certain cases as being fibrillar, it clearly does not have a well-defined structure such as that encountered in the intercellular cleft of the desmosome (Kelly, 1966). At present, there are three possible explanations for the presence of these fibers in and around presumptive intermediate junctions. They may be completely artifactual, representing merely bits of the glycocalyx pulled out by shrinkage of the monolayer during preparation. Alternatively, fiber-like structures could be precipitated from a truly amorphous intercellular cleft material by the combined effects of dehydration, critical point drying, and the heating and shrinkage that accompany vacuum coating. Finally, there may,

in fact, be fibers in the intercellular cleft, possibly exposed by leaching out of other amorphous components of the intercellular material during preparation. The data presented here are insufficient to distinguish between these possibilities. However, freeze-etching has revealed some suggestion of fibers near presumptive intermediate junctions (Chapter 5). The presence of fibrous material in this region is not unreasonable, since the force generated by the contractile system is concentrated at the intermediate junction, and the intercellular attachment at these points must be particularly strong. Fibers embedded in the intercellular substance would probably increase the tensile strength of the junction considerably. It may be possible to examine this question further by impregnation of the intercellular material with lanthanum hydroxide (Revel and Karnovsky, 1967) or similar materials.

The presence of long filaments (Figs. 27 and 29) on the surface of Balb 3T3 monolayers suggests an explanation for the occasional reports of cytoplasmic filaments penetrating the cell membrane and extending into the extracellular space (Lucky et al., 1975; Perdue, 1973). McNutt et al. (1971) reported that filamentous extracellular material tended to adhere preferentially to the cell surface over regions where cytoplasmic microfilament bundles attached to the inner surface of the plasma membrane. Micrographs such as Fig. 30 show that such aggregations of filamentous material on the outer cell surface can very easily give the impression of continuity between cytoplasmic and extracellular filaments. In fact, Perdue (1973) has reported that the extracellular filaments have a different appearance from those found within the cell, which suggests that the filaments are not continuous across the plasma

membrane.

Recently, much emphasis has been placed on the role of LETS protein in cell adhesion. This 250,000 molecular weight surface glycoprotein, which forms long filaments on the cell surface, is present in the regions of contact between normal fibroblasts but is reduced markedly in transformed cultures (Chen et al., 1976). It does not seem to be involved in the regulation of cell division (Blumberg and Robbins, 1975; Teng and Chen, 1975), but does appear to have a role in cell-cell adhesion (Chen et al., 1976) and its addition to cultures of transformed cells has been observed to increase their adhesion to the substratum and stimulate formation of actin filament bundles (Ali et al., 1977). It is possible that either the fibers observed at presumptive intermediate junctions or the surface filaments could be LETS protein. This idea is worthy of further study, perhaps by the use of anti-LETS antibody coupled to a marker like ferritin or hemocyanin (Karnovsky et al., 1972) which would be visible in thin section or HRSEM preparations.

Chapter 5

In Situ Freeze-Fracture Studies on Balb 3T3 Monolayers⁵

As described in Chapter 2, the customary method of preparing tissue culture cells for freeze-fracture has involved gently scraping fixed or unfixed cell layers off the culture dish, centrifuging the resulting suspension, and freezing portions of the pelleted cell layer. Although aldehyde-fixed, confluent cell layers will retain some of their integrity during this procedure, a great deal of information regarding morphology in situ and intercellular relationships is unavoidably lost. Delicate structures such as filopodia are usually broken during removal of the cell layer, and it is often difficult to orient regions of membrane specialization with respect either to the cell as a whole or to regions of interaction with neighboring cells.

Recently, Pfenninger and Rinderer (1975) have described a method for the in situ freeze-fracture of cells growing on 3-mm gold grids embedded in a thin collagen substratum. This apparatus has given excellent results, but has the disadvantages of complexity and high cost. Furthermore, in applications such as cell cycle studies where growth parameters may be dependent on the substratum upon which the culture is grown, it may be necessary to compare the biochemical properties and ultrastructure of cells grown on the same substratum, and collagen may not always be the substratum of choice. This chapter describes a simple technique for the freeze-fracture in situ of cultures grown on gold carriers coated

⁵ Portions of the material described in this chapter have been published previously (Collins et al., 1974 and 1975).

with a thin layer of vacuum-deposited silicon monoxide. This coating can be deposited on growth chambers of any size and appears to be a suitable substratum for the growth of a number of cell lines. The method is inexpensive, yields large areas of cell membrane, and should be adaptable to use with other cell culture substrata. The results of the freeze-fracture studies will be correlated with the HRSEM data presented in Chapter 4.

Materials and Methods

Cell culture. Swiss 3T3 4A RK2 and Balb 3T3 cells were cultured as described in Chapter 2 and 3, respectively. Because of mycoplasma contamination, Swiss 3T3 4A RK2 cultures were used only during development of the freeze-fracture methodology, and all morphological studies were carried out on confluent monolayers of Balb 3T3 cells. The observed morphology of the Swiss 3T3 cells was essentially the same as that of Balb 3T3.

Preparation of cultures for freeze-fracture. Swiss 3T3 4A RK2 cultures were fixed and glycerinated by Method III described in Chapter II. Balb 3T3 cultures were prepared by a procedure similar to that used for HRSEM studies (Chapter 4). Cultures were fixed for 45-65 min. in 2% glutaraldehyde (Polysciences, Inc., Warrington, Pa.) containing 0.1 M phosphate buffer, 12 mM sucrose, and 0.14 mM $\text{CaCl}_2 \cdot 2\text{H}_2\text{O}$. The fixative was first added directly to the culture medium without any prior washing; after the fixative had been added slowly and excess medium removed for approximately 5 min., the mixture of fixative and medium was drawn off and the cells were covered with pure fixative. Culture dishes and fixative were maintained in a water bath at 36-37°C during this procedure. Each dish was then washed three times in ice-cold 0.15 M phosphate buffer

containing 0.14 mM $\text{CaCl}_2 \cdot 2\text{H}_2\text{O}$, and incubated for 45 min. in cold 30% glycerol in 0.1 M phosphate buffer. Culture dishes were kept on an ice-water slush during washing and glycerination. Washing and glycerination in the cold was suggested by Dr. K. H. Pfenninger as a means of minimizing any enzyme activity remaining in the cell after glutaraldehyde fixation. All solutions had a pH of 7.0-7.4 at the temperature employed, and each solution was gradually replaced by the next one to minimize the osmotic shock to the cells. Observation of the cells on the culture dish with 100X phase contrast optics at intervals during these procedures did not reveal any morphological changes resulting from this treatment.

Freeze-fracture. The device first used for in situ freeze-fracture consisted of a 2 cm square brass block screwed onto the specimen post of the Balzers apparatus in place of the standard specimen table. Swiss 3T3 4A RK2 cultures were grown on 6 mm squares cut from glass coverslips, then fixed and glycerinated in the dish. A small copper hat slightly larger than those shown in Fig. 31 was placed over the coverslip and the assembly was frozen in Freon 22. The coverslip with its attached hat was then transferred to the top of the brass block, where it was held in place by two small brass clips. Fracturing was accomplished by knocking off the hat with the knife. Membrane fracture faces could be recognized in replicas prepared by this method, but the P and E faces were indistinguishable, both having particles that appeared stringy and of low profile. Also, the usually sharp edges of membrane fracture faces seemed to have been rounded off. This appearance of the fracture faces suggested that the specimens had been melted at some point in the freeze-fracture procedure, most likely during replication

(K. H. Pfenninger, personal communication). Overheating of the fracture faces was attributed to the poor thermal conductivity of the glass substratum.⁶ The experiment was repeated using 3 mm disks ground from quartz coverslips. These could be placed directly into the specimen wells on top of the four position Balzers specimen table. However, in spite of the improved thermal conductivity of the quartz,⁷ the results were no better. Since heat transfer could be improved either by increasing the conductivity of the substratum or by reducing its thickness, this problem was solved by vacuum-depositing a very thin film of the tissue culture substratum onto the surface of a metal support. Silicon monoxide was suggested as the material of choice for this purpose (J. Murchio, personal communication).

In the procedure which was finally adopted for routine in situ freeze-fracture, 3T3 cells were grown to their saturation density on silicon monoxide-coated, 3 mm diameter Balzers specimen carriers (95% gold, 5% nickel) placed in the bottom of Falcon plastic dishes. After the cells had been fixed and glycerinated, the carriers were removed from the dish and the excess liquid carefully drained off with filter paper. The carrier was then sprayed with a 1% suspension of 9.7 μm polystyrene latex beads (Particle Information Service, Los Altos, California), using a Pelco nebulizer (Ted Pella Company, Tustin, California). A small copper hat (Fig. 31) was then placed over the cell

⁶ Approximately 5×10^{-3} watts/cm $^{\circ}\text{K}$ at 100 $^{\circ}\text{K}$ for glass as opposed to 3.4 watts/cm $^{\circ}\text{K}$ for gold at the same temperature. American Institute of Physics Handbook, Second edition (1963).

⁷ Approximately 0.2 - 0.6 watts/cm $^{\circ}\text{K}$ at 100 $^{\circ}\text{K}$, depending on the orientation of the crystal axis.

Figure 31. Copper hats with a Balzers flat-topped specimen carrier.
21X.

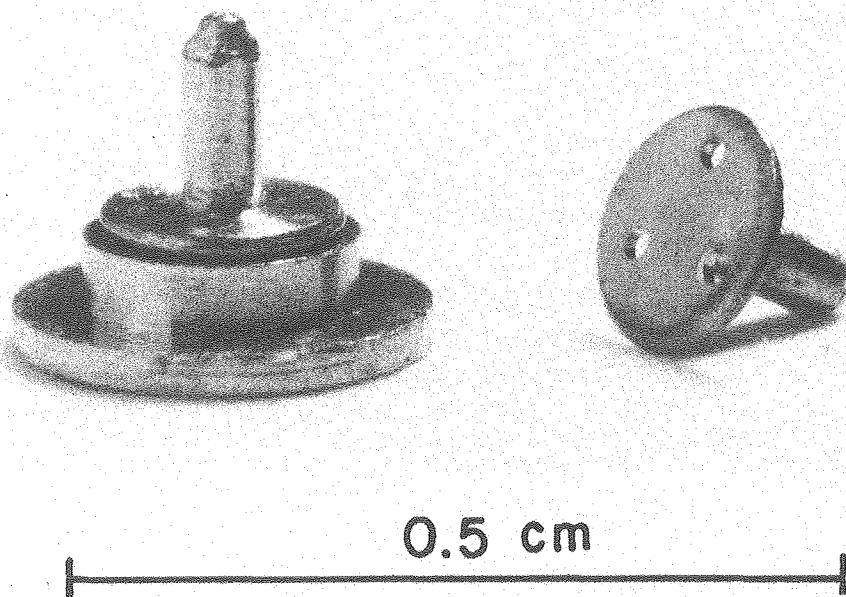


Fig. 31

XBB746 3706

layer on the raised central portion of the Balzers carrier, and the whole assembly was frozen rapidly against the solid phase of partially solidified Freon 22. The polystyrene latex spheres functioned as spacers to prevent the copper hat from resting directly on the cell layer. Good mechanical contact between the copper hat and the ice layer above the cells was insured by drilling three 0.008 mm holes in the base of each hat, and sonicating the hats in the 30% glycerol cryoprotectant to remove any air bubbles from the holes. The carriers with their attached hats were then placed in the depressions on the four-position specimen table of a Balzers BA 360M freeze-etching apparatus and held firmly in place by the specimen table clip and clamping ring. Specimens were fractured at a stage temperature of -100°C by knocking off the hats with a knife, and were then either etched for 1 min. with the cold knife positioned over the specimen table, or immediately shadowed with platinum-carbon (7 sec at 7.4 V using 10 cm of 0.1 mm cleaned platinum wire on a standard Balzers carbon electrode) followed by carbon (10 sec at 8.6 V). The specimens were then thawed and the cellular material digested away from the replica by chlorine bleach (5.25% sodium hypochlorite, 30 min.) followed by two washes with distilled water. The replicas were quite firmly attached to the cell layer and tended to tear when the carriers were introduced into bleach. However, it was possible to alleviate this problem by soaking the specimen carriers overnight in 100% methanol and gradually replacing the methanol with distilled water before treatment with bleach. Replicas were picked up on flamed 75 x 300 mesh copper grids and examined in a Siemens Elmiskop I electron microscope at an accelerating voltage of 80 or 100 kV. The hats were cleaned before each run by a brief immersion in dilute ammonium hydroxide followed by soni-

cations in acetone, absolute ethanol and petroleum ether. Only the E face of the membrane at the lower cell surface and the P face of the membrane at the upper surface can be seen by this technique, as the other two fracture faces are attached to the hat and cannot be retrieved at present.

In cases where very flat cells were fractured or when the opposing surfaces of the hat and carrier were slightly rounded, the fracture plane would frequently pass above the cell layer, either exposing only the tops of the cells or missing the monolayer altogether. This problem could be rectified by reducing the thickness of the layer of ice above the cells; this was accomplished by reducing the bead diameter to 4.7 μm , and grinding the upper surface of the carrier and the bottom of the hat flat against a large piece of 0.25 in thick double ground and polished plate glass. The carriers were most conveniently ground by using no. 70C cement (Hugh Courtwright & Co., Chicago, Illinois) to attach a number of carriers to a small square of 0.125 in thick plate glass, then inverting the glass square over the grinding surface. Grinding was carried out in three stages, using a slurry of 800 mesh boron carbide (Norbite; Norton Co., Industrial Ceramics Div., Worcester, Mass; particle size approximately 20 μm) followed by 6 μm and 1 μm diamond paste (Buehler Ltd., Evanston, Illinois). A slurry of aluminum oxide in 20, 5, and 1 μm particle sizes (Universal Shellack and Supply Co. Ltd., Brooklyn, New York) was also used for this purpose, and was found to be equally effective and much less expensive. Unfortunately, grinding left the upper surface of the carriers quite rough, which caused severe problems with the HRSEM studies (Chapter 4). In addition, it is possible that the roughness of the surface might alter the growth properties of

the cells. These problems could probably be circumvented by abandoning grinding in favor of using polyvinyl alcohol (Pauli et al., 1977; see Discussion) to induce fracturing through the monolayer.

Another problem encountered with this method of in situ freeze-fracturing was its sensitivity to "orange-peel" contamination of the sort described by Moor (1971; see especially Fig. 12), Dunlop and Robards (1972), and Staehelin and Bertaud (1971). However, this type of contamination should not pose a serious obstacle to the use of this technique, since it could be eliminated by fracturing at -100°C .

The results reported in this chapter were derived from replicas of two separate preparations of Balb 3T3 cells, including portions of the membranes of 27 cells. For purposes of identification, each cell was given a number, and each of the fracture faces associated with that cell was listed according to the number of the cell, e.g. P_6 and E_6 represent the P face of the upper surface and the E face of the lower surface, respectively, of Cell 6 (Fig. 32). This system is used in all of the figures in this chapter. P and E faces were determined by a combination of low and high magnification micrographs as described in Chapter 2. Shadow direction is indicated by an arrow on each print.

Results

Balb 3T3 cells prepared by freeze-fracture were similar in size and appearance to those observed by HRSEM (Fig. 32). The collapse of the cell membrane over the nucleus observed in some of the HRSEM preparations was never seen in freeze-fractured cultures, which suggests that this was an artifact resulting from the use of the Freon critical point drying apparatus. Varying numbers of microvilli were present on the

Figure 32. Replica of one entire Balb 3T3 cell fractured in situ using the copper hats. The fracture plane has followed the upper surface of this cell (P_6) as well as portions of the upper surfaces of four neighboring cells (P_7 , P_8 , P_9 , and P_{10}). Cellular interactions primarily involve interdigitation of the cell edges, although there are some regions of overlap where E faces (E_6 , E_6' , and E_8) can be seen. The enclosed area between P_6 and P_8 is shown at higher magnification in Fig. 33. The broken stumps of numerous microvilli (arrowheads) can be seen on P_6 , P_7 , and P_8 . White areas represent breaks in the replica. gly, glycerol matrix. Specimen etched for 1 min. 2800X.

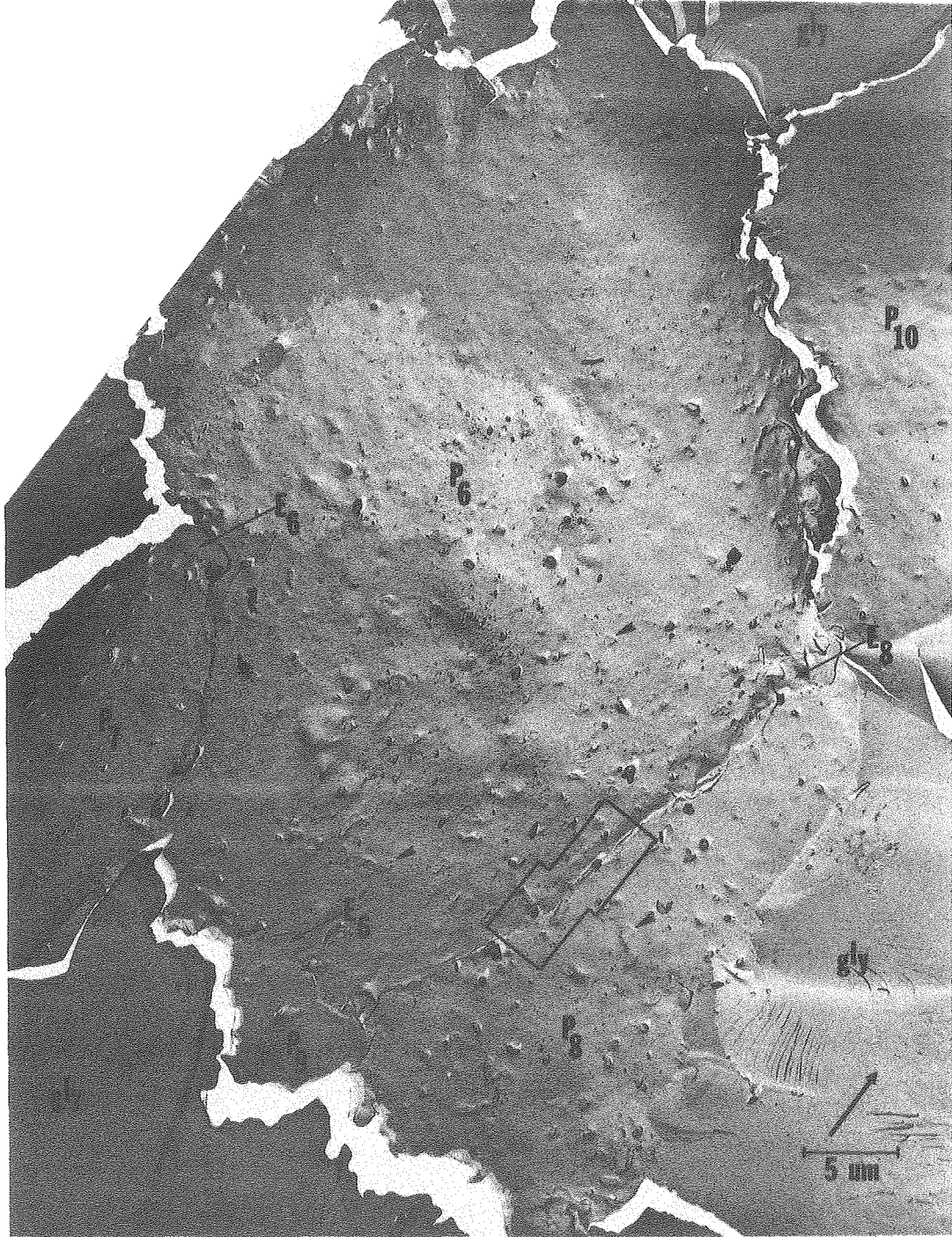


Fig. 32

XBB767 6519

upper surface (P fracture face) of the cells. Microvilli were almost always cleaved away during fracturing, appearing only as broken stumps on the cell surface. In favorable fractures, filopodia could be observed at the cell periphery. These were usually fractured in cross-section, but in some cases the fracture plane would follow the membrane of a filopodium for some distance (Fig. 40). Some cells displayed patches of vesicular stomata in certain regions of the plasma membrane, as shown by fracture face P₁₇ of Fig. 38. Vesicular stomata were particularly numerous in Swiss 3T3 4A RK2 cultures, where the boundary between regions with and without vesicles was often very sharp, and the stomata frequently gave the impression of being arranged in rows.

The scheme for classification of cell interactions used with the HRSEM observations was also useful with cultures prepared by freeze-fracture, and most of the interactions observed in replicas could be described as examples of overlap, interdigitation, or filopodial interactions. Examples of cell overlap are shown on a low magnification montage in Fig. 35, and at higher magnification in Figs. 36 and 37. Interdigitation can be seen to occur between Cell 6 and its neighbors in Figs. 32 and 33. Finally, a region where numerous filopodia seem to be interacting is shown in Fig. 40. True edge-to-edge contacts of the sort shown in Figs. 18 and 21 of Chapter 4 were not seen, probably because these interactions were relatively rare in the dense cultures employed in this study, and the chances of the fracture plane passing through such a region would therefore be small.

Both the P and E fracture faces were covered with IMP whose diameter, measured on the P face, was 98 Å (N = 140, standard deviation = 17 Å). Particle density on the E face was lower than that on the P

Figure 33. Higher magnification view of Fig. 32, showing part of the region of interdigitation between P_6 and P_8 . Localized regions where surfaces of the two cells are in close apposition are labelled as $A_1 - A_5$. Note that in the region of overlap which contains A_5 , an E face (E_8) interacts with a P face (P_6), while at $A_1 - A_4$, the fracture faces at the point of close apposition of the cell surfaces are both P faces. The significance of this difference is discussed in the text. The area within the rectangle is shown at higher magnification in Fig. 34. Cyt, cytoplasm; gly, glycerol matrix; Ves, vesicles in cytoplasm. 36,000X.

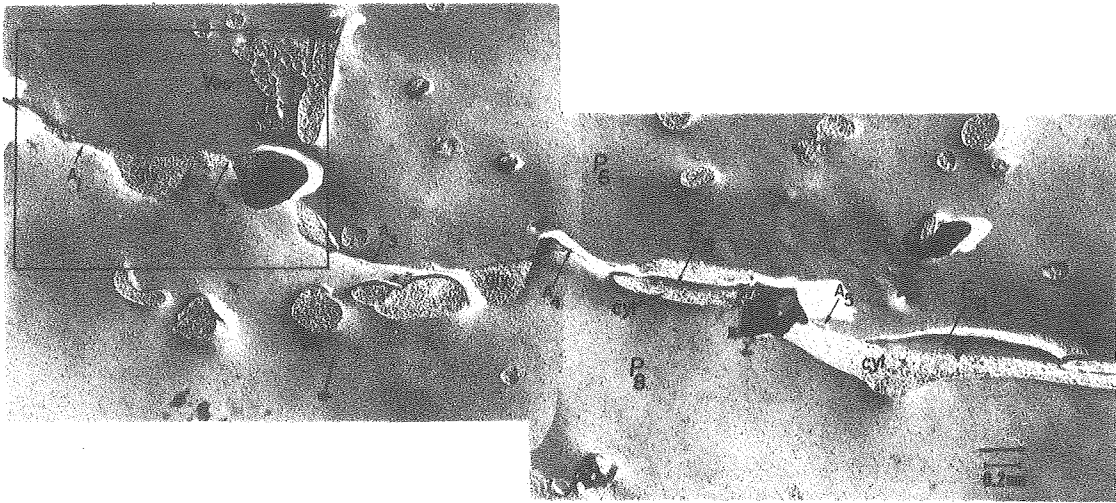


Fig. 33

XBB767 6285

Figure 34. Photographic enlargement of Fig. 33, showing two presumptive intermediate junctions, A_1 and A_2 . In the region delimited by the arrowheads, etching of the glycerol matrix (gly) appears to have exposed numerous short fibers connecting the surfaces of Cells 6 and 8. 110,000X.

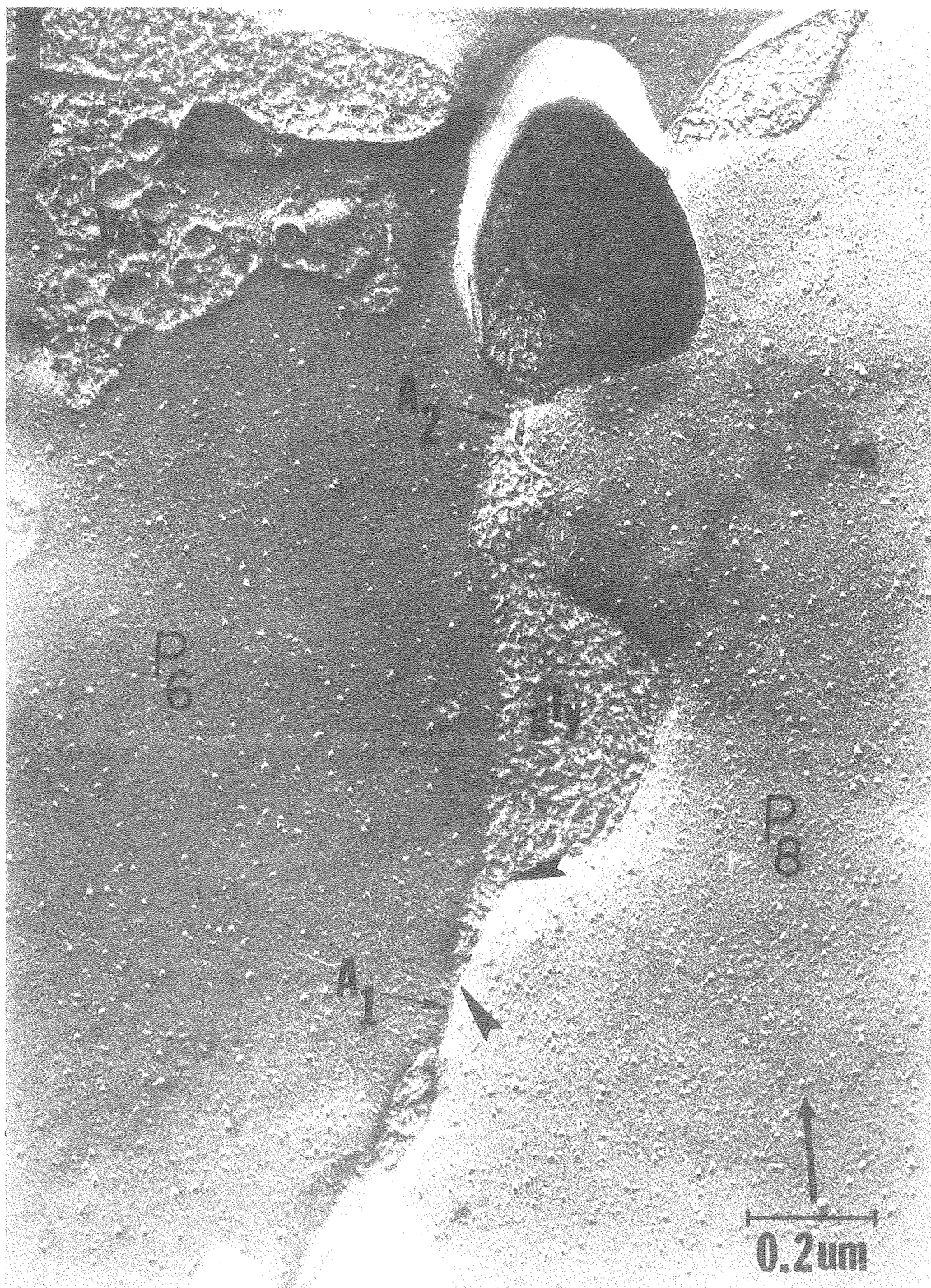


Fig. 34 .

XBB767 6280

Figure 35. Replica of a Balb 3T3 monolayer, showing overlap of Cell 17 by Cell 18, and Cell 16 by Cell 15. The numbered rectangles indicate regions selected for examination at high magnification. The areas of interaction of Cell 15 with Cell 16 and Cell 17 with Cell 18 are shown in Figs. 36 and 37, respectively. Gap junctions are circled. This montage of 14 photographs includes portions of the membranes of 8 cells. Specimen fractured and replicated without etching. 2500X.

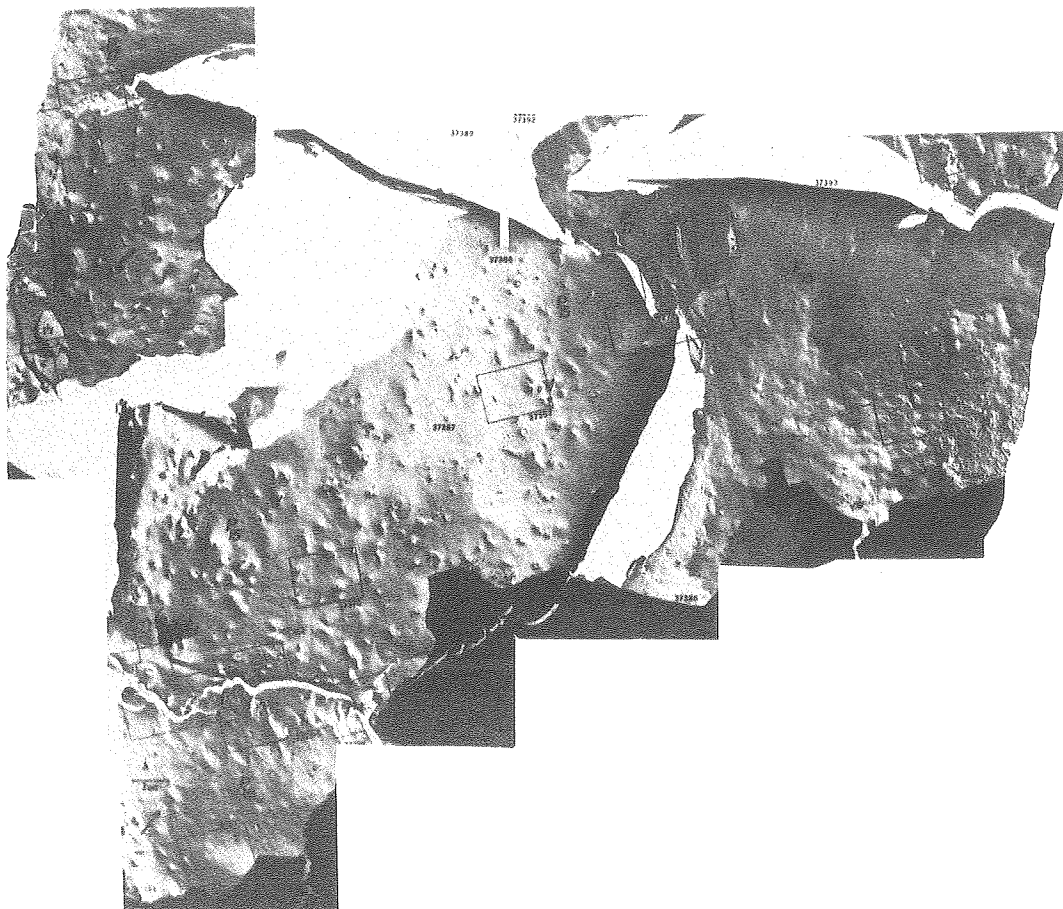


Fig. 35

XBB764 3824

Figure 36. Higher magnification view of Fig. 35, showing the area where the lower surface of Cell 15 (E_{15}) overlaps the upper surface of Cell 16 (P_{16}). There are extensive areas of close apposition between E_{15} and P_{16} , but with the exception of a few gap junctions (circled), there does not appear to be any difference in particle distribution or density between these regions and the rest of the cell membrane. Montage of 7 photographs. 34,000X.

Figure 36 has been omitted from the text.

Figure 37. Higher magnification view of Fig. 35, showing a region where the lower surface of Cell 18 (E_{18}) is overlapping the upper surfaces of Cells 17 and 20 (P_{17} and P_{20}). Areas of close apposition between the cell membranes are restricted in this case to fairly small regions (lower left, for example). A large gap junction (circled) has formed between P_{17} and E_{18} in one such area. This junction, approximately $0.3 \mu\text{m}$ in diameter, was one of the largest seen with Balb 3T3 cells. 15,000X.



Fig. 37

XBB764 3823

Figure 38. Montage from an area adjacent to that seen in Fig. 35. Note patches of vesicular stomata (V) and absence of microvilli on P₁₇. Gap junctions are circled, and the region with many gap junctions at the bottom of P₂₅ is shown at higher magnification in Fig. 39. This montage of 10 photographs includes portions of the membranes of 4 cells. 2700X.



Fig. 38

XBB764 3821

Figure 39. Higher magnification view of Fig. 38, showing area of close apposition between E₂₆ and P₂₅. A linear array of gap junctions appears to be forming from, or disaggregating into, small clusters of IMP. Montage of 3 photographs. 34,000X.

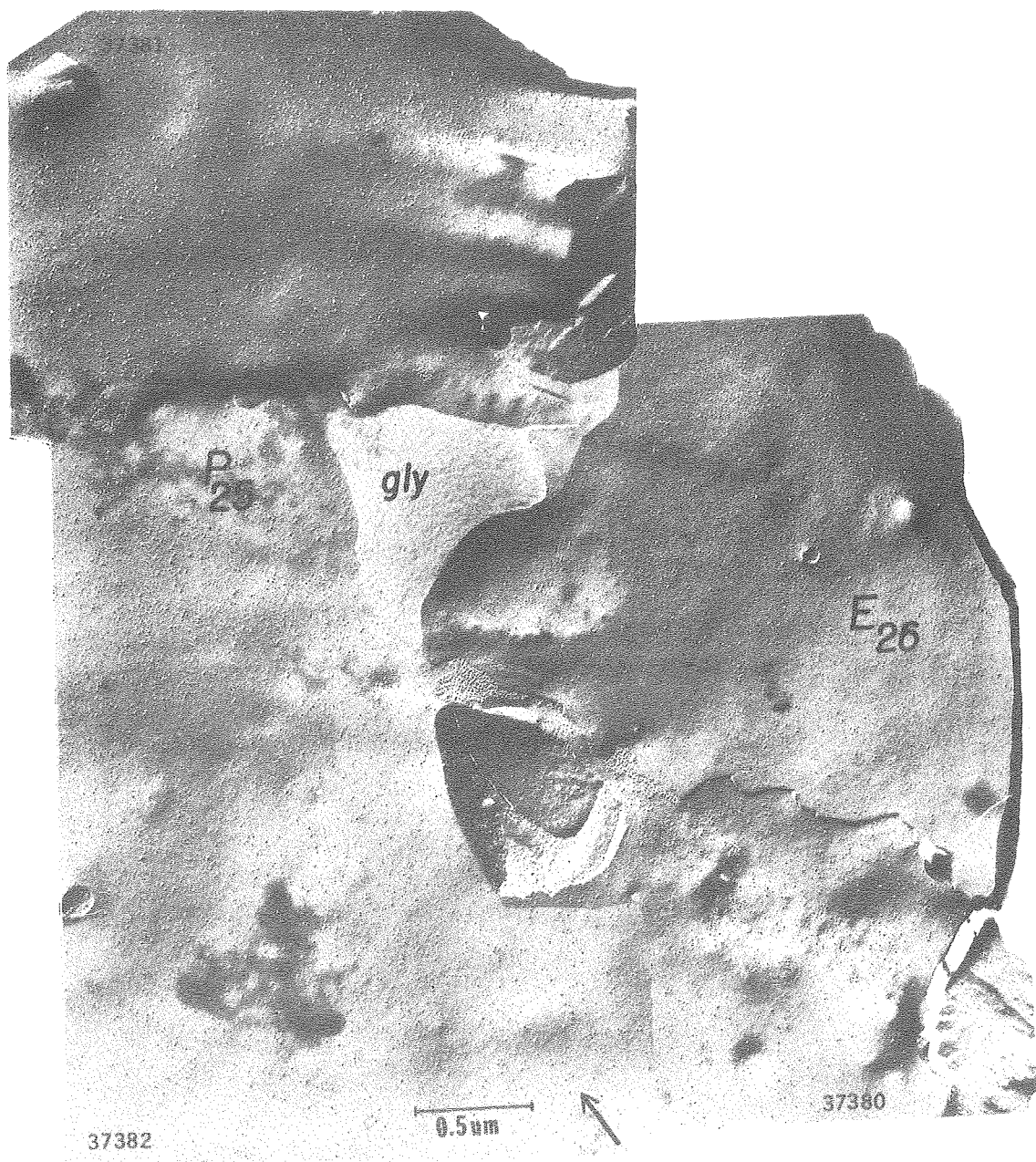


Fig. 39

XBB764 3820

Figure 40. Freeze-fracture replica of a region of filopodial interaction. The micrograph shows the upper surfaces of two neighboring cells, P₆₁ and P₆₂. Most of the filopodia have been broken off during fracturing, leaving behind only the stumps of their basal portions (arrowheads). In the lower half of the micrograph, the filopodia appear to have been concentrated into apposing regions of the two cell edges. It is likely that in this area, the two cells put forth a complex tangle of interlocking filopodia similar to that shown in Fig. 20. The appearance of this region contrasts sharply with the upper portion of the micrograph, where there are few filopodia. A filopodium fractured lengthwise (Fil) appears at the bottom of the figure. Cyt, cytoplasm; gly, glycerol matrix. Bar equals 1 μ m. 13,000X.

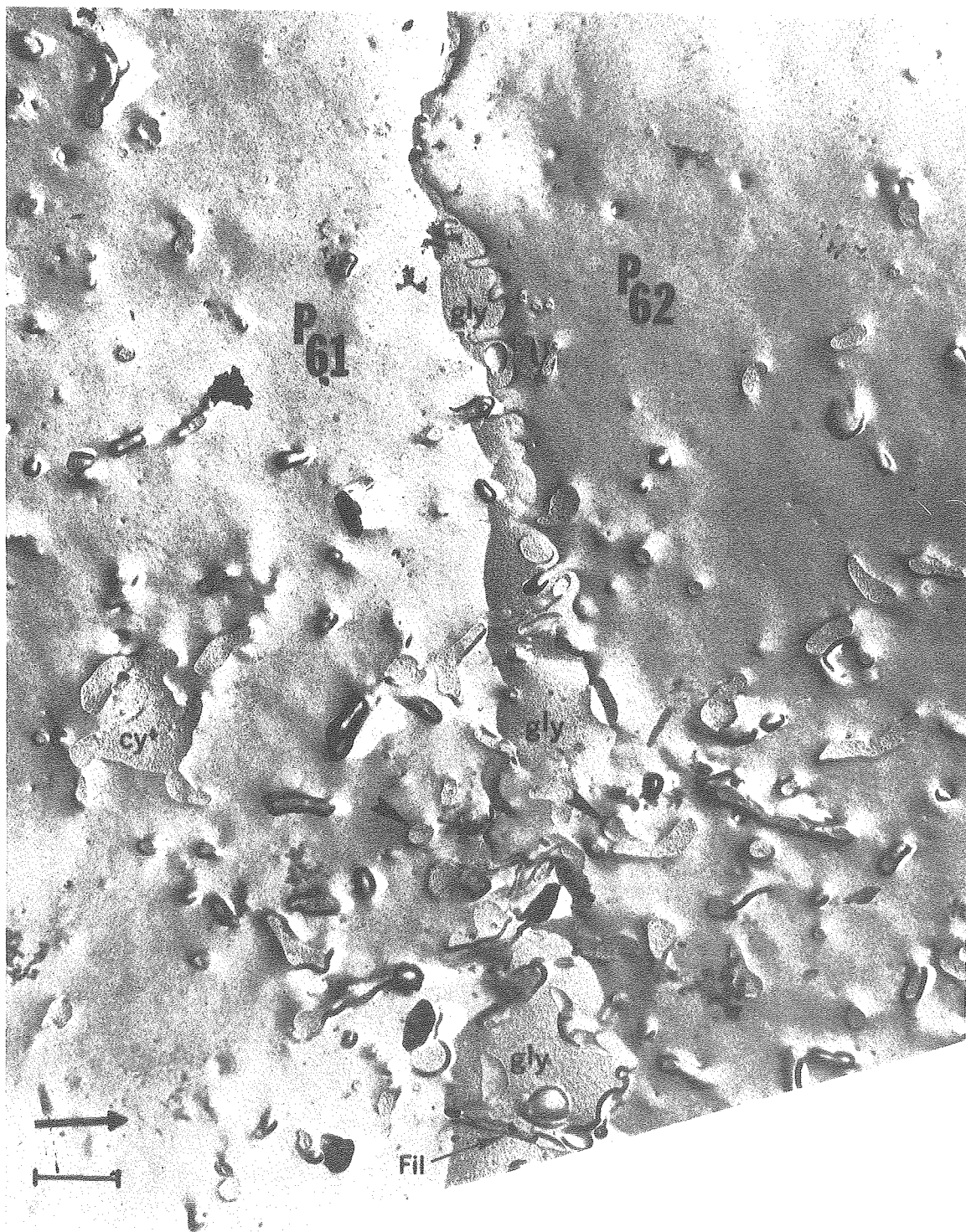


Fig. 40

XBB767 6586

face. In order to determine whether cell contact induced any alteration in the density or distribution of IMP, photographs were taken at high magnification (approximately 80,000X on the final print) of the membrane at the cell center, where cell interaction was presumed to be minimal, and at the periphery, where maximal cell interaction was presumed to occur. With the exception of small gap junctions, visual observation of these areas revealed in all cases only IMP scattered uniformly over both P and E fracture faces. There appeared to be no difference in particle distribution between central and peripheral regions of the cell. This result is in agreement with the work of Gilula et al. (1975) and Pinto da Silva and Martinez-Palomo (1975) who also found that the intrinsic distribution of IMP in fibroblasts is uniform. There was no evidence of the particle aggregation at confluency reported by Furcht and Scott (1975) and Scott et al. (1973). In spite of this apparent uniformity in all regions of the membrane, it is possible that a numerical method of analyzing particle distributions (Weinstein, 1974) might reveal more subtle variations in the topography of the membrane.

Particle densities were estimated on one of the two Balb 3T3 preparations by counting the number of particles in 0.25 μm squares drawn on the prints in regions where overlap or interdigitation was clearly occurring. These values were compared to particle densities found by counting similar squares drawn on photographs taken in the cell center or where this was not possible, some distance from the region of interaction (Table II). Although based on a small sample, the results suggest that there were no significant differences in particle density between different regions of the same cell, and therefore it seems likely that cell contact does not have any obvious effect on the density or native distribution of IMP in

Table II

Regional Particle Densities in Balb 3T3 Cells

Face Number	Region of cell interaction		Intermediate area (0.5-3.0 μm from region of cell interaction)		Cell center	
	Area counted, $(\mu\text{m})^2$	Density, $\text{IMP}/(\mu\text{m})^2$	Area counted, $(\mu\text{m})^2$	Density $\text{IMP}/(\mu\text{m})^2$	Area counted, $(\mu\text{m})^2$	Density $\text{IMP}/(\mu\text{m})^2$
P ₆	2.50	820 \pm 230	2.25	740 \pm 130	2.25	910 \pm 210
P ₇	1.50	850 \pm 100				
P ₈	2.25	1020 \pm 110			1.75	950 \pm 150
P ₁₀	1.00	780 \pm 350				
P ₁₂	1.00	670 \pm 100	2.50	670 \pm 90		

The indicated uncertainty limits represent one standard deviation. Total number of IMP counted was 14,119.

Balb 3T3 cultures. A one-way analysis of variance (Minium, 1970) performed on the values for the particle density in regions of cell interaction (Table II, Column 3) showed a statistically significant difference ($p < .05$) between the IMP densities found for this region in different cells; i.e., it appears that the variation in particle density between cells is significant whereas that between different regions of the same cell is not significant.

The membranes of adjoining cells were generally separated by an extracellular space of at least 300 - 500 Å. However, in areas showing overlap or interdigitation of the cells' peripheral zones, there were numerous localized regions of close apposition between the cell surfaces. Typical examples of the appearance of these loci in a region of interdigitation are shown in Fig. 33, where the P faces (i.e., the upper surfaces) of Cells 6 and 8 come into very close proximity at points A_1 , A_2 , A_3 , and A_4 . By considering which fracture faces were in apposition in each of these loci, it was possible to show that many of the regions of close apposition were located at or near the cell periphery.⁸ Regions such as these ranged in width from 0.05 to 0.5 μm . The similarities in size, appearance, and location between the regions of close apposition seen by

⁸Determination of the location of regions of close apposition was based on the fact that there are only two instances where two P faces can approach each other, namely, at a contact between the edges of two cells or where the edge of one cell is contacting the upper surface of its neighbor. It therefore follows that regions such as $A_1 - A_4$ must be at the periphery of at least one of the cells concerned--in this case probably Cell 8. If $A_1 - A_4$ were located beneath one of the cells rather than at the edge, then one of the interacting fracture faces would have to be an E face. This latter case occurs at A_5 , where E_8 and P_6 interact in a small region of overlap some distance underneath Cell 8.

freeze-fracture and the adhesions found in HRSEM preparations suggest that these may be different views of the same structures. The fracture face in the regions of close apposition was not significantly different from that of the rest of the cell membrane, a fact which lends credence to their interpretation as regions of intermediate junction formation (see Chapter 4). It is unfortunate that the thin section studies (Chapter 6) did not yield better results, because intermediate junctions have a characteristic appearance in sections, and the nature of these regions could probably have been decided conclusively by careful examination of sections through the cell periphery. For the present, the adhesions seen by HRSEM and the regions of close apposition seen in replicas will both be referred to as "presumptive intermediate junctions."

In some cases, etching seemed to have exposed small fibrous elements approximately 100 A in diameter and 300-400 A long in close association with the presumptive intermediate junctions at the cell periphery (Fig. 34). These structures may correspond to the short fibers seen by HRSEM (Figs. 23-26 and 28).

Regions of close apposition were also common in regions of cell overlap located at varying distances from the actual edge of the cell. The area involved could be quite small (A_5 in Fig. 33; see also Fig. 37) or quite extensive (Fig. 36). With the exception of occasional small gap junctions, there was no specialization of the fracture face in these regions. Intercellular fibers were not observed in overlap regions. The width of the step between the overlapping E and underlying P fracture faces was 110-220 A. Since other workers (Cherny et al., 1975; Heaysman and Pegrum, 1973; Ross and Greenlee, 1966) have observed intermediate junctions in regions of close apposition between overlapping fibroblasts,

it is possible that some or all of these regions may represent intermediate junctions, but it is impossible with the data at hand to know what fraction of these areas might contain junctions or how much of each area of close apposition would be occupied by the junctional complex. Better results from the thin section studies (Chapter 6) would have resolved this question.

Occasionally, filopodia could also be observed to interact closely with each other or with the cell surface. There was no evidence of any specialization of the membrane at these points. The distribution and density of IMP on filopodia was similar to that of the rest of the cell membrane.

Gap junctions were almost never observed with Swiss 3T3 4A RK2 cultures, but a few gap junctions could be found in replicas of Balb 3T3 cells (Figs. 36, 37, and 39). Their location has been indicated by circles in all of the micrographs in this chapter. Gap junctions ranged in size from very small junctions containing only a few particles, to longer junctions 0.2 to 0.3 μm in diameter. In one isolated case (Fig. 39), a row of gap junctions appeared to be forming from or disaggregating into small clusters of IMP. Gap junctions formation and disassembly has also been described by Albertini et al. (1975), Decker and Friend (1974), Johnson et al. (1974), and Revel et al. (1973).

When they occurred, gap junctions were frequently encountered in regions of close apposition between overlapping cell surfaces (Figs. 36 and 39). However, since they account for only a small percentage of the total area of such regions, it is unlikely that they represent the major component of whatever cell interaction occurs at these locations. This point becomes obvious after a simple calculation; in two montages (Figs.

35 and 38) comprising approximately $2700 \mu\text{m}^2$ of membrane fracture faces, there were only 17 recognizable gap junctions (i.e., one gap junction per $160 \mu\text{m}^2$ of membrane). Assuming as in Chapter 4 that the cell is a circle of radius $40 \mu\text{m}$ and area $1260 \mu\text{m}^2$, with this density of gap junctions one would expect only approximately 16 gap junctions over the whole of both the upper and lower surfaces of an average cell. Since the number of gap junctions at the cell periphery would be only a fraction of this number, it seems clear that the numerous adhesions seen by HRSEM cannot be gap junctions.

Discussion

The data presented here indicate that in clone A31 HYF of Balb 3T3 cells, there is no visible alteration in the density or distribution of IMP in regions of cell contact. The next step in the search for contact-induced alterations in membrane structure therefore involved using glycerol to induce particle redistribution in an effort to determine whether cell contact changed the mobility of the IMP in any way. Preliminary results of these experiments are described in Chapter 7.

The freeze-fracture technique described here has proven to be a simple and inexpensive method for fracturing a monolayer culture without removing it from the substratum. Experience with freeze-fracture of cultures prepared by traditional methods (Chapter 2) suggests that with these preparations, it is very difficult to interpret regional membrane specializations such as variations in the density of vesicular stomata or IMP. Preservation of the native cell shape by in situ fixation and fracturing makes it possible to determine how areas of membrane specialization are related to the cell as a whole and to regions of cellular interaction. Furthermore, since the cell layer remains attached to the

substratum during preparation for fracturing, delicate structures such as filopodia (Fig. 40) can be preserved intact.

This method of in situ fracturing presents several improvements over techniques I and II described by Pfenninger and Rinderer (1975). Use of the silicon monoxide coating eliminates the necessity for the collagen-coated cellophane supporting film employed with cell cultures in technique I, while avoiding the complex apparatus required by technique II. The design of the hat minimizes the amount of metal separating the cell monolayer from the coolant during freezing and should provide faster freezing than the brass cylinders used in technique I. Since the carriers fit onto the standard Balzers specimen table, a special specimen stage is not required. The method should be adaptable to a number of different substrata, the only condition being that the layer of substratum applied to the gold-nickel carrier must be thin enough to permit good heat conduction during replication. For example, Hamamoto et al. (1974) have used this technique to examine epithelial cell layers grown on Nucleopore filters. At present, the main limitation encountered with this method results from the necessity of using a vertical illumination system to observe the cells growing on the carrier. This problem does not arise with the method of Pfenninger and Rinderer, where the transparent collagen substratum extends across the open squares of the supporting gold grid.

Recently, Pauli et al. (1977) have developed a method for in situ freeze-fracturing which eliminates some of the problems encountered with the technique used in this study. In their method, cells are grown on plastic coverslips placed in the bottom of Falcon plastic dishes. Cultures are fixed and glycerinated in situ, and the coverslips are removed

and cut into pieces. Each piece of coverslip with its attached cells is inverted onto a droplet of polyvinyl alcohol placed on a Balzers 3 mm flat-topped carrier, and the assembly is frozen. Cleavage is accomplished by lifting off the coverslip with the knife.

Since the plastic substratum is transparent, this method permits observation of the cell layer before fracturing, enabling one to correlate cell ultrastructure with the growth characteristics seen by light microscopy. More important is the fact that the polyvinyl alcohol causes the fracture plane to propagate through the monolayer, thus eliminating the problems associated with grinding flat surfaces onto the hats and carriers. There is, however, one serious drawback with this technique; etching experiments require cells to be frozen in distilled water, and this precludes the use of polyvinyl alcohol in cases where the cell surface is to be revealed by deep etching. In addition, while the technique described in this chapter only permits visualization of the E face of the membrane at the lower cell surface and the P face of the membrane at the upper cell surface, the method of Pauli et al. suffers from the similar limitation of revealing only the complementary two fracture faces, i.e., the P face at the lower cell surface and the E face at the upper cell surface. The optimum methodology for in situ freeze-fracture would probably involve employing either both techniques or a double replica device in order to reveal all four possible fracture faces, together with the use of polyvinyl alcohol to control fracturing in cases where etching is not necessary. Surface studies requiring deep etching could be carried out with cells frozen in distilled water if grinding were used to ensure that the surfaces above and below the cell layer were sufficiently flat.

Chapter 6

In Situ Thin Sectioning with Balb 3T3 Monolayers

Recently, a variety of techniques for in situ thin sectioning of cultured cells have become available (Abercrombie et al., 1971; Cherny et al., 1975; Lucky et al., 1975; McNutt et al., 1971; Pegrum and Maroudas, 1975; Reaven and Axline, 1973). This chapter describes experiments aimed at adapting these standard techniques for use with the silicon monoxide substratum.

Materials and Methods

Balb 3T3 A31 cells were used for thin sectioning prior to cloning (see Chapter 2). Cultures were grown to confluency in silicon monoxide-coated 60 mm Pyrex petri dishes. The monolayer was first washed three times in saline G (a 2 mM phosphate buffer containing 0.14 M NaCl, 6.1 mM glucose, 5.4 mM KCl, 0.63 mM $MgSO_4 \cdot 7H_2O$, and 0.14 mM $CaCl_2 \cdot 2H_2O$) and then fixed for 1 hr in 2% glutaraldehyde (Electron Microscopy Sciences, Fort Washington, Pennsylvania) containing 0.1 M phosphate buffer, 12 mM sucrose, and 0.14 mM $CaCl_2 \cdot 2H_2O$. Culture dishes and solutions were maintained at 37°C in a water bath during washing and fixation. Each dish was then washed three times at room temperature in 0.15 M phosphate buffer containing 0.14 mM $CaCl_2 \cdot 2H_2O$ and postfixed for 1 hr. in 1% osmium tetroxide (Fisher Scientific Co., Fairlawn, New Jersey) in 0.1 M phosphate buffer at room temperature. The pH of the saline G, fixative, and phosphate buffer solutions was between 7.0 and 7.5 at the temperature employed. The fixed monolayers then received three 15 min. washes in cold Michaelis' veronal acetate buffer, pH 6.3, followed by a 1 hr. en

bloc staining (Farquhar and Palade, 1965) with 0.5% uranyl acetate (Mallinckrodt Analytical Reagent Grade) in cold veronal acetate buffer. The cells were then washed three times in glass-distilled water and dehydrated through a graded ethanol series (50, 70, and 95% ethanol, 5 min. each; 100% ethanol twice, 15 min. each). Cultures were then treated with two changes of propylene oxide followed by 1 hr. in a 1:1 mixture of propylene oxide with Spurr's epoxy embedding medium (Polysciences, Inc. Warrington, Pennsylvania; Spurr, 1969). This mixture was removed and replaced by a thin layer of Spurr's medium, which was cured for 24 hr. at 60°C. The disc of epoxy containing the cells was then removed from the dish by cracking away the edges of the dish with pliers, inserting a heavy single-edged razor blade between the epoxy disc and the bottom of the dish, and prying the epoxy away from the glass. In most cases the silicon monoxide layer readily came away from the glass, while remaining firmly attached to the bottom surface of the epoxy disc. This was a very desirable result, since the experience of other researchers who have employed in situ embedding techniques suggests that it is frequently difficult to separate the epoxy from the substratum, and that portions of the cell layer often tear out of the epoxy (S. Hamamoto, personal communication, and Elias et al., 1971).

Removal of the silicon monoxide from the lower surface of the epoxy disc represented the major obstacle to development of an in situ thin sectioning technique. It was impossible to section specimens with the oxide layer intact because it was quite hard and blunted glass knives almost immediately. An attempt to polish the silicon monoxide off with 300 mesh carborundum also failed because it was almost impossible to avoid grinding off part of the cell layer with the silicon monoxide. The

oxide layer could be removed successfully by holding the epoxy disc for one or two minutes above the surface of 70% hydrofluoric acid, then gently rubbing off the silicon monoxide with a soft tissue. Selected areas could then be cut out and sectioned with or without re-embedding. Unfortunately, cells prepared in this manner lacked a well-defined plasma membrane and many of the cytoplasmic membranes, an artifact which was attributed to penetration of the hydrofluoric acid into the cell layer. These problems were partially solved when it was noted that during routine cleaning of the vacuum evaporator with acetone and ethanol, the excess silicon monoxide film would begin to wrinkle up and detach from the bell jar within a few minutes after being wetted with acetone. Immersion of epoxy discs in acetone likewise caused the silicon monoxide coating to peel away from the epoxy at each microscopic scratch in the oxide film. Gentle rubbing with a tissue soaked in acetone was usually sufficient to remove the remaining silicon monoxide.

After removal of the silicon monoxide, selected areas were cut from the disc and sectioned with a diamond knife on a Porter-Blum MT-2 ultramicrotome. Sections were picked up on clean 300 mesh grids and stained with 0.5% uranyl acetate in 50% methanol followed by Reynolds lead citrate (Reynolds, 1962). Thin sections were photographed in the Siemens Elmiskop I electron microscope at an accelerating voltage of 80 kV. Thick sections for light microscopy were cut using glass knives, stained with Mallory's Azure II-Methylene Blue (Richardson et al., 1960), and photographed on Kodak Panatomic-X film using a Zeiss Photomicroscope with a #53 orange filter to improve contrast.

Results and Discussion

The appearance of Balb 3T3 A31 cells in light micrographs (Fig. 41) and low power electron micrographs (Figs. 42 and 43) was similar to that observed in other studies of fibroblasts sectioned perpendicular to the substratum (Abercrombie et al., 1971; Cherny et al., 1975; Luckey et al., 1957). With the exception of a small population of rounded cells (Fig. 41), Balb 3T3 A31 cells were very flat, with the thickest portion (2 - 5 μm) over the nucleus tapering gently to extensive peripheral regions 0.07 - 0.4 μm thick. There was no evidence of filamentous intercellular material in any of the sectioned preparations. Most membrane-bound organelles were located in the central or perinuclear region of the cell, while the peripheral regions appeared to contain primarily microfilaments, microtubules, and ribosomes. At higher magnification (Fig. 43), mitochondria, sacs of rough endoplasmic reticulum, and lysosomal residual bodies could be identified in the perinuclear cytoplasm. Bundles of cytoplasmic microfilaments in longitudinal and cross section could be seen in both the central and peripheral regions. Microfilaments occurred both directly under the plasma membrane and deeper into the cytoplasm.

Although the silicon monoxide layer had been removed before sectioning, its position was marked by an electron-dense deposit, probably derived from protein components of the serum (Pegrum and Maroudas, 1975), at the edge of the section. The preparation used for Figs. 41, 42, and 43 was sectioned without being re-embedded, so the edge of the section underneath the monolayer represents the part of the epoxy disc which was originally applied to the silicon monoxide film. The lower surfaces of the cells were usually less than 0.1 μm from the substratum, and appeared to contact the oxide layer in small localized areas (Fig. 42) which may

Figure 41. Thick section cut from a confluent monolayer of Balb 3T3 A31 cells fixed and embedded in situ. Since these cells were prepared before the Balb 3T3 cells were recloned, some cells tended to overgrow the monolayer, forming the localized mounds of cells which can be seen in (a). (a) Bar equals 50 μm , 210 X; (b) bar equals 10 μm , 1300X.

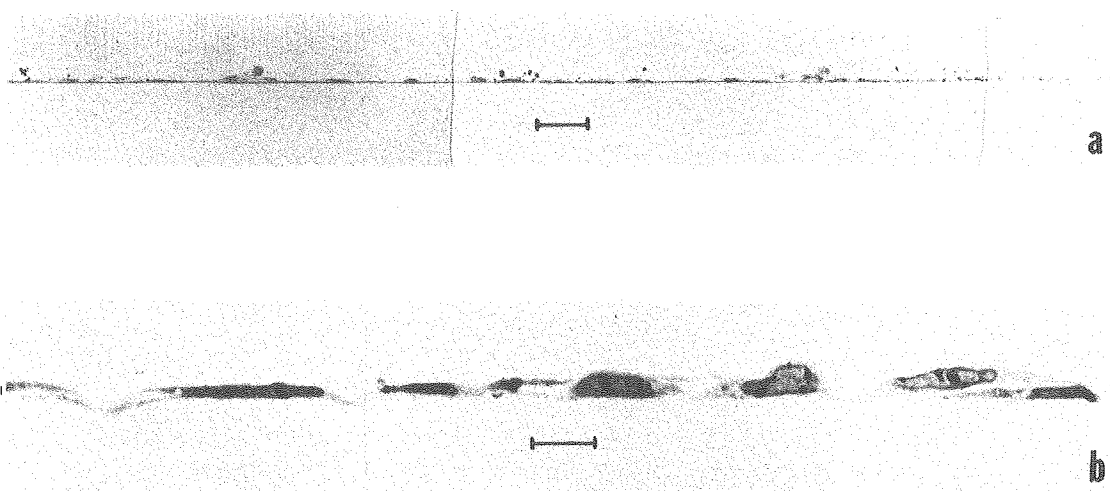


Fig. 41

XBB767 6284

Figure 42. Electron micrograph of a confluent monolayer of Balb 3T3 A31 cells, showing parts of three cells (1, 2, and 3) and numerous smaller processes from other cells. This montage of nine micrographs originally formed a continuous strip, but was cut into three sections for this figure. The silicon monoxide was removed from the embedded monolayer with acetone; however, its position is marked by an electron-dense deposit at the underside of the monolayer. The dark objects adhering to the underside of the monolayer are probably silicon monoxide fragments. The cells are flattened, with most of the membranous organelles restricted to the central portion of the cell. Cells appear to contact the substratum only in localized regions (arrowheads). Occasionally, a line of electron-dense material can be seen in such regions (double arrowheads). Mfl, microfilaments in longitudinal section; Mfx, cross-sectioned microfilaments; Mv, microvilli; RER, rough endoplasmic reticulum. 14,000X.

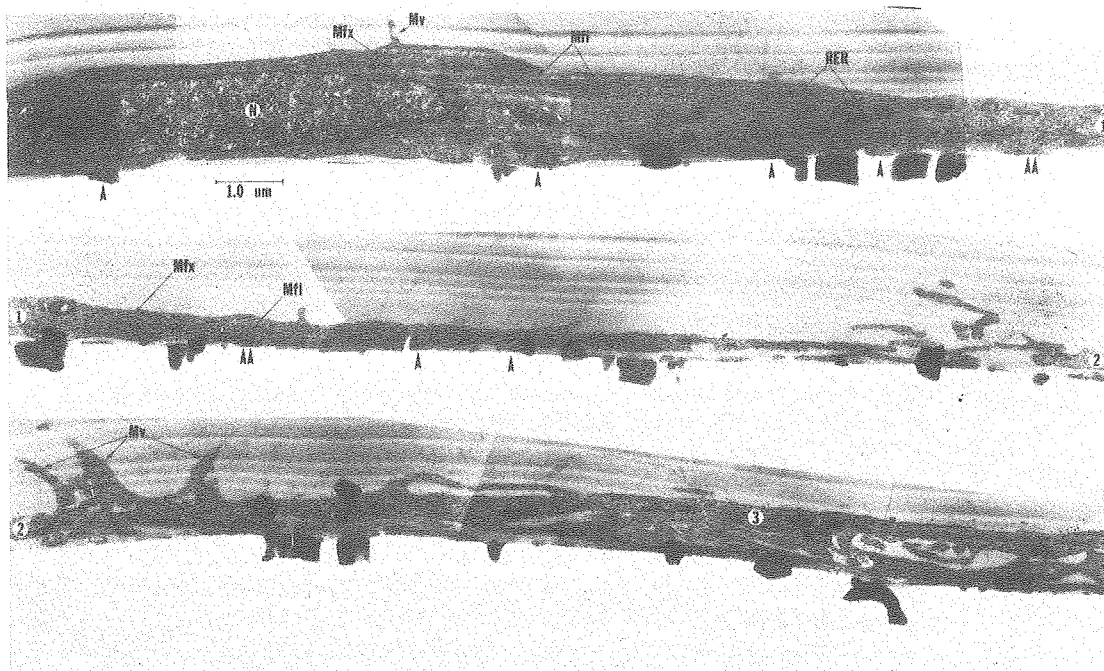


Fig. 42

XBB767 6286

Figure 43. Appearance of the cytoplasm of a typical Balb 3T3 A31 cell. The dark line (arrowheads) marks the position of the silicon monoxide substratum. LRB, lysosomal residual body; M, mitochondria; Mfl, microfilaments in longitudinal section; Mfx, cross-sectioned microfilaments; Mt, microtubules; Mv, microvilli; N, nucleus; RER, rough endoplasmic reticulum. Bar equals 0.2 μm . 70,000X.

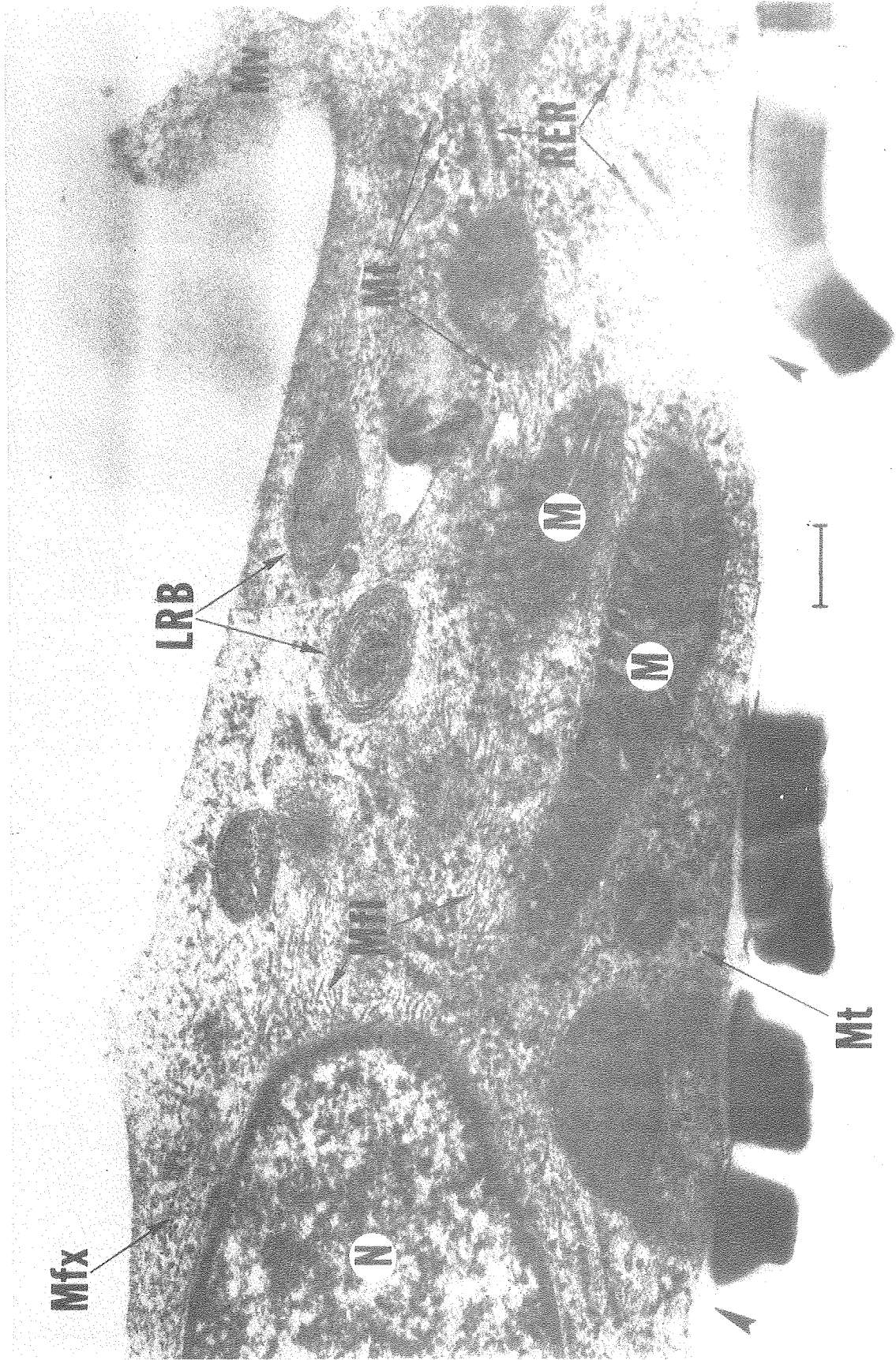


Fig. 43

XBB767 6275

correspond to the adhesion plaques described by Abercrombie et al. (1971) and Pegrum and Maroudas (1975). Certain of these regions displayed a condensation of electron-dense material parallel to the substratum.

There did not appear to be significant overlap of the nuclear regions of Balb 3T3 A31 cells, but there was a great deal of overlapping between the peripheral regions. In some places, this resulted in the stacking of peripheral extensions from four or five cells (Fig. 42). These peripheral sheets were in some cases observed to extend underneath the nuclei of neighboring cells. The presence of such extensive overlapping suggests that this kind of interaction probably involved more of the cellular surface area than did edge-to-edge interactions, interdigitation, or filopodial interactions. Numerous regions could be seen where the surfaces of these peripheral extensions approached each other closely, and other workers have found intermediate junctions in such locations (Cherry et al., 1975; Heaysman and Pegrum, 1973; Ross and Greenlee, 1966). Unfortunately, although the use of acetone rather than hydrofluoric acid to remove the silicon monoxide had improved the preservation of cytoplasmic membranes, the plasma membrane still could not be seen in any of the sections examined. For this reason, it was not possible to use these preparations to substantiate previous speculation regarding the formation of intermediate junctions in areas of cell interaction (Chapters 4 and 5). However, Spurr's embedding medium has been found to induce fading of plasma membranes in some cases (N. S. McNutt, personal communication; P. Satir, personal communication). If use of Spurr's medium is responsible for the poor preservation of the plasma membranes in these sections, then future studies using monolayers

embedded in situ utilizing more traditional embedding media such as Araldite or Epon may yield valuable information regarding the nature of the cell junctions in regions of interaction between fibroblasts.

Chapter 7

Effect of Glycerol on Balb 3T3 Cell Membranes;

Preliminary Results

The discovery by Gilula et al. (1975) that glycerol solutions aggregate IMP in nontransformed but not in transformed cultures of fibroblasts suggests that glycerol may be used as a perturbing agent for the purpose of revealing hidden alterations in membrane structure. The results of preliminary studies on in situ freeze-fracture of glycerinated cultures are presented in this chapter, together with some conclusions regarding the effects of other components of the incubation medium on cell morphology.

Materials and Methods

Incubation of cell monolayers in different buffer systems. The following buffer systems were tested for their ability to maintain pH and cell monolayer stability during incubation of cell monolayers in air at 37°C: 1) isotonic tris buffer (see Chapter 3), 2) saline G (see Chapter 3), 3) DME, 4) DME without Phenol Red but with 25 mM HEPES buffer, and 6) DME without bicarbonate, Phenol Red, or vitamins, but with 100 mM HEPES buffer (hereafter referred to as HEPES-DME). All buffer systems had an osmotic concentration of approximately 300 milliosmolal. Phenol Red and vitamins were removed from the DME-based buffer systems because these buffer systems were also intended for use in other fluorometric experiments being carried out in the laboratory, and these substances are themselves fluorescent.

In Experiment I, FNE cells were grown to high density in DME supplemented with 10% newborn calf serum in 72 35 mm Falcon plastic dishes.

FNE cells are a highly rounded line of SV40-transformed Balb 3T3 clone A31 cells, obtained from Dr. Helene Smith. The medium was removed from the cells, the plates were washed twice with isotonic tris buffer, and a Polaroid photograph was taken to use as a standard for evaluation of changes in cell morphology. The plates were divided into six groups of twelve, and each group was incubated with 2.0 ml per dish of one of the above buffer systems. The plates were incubated at 37°C in a non-CO₂ incubator, and time points were taken after 15, 30, 45, 60, and 120 min. of incubation, with an additional time point being taken at 24 hr.

At each time point, the cell monolayer was photographed, the buffer was removed from two plates, and 2.0 ml trypsin were added to each plate. The pH of the buffer was measured, and the buffer was transferred to tubes containing 8 ml Isoton. The trypsinized cells were removed to tubes containing 8 ml Isoton and both the cells detached into the buffer and the cells removed from the plate were counted (see Chapter 3). The reported values for cell counts and pH are the average of values for both dishes. The fraction of cells detached from the dish during incubation was calculated from the formula:

$$\frac{\text{Cells detached}}{\text{Total cell number}} = \frac{\text{Cells in buffer}}{\text{Cells on dish} + \text{cells in buffer}}$$

In Experiment II, 60 35 mm dishes of Balb 3T3 cells were seeded at 5×10^4 cells/plate and allowed to reach saturation density. The conditions of Experiment I were duplicated using buffer systems 1, 3, and 6 (20 plates per buffer) and time points at 15, 30, 45, 60, 75, 90, 105, and 120 min. and 24 hr.

Incubation in glycerol. Balb 3T3 cells were grown to confluency on silicon monoxide coated coverslips, Balzers carriers, and coated or

uncoated Falcon or Corning plastic dishes depending on whether they were to be used for HRSEM, freeze-fracture, or light microscopy. In each experiment, cultures were first washed twice with HEPES-DME and then divided into two groups, one of which was incubated for 35-45 min. HEPES-DME, and the other which was incubated with glycerol. The glycerol series used here was the same as that employed by Gilula et al. (1975), but with HEPES-DME substituted for phosphate-buffered saline (PBS) as the buffer vehicle, i.e., 5% glycerol in HEPES-DME for 5 min., 10% glycerol in HEPES-DME for 10 min., 20% glycerol in HEPES-DME for 20-30 min. Solutions and culture dishes were kept in a water bath at 37°C during the incubation. All HEPES-DME and glycerol solutions had a pH between 7.1 and 7.3 at this temperature. At regular intervals during incubation, cultures were photographed in Tri-X film using a Nikon inverted tissue culture microscope with 100X phase contrast optics. After incubation was completed, specimens were fixed and processed for HRSEM (see Chapter 4) or freeze-fracture (see Chapter 5) without any intermediate washing, i.e. the 2% glutaraldehyde fixative was added directly to the 20% glycerol solution, and the glycerol/fixative mixture was then gradually replaced by pure fixative. The results described here are based on 128 photographs of living cells from six separate preparations, HRSEM photographs from two preparations, and in situ freeze-fracture replicas of 33 cells taken from one preparation.

Results

Incubation in different buffer systems. Since the proposed studies required cultures to be incubated for extended periods of time outside of a CO₂ incubator, it was necessary to develop a buffer system that

would maintain native cell morphology and medium pH under these conditions. Some preliminary experiments showed that incubation of monolayer cultures in simple isotonic buffers resulted in severe morphological changes and detachment of many cells from the dish within 30 min., and that alterations in cell morphology were particularly severe at basic pH. For this reason, FNE cells were chosen to evaluate the effect of buffers because this cell line is highly rounded, weakly attached to the dish, and should be very sensitive to any deleterious effects of the buffer.

Although isotonic tris buffer (Fig. 44) maintained medium pH adequately, it proved to be unsuitable for even short-term incubations, because cells rapidly rounded up and began to detach from the dish. Saline G (Fig. 45) maintained monolayer stability much better than did isotonic tris buffer, with relatively few cells being lost after 2 hr. of incubation. DME (Fig. 46) was unsuitable because it very rapidly became basic when exposed to air. Similar difficulties with pH changes occurred with both formulations of DME buffered with 25 mM HEPES (Figs. 47 and 48). Apparently the buffering capacity of the 25 mM HEPES was insufficient to counteract the basicity of the bicarbonate in DME. Replacement of the bicarbonate in DME with 100 mM HEPES buffer (Fig. 49) resulted in a stable pH and minimal cell detachment. This mixture appeared to be the best of the modified DME formulations. Although saline G also maintained the monolayer well, further experiments were done with HEPES-buffered DME rather than saline G because the DME formulations were closer to the normal growth medium of the cultures.

Incubation of Balb 3T3 cells with buffer systems 1, 3, and 6 produced results similar to those obtained with FNE cells. Balb 3T3 cells

Figure 44. Changes in the pH (·-·-·) and the fraction of cells detached from the dish (o-o-o) during incubation of FNE cells with isotonic tris buffer.

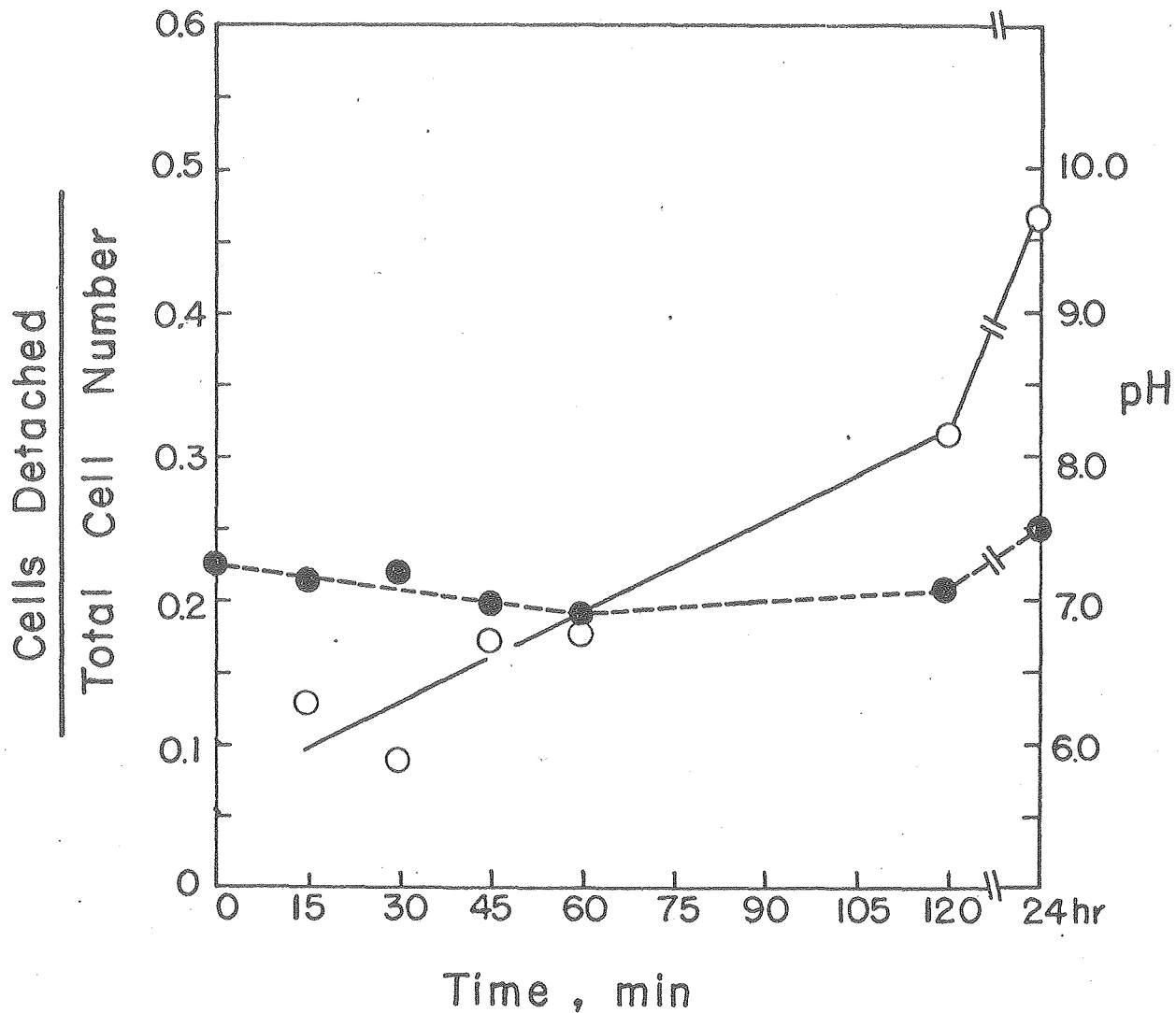


Figure 45. Changes in the pH (·-·-·) and the fraction of cells detached from the dish (o-o-o) during incubation of FNE cells with saline G.

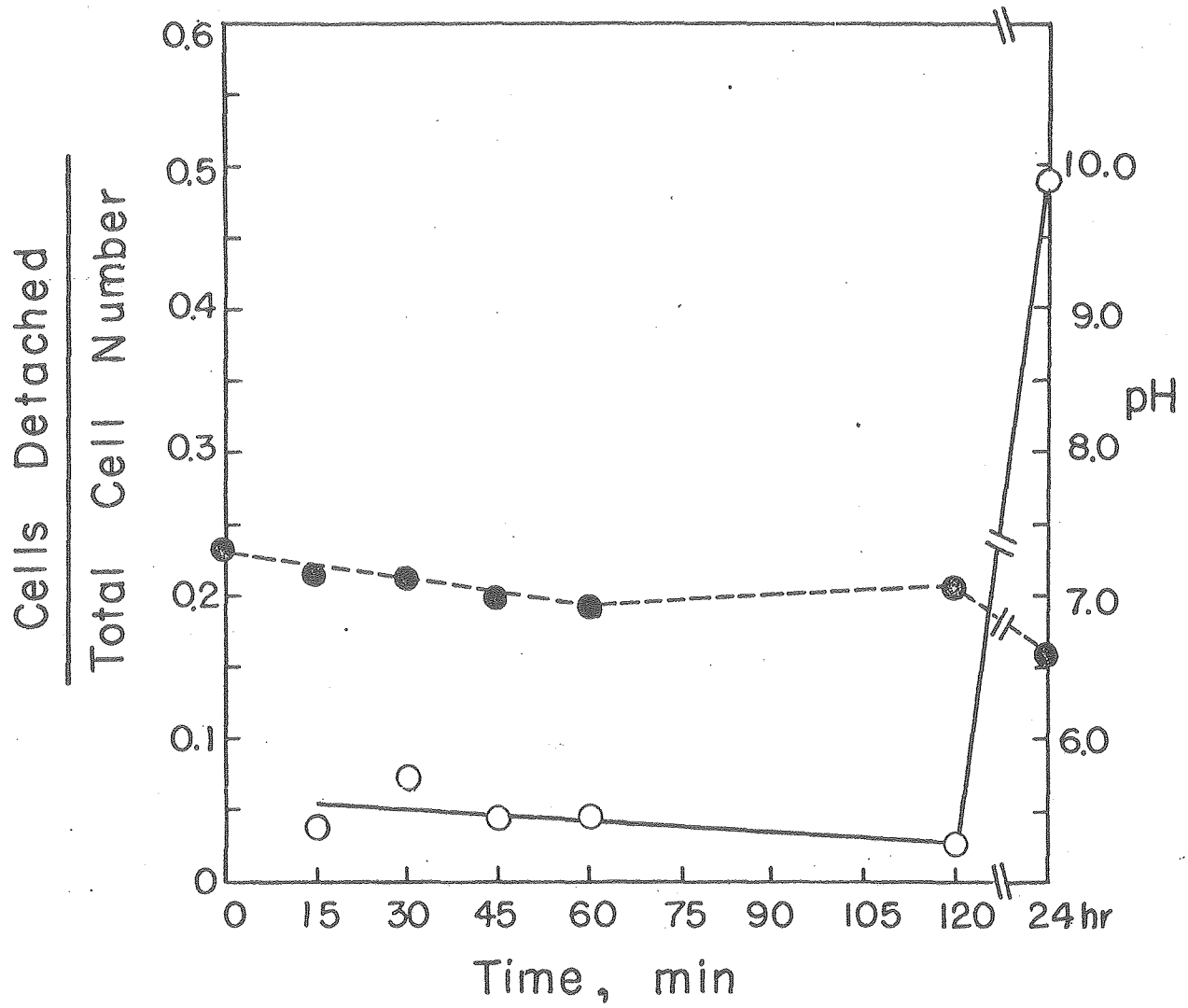


Figure 46. Changes in the pH (·-·-·) and the fraction of cells detached from the dish (o-o-o) during incubation of FNE cells with DME.

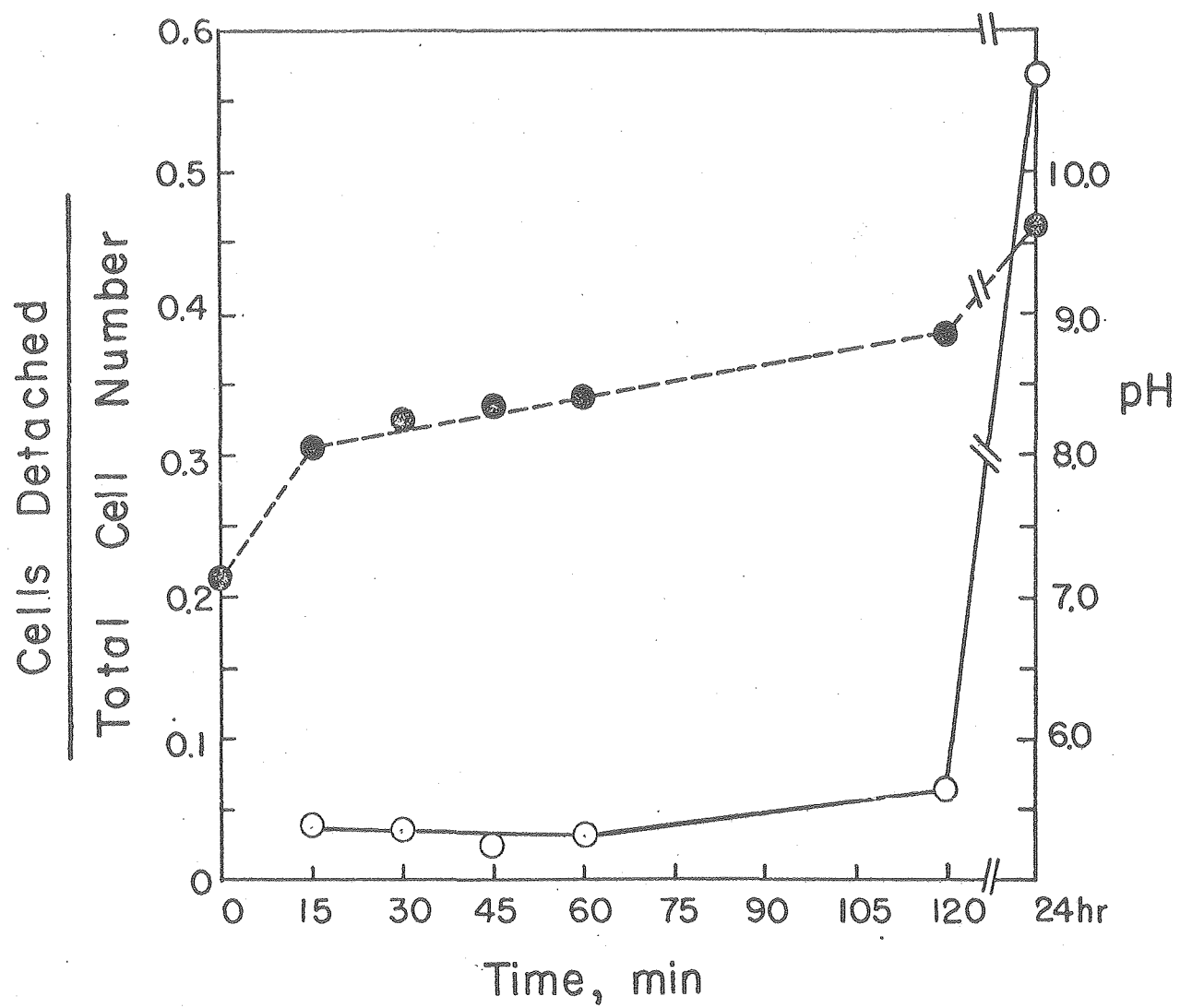


Figure 47. Changes in the pH (---) and the fraction of cells detached from the dish (o-o-o) during incubation of FNE cells with DME containing 25 mM HEPES but minus Phenol Red.

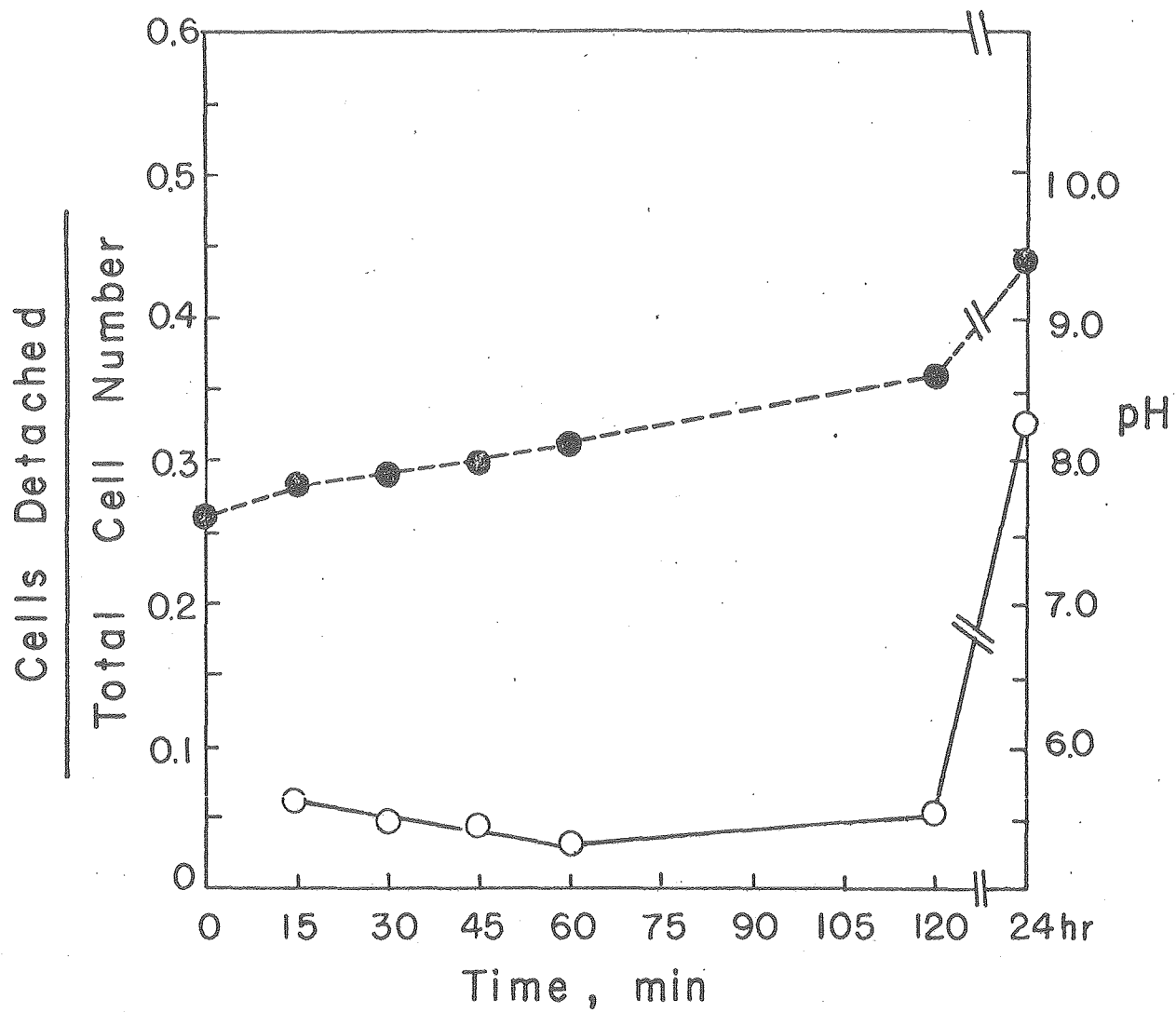


Figure 48. Changes in the pH (·-·-·) and the fraction of cells detached from the dish (o-o-o) during incubation of FNE cells with DME containing 25 mM HEPES but minus Phenol Red and vitamins.

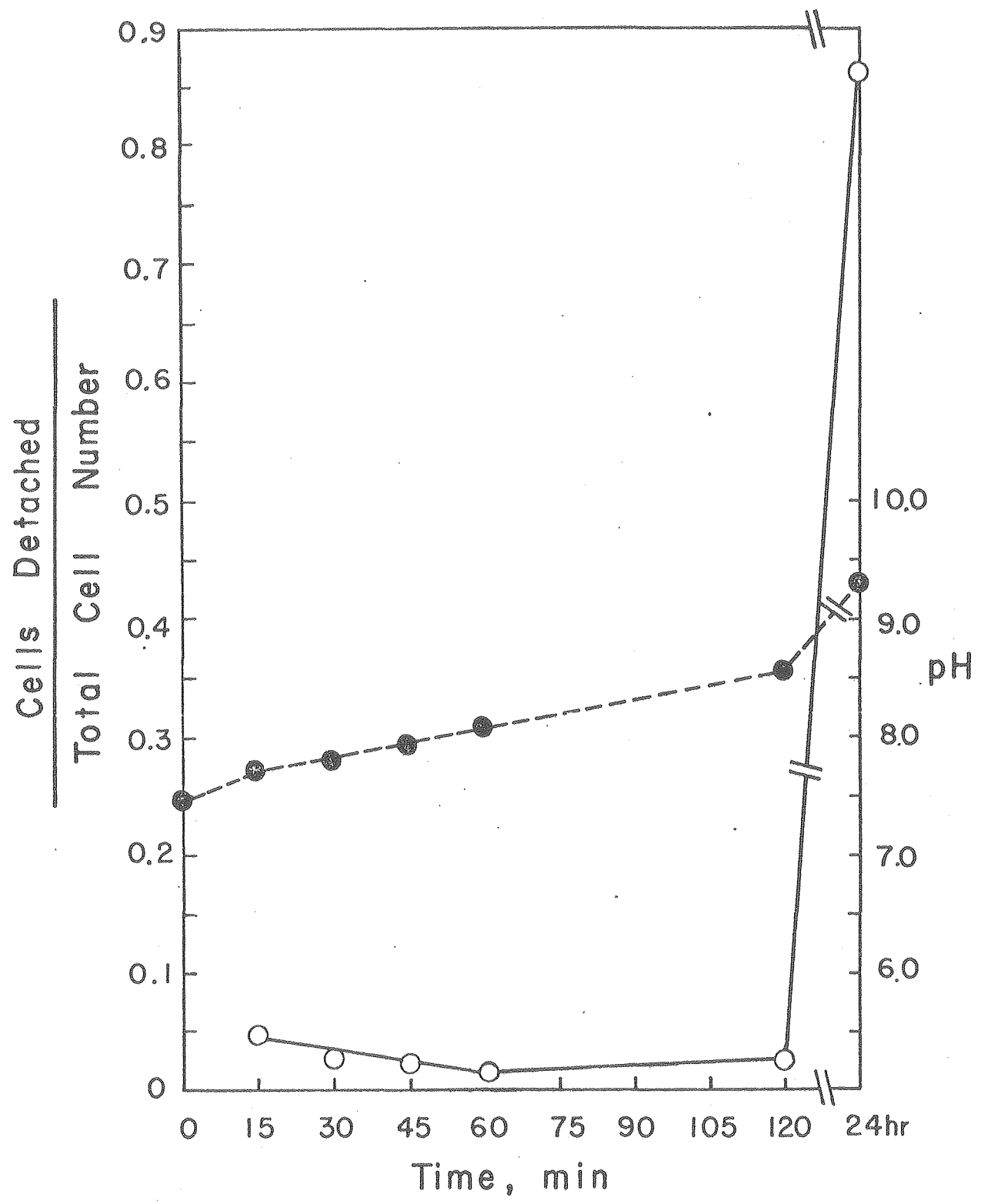
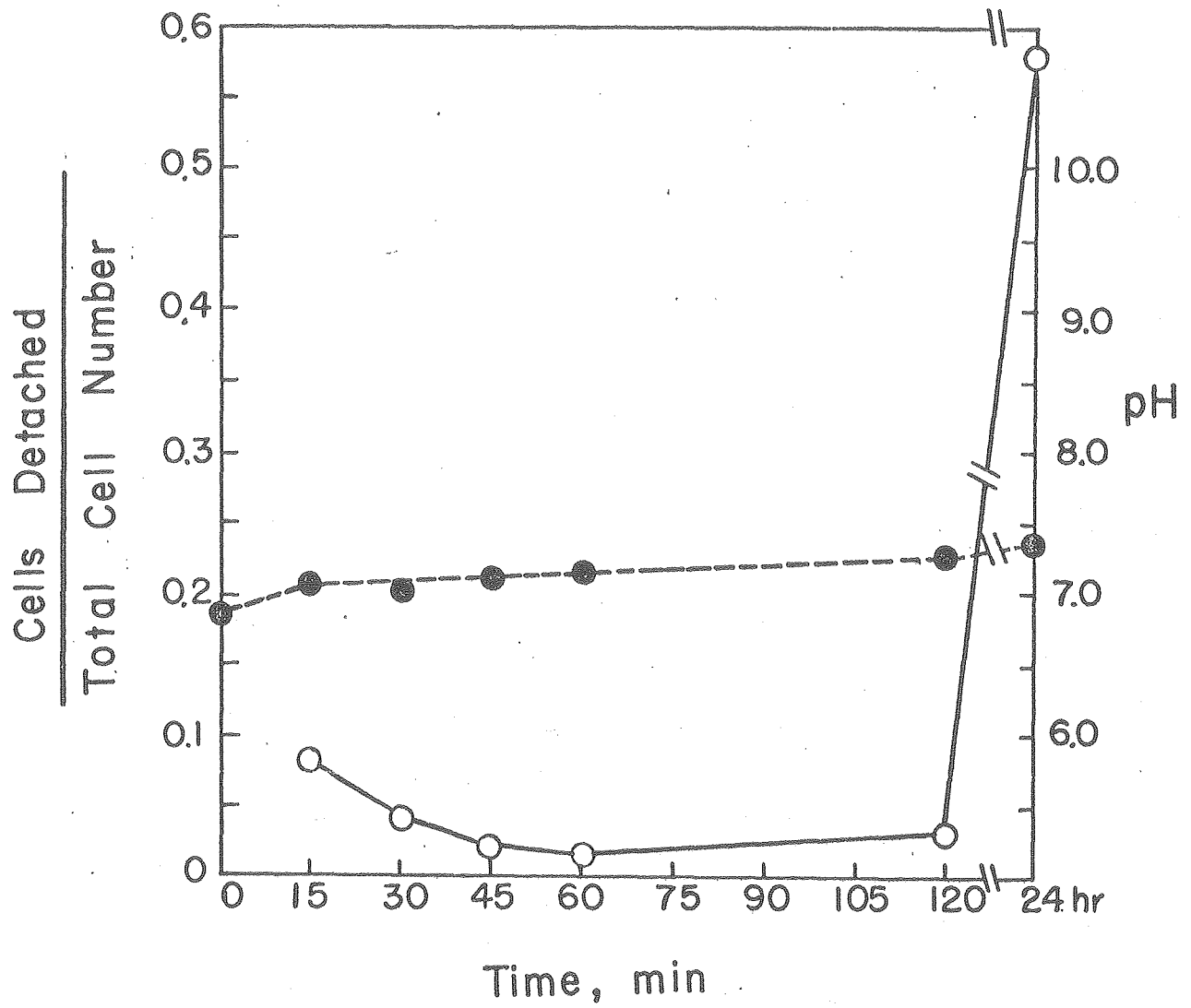


Figure 49. Changes in the pH (·-·-·) and the fraction of cells detached from the dish (o-o-o) during incubation of FNE cells with DME containing 100 mM HEPES but minus Phenol Red, vitamins, and bicarbonate.



rounded up and came off the plates very quickly in isotonic tris buffer (Fig. 50). The scatter in the cell counts in Fig. 50 is due to the fact that cells in isotonic tris buffer were only weakly attached to the substratum and could be dislodged by even gentle vibrations. In spite of the basicity of the medium when cells were incubated with DME alone (Fig. 51), there was, surprisingly, little morphological change in cultures even after 2 hr. of incubation. Apparently the extra components in DME protected the culture against the damaging effects of basic pH. Balb 3T3 cells incubated in DME buffered with 100 mM HEPES (Fig. 52) appeared normal even after 2 hr., and this solution was accordingly chosen as a buffer vehicle for the glycerol incubation studies. All of the six formulations caused extensive cell rounding and detachment by 24 hr.

Incubation in HEPES-DME and glycerol/HEPES-DME. Although treatment with HEPES-DME produced little alteration in the morphology of Balb 3T3 cells during Experiment II, further studies with cultures incubated in HEPES-DME and the glycerol/HEPES-DME series showed that the effect of these solutions on Balb 3T3 cells was quite variable. With three of the six cultures photographed during incubation with HEPES-DME, morphological changes after 35 min. were minimal and the treated dishes could easily have been mistaken for untreated cultures. In two of the preparations, a number of the cells began to round up within 10 min., and by the time this process was completed (20 min.), a sizable fraction of the cells had rounded up to various degrees (Fig. 53). The other preparation was intermediate in appearance between these two extremes.

The appearance of monolayers incubated in glycerol/HEPES-DME was more uniform. The cytoplasm of glycerinated cells had a characteristic granular appearance, and there was a condensation of material into the

Figure 50. Changes in the pH(-----) and the fraction of cells detached from the dish (o-o-o) during incubation of Balb 3T3 cells with isotonic tris buffer.

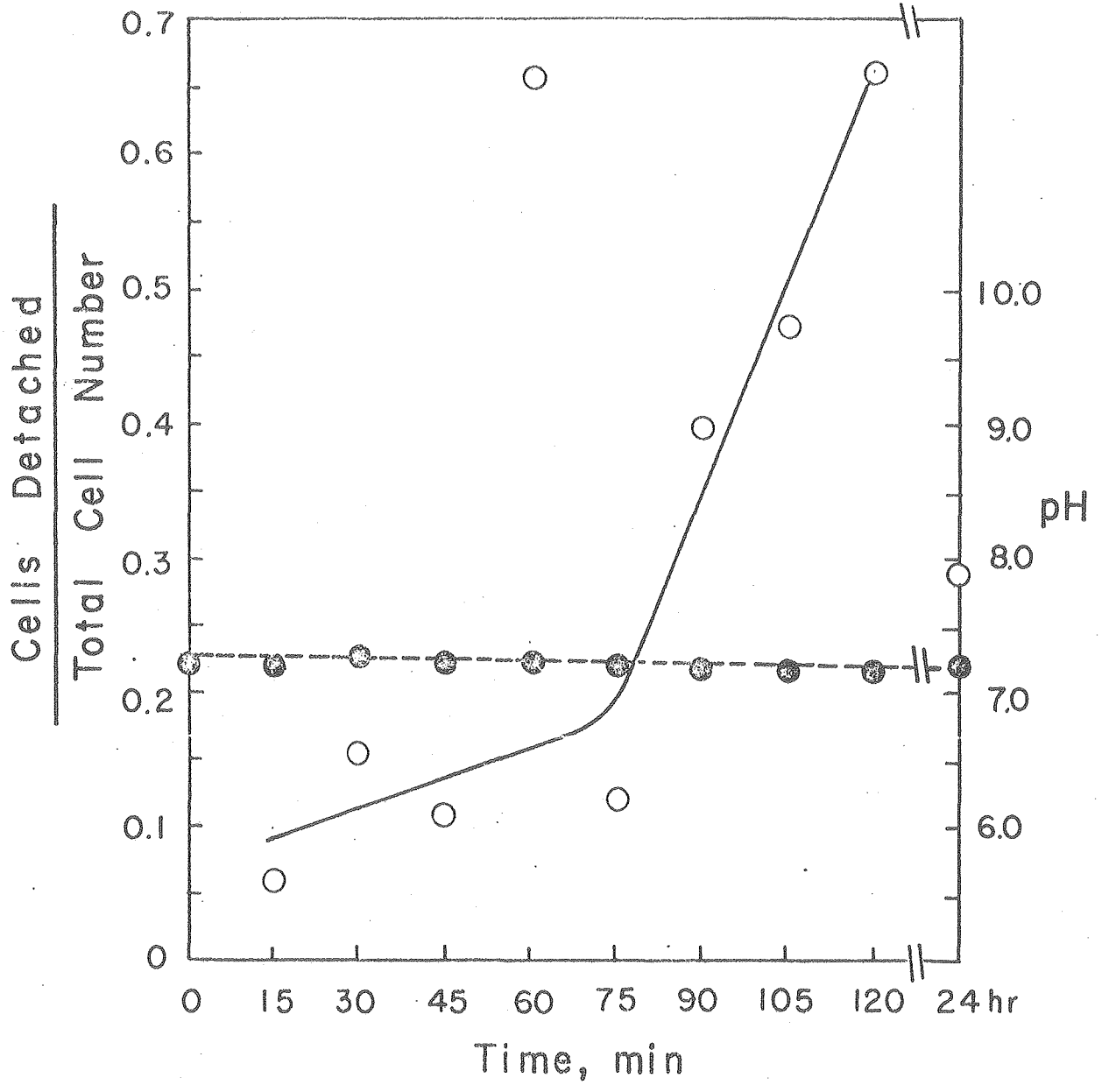


Figure 51. Changes in the pH(·-·-·) and the fraction of cells detached from the dish (o-o-o) during incubation of Balb 3T3 cells with DME.

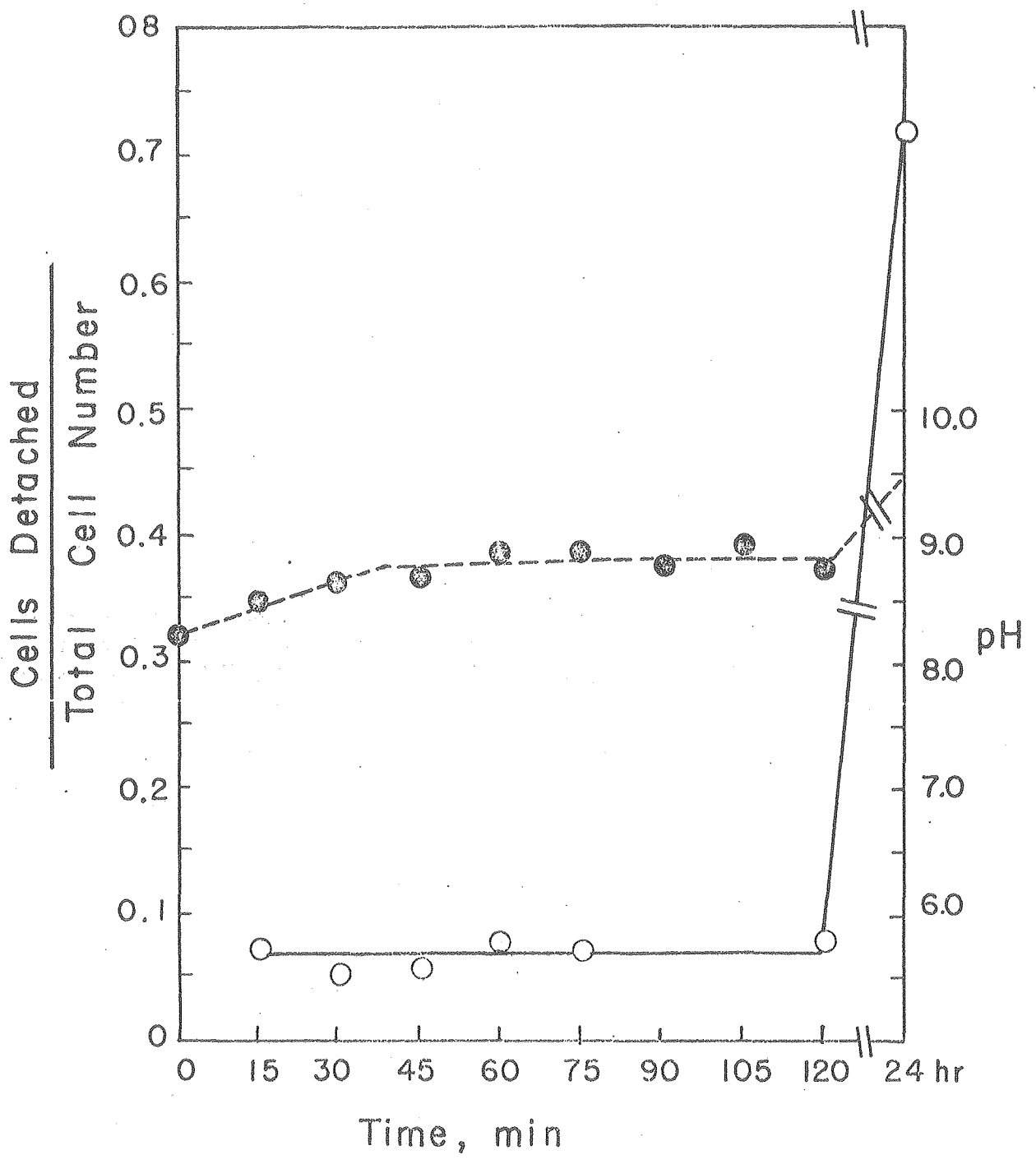


Figure 52. Changes in the pH (·-·-·) and the fraction of cells detached from the dish (o-o-o) during incubation of Balb 3T3 cells with DME containing 100 mM HEPES but minus Phenol Red, vitamins, and bicarbonate.

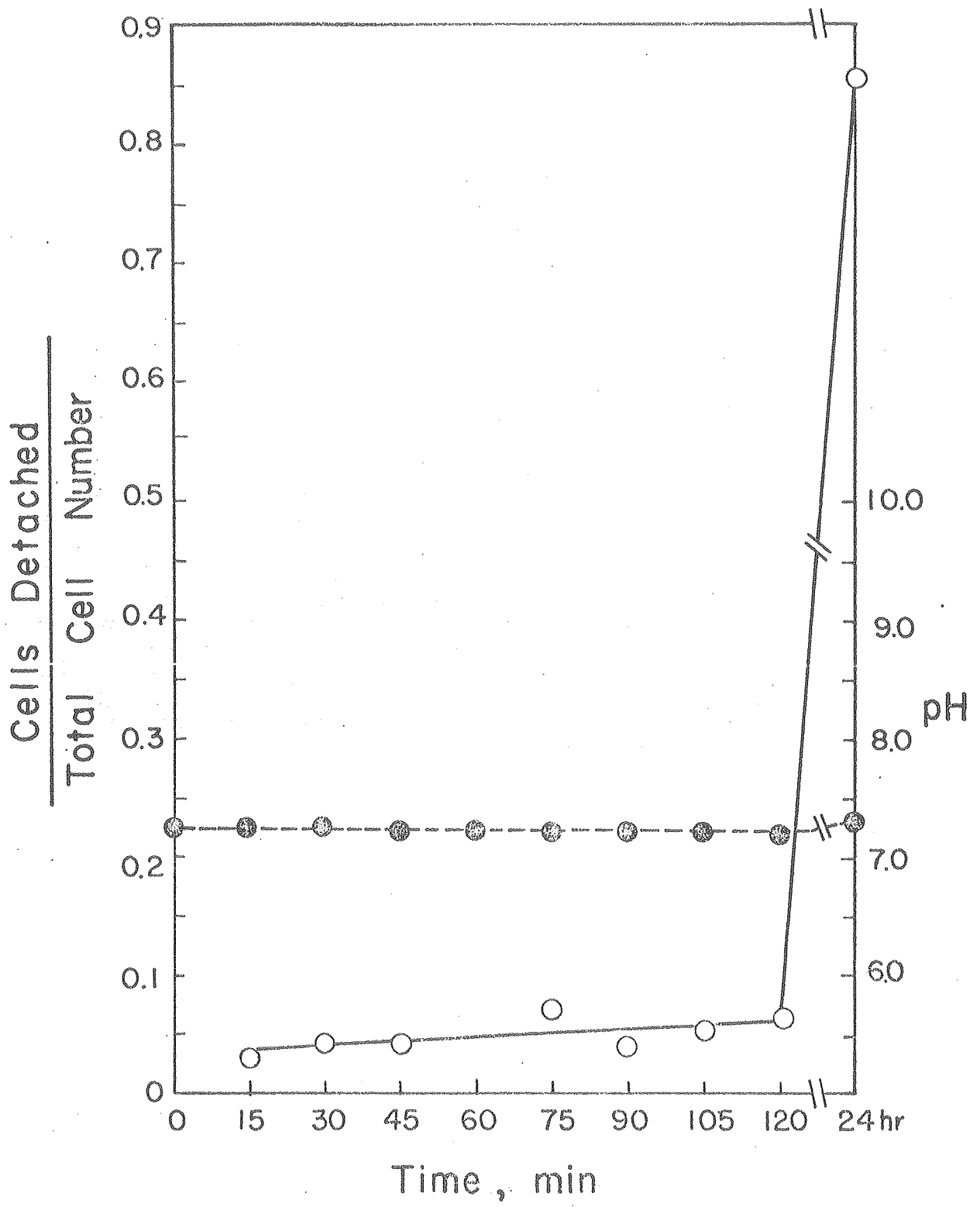


Figure 53. Balb 3T3 fibroblasts photographed during incubation at 37°C with HEPES-DME (left) and glycerol/HEPES-DME (right). The number of minutes elapsed after the beginning of incubation is indicated on each photograph. Cells for the zero time point were photographed before the medium was removed. Cultures incubated with glycerol/HEPES-DME in this particular experiment were transferred from 5% to 10% glycerol at 6 min., from 10% to 20% glycerol at 18 min., and were fixed after 45 min. total incubation. All of the scanning electron micrographs shown in this chapter were taken using the preparations shown here. 100X.

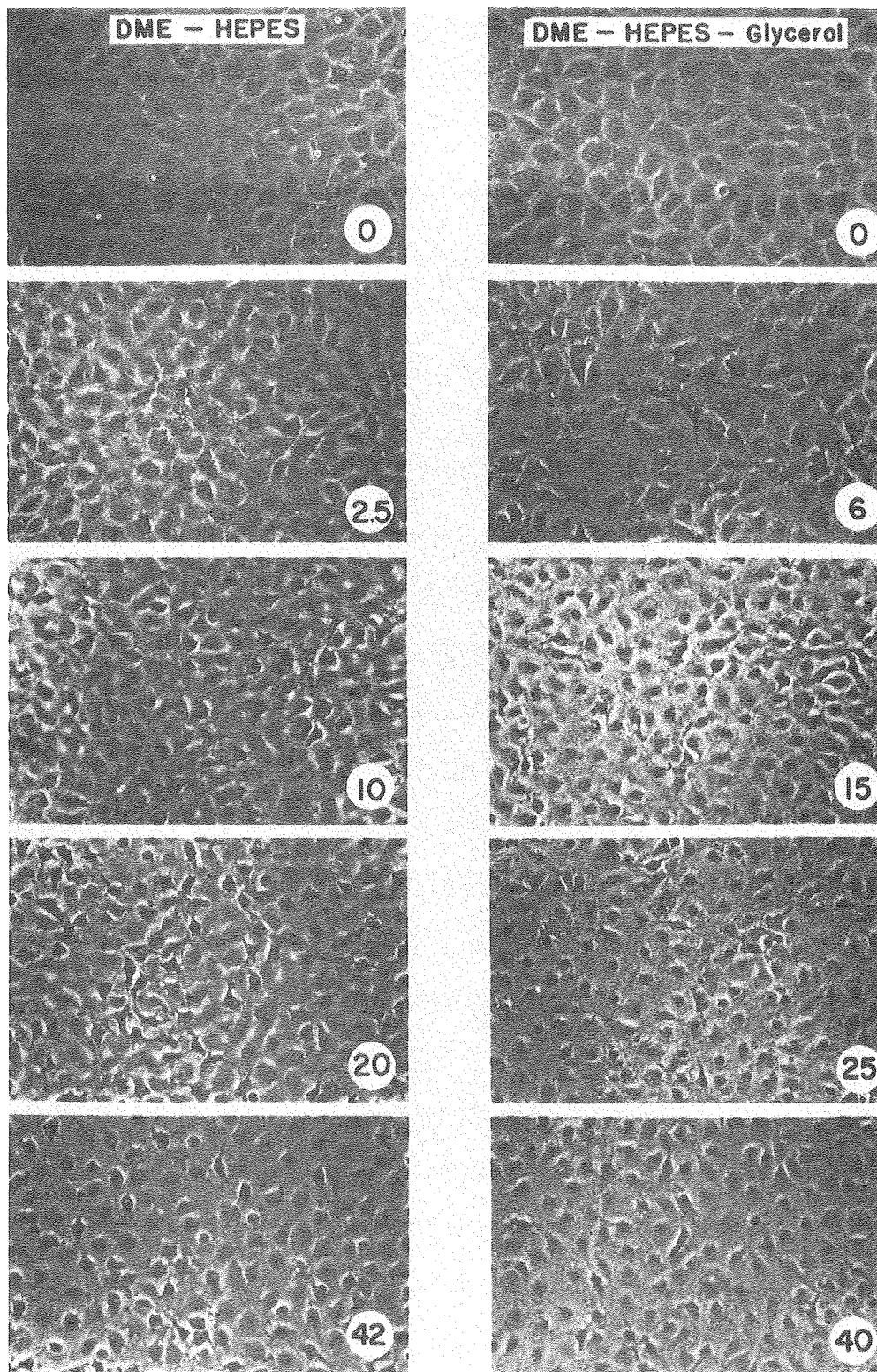


Fig. 53

XBB767 6587

cell center, so that the perinuclear region appeared as a dark central spot (Fig. 53). In preparations where rounding up of the cells occurred, it was generally much less pronounced in glycerinated cultures than in HEPES-DME-treated cells. The time course of these events was similar to that observed for cultures incubated in HEPES-DME alone, with morphological alterations beginning by 6-10 min. and being essentially complete by 20-25 min. There was no satisfactory explanation for the variability in the effect of the HEPES-DME and glycerol/HEPES-DME solutions, since the degree of morphological alteration did not seem to be correlated with the age of the culture, the substratum (silicon monoxide, Falcon plastic, or Corning plastic) or the age of the solutions used.

These observations were confirmed by HRSEM. The HRSEM data consisted of ninety-two photographs at varying magnifications of the preparation shown in Fig. 53 (including all of the micrographs shown here), plus eighteen photographs of one culture in which little morphological change could be seen by light microscopy.

Cells incubated in HEPES-DME displayed various degrees of rounding up (Fig. 54). Rounded cells (Fig. 54, Cell 5; Fig. 55) were stellate in appearance, with a roughly spherical cell body attached to the dish by numerous slender radiating processes. The cell body was covered with blebs 0.5-1.5 μm in diameter; these usually appeared in large numbers only on fully rounded cells. The majority of the cells in HEPES-DME treated cultures remained flattened onto the substratum (Fig. 54, Cell 1; Fig. 56) but without exception even these cells displayed a very characteristic pattern of retraction of the peripheral regions. Retraction appeared to begin at the cell periphery, where the withdrawing edge formed a web of filopodia and left behind numerous foot-like pads of cytoplasm

Figure 54. Scanning electron micrograph of Balb 3T3 cells after 45 min incubation in HEPES-DME. Cell shape varied from flattened (Cell 1) to stellate (Cell 5). Cells in the process of rounding up (Cells 2, 3, and 4) left behind foot-like pads of cytoplasm which were attached to the cell body by long processes. 1300X.

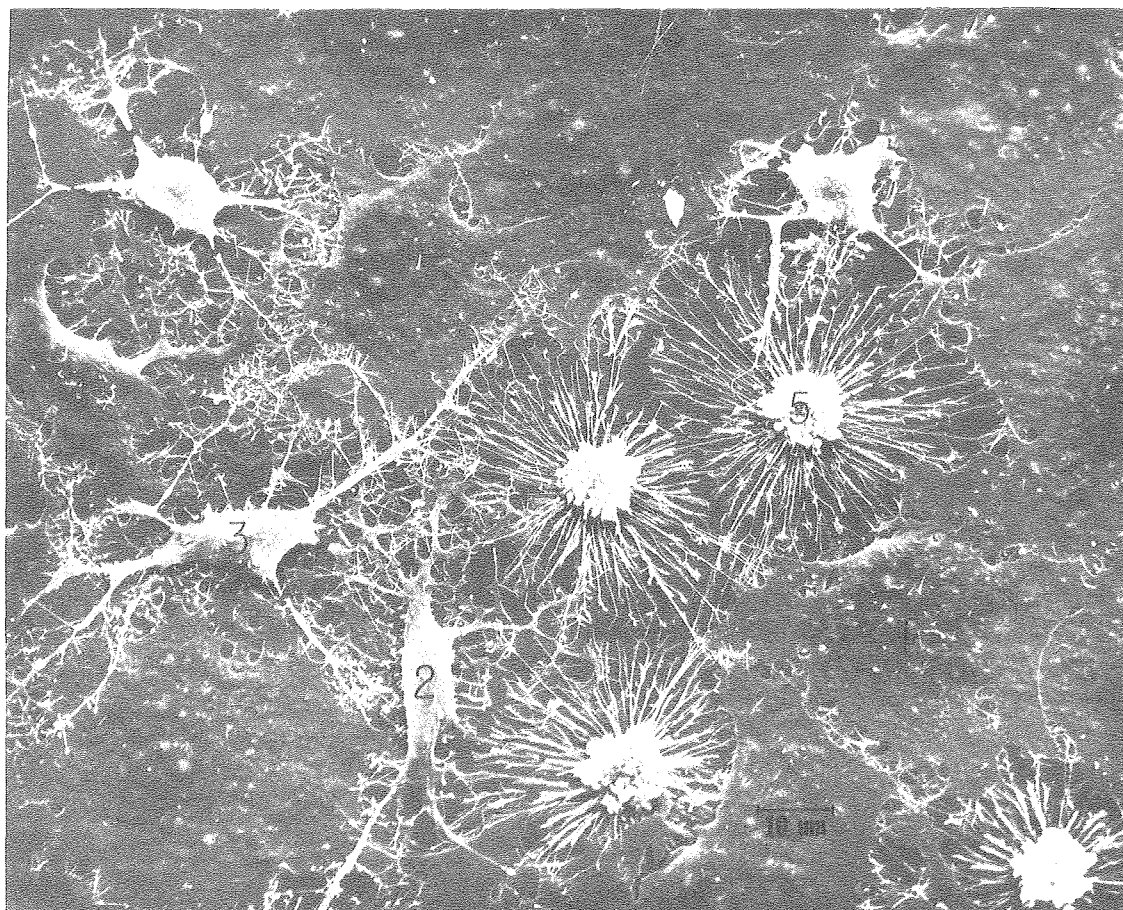


Fig. 54

XBB767 6505

Figure 55. Typical fully rounded cell from a preparation incubated 45 min. in HEPES-DME. 3400X.

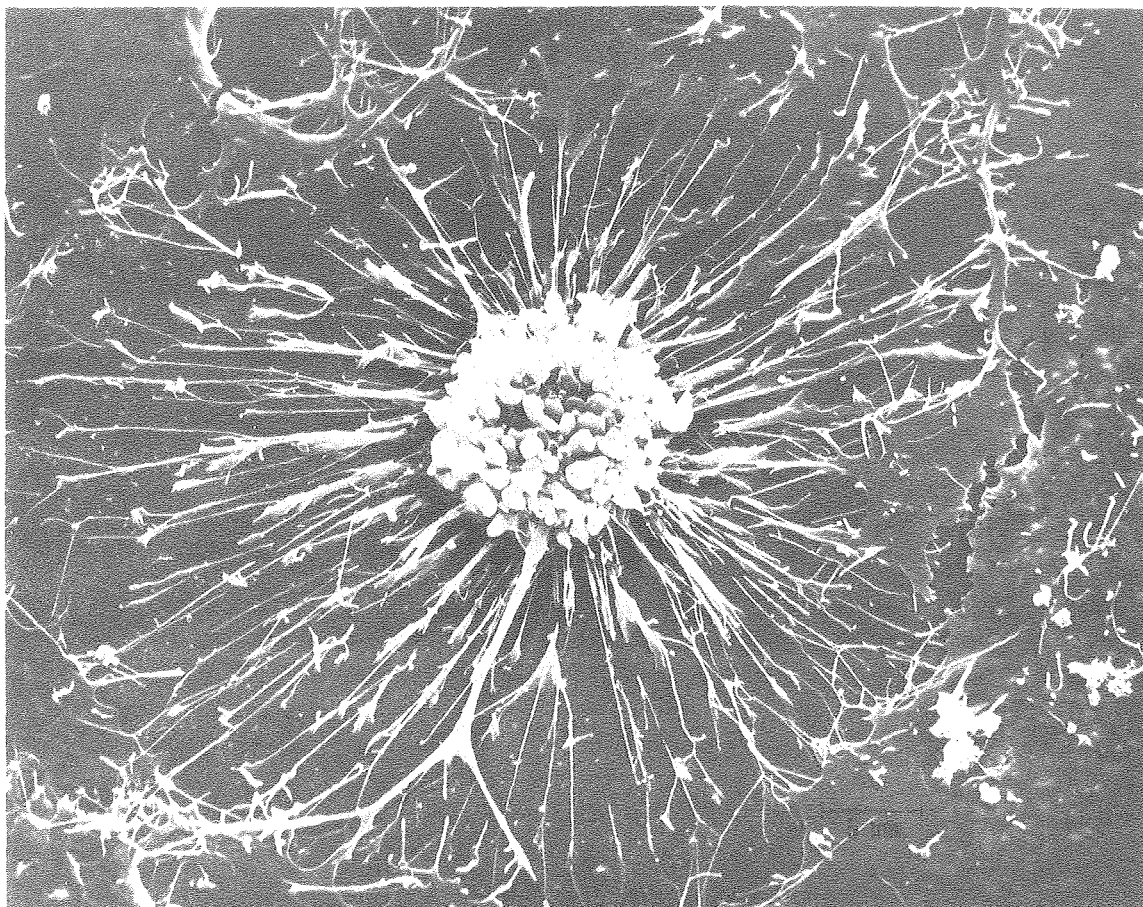


Fig. 55

XBB767 6503

Figure 56. Typical flattened cell from a preparation incubated 45 min. in HEPES-DME. Some retraction of the peripheral cytoplasm has occurred, resulting in a web of filopodia and cytoplasmic processes around the cell periphery. A patch of microvilli (arrowhead) can be seen on the upper surface of a neighboring cell. 1500X.

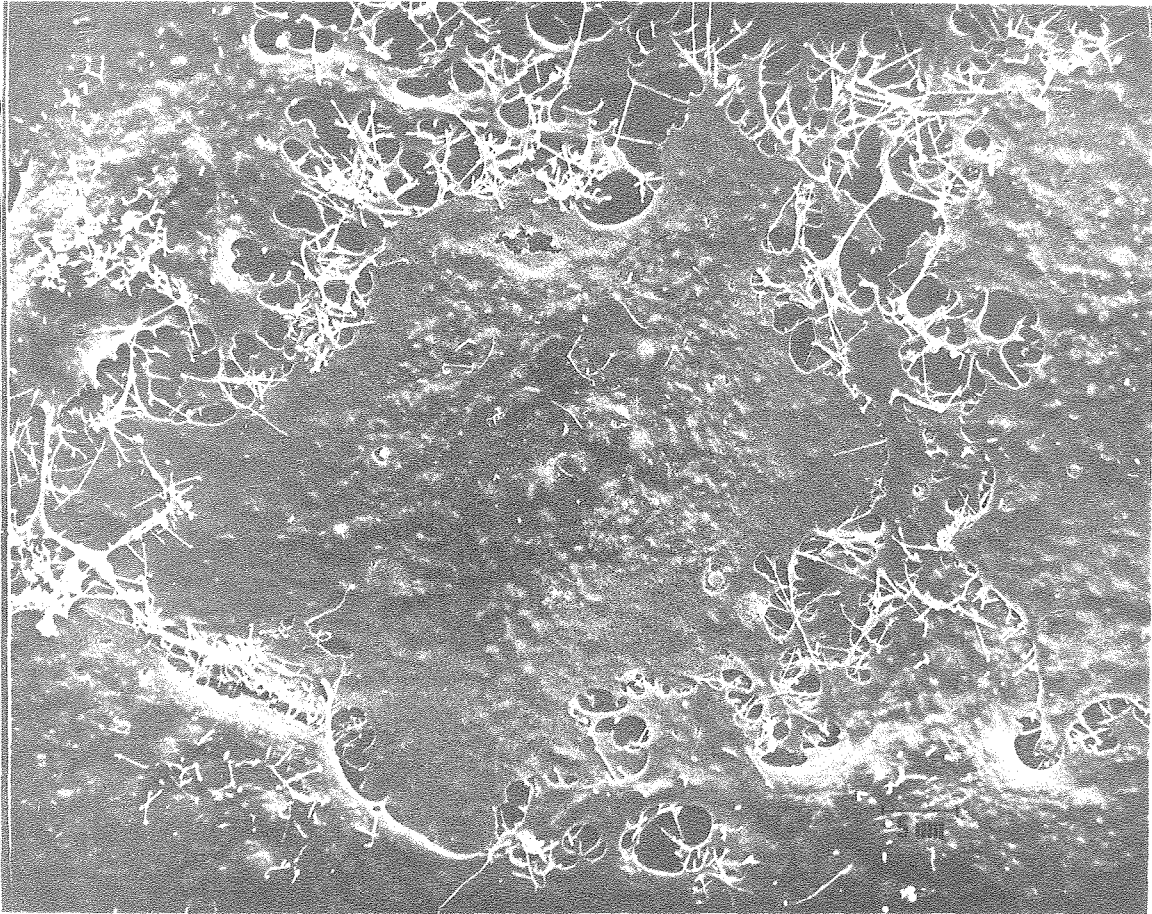


Fig. 56

XBB767 6504

(possibly remnants of adhesion plaques) which were attached to the cell body by slender processes. With partially rounded cells (Fig. 54, Cells 2, 3, and 4) these processes often extended for long distances. These morphological alterations were instructive in that they revealed the extensive overlapping which occurred in these "monolayer" cultures. In cases such as Cell 3 of Fig. 54, for example, it is clear that the cell has extended processes completely underneath its immediate neighbors and is interacting with cells some distance away. HRSEM observations on the culture which showed little morphological alteration by light microscopy revealed that, although this culture had fewer rounded cells, the flattened cells had similar morphology to those shown here and displayed the same pattern of peripheral retraction as did cells from more obviously altered cultures.

Glycerinated cultures (Fig. 57) had a majority of flattened cells (Fig. 58) and few rounded cells (Fig. 59). The nuclear region of flattened cells was typically raised up into a gentle hump, which probably corresponded to the dark central spot seen with the phase contrast microscope (Fig. 53). Varying numbers of microvilli were present on the upper cell surface; these were sometimes concentrated into a patch over the nucleus. Large vesicular stomata 0.2 - 0.8 μm in diameter were fairly common in the membranes of glycerinated cells. Unlike HEPES-DME treated monolayers, where peripheral retraction had separated most of the regions of cell interaction, glycerinated cells displayed overlapping and interdigitating regions, as well as considerable numbers of presumptive intermediate junctions (Fig. 60) which seemed similar in size and distribution to those described in Chapter 4. However, presumptive intermediate junctions in glycerinated cultures possessed none of the short

Figure 57. Balb 3T3 cells after incubation for 45 min. in glycerol/HEPES-DME. Retraction of the cell periphery is much less pronounced than with HEPES-DME alone. The majority of cells are flattened (Cell 1), with a central hump over the nucleus. Stubby microvilli, common on the upper cell surface, are sometimes concentrated into a patch over the nucleus (Cell 3). A few rounded cells (Cell 2) occurred in glycerinated cultures, but they were much less common than in cultures treated with HEPES-DME alone. Cells 1 and 2 are shown at higher magnification in Figs. 58 and 59, respectively. 1200X.

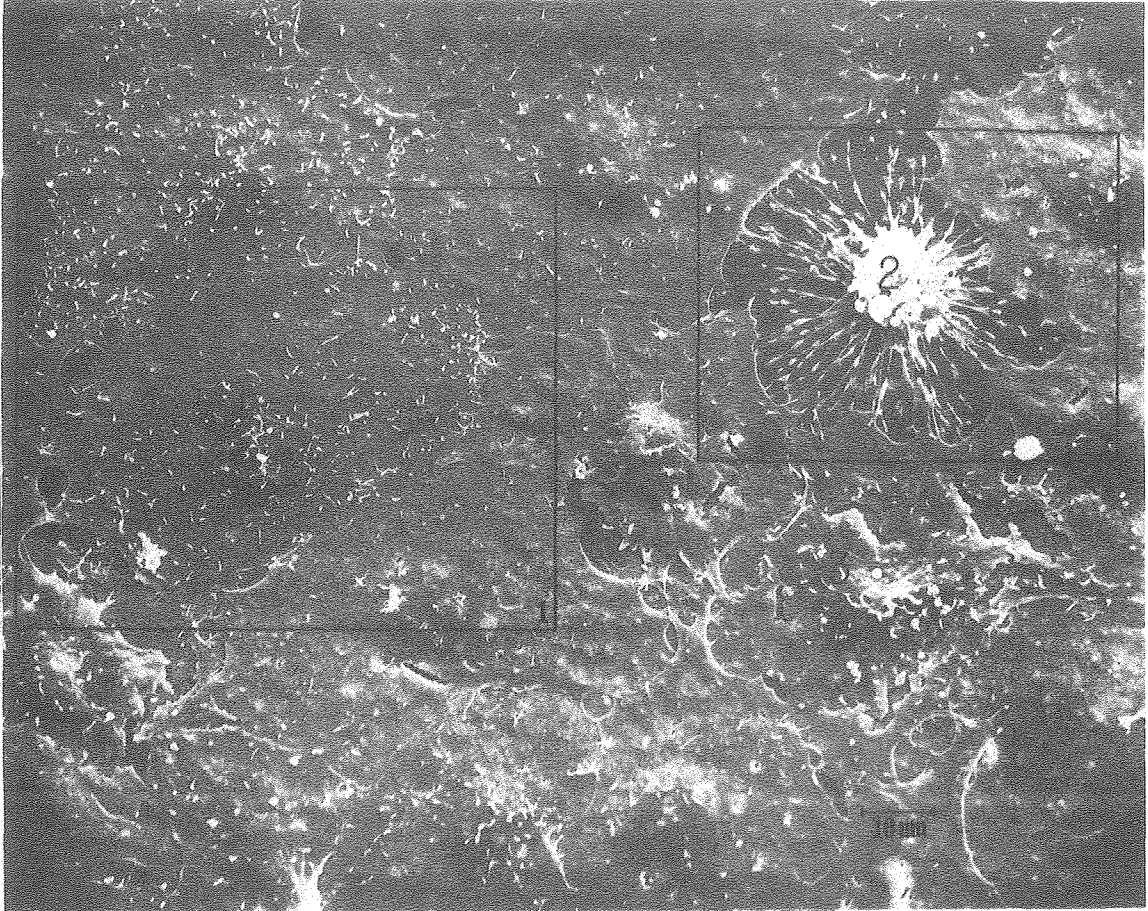


Fig. 57

XBB767 6502

Figure 58. Higher magnification view of Fig. 57, showing a typical flattened cell from a culture incubated 45 min. in glycerol/HEPES-DME. Cells such as this one retain many of the interactions with neighboring cells, but the numerous filopodia which occur around the periphery of untreated (Fig. 20) or HEPES-DME incubated cells (Fig. 56) are absent and may have retracted into stubby knobs (arrowheads). The areas marked 1 and 2 are shown at higher magnification in Figs. 61 and 60, respectively. 2500X.

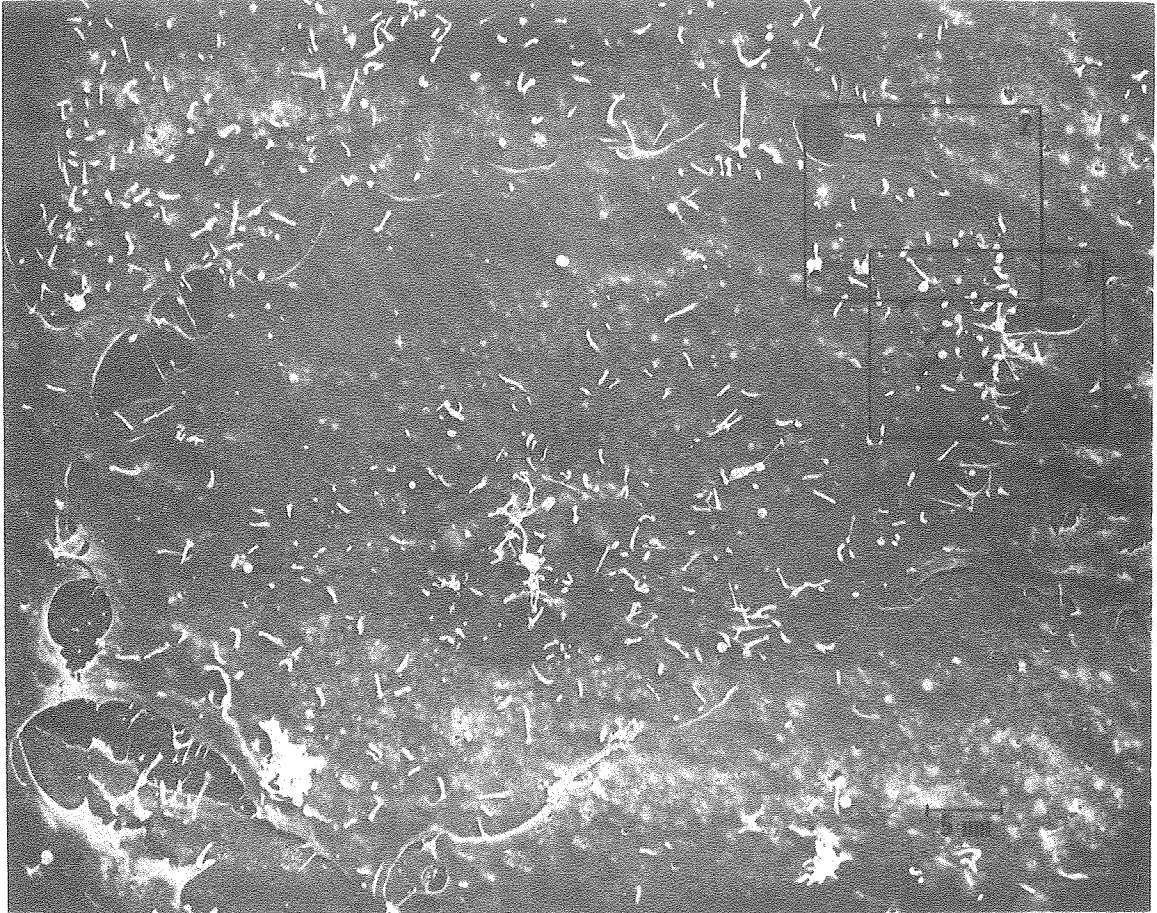


Fig. 58

XBB767 6500

Figure 59. Higher magnification view of Fig. 57, showing a typical rounded cell. The plasma membrane of this cell appears rougher and more porous than that of the unglycerinated cell shown in Fig. 55. 3000X.

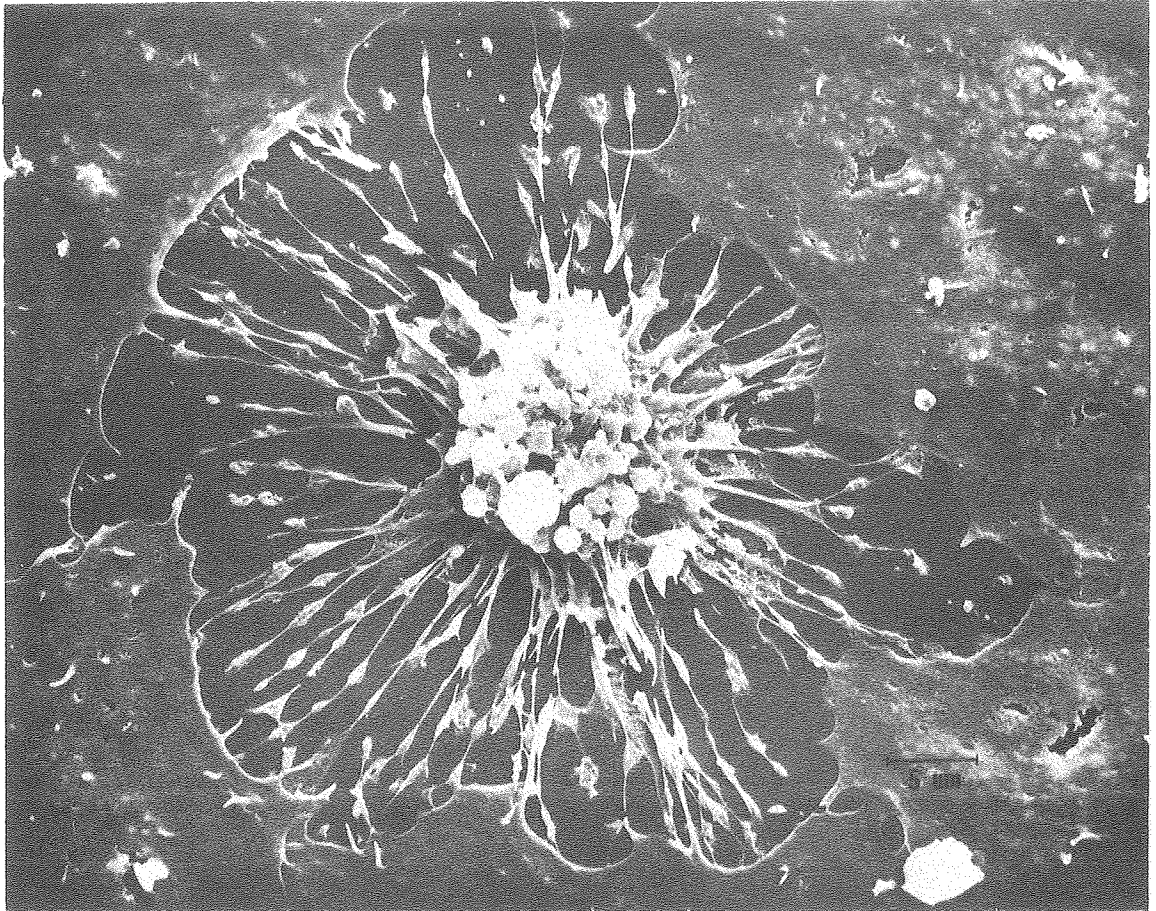


Fig.59

XBB767 6501

Figure 60. Higher magnification view of area 2 of Fig. 58, showing presumptive intermediate junctions (A_1 , A_2 , A_3 , and A_4) as well as smaller regions of intercellular adhesion (arrowheads). Tapered microvilli (arrows) and vesicular stomata (V) are also visible in this micrograph. 12,000X.

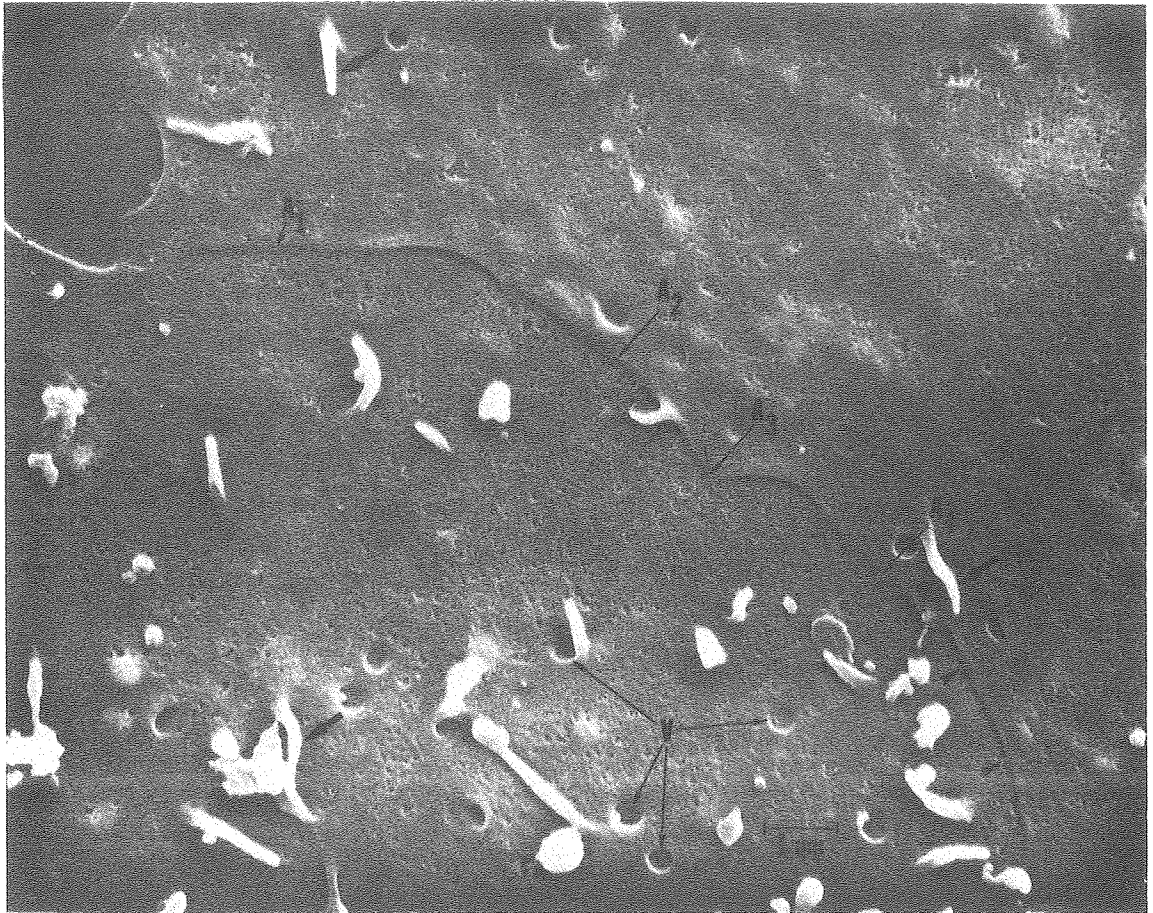


Fig. 60

XBB767 6495

fibers seen in untreated cells. Patches of membrane with a roughened, pitted appearance were common in glycerinated cultures (Fig. 61; note also the differences in surface texture between the glycerinated and unglycerinated rounded cells shown in Figs. 59 and 55) and may represent regions of membrane damage resulting from too rapid deglycerination at the end of the glycerol/HEPES-DME series (N. S. McNutt, personal communication).

One very interesting difference between glycerinated and either untreated or HEPES-DME incubated cultures was the alterations which occurred in the microvilli and filopodia of glycerinated cells. Microvilli and filopodia on untreated Balb 3T3 cells were cylindrical structures with approximately the same diameter along their whole length (Figs. 17, 20, 21, 22, 25, and 26). The majority of microvilli on glycerinated cells were shorter than on untreated cells and could be divided into two types: one group which tapered from a base 0.2 - 0.5 μm in diameter to a rounded end 0.09 - 0.14 μm in diameter (Figs. 60 and 61), and a second group which consisted of bulbs 0.3 - 0.6 μm in diameter, connected to the cell surface by a short stalk (Fig. 61). Filopodia were notable mostly by their absence. Fully or partially rounded cells exhibited slender processes radiating from the cell body, but the flattened cells had very few filopodia around the cell periphery. In some cases, patches of the bulbous structures were associated with a few short filopodia at the cell edge (Figs. 58 and 61). This association suggested that rather than being microvilli, some of the bulbous structures may have resulted from retraction of filopodia, with the bulb representing filopodial membrane which had not yet been integrated into the cell membrane. These alterations in the morphology of microvilli and filopodia

Figure 61. Higher magnification view of area 1 of Fig. 58. This region may have originally possessed a tangle of filopodia similar to that shown in Fig. 20. After glycerination, only a few short filopodia (Fil) are present. It is possible that many of the filopodia have retracted into short bulbous structures (arrowheads). The microvilli are shorter than in untreated cultures, and frequently taper to a point at the tip (arrows). Patches of roughened membrane (RM) were common in glycerinated preparations and may represent localized regions of membrane damage. In areas where the silicon monoxide substratum (SM) is visible, adhesions (A) between the cell membrane and the substratum are visible. V, vesicular stomata. 12,000X.

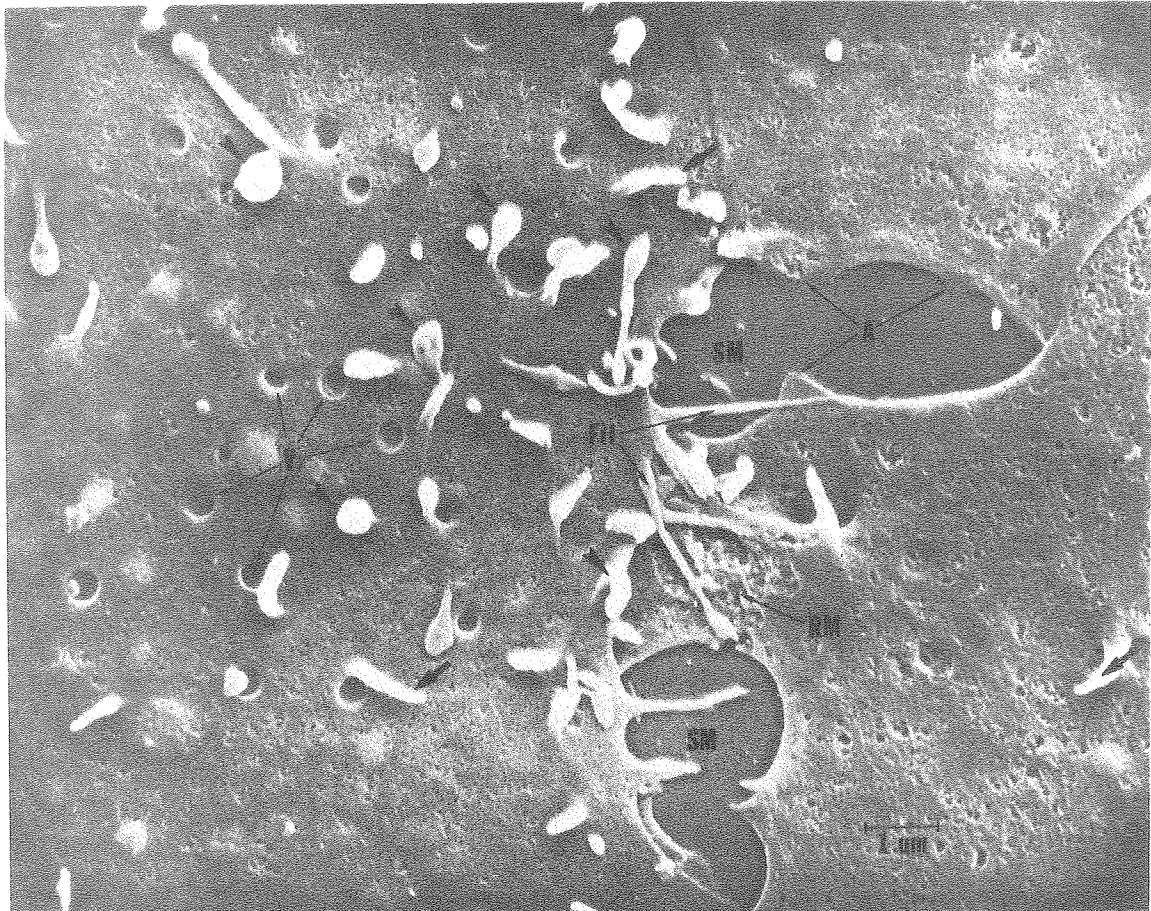


Fig. 61

XBB767 6499

were presumably induced by glycerination, and it would be extremely interesting to determine whether they represent a primary effect of glycerol on the filamentous central core of the microvilli and filopodia or whether they were merely a secondary consequence of the influence of glycerol on other cytoplasmic elements.

The freeze-fracture data consisted of twelve fracture faces from eleven cells incubated in HEPES-DME and twenty-six fracture faces from twenty-two glycerinated cells. These were obtained using a culture which showed little morphological alteration by light microscopy. The preparation which showed a moderate number of rounded cells was also fractured, but most of the micrographs from this experiment were ruined by an instability in the microscope. However, similar results were obtained with both of these preparations.

The appearance of cells incubated in HEPES-DME or the glycerol series before fracturing was consistent with the HRSEM data. Of the nine cells examined after HEPES-DME incubation, all were quite flat, with few microvilli and varying numbers of vesicular stomata 0.03 - 0.15 μm in diameter. The distribution of IMP was essentially uniform, although it was possible to pick out a few small regions 0.08 - 0.12 μm in diameter where the density of particles and subparticles seemed lower than in the rest of the membrane. The average size of the IMP on the P face was 106 A (N - 140, standard deviation = 23 A). Fractures through the cells' peripheral regions revealed a network of filopodia and small cytoplasmic processes. Numerous regions of close apposition occurred between filopodia and processes from neighboring cells, but with the exception of occasional gap junctions, the fracture face in these regions was not visibly different from that of the rest of the cell membrane.

As predicted by the HRSEM data, glycerinated Balb 3T3 cells (Fig. 62) were generally flattened with a central hump, few peripheral filopodia, and numerous vesicular stomata 0.016 - 0.8 μm in diameter. The small bulbous structures tentatively identified as retracting microvilli or filopodia were almost never seen in the fracture faces examined here.

The alterations in IMP distribution observed with glycerinated Balb 3T3 cells were quite different from those described by Gilula et al. (1975). In portions of some cells, the particle distribution appeared uniform (Fig. 63) and it would have been hard to distinguish between these regions and the fracture faces of untreated cells (Chapter 5). When aggregation did occur, it was usually not pronounced, manifesting itself mostly in the formation of small aisles free of both particles and subparticles and in a tendency for the particles to gather together (Fig. 64a) without forming real clusters or aggregates of the type described by Gilula et al. (1975); (see especially Figs. 2, 8, and 11 of this reference). This pattern of aggregation is suggestive of the beginning of a network of aggregated IMP similar to that described by Pinto da Silva and Martinez-Palomo (1975). Aggregation of this type was most obvious on the P face. The average IMP diameter measured on P₂₈ was 102 Å (N = 140, standard deviation = 17 Å). The degree of aggregation varied from cell to cell and between different regions of the same cell, with twelve of the twenty-two cells (55%) showing visible aggregation. The presence or absence of aggregation did not appear to be correlated with cell shape; three of the twenty-three cells examined were partially rounded and had surface blebs (Fig. 63), yet these cells had almost uniform particle distributions. There seemed to be a slight tendency for aggregation to be more pronounced at the cell center than in the peripheral regions,

Figure 62. Freeze-fracture replica of a confluent monolayer of Balb 3T3 cells incubated for 46 min. in glycerol/HEPES-DME, then fractured in situ at -100°C with 2 min. of etching. This micrograph shows large portions of the membranes of three cells (27, 29, and 31) and smaller portions of several other cells. The majority of the cells seen in glycerinated preparations appeared similar to those shown here. The dotted lines enclose regions of particle aggregation on E_{29} and E_{31} (see text). Gap junctions are circled. The regions enclosed within numbered rectangles were selected for examination at higher magnification. Montage of twenty-one micrographs. Gly, glycerol matrix; N, nucleus. 1900X.

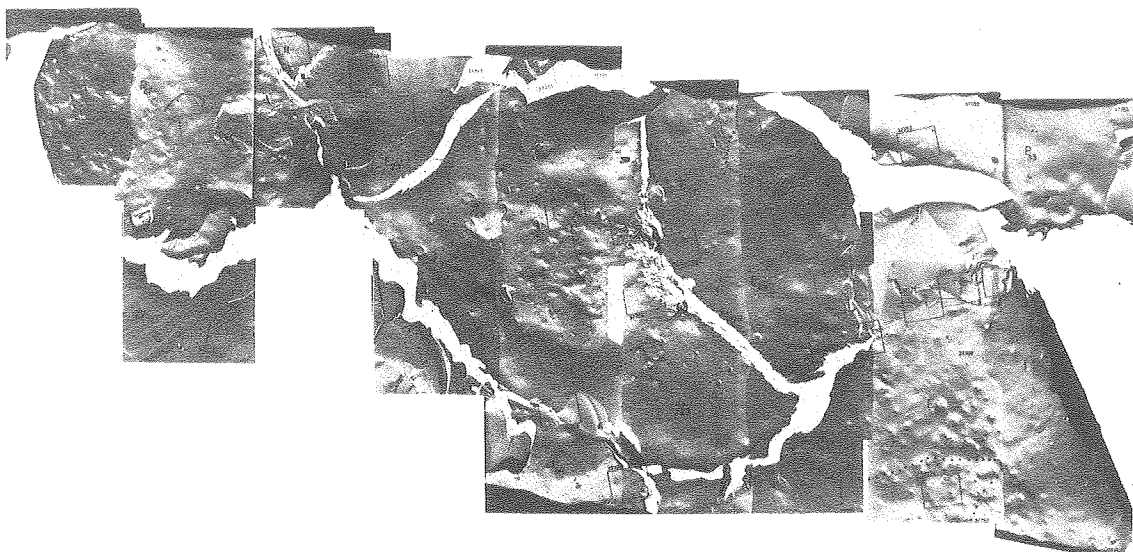


Fig. 62

XBB767 6281

Figure 63. Low magnification (a) and high magnification (b) views of a cell which developed numerous blebs after incubation with glycerol/HEPES-DME. The area enclosed by the rectangle in (a) is shown at higher magnification in (b). Although the cell has become highly contorted as a result of incubation in the glycerol solution, the distribution of the IMP appears to be essentially uniform, with the exception of two small, particle-free blisters (arrowheads). (a) 11,000X, bar equals 1 μm ; (b) 53,000X, bar equals 0.25 μm .

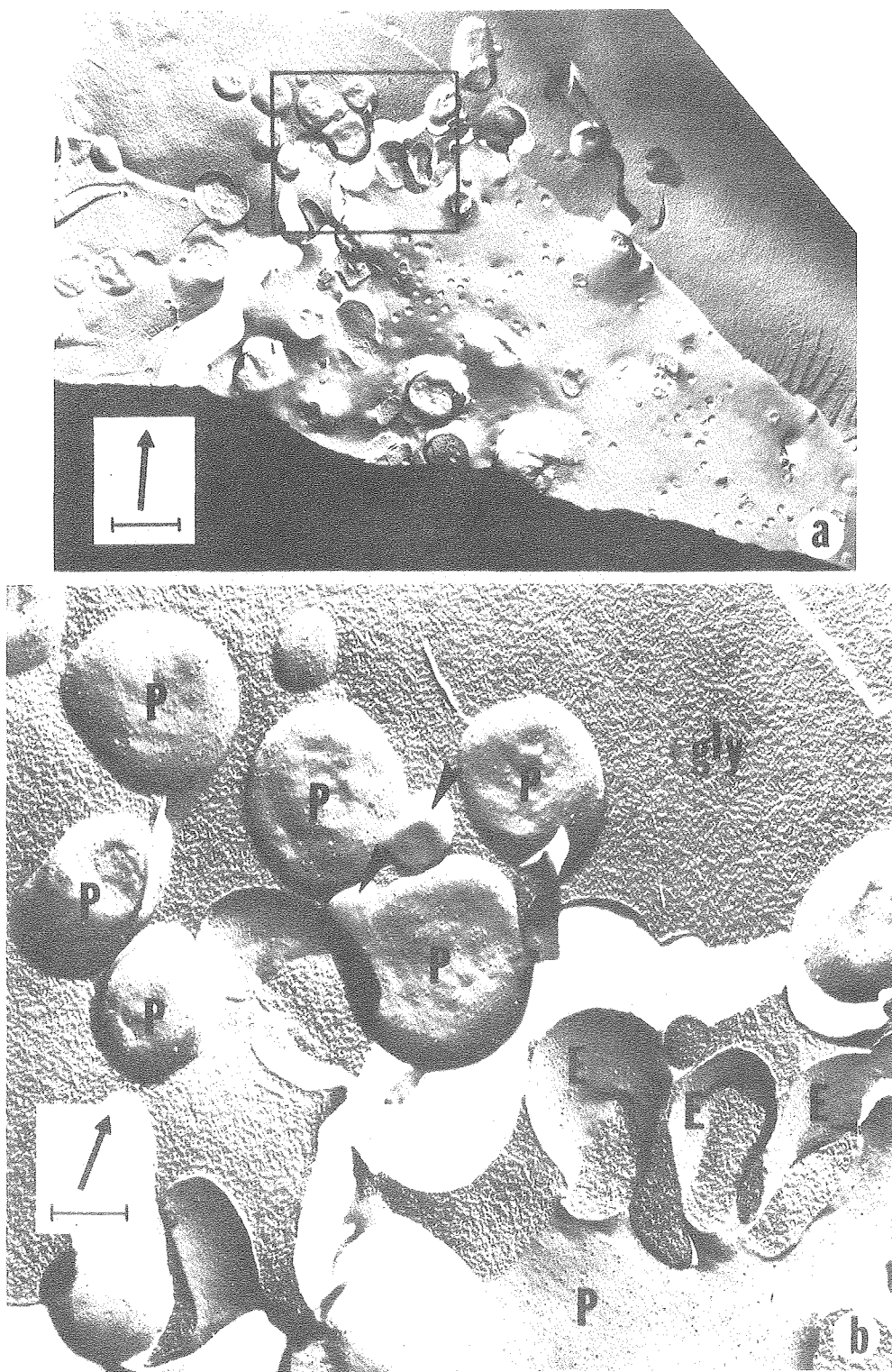


Fig. 63

XBB767 6589

Figure 64. (A) Appearance of a typical P face from a cell incubated 45 min. at 37°C with glycerol/HEPES-DME. The slight degree of particle aggregation which occurred with these cultures is evident in the particle-free aisles (A) which appear at random over the fracture face. The arrowheads point to annuli of particles which appear around the stomata of vesicles which are in the process of forming from, or fusing with, the plasma membrane.

(b) Appearance of an E face (E₃₁) where lines of IMP formed in a specific area on the underside of the cell. The arrowhead points to a very small particle annulus with a raised central stoma. The inset shows a small particle annulus with no central stoma, and a linear aggregate of IMP which passes through a stoma with no annulus. Bar equals 0.2 μ m. 62,000X.

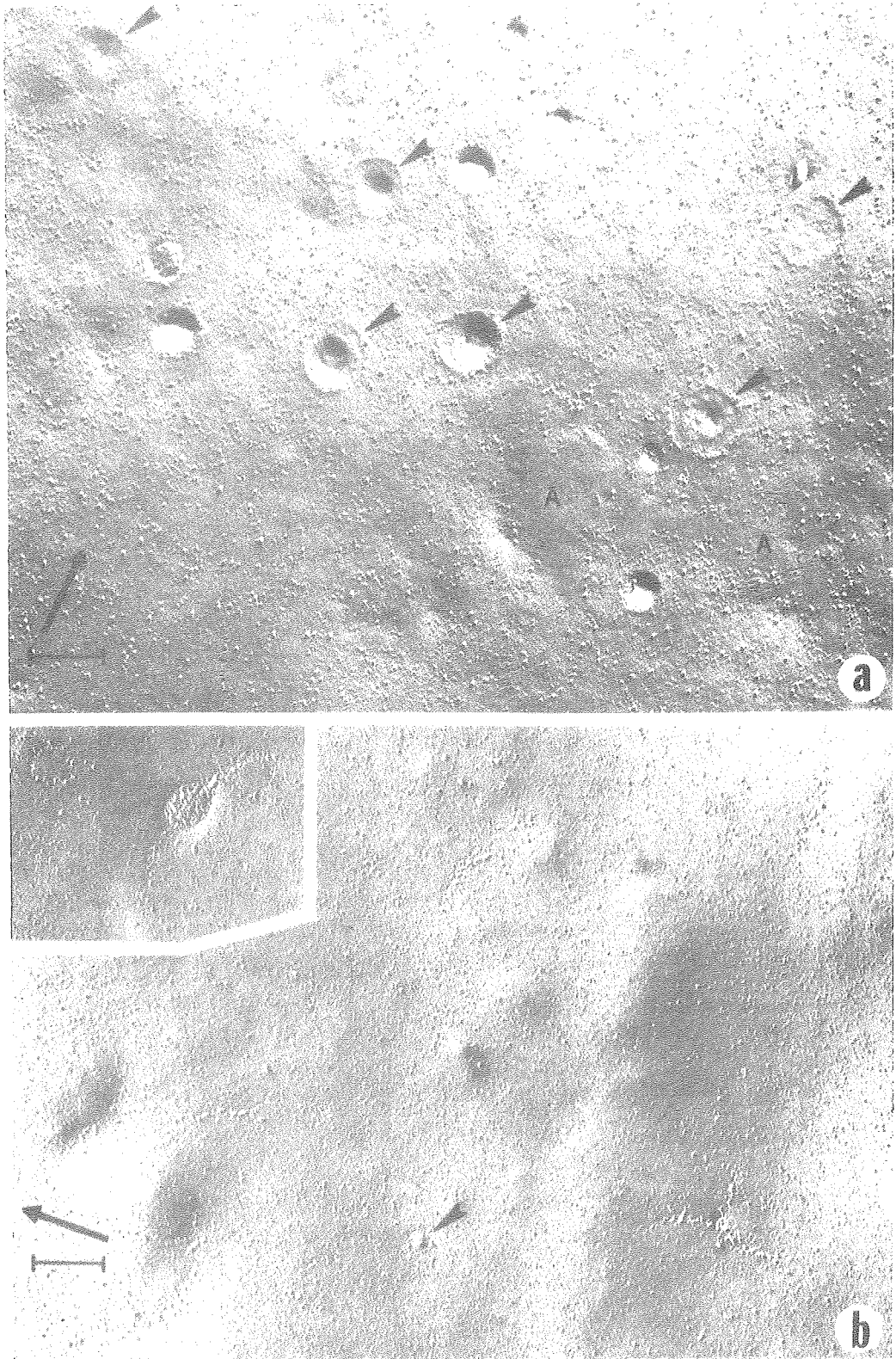


Fig. 64

XBB767 6588

but the degree of aggregation was so small that it was very difficult to make comparisons between different regions. Numerous regions of close apposition were present between the surfaces of neighboring cells, but with the exception of occasional gap junctions, there was no specialization of the membrane at these points.

Two of the E fracture faces, E₂₉ and E₃₁, had localized regions (delimited by dotted lines in Fig. 62) with unusual alterations in IMP distribution. Within the area shown in Fig. 62, E₃₁ displayed scattered rows of IMP on an otherwise uniform background (Fig. 64b). Outside of this localized region, E₃₁ was indistinguishable from other E fracture faces. Face E₂₉ possessed an area approximately 8 μm in diameter which displayed an abundance of large IMP (Fig. 65a). The average IMP diameter in this particle-rich area was 133 \AA ($N = 50$, standard deviation = 27 \AA). A student's t-test (Minium, 1970) revealed that the difference in diameter between particles in this region and those on face P₂₈ was statistically significant ($p < 0.01$). The boundary between the particle-rich area and the rest of E₂₉ was very distinct and was marked in places by a slight low step (arrowheads in Fig. 65), with the particle-rich area being slightly depressed with respect to the rest of the fracture face. In part of this region the fracture face appeared to have a very rough texture (Fig. 65b). It is possible that the roughened appearance of the fracture face resulted from damage to the membrane and that such a region may be analogous to the areas of roughened membrane seen with HRSEM (Fig. 61). At high magnification (Fig. 66), many of the IMP in the particle-rich area appeared to be encircled by a necklace made up of subparticles approximately 20 $\overset{\circ}{\text{\AA}}$ in diameter. These necklaces may simply represent decoration artifacts caused by creeping of platinum after it arrives on

Figure 65. Higher magnification view of Fig. 62. This micrograph shows two regions from E₂₉, an E face where large (130 Å) particles aggregated into a localized area of the lower cell surface. (a) shows the striking difference between the appearance of the aggregated region (right-hand side) and the rest of the fracture face (left-hand side). There appears to be a definite boundary (arrowheads) between the two regions. (b) was taken at the edge of a different part of this particle-rich area, and shows a region where the membrane appears to be roughened. The arrowheads point to the boundary of the aggregated region. The area enclosed in the rectangle in (a) is shown at higher magnification in Fig. 66. Bar equals 0.2 μm. 62,000X.

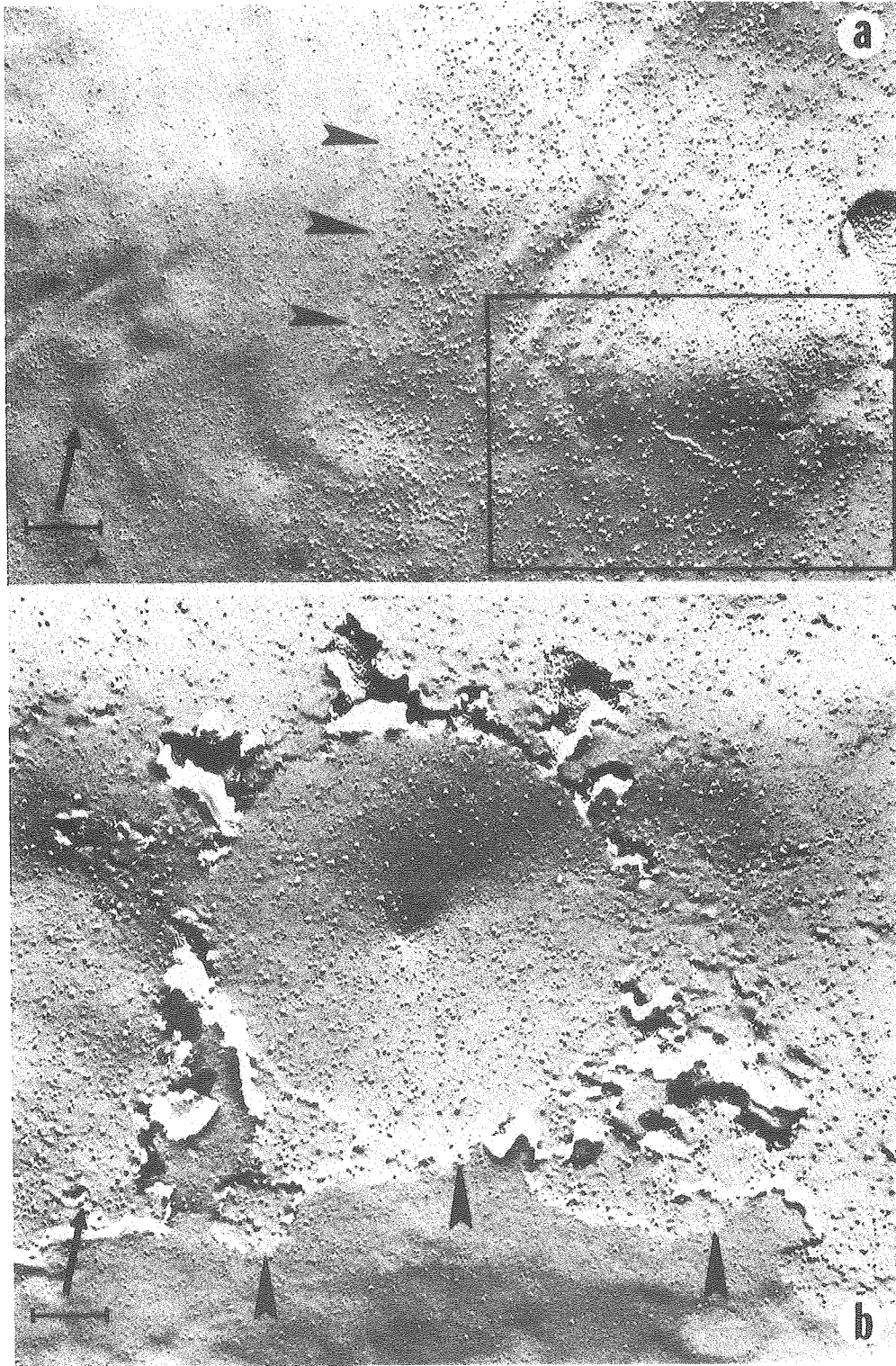


Fig. 65

XBB767 6590

Figure 66. Photographic enlargement of Fig. 65. Many of the 130 A particles appear to be encircled by a necklace made up of subparticles approximately 20 A in diameter (small arrowheads). Subparticle rings are especially noticeable around a linear aggregate of 130 A IMP (asterisk). The structure indicated by the large arrowhead is a beginning of membrane roughening similar to that shown in Fig. 65b. Bar equals 500 A. 190,000X.

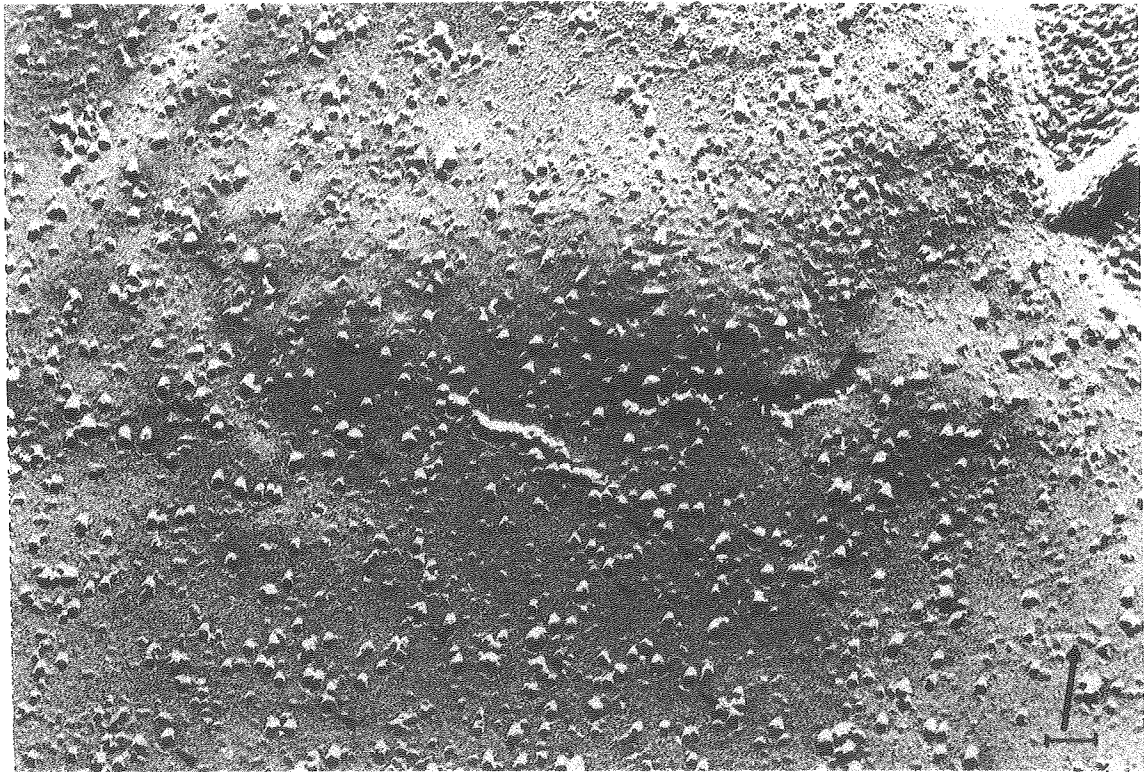


Fig. 66

XBB767 6591

the fracture face, or they may be real elements of the hydrophobic region of the membrane. The recent demonstration of substructure within IMP (Fisher and Stockenius, 1977; Margaritis et al., 1976) would tend to support the latter hypothesis. Subparticle necklaces around large IMP were observed only in the particle-rich area of face E₂₉.

One interesting result of glycerination was the appearance of annuli of IMP around some of the vesicular stomata (Fig. 64). These recurred mostly on the P face (upper cell surface), where stomata were most numerous, but could occasionally be seen on the E face (lower cell surface). In some cases, the IMP appeared to be resting upon a low ridge which encircled the stomatum. Particle annuli sometimes encircled only a flat, particle-free area; these may represent regions where a vesicle has completely fused with the plasma membrane, leaving only the annulus to mark the site of fusion. The fact that particle annuli were seen only in Balb 3T3 cells pretreated with glycerol and never in untreated fixed Swiss 3T3 4A RK2 (Chapter 2) or Balb 3T3 cells (Chapter 5) indicates that formation of these structures in mammalian cells is probably an artifact of glycerination rather than being a customary step in vesicle formation or fusion, as has been suggested in some studies (Orci and Perrelet, 1973; Simionescu et al., 1974). This conclusion is supported by the fact that freeze-fracture studies on several mammalian secretory tissues (Elias et al., 1973; Orci et al., 1973; Smith et al., 1973) have not revealed any evidence of specific IMP configurations at sites where vesicles are attached to the plasma membrane. However, it is possible that artifactual formation of IMP annuli during glycerination reflects alterations in the internal structure of the membrane at the site of attachment of the vesicle. This is an extremely interesting and potentially useful

observation, since specialization of the fracture face at the site of vesicle formation or fusion has been demonstrated and studied in Tetrahymena (Satir et al., 1972 and 1973) but has only infrequently been observed in mammalian cells (Orci and Perrelet, 1973; Simionescu et al., 1974). If conditions can be defined under which glycerination reproducibly causes reorganization of the IMP around vesicular stomata, then it is possible that glycerol might be used as a membrane-perturbing agent for examining the mechanism of vesicle formation from, and fusion with, the plasma membrane. Correlation of results from such glycerination experiments with studies of membrane-vesicle interactions in sectioned preparations (Palade and Bruns, 1968) could provide valuable information about the mechanism of interaction between vesicles and the plasma membrane.

Discussion

The results presented in this chapter must be viewed with a great deal of caution, since they are based on a small sample of cells from cultures which displayed considerable variability in their response to incubation in HEPES-DME and glycerol/HEPES-DME solutions. For this reason, further experimental work will be required before firm conclusions can be drawn regarding the effect of glycerol on the morphology and membrane structure of fibroblasts.

With this qualification in mind, it is possible to make some general observations on the effect of HEPES-DME and glycerol/HEPES-DME on cell monolayers. First, it is clear that the buffer vehicle itself can induce pronounced changes in cell morphology. In the case of Balb 3T3 cells, these changes involve peripheral retraction, rounding up, and eventual detachment of a fraction of the cells from the substratum, with different

buffer systems producing varying degrees of morphological alteration. These effects are reversed to some extent by adding glycerol to the incubation medium, but the mechanism by which reversal occurs is unknown at present, and it is somewhat unsatisfactory to have to examine the effects of glycerol against a background of buffer-induced changes. Future experiments should be aimed at developing a buffer system, possibly based on HEPES-DME with added serum components, which would reliably preserve the native morphology of the monolayer for a period of two or three hours outside of the CO₂ incubator. Use of in situ techniques would be essential in these experiments, since it is extremely difficult to evaluate changes in cell morphology and interactions once the monolayer has been detached from the substratum.

In this study, glycerination has been found to induce a number of interesting and potentially informative plasma membrane alterations, including modification of the structure of microvilli and filopodia, induction of various patterns of particle aggregation, formation of subparticle necklaces around large IMP, and formation of particle annuli around vesicular stomata. However, it is difficult to interpret these changes at present, because the effects of glycerol seem to be extremely variable. For example, Swiss 3T3 4A cells glycerinated by Method I or Method II (Chapter 2) exhibited patches and clumps of IMP, but did not display annuli around vesicular stomata, while Balb 3T3 cells treated with glycerol/HEPES-DME showed only the beginnings of a reticular network of aggregated IMP, but had numerous particle annuli. In other studies, Gilula et al. (1975) were able to distinguish clearly between Balb 3T3 A31 cells, which showed numerous patches of IMP after treatment with glycerol in PBS, and SV40 transformants of this cell line, which exhibited only a minimal

degree of particle aggregation after this treatment. However, results directly contradictory to these were reported by Pinto da Silva and Martinez-Palomo (1975), who observed that the particles of both untransformed and SV40-transformed Balb 3T3 A31 cells aggregated into a reticular network after treatment with PBS alone; incubation in glycerol in PBS yielded a "similar, although less clear" pattern of aggregation. Although time did not permit observation of transformed cultures after glycerination, the results of the present study suggest that the effect of glycerol on the membranes of untransformed Balb 3T3 cells was similar to that reported by Pinto da Silva and Martinez-Palomo (1975). It seems likely that much of this variability is the result of the different conditions under which cells were incubated in each experiment. Clearly, what is needed here are carefully designed experiments in which factors such as pH, temperature, the incubation medium, and the presence or absence of glycerol or metal ions can be controlled in order to isolate those factors influencing IMP redistribution.

Some of these inconsistencies may also be due to differences between the intrinsic properties of various subclones of Swiss and Balb 3T3 cells. For example, Gilula (personal communication) has reported that the different subclones of Balb 3T3 A31 cells used in several laboratories vary widely in their tendency to exhibit glycerol-induced particle aggregation. Also, since aggregation is a time-dependent process which probably occurs at different rates in different cell lines, many of the apparent inconsistencies may result from sampling different stages in this process. Future work should be aimed at understanding the factors controlling lateral movements of the IMP. Elucidation of the mechanisms influencing the distribution and mobility of the particles may provide important

information concerning the interactions between the IMP and other elements of the plasma membrane and cytoskeleton.

Chapter 8

Conclusions and Suggestions for Future Studies

This study has accomplished several goals. After available methods for freeze-fracture of cell cultures were evaluated and determined to be inadequate, an in situ technique for freeze-fracture was perfected and was found to increase greatly the amount of information available from replicas of cell monolayers. Since growing cells on different substrata has been shown to change the growth characteristics of the culture (see Chapter 3), it was necessary to develop methods whereby cultures could be grown on the same material for all types of experiments. Silicon monoxide, which can easily be evaporated onto most surfaces, was therefore evaluated as a substratum for cell culture and was found to have excellent properties for the growth of a variety of cell types. Existing techniques of HRSEM and thin sectioning were then modified for use with silicon monoxide. As a result of these developments, monolayer cultures can now be subjected to both biochemical analysis and high resolution electron microscopy under identical growth conditions. Using these methods, the interactions between Balb 3T3 cells in culture were for the first time carefully observed and classified using freeze-fracture and HRSEM, and the ultrastructure of the plasma membrane in areas of cell interaction was examined. Preliminary studies were then carried out using glycerol to perturb the structure of the plasma membrane, with the aim of revealing any possible contact-induced changes in the mobility of the IMP.

The HRSEM and freeze-fracture data suggest that, with the exception of the formation of gap junctions and the presumptive intermediate junctions, cell interaction does not induce any change in the native membrane

structure of untransformed Balb 3T3 cells that is visible at the resolution (20-40 Å) available in this study. This result is not surprising in view of the fact that other studies published during the course of this project (see Chapter 1) have demonstrated that various membrane components such as the IMP and the different classes of surface receptors, have been found to be distributed uniformly across the plasma membrane in all cases. The general consensus of all the work published to date is that a change in the metabolic state of a cell manifests itself as an alteration in the lateral mobility of these sites without affecting their inherent distribution. Since there is now reasonably good evidence that some membrane proteins possess linkages to a submembranous assembly of microfilaments and microtubules, it seems likely that such variations in mobility reflect either changes in the anchorage of these proteins to the assembly, or alterations in the state of the assembly itself. Since the native distribution of these sites does not change with alterations in the metabolic state of the cell, variations in lateral mobility become apparent only when the cell is treated with agents capable of perturbing the membrane and inducing redistribution of specific proteins; changes in mobility are then revealed as variations in the rapidity and extent of redistribution. The results of the present study indicate that the effects of cell interaction on the membranes of fibroblasts, if any, will probably not become apparent unless such membrane-perturbing agents are employed.

Future studies on the effect of cell interactions on membrane structure should employ in situ techniques for all electron microscopy, since the value of these techniques over conventional methods has been clearly demonstrated here. Initially, efforts should be concentrated on perfec-

tion of the method for in situ thin sectioning of cells grown on silicon monoxide. Once sections suitable for examination of the plasma membrane at high resolution have been obtained, an attempt should be made to determine the type of junction, if any, responsible for the regions of intercellular adhesion seen by HRSEM and freeze-fracture. Further investigation of the structure of these junctions, possibly involving the use of metal tracers such as lanthanum hydroxide (Revel and Karnovsky, 1967), may reveal clues to the nature of the short fibers which were so often associated with these regions in HRSEM preparations. This would complete the morphological studies on untransformed, untreated Balb 3T3 cells.

Attention should then be focused on perfection of techniques for glycerination of cell monolayers. The preliminary experiments on glycerination of Balb 3T3 cells suggest that this may not be a trivial task, since even the simple act of changing the incubation medium results in severe morphological changes in the monolayer. If possible, an incubation medium should be developed which does not have these adverse effects on cell morphology. Alternatively, it may be necessary to use standard culture media as the vehicle for glycerination, which means carrying out all incubation procedures in a CO₂ atmosphere.

Since the subclone of Balb 3T3 used here shows very little aggregation of the IMP during glycerination, it is probably not a good choice for examining the effect of cell interactions on the lateral mobility of membrane elements. The initial in situ glycerination studies should therefore employ a cell line such as CEF (Gilula et al., 1975) which exhibits obvious particle aggregation. Once a reliable protocol for glycerination has been established, it should be possible to determine

whether cell contact affects glycerol-induced IMP aggregation. Extension of these studies to other cell lines should reveal how commonly glycerol-induced particle aggregation occurs, and whether or not cell interaction can affect the rate or extent of aggregation in other types of cultures. Ideally, one would like to isolate from some parent cell line a number of subclones which differ only in the degree of IMP aggregation produced by a standard glycerol treatment. It might then be possible to correlate the tendency of a given subclone to exhibit IMP aggregation during a standard exposure to glycerol with the presence or absence of potential IMP-anchoring structures such as microtubules, subplasmalemmal microfilaments, spectrin-like molecules, or possibly even surface LETS protein. Recently developed fixatives which show enhanced preservation of microfilaments and microtubules (Luftig et al., 1976) would probably be very useful in this kind of experiment. These experiments could then be repeated on viral transformants of the same parent cell line in order to evaluate the effect of transformation on the lateral mobility of the IMP.

Present evidence suggests that experiments of the sort outlined here have considerable promise. Although the nature of the IMP is poorly understood, data from studies on the erythrocyte membrane (Chapter 1) indicate that membrane particles are proteins which, in some cases, span the plasma membrane and may connect surface receptors with enzyme complexes and filaments on the cytoplasmic side of the membrane. Thus, they have the potential for transferring information between the cell's interior and its outside environment. The fact that changes in particle density, distribution, or mobility have been observed to accompany alterations in the metabolic state of some cell types (Chapter 1) suggests that the IMP are, in fact, responsive to the growth conditions of the cell. They may

therefore provide a useful marker for alterations in the plasma membrane or the submembranous cytoskeleton. This view is supported by the observation that glycerol-induced particle annuli appear at sites where vesicles are fusing with or forming from the plasma membrane (Chapter 7). Finally, future studies should not neglect examination of the presumptive intermediate junctions by HRSEM and thin sectioning, since these structures appear to be essential to both cell motility and intercellular adhesion, and are intimately related to the contractile cytoskeleton. If carefully executed, these studies could provide valuable information regarding membrane dynamics and its role in communication between the cell and its environment.

References

- Abercrombie, M. 1961. The bases of the locomotory behavior of fibroblasts. Exp. Cell Res. Suppl. 8, 188-198.
- Abercrombie, M. 1970. Contact inhibition in tissue culture. In Vitro 6, 128-142.
- Abercrombie, M., and E. J. Ambrose. 1958. Interference microscope studies of cell contacts in tissue culture. Exp. Cell Res. 15, 332-345.
- Abercrombie, M., and J. E. M. Heaysman. 1954. Observations on the social behavior of cells in tissue culture. II. "Monolayering" of fibroblasts. Exp. Cell Res. 6, 293-306.
- Abercrombie, M., J. E. M. Heaysman, and H. M. Karthausner. 1957. Social behavior of cells in tissue culture. III. Mutual influence of sarcoma cells and fibroblasts. Exp. Cell Res. 13, 276-291.
- Abercrombie, M., J. E. M. Heaysman, and S. M. Pegrum. 1970. The locomotion of fibroblasts in culture. II. Ruffling. Exp. Cell Res. 60, 437-444.
- Abercrombie, M., J. E. M. Heaysman, and S. M. Pegrum. 1976. The locomotion of fibroblasts in culture. IV. Electron microscopy of the leading lamella. Exp. Cell Res. 67, 359-367.
- Albertini, D. F., and J. I. Clark. 1975. Membrane-microtubule interaction: concanavalin A capping induced redistribution of cytoplasmic microtubules and colchicine binding proteins. Proc. Natl. Acad. Sci. USA. 72, 4976-4980.
- Albertini, D. F., D. W. Fawcett, and P. J. Olds. 1975. Morphological variations in gap junctions of ovarian granulosa cells. Tissue & Cell. 7, 389-405.
- Ali, I. U., V. Mautner, R. Lanza, and R. O. Hynes. 1977. Restoration of normal morphology, adhesion and cytoskeleton in transformed cells by addition of a transformation-sensitive surface protein. Cell 11, 115-126.
- Aub, J. C., B. H. Sanford, and M. N. Cote. 1965. Studies on reactivity of tumor and normal cells to a wheat germ agglutinin. Proc. Natl. Acad. Sci. USA 54, 396-399.
- Aub, J. C., C. Tieslau, and A. Lankester. 1963. Reaction of normal and tumor cell surfaces to enzymes. I. Wheat-germ lipase and associated mucopolysaccharides. Proc. Natl. Acad. Sci. USA. 50, 613-619.

- Axline, S. G. and E. P. Reaven. 1974. Inhibition of phagocytosis and plasma membrane mobility of the cultivated macrophage by cytochalasin B. J. Cell Biol. 62, 647-659.
- Barkla, D. H. and P. J. M. Tutton. 1976. Comparison between membranes of malignant and of non-malignant rat colonic epithelial cells. J. Cell Biol. 70, 63a (Abstr.).
- Bartholomew, J. C., H. Yokota, and P. A. Ross. 1976. Effect of serum on the growth of Balb 3T3 A31 mouse fibroblasts and an SV40-transformed derivative. J. Cell. Physiol. 88, 277-286.
- Becker, J. S., J. M. Oliver, and R. D. Berlin. 1975. Fluorescence techniques for following interactions of microtubule subunits and membranes. Nature 254, 152-154.
- Benjamin, T. L. and M. M. Burger. 1970. Absence of a cell membrane alteration function in non-transforming mutants of polyoma virus. Proc. Natl. Acad. Sci. USA 67, 929-934.
- Bererhi, A. and K. Malkani. 1969. Cryodécapage de cellules en cultures. J. Microscopie 8, 841-844.
- Berlin, R. D., J. M. Oliver, T. E. Ukena, and H. H. Yin. 1974. Control of cell surface topography. Nature 247, 45-46.
- Bissell, M. J., C. Hatie, A. N. Tischler, and M. Calvin. 1974. Preferential inhibition of the growth of virus-transformed cells in culture by Rifazone-8, a new Rifamycin derivative. Proc. Natl. Acad. Sci. USA 71, 252-2524.
- Blumberg, P. M. and P. W. Robbins. 1975. Effect of proteases on activation of resting chick embryo fibroblasts and on cell surface proteins. Cell 6, 137-147.
- Boyde, A. and P. Vesely. 1972. Comparison of fixation and drying procedures for preparation of some cultured cell lines for examination in the SEM. In Scanning Electron Microscopy/1972, O. Johari and I. Corvin (Eds.), IIT Research Institute, Chicago, Ill. pp. 265-272.
- Boyde, A., R. A. Weiss, and P. Vesely. 1972. Scanning electron microscopy of cells in culture. Exp. Cell Res. 71, 313-324.
- Branton, D. 1971. Freeze-etching studies of membrane structure. Phil. Trans. Roy. Soc. Lond. B. 261, 133-138.
- Branton, D., S. Bullivant, N. B. Gilula, M. J. Karnovsky, H. Moor, K. Muhlethaler, D. H. Northcote, L. Packer, B. Satir, P. Satir, V. Speth, L. A. Staehlin, R. L. Steere, and R. S. Weinstein. 1975. Freeze-etching nomenclature. Science 190, 54-56.
- Branton, D. and D. Deamer. 1972. Membrane structure. Protoplasmatologia. II/E/1, 1-70.

- Bretscher, M. S. 1973. Membrane structure: some general principles. Science 181, 622-629.
- Brinkley, B. R., G. M. Fuller, and D. P. Highfield. 1975. Cytoplasmic microtubules in normal and transformed cells in culture: analysis by tubulin antibody immunofluorescence. Proc. Natl. Acad. Sci. USA 72, 4981-4985.
- Brown, S., M. Teplitz, and J. P. Revel. 1974. Interaction of mycoplasmas with cell cultures as visualized by electron microscopy. Proc. Natl. Acad. Sci. USA 71, 464-468.
- Brunk, U., P. Bell, P. Colling, N. Forsby, and B. A. Fredriksson. 1975. SEM of *in vitro* cultivated cells. Osmotic effects during fixation. In Scanning Electron Microscopy/1975, O. Johari (Ed.), IIT Research Institute, Chicago, Ill. pp. 379-386.
- Burger, M. M. 1969. A difference in the architecture of the surface membrane of normal and virally transformed cells. Proc. Natl. Acad. Sci. USA. 62, 994-1001.
- Burger, M. M. 1970. Proteolytic enzymes initiating cell division and escape from contact inhibition of growth. Nature 227, 170-171.
- Burger, M. M. 1971. The significance of surface structure changes for growth control under crowded conditions. In Ciba Foundation Symposium on Growth Control in Cell Cultures, G. E. W. Wolstenholme and J. Knight (Eds.), Churchill-Livingstone, London. pp. 45-69.
- Burger, M. M. and A. R. Goldberg. 1967. Identification of a tumor-specific determinant on neoplastic cell surfaces. Proc. Natl. Acad. Sci. USA 57, 359-366.
- Burger, M. M. and G. S. Martin. 1972. Agglutination of cells transformed by Rous sarcoma virus by wheat germ agglutinin and concanavalin A. Nature New Biol. 237, 9-12.
- Chen, L. B., P. H. Gallimore, and J. I. McDougall. 1976. Correlation between tumor induction and the large external transformation sensitive protein on the cell surface. Proc. Natl. Acad. Sci. USA 73, 3570-3574.
- Cherny, A. P., J. M. Vasiliev, and I. M. Gelfand. 1975. Spreading of normal and transformed fibroblasts in dense cultures. Exp. Cell Res. 90, 317-327.
- Clark, A. W. and D. Branton. 1968. Fracture faces in frozen outer segments from the guinea pig retina. Z. Zellforsch. 91, 586-603.
- Cline, M. J. and D. C. Livingston. 1971. Binding of ³H-concanavalin A by normal and transformed cells. Nature New Biol. 232, 155-156.

- Cohen, A. L., D. P. Marlow, and G. E. Garner. 1968. A rapid critical point method using fluorocarbons (Freon) as intermediate and transitional fluids. J. Microscopie 7, 331-342.
- Collins, T. R., J. C. Bartholomew, and M. Calvin. 1974. A simple method for freeze-fracture of monolayer cultures. J. Cell Biol. 63, 67a (Abstr.)
- Collins, T. R., J. C. Bartholomew, and M. Calvin. 1975. A simple method for freeze-fracture of monolayer cultures. J. Cell Biol. 67, 904-911.
- Comoglio, P. M. and R. Guglielmo. 1972. Two dimensional distribution of concanavalin A receptor molecules on fibroblast and lymphocyte plasma membranes. FEBS Letters 27, 256-258.
- Culp, L. A. and P. H. Black. 1972. Contact-inhibited revertant cell lines isolated from simian virus 40-transformed cells. III. Concanavalin A-selected revertant cells. J. Virology 9, 611-620.
- Decker, R. S. and D. S. Friend. 1974. Assembly of gap junctions during amphibian neurulation. J. Cell Biol. 62, 32-47.
- dePetris, S. 1974. Inhibition and reversal of capping by cytochalasin B, vinblastine, and colchicine. Nature 250, 54-55.
- Dulbecco, R. 1969. Cell transformation by viruses. Science 166, 962-968.
- Dulbecco, R. and J. Elkington. 1973. Conditions limiting multiplication of fibroblastic and epithelial cells in dense cultures. Nature 246, 197-199.
- Dunlop, W. F. and A. W. Robards. 1972. Some artifacts of the freeze-etching technique. J. Ultrastruc. Res. 40, 391-400.
- Eagle, H. 1959. Amino acid metabolism in mammalian cell cultures. Science 130, 432-437.
- Edelman, G. M. 1976. Surface modulation in cell recognition and cell growth. Science 192, 218-226.
- Edelman, G. M., B. A. Cunningham, G. N. Reeke, J. W. Becker, M. J. Waxdal, and J. L. Wang. 1972. The covalent and three-dimensional structure of concanavalin A. Proc. Natl. Acad. Sci. USA 69, 2580-2584.
- Edelman, G. M. and I. Yahara. 1976. Temperature-sensitive changes in surface modulating assemblies of fibroblasts transformed by mutants of Rous sarcoma virus. Proc. Natl. Acad. Sci. USA 73, 2047-2051.

- Edelman, G. M., Y. Yahara, and J. L. Wang. 1973. Receptor mobility and receptor-cytoplasmic interactions in lymphocytes. Proc. Natl. Acad. Sci. USA 70, 1442-1446.
- Eddin, M. and D. Fambrough. 1973. Fluidity of the surface of cultured muscle fibers. Rapid lateral diffusion of marked surface antigens. J. Cell Biol. 57, 27-37.
- Eddin, M. and A. Weiss. 1972. Antigen cap formation in cultured fibroblasts: A reflection of membrane fluidity and of cell motility. Proc. Natl. Acad. Sci. USA 69, 2456-2459.
- Elgsaeter, A. and D. Branton. Intramembrane particle aggregation in erythrocyte ghosts. I. The effects of protein removal. J. Cell Biol. 63, 1018-1030.
- Engstrom, L. H. 1970. Structure in the erythrocyte membrane. Ph.D. dissertation. University of California, Berkeley, California.
- Elias, J. J., D. R. Pitelka, and R. C. Armstrong. 1973. Changes in fat cell morphology during lactation in the mouse. Anat. Rec. 177, 533-548.
- Elias, P. M., L. Ornstein, M. A. Lutzner, and J. H. Robbins. 1971. A method for studying the ultrastructure of intercellular contacts in leukocyte cultures. Experientia 27, 116-118.
- Fanger, M. W., D. A. Hart, J. V. Wells, and A. Nisoneff, 1970. Requirement for cross-linkage in the stimulation of transformation of rabbit peripheral lymphocytes by anti-globulin reagents. J. Immunol. 105, 1484-1492.
- Farquhar, M. G. and G. Palade. 1963. Junctional complexes in various epithelia. J. Cell Biol. 17, 375-412.
- Farquhar, M. G. and G. Palade. 1965. Cell junctions in amphibian skin. J. Cell Biol. 26, 263-291.
- Fawcett, D. W. and N. S. McNutt. 1969. The ultrastructure of the cat myocardium. I. Ventricular papillary muscle. J. Cell Biol. 42, 1-45.
- Feagler, T. R., T. N. Tillack, D. P. Chaplin, and P. W. Majerus. 1974. The effects of thrombin on phytohemagglutinin receptor sites in human platelets. J. Cell Biol. 60, 541-553.
- Findlay, J. B. C. 1974. The receptor proteins for concanavalin A and Lens culinaris phytohemagglutinin in the membrane of the human erythrocyte. J. Biol. Chem. 249, 4398-4403.
- Fisher, K. A. and W. Stockenius. 1977. Freeze-fractured purple membranes: protein content. Science 197, 72-74.

- Frye, L. D. and M. Edidin. 1970. The rapid intermixing of cell surface antigens after formation of mouse-human heterokaryons. J. Cell Sci. 7, 319-335.
- Fukuda, M. and T. Osawa. 1973. Isolation and characterization of a glycoprotein from human group O erythrocyte membrane. J. Biol. Chem. 248, 5100-5105.
- Fuller, G. M., C. S. Artus, and J. J. Ellison. 1976. Calcium as a regulator of cytoplasmic microtubule assembly and disassembly. J. Cell Biol. 70, 68a (Abstr.).
- Furcht, L. T. and R. E. Scott. 1974. Influence of cell cycle and cell movement on the distribution of intramembranous particles in contact-inhibited and transformed cells. Exp. Cell Res. 88, 311-318.
- Gilula, N. B., R. R. Eger, and D. B. Rifkin. 1975. Plasma membrane alteration associated with malignant transformation in culture. Proc. Natl. Acad. Sci. USA 72, 3594-3598.
- Gilula, N. B., O. R. Reeves, and A. Steinbach. 1972. Metabolic coupling, ionic coupling, and cell contacts. Nature 235, 262-265.
- Glynn, R. D., C. R. Thrash, and D. D. Cunningham. 1973. Maximal concanavalin A-specific agglutinability without loss of density-dependent growth control. Proc. Natl. Acad. Sci. USA 70, 2676-2677.
- Goldman, R. D., E. Lazarides, R. Pollack, and K. Weber. 1975. The distribution of actin in non-muscle cells. Exp. Cell Res. 90, 333-334.
- Gonzalez-Robles, A., A. Martinez-Palomo, S. Villa-Trevino, and M. Segura. 1976. Increased density of intramembranous particles in plasma membranes of murine leukemic cells. J. Cell Biol. 70, 416a (Abstr.).
- Greaves, M. F. and G. Janossy. 1972. Activation of lymphocytes by phytoimitogens and antibodies to cell surface components--a model for antigen induced differentiation. In Cell Interactions: Proceedings of the Third Lepetit Colloquium on Biology and Medicine, L. G. Silvestri (Ed.), Elsevier, New York. pp. 143-155.
- Gruenstein, E., A. Rich, and R. R. Weihing. 1975. Actin associated with membranes from 3T3 mouse fibroblast and HeLa cells. J. Cell Biol. 64, 223-234.
- Gunther, G. R., J. S. Wang, I. Yahara, B. A. Cunningham, and E. M. Edelman. 1973. Concanavalin A derivatives with altered biological activities. Proc. Natl. Acad. Sci. USA 70, 1012-1016.
- Hakamori, S. 1975. Structures and organization of cell surface glycolipids. Dependency on cell growth and malignant transformation. Biochem. Biophys. Acta. 417, 55-89.

- Hamamoto, S. T., D. R. Pitelka, T. R. Collins, and D. S. Misfeldt. 1974. Transepithelial transport and tight junctions in normal and neoplastic cells in culture. J. Cell Biol. 63, 129 a (Abstr.).
- Heaysman, J. E. M., and S. M. Pegrum. 1973 (a). Early contacts between fibroblasts. Exp. Cell Res. 78, 71-78.
- Heaysman, J. E. M., and S. M. Pegrum. 1973 (b). Early contacts between normal fibroblasts and mouse sarcoma cells. Exp. Cell Res. 78, 479-481.
- Hirschauer, M., and J. Prioul. 1969. Essai de restitution du relief sur des clichés de répliques obtenues par cryodécoupage. C. R. Acad. Sci. Paris. 268, 3064-3067.
- Holley, R. W., and J. A. Kiernan. 1968. "Contact inhibition" of cell division in 3T3 cells. Proc. Natl. Acad. Sci. USA 60, 300-304.
- Huxley, H. E. 1973. Muscular contraction and cell motility. Nature, 243, 445-449.
- Hynes, P. O. 1976. Cell surface proteins and malignant transformation. Biochim. Biophys. Acta. 458, 73-107.
- Inbar, M. and L. Sachs. 1969. Interaction of the carbohydrate-binding protein concanavalin A with normal and transformed cells. Proc. Natl. Acad. Sci. USA 63, 1418-1425.
- Inbar, M., H. Ben-Bassat, and L. Sachs. 1973. Temperature-sensitive activity on the surface membrane in the activation of lymphocytes by lectins. Exp. Cell Res. 76, 143-151.
- Ishizaka, K. and T. Ishizaka. 1969. Immune mechanisms of reversed type reaginic hypersensitivity. J. Immunol. 103, 588-595.
- Ishizaka, K. and T. Ishizaka. 1970. Biological functions of γE antibodies and mechanisms of reaginic hypersensitivity. Clin. Exp. Immunol. 6, 25-42.
- Johnson, R., M. Hammer, J. Sheridan, and J. P. Revel. 1974. Gap junction formation between reaggregated Novikoff Hepatoma cells. Proc. Natl. Acad. Sci. USA 71, 4536-4540.
- Karnovsky, M. J. 1965. A formaldehyde-glutaraldehyde fixative of high osmolarity for use in electron microscopy. J. Cell Biol. 27, 137a-138a.
- Karnovsky, M. J. and E. R. Unanue. 1973. Mapping and migration of lymphocyte surface macromolecules. Fed. Proc. 32, 55-59.
- Karnovsky, M. J., E. R. Unanue, and M. Leventhal. 1972. Ligand-induced movement of lymphocyte membrane macromolecules. II. Mapping of surface moieties. J. Exp. Med. 136, 907-930.

- Kelly, D. E. 1966. Fine structure of desmosomes, hemidesmosomes, and a dermal globular layer in developing newt epidermis. J. Cell Biol. 28, 51-72.
- Kelley, R. O., R. A. F. Dekker, and J. G. Bluemink. 1973. Ligand-mediated osmium binding: Its application in coating biological specimens for scanning electron microscopy. J. Ultrastruc. Res. 45, 254-258.
- Kiehart, D. P. and S. Inoue, 1976. Local depolymerization of spindle microtubules by microinjection of calcium ions. J. Cell Biol. 70, 230a (Abstr.).
- Kouri, J., G. Kouri, E. Bravo, P. Rodriguez, and A. Aguilera. Ultrastructure of BHK-21 cells as revealed by freeze-etching and fixation methods. J. Microscopie. 11, 331-338.
- Kraemer, P. M., R. A. Tobey, and M. A. Van Dilla. 1973. Flow microfluorometric studies of lectin binding to mammalian cells. I. General Features. J. Cell Physiol. 81, 305-314.
- Kruse, P. F. and E. Miedema. 1965. Production and characterization of multiple-layered populations of animal cells. J. Cell Biol. 27, 273-279.
- Lauweryns, J. M., J. Baert, and W. de Loecker. 1976. Fine filaments in lymphatic endothelial cells. J. Cell Biol. 68, 168-167.
- Lazarides, E. 1975. Tropomyosin antibody: the specific localization of tropomyosin in nonmuscle cells. J. Cell Biol. 65, 549-561.
- Lazarides, E. 1976. Actin, α -actinin, and tropomyosin interaction in the structural organization of actin filaments in nonmuscle cells. J. Cell Biol. 68, 202-219.
- Lazarides, E. and K. Weber. 1974. Actin antibody: the specific visualization of actin filaments in non-muscle cells. Proc. Natl. Acad. Sci. USA 71, 2268-2272.
- Lewis, E. R. and M. K. Nemanic. 1973. Critical point drying techniques. In Scanning Electron Microscopy/1973, O. Johari (Ed.), IIT Research Institute, Chicago, Ill. pp. 768-774.
- Liske, R. and D. Franks. 1968. Specificity of the agglutinin in extracts of wheat germ. Nature 217, 860-861.
- Lucky, A. W., M. J. Mahoney, R. J. Barnett, and L. E. Rosenberg. 1975. Electron microscopy of human skin fibroblasts in situ during growth in culture. Exp. Cell Res. 92, 383-393.
- Luftig, R. B., P. N. McMillan, J. A. Weatherbee, and R. R. Weining. 1976. Increased visualization of microtubules by an improved fixation procedure. J. Cell Biol. 70, 230a (Abstr.).

- Malkani, K. and A. Bererhi. 1970. Cryodécapage de cellules KB infectées par l'adenovirus Type 7. J. Microscopie, 9, 671-674.
- Mandel, T. E. 1972. Intramembranous marker in T lymphocytes. Nature New Biol. 239, 112-114.
- Marchesi, V. T., T. W. Tillack, R. L. Jackson, J. P. Segrest, and R. E. Scott. 1972. Chemical characterization and surface orientation of the major glycoprotein of the human erythrocyte membrane. Proc. Natl. Acad. Sci. USA 69, 1445-1449.
- Margaritis, L. H., J. Yu, and D. Branton. 1976. Biochemical and structural analysis of intramembrane particles using recombination experiments and rotary shadow freeze-etch microscopy. J. Cell Biol. 70, 73a (Abstr.).
- Martinez-Palomo, A., W. de Souza, and A. Gonzalez-Robles. 1976. Topographical differences in the distribution of surface coat components and intramembrane particles. J. Cell Biol. 69, 507-513.
- Martz, E. and M. S. Steinberg. 1973 (a). Contact inhibition of what? An analytical review. J. Cell Physiol. 81, 25-38.
- Martz, E. and M. S. Steinberg. 1973 (b). Contact inhibition of speed in 3T3 and its independence from postconfluence inhibition of cell division. J. Cell Physiol. 81, 39-48.
- Minium, E. W. 1970. Statistical Reasoning in Psychology and Medicine. John Wiley and Sons, Inc., New York.
- Moor, H. 1971. Recent progress in the freeze-etching technique. Philos. Trans. Roy. Soc. Lond. B. Biol. Sci. 261, 121-131.
- Moore, E. G. and H. M. Temin. 1971. Lack of correlation between conversion by RNA tumor viruses and increased agglutinability of cells by concanavalin A and wheat germ agglutinin. Nature 231, 117-118.
- Mooseker, M. S. and L. G. Tilney. 1975. Organization of an actin filament membrane complex. J. Cell. Biol. 67, 725-743.
- McIntyre, J. A., N. B. Gilula, and M. J. Karnovsky. 1974. Cryoprotectant-induced redistribution of intramembranous particles in mouse lymphocytes. J. Cell Biol. 60, 192-203.
- McIntyre, J. A., M. J. Karnovsky, and N. B. Gilula. 1973. Intramembranous particle aggregation in lymphoid cells. Nature New Biol. 245, 147-148.
- McNutt, N. S. 1970. Ultrastructure of intercellular junctions in adult and developing cardiac muscle. Am. J. Cardiol. 25, 169-183.

- McNutt, N. S. 1975. Ultrastructure of the myocardial sarcolemma. Circ. Res. 37, 1-13.
- McNutt, N. S. 1976. Plastic deformation of actin in the production of filaments on the E faces of freeze-fractured plasma membranes. J. Cell Biol. 70, 188a (Abstr.).
- McNutt, N. S., L. A. Culp, and P. H. Black. 1971. Contact-inhibited revertant cell lines isolated from SV40-transformed cells. II. Ultrastructural study. J. Cell Biol. 50, 691-708.
- McNutt, N. S., L. A. Culp, and P. H. Black. 1973. Contact-inhibited revertant cell lines isolated from SV40-transformed cells. IV. Microfilament distribution and cell shape in untransformed, transformed, and revertant Balb/c 3T3 cells. J. Cell Biol. 56, 412-428.
- McNutt, N. S. S. Grayson, and L. L. Mak. 1977. Microfilament-membrane attachments in microvilli of intestinal and choroid plexus epithelium. J. Cell Biol. 75, 256a (Abstr.).
- McNutt, N. S. and R. S. Weinstein. 1970. The ultrastructure of the nexus. A correlated thin-section and freeze-cleave study. J. Cell Biol. 47, 666-688.
- McNutt, N. S. and R. S. Weinstein. 1973. Membrane ultrastructure at mammalian intercellular junctions. Progr. Biophys. Mol. Biol. 26, 45-101.
- Nicolson, G. L. 1971. Difference in topology of normal and tumor cell membranes shown by different surface distributions of ferritin-conjugated concanavalin A. Nature New Biol. 233, 244-246.
- Nicolson, G. L. 1972. Topography of membrane concanavalin A sites modified by proteolysis. Nature New Biol. 239, 193-197.
- Nicolson, G. L. 1973 (a). Anionic sites of human erythrocyte membranes. I. Effects of trypsin, phospholipase C, and pH on the topography of bound positively charged colloidal particles. J. Cell Biol. 57, 373-387.
- Nicolson, G. L. 1973 (b). Cis- and transmembrane control of cell surface topography. J. Supramol. Struct. 1, 410-416.
- Nicolson, G. L. 1973 (c). Temperature-dependent mobility of concanavalin A sites on tumor cell surfaces. Nature New Biol. 243, 218-220.
- Nicolson, G. L., V. T. Marchesi, and S. J. Singer. 1971. The localization of spectrin on the inner surface of human red blood cell membranes by ferritin-conjugated antibodies. J. Cell Biol. 51, 265-272.
- Nicolson, G. L. and R. G. Painter. 1973. Anionic sites of human erythrocyte membranes. II. Antispectrin-induced transmembrane aggregation of the binding sites for positively charged colloidal particles. J. Cell Biol. 49, 395-406.

- Nicolson, G. L., J. R. Smith, and G. Poste. 1976. Effects of local anesthetics on cell morphology and membrane-associated cytoskeletal organization in Balb/3T3 cells. J. Cell Biol. 68, 395-402.
- Nicolson, G. L. and R. Yanagimachi. 1974. Mobility and the restriction of mobility of plasma membrane lectin-binding components. Science 184, 1294-1296.
- Nilausen, K. and H. Green. 1965. Reversible arrest of growth in G₁ of an established fibroblast line (3T3). Exp. Cell Res. 40, 166-168.
- Noonan, K. D. and M. M. Burger. 1973. The relationship of concanavalin A binding to lectin-initiated cell agglutination. J. Cell Biol. 59, 134-142.
- Nordquist, R. E., J. H. Anglin, and M. P. Lerner. 1977. Antibody-induced antigen redistribution and shedding from human breast cancer cells. Science 197, 366-367.
- Novogrodsky, A. and E. Katchalski. 1971. Lymphocyte transformation induced by concanavalin A and its reversion by methyl- α -D-mannopyranoside. Biochim. Biophys. Acta. 228, 579-583.
- Novogrodsky, A. and E. Katchalski. 1972. Membrane sites modified on induction of the transformation of lymphocytes by periodate. Proc. Natl. Acad. Sci. USA 69, 3207-3210.
- Novogrodsky, A. and E. Katchalski. 1973. Induction of lymphocyte transformation by sequential treatment with neuraminidase and galactose oxidase. Proc. Natl. Acad. Sci. USA 70, 1824-1827.
- Oliver, J. M., T. E. Ukena, and R. D. Berlin. 1974. Effects of phagocytosis and colchicine on the distribution of lectin-binding sites on cell surfaces. Proc. Natl. Acad. Sci. USA 71, 394-398.
- Orci, L., M. Amherdt, F. Malaisse-Lagae, C. Rouiller, and A. E. Renold. 1973. Insulin release by emiocytosis. Demonstration with freeze-etching technique. Science 179, 82-84.
- Orci, L. and A. Perrelet. 1973. Membrane-associated particles: Increase at sites of pinocytosis demonstrated by freeze-etching. Science 181, 868-869.
- Overton, J. 1974. Selective formation of desmosomes in chick cell reaggregates. Dev. Biol. 39, 210-225.
- Overton, J. 1975. Experiments with junctions of the adhaerens type. Dev. Biol. 10, 1-34.
- Owens, R. B. 1974. Glandular epithelial cells from mice: a method for selective cultivation. J. Natl. Cancer Inst. 52, 1375-1378.

- Ozanne, B. and J. Sambrook. 1971 (a). Isolation of lines of cells resistant to agglutination by concanavalin A from 3T3 cells transformed by SV40. In Biology of Oncogenic Viruses: Proceedings of the Second Lepetit Colloquium on Biology and Medicine, L. G. Silvestri (Ed.), Elsevier, New York. pp. 248-257.
- Ozanne, B. and J. Sambrook. 1971 (b). Binding of radioactively labelled concanavalin A and wheat germ agglutinin to normal and virus-transformed cells. Nature New Biol. 232, 156-160.
- Palade, G. E. and R. R. Bruns. 1968. Structural modulations of plasmalemmal vesicles. J. Cell Biol. 37, 633-649.
- Pardee, A. B. 1975. The cell surface and fibroblast proliferation. Some current research trends. Biochim. Biophys. Acta. 417, 153-172.
- Parker, J. W., R. L. O'Brien, J. Steiner, and P. Paolilli. 1973. Periodate-induced lymphocyte transformation. II. Character of response and comparison with phytohemagglutinin and pokeweed mitogen stimulation. Exp. Cell Res. 78, 279-286.
- Parker, J. W., R. L. O'Brien, J. Steiner, and P. Paolilli. 1974. Periodate-induced lymphocyte transformation. III. Effects of temperature and pH. Exp. Cell Res. 83, 220-224.
- Pauli, B. U., R. S. Weinstein, L. W. Soble, and J. Alroy. 1977. Freeze-fracture of monolayer cultures. J. Cell Biol. 72, 763-768.
- Pegrum, S. M. and N. G. Maroudas. 1975. Early events in fibroblast adhesion to glass. Exp. Cell Res. 96, 416-422.
- Pfenninger, K. H. and R. P. Bunge. 1974. Freeze-fracturing of nerve growth cones and young fibers. J. Cell Biol. 63, 180-196.
- Pfenninger, K. H. and E. R. Rinderer. 1975. Methods for the freeze-fracturing of nerve tissue cultures and cell monolayers. J. Cell Biol. 65, 15-28.
- Pickett, P. B., D. R. Pitelka, S. T. Hamamoto, and D. S. Misfeldt. 1975. Occluding junctions and cell behavior in primary cultures of normal and neoplastic mammary gland cells. J. Cell Biol. 66, 316-332.
- Pinto da Silva, P. 1972. Translational mobility of the membrane intercalated particles of human erythrocyte ghosts. pH-dependent, reversible aggregation. J. Cell Biol. 53, 777-787.
- Pinto da Silva, P., and D. Branton. 1972. Membrane intercalated particles: the plasma membrane as a planar fluid domain. Chem. Phys. Lipids. 8, 265-278.
- Pinto da Silva, P. and N. B. Gilula. 1972. Gap junctions in normal and transformed fibroblasts in culture. Exp. Cell Res. 71, 393-401.

- Reaven, E. P. and S. G. Axline. 1973. Subplasmalemmal microfilaments and microtubules in resting and phagocytosing macrophages. J. Cell Biol. 59, 12-27.
- Reith, A. and R. Oftebro. 1971. Structure of HeLa cells after treatment with glycerol as revealed by freeze-etching and electron microscopic methods. Exp. Cell Res. 66, 385-395.
- Revel, J. P. and M. J. Karnovsky. 1967. Hexagonal array of subunits in intercellular junctions of the mouse heart and liver. J. Cell Biol. 33, c7-c12.
- Revel, J. P., A. G. Yee, and A. J. Hudspeth. 1971. Gap junctions between electronically coupled cells in tissue culture and in brown fat. Proc. Natl. Acad. Sci. USA 68, 2924-2927.
- Revel, J. P., P. Yip, and L. L. Chang. 1973. Cell junctions in the early chick embryo--a freeze etch study. Dev. Biol. 35, 302-317.
- Reynolds, E. S. 1962. The use of lead citrate at high pH as an electron-opaque stain in electron microscopy. J. Cell Biol. 17, 208-213.
- Richardson, K. C., L. Jarret, and E. H. Fincke. 1960. Embedding in epoxy resins for ultrathin sectioning in electron microscopy. Stain Techn. 35, 313-323.
- Rodewald, R., S. B. Newman, and M. J. Karnovsky. 1976. Contraction of isolated brush borders from the intestinal epithelium. J. Cell Biol. 70, 541-554.
- Romeo, D., G. Zabucchi, and F. Rossi. 1973. Reversible metabolic stimulation of polymorphonuclear leukocytes and macrophages by concanavalin A. Nature New Biol. 243, 111-112.
- Rosenblith, J. Z., T. E. Ukena, H. H. Yin, and R. D. Berlin, and M. J. Karnovsky. 1973. A comparative evaluation of the distribution of concanavalin A-binding sites on the surfaces of normal, virally transformed, and protease-treated fibroblasts. Proc. Natl. Acad. Sci. USA 70, 1625-1629.
- Ross, R. R. and T. K. Greenlee. 1966. Electron microscopy: attachment sites between connective tissue cells. Science 153, 997-999.
- Roth, S. and D. White. 1972. Intercellular contact and cell-surface galactosyl transferase activity. Proc. Natl. Acad. Sci. USA 69, 485-489.
- Roth, S., A. Patteson, and D. White. 1974. Surface glycosyltransferases on cultured mouse fibroblasts. J. Supramol. Struc. 2, 1-6.
- Rutishauser, U., I. Yahara, and G. N. Soltman. 1974. Morphology, motility, and surface behavior of lymphocytes bound to nylon fibers.

- Proc. Natl. Acad. Sci. USA 71, 1149-1153.
- Ryan, G. B., J. Z. Borysenko, and M. J. Karnovsky. 1974. Factors affecting the redistribution of surface-bound concanavalin A on human polymorphonuclear leukocytes. J. Cell Biol. 62, 351-365.
- Satir, B., C. Schooley, and P. Satir. 1972. Membrane reorganization during secretion in Tetrahymena. Nature 235, 53-54.
- Satir, B., C. Schooley, and P. Satir. 1973. Membrane fusion in a model system. Mucocyst secretion in Tetrahymena. J. Cell Biol. 56, 153-176.
- Satir, P. and N. G. Gilula. 1973. The fine structure of membranes and intercellular communication in insects. Ann.Rev. Entymol. 18, 143-166.
- Schliwa, M. 1976. Regulation by calcium of microtubule assembly in vivo. J. Cell Biol. 70, 12a (Abstr.).
- Schollmeyer, J. V., D. E. Goll, L. G. Tileny, M. Mooseker, R. Robston, and M. Stromer. 1974. Localization of α -actinin in nonmuscle material. J. Cell Biol. 63, 304a (Abstr.).
- Scott, R. E., L. T. Furcht, and J. H. Kersey. 1973. Changes in membrane structure associated with cell contact. Proc. Natl. Acad. Sci. USA 73, 3631-3635.
- Sharon, N. and H. Lis. 1972. Lectins: cell-agglutinating and sugar-specific proteins. Science 177, 949-959.
- Simionescu, M., N. Simionescu, and G. E. Palade. 1974. Morphometric data on the endothelium of blood capillaries. J. Cell Biol. 60, 128-152.
- Singer, S. J. and G. L. Nicolson. 1972. The fluid mosaic model of the structure of cell membranes. Science 175, 720-731.
- Smith, U., D. S. Smith, H. Winkler, and J. W. Ryan. 1973. Exocytosis in the adrenal medulla demonstrated by freeze-etching. Science 179, 79-82.
- Spurr, A. R. 1969. A low-viscosity epoxy resin embedding medium for electron microscopy. J. Ultrastruc. Res. 26, 31-43.
- Stackpole, C. W., L. T. DeMilo, J. B. Jacobson, U. Hammerling, and M. P. Lardis. 1974. A comparison of ligand-induced redistribution of surface immunoglobulins, alloantigens, and concanavalin A receptors on mouse lymphoid cells. J. Cell Physiol. 83, 441-448.
- Stachelin, L. A. and W. S. Bertaud. 1971. Temperature and contamination-dependent images of frozen water and glycerol solutions. J. Ultrastruc. Res. 37, 146-168.

- Steck, T. L. 1974. The organization of proteins in the human red blood cell membrane. J. Cell Biol. 62, 1-19.
- Stoker, M. G. P. 1972. Tumor viruses and the sociology of fibroblasts. Proc. Roy. Soc. Lond. B. 181, 1-17.
- Stoker, M. G. P. 1973. Role of diffusion boundary layer in contact inhibition of growth. Nature 246, 200-203.
- Stoker, M. G. P. and H. Rubin. 1967. Density dependent inhibition of cell growth in culture. Nature 215, 171-172.
- Taylor, A. C. 1961. Attachment and spreading of cells in culture. Exp. Cell Res. Suppl. 8, 154-173.
- Taylor, R. B., W. P. H. Duffus, M. C. Raff, and S. de Petris. 1971. Redistribution and pinocytosis of lymphocyte surface immunoglobulin molecules induced by anti-immunoglobulin antibody. Nature New Biol. 233, 225-229.
- Teng, N. N. H. and L. B. Chen. 1975. The role of surface proteins in cell proliferation as studied with thrombin and other proteases. Proc. Natl. Acad. Sci. USA 72, 413-417.
- Tillack, T. W., R. E. Scott, and V. T. Marchesi. 1972. The structure of erythrocyte membranes studied by freeze-etching. II. Localization of receptors for phytohemagglutinin and influenza virus to the intramembranous particles. J. Exp. Med. 135, 1209-1227.
- Todaro, G. J. and H. Green. 1963. Quantitative studies of the growth of mouse embryo cells in culture and their development into established lines. J. Cell Biol. 17, 299-313.
- Torpiere, G., L. Montagnier, J. M. Biquard, and P. Vigier. 1975. A structural change of the plasma membrane induced by oncogenic viruses: quantitative studies with the freeze-fracture technique. Proc. Natl. Acad. Sci. USA 72, 1695-1698.
- Trujillo, T. T. and M. A. Van Dilla. 1972. Adaptation of the fluorescent Feulgen reaction to cells in suspension for flow microfluorometry. Acta. Cytol. 16, 26-30.
- Tsan, M. F. and R. D. Berlin. 1971. Effect of phagocytosis on membrane transport of nonelectrolytes. J. Exp. Med. 134, 1016-1033.
- Ukena, T. E. and R. D. Berlin. 1972. Effect of colchicine and vinblastine on the topographical separation of membrane functions. J. Exp. Med. 136, 1-17.
- Ukena, T. E., J. Z. Borysenko, M. J. Karnovsky, and R. D. Berlin. 1974. Effect of colchicine, cytochalasin B, and 2-deoxyglucose on the topographical organization of surface-bound concanavalin A in normal and transformed fibroblasts. J. Cell Biol. 61, 70-82.

- Unanue, E. R., M. J. Karnovsky, and H. D. Engers. 1973. Ligand-induced movement of lymphocyte membrane macromolecules. J. Exp. Med. 137, 675-689.
- Unanue, E. R., W. D. Perkins, and M. J. Karnovsky. 1972. Ligand-induced movement of lymphocyte membrane macromolecules. I. Analysis by immunofluorescence and ultrastructural radioautography. J. Exp. Med. 136, 885-906.
- Vaheri, A., E. Ruoslahti, M. Sarvas, and M. Nurminen. 1973. Mitogenic effect by lipopolysaccharide and pokeweed lectin on density-inhibited chick embryo fibroblasts. J. Exp. Med. 138, 1356-1364.
- Vogt, M. and R. Dulbecco. 1963. Steps in the neoplastic transformation of hamster embryo cells by polyoma virus. Proc. Natl. Acad. Sci. USA 49, 171-179.
- Waymouth, C. 1959. Rapid proliferation of sublines of NCTC clone 929 "strain L" mouse cells in a simple chemically defined medium (MB752/1). J. Natl. Cancer Inst. 22, 1003-1017.
- Webb, G. C. and S. Roth. 1974. Cell contact dependence of surface galactosyltransferase activity as a function of the cell cycle. J. Cell Biol. 63, 796-805.
- Weber, J. 1973. Relationship between cytoagglutination and saturation density of cell growth. J. Cell. Physiol. 81, 49-54.
- Weber, K. and U. Groeschel-Stewart. 1974. Antibody to myosin: the specific visualization of myosin-containing filaments in nonmuscle cells. Proc. Natl. Acad. Sci. USA 71, 4561-4564.
- Weinstein, R. S. 1974. Changes in cell membrane structure associated with neoplastic transformation in human urinary bladder epithelium. J. Cell Biol. 63, 367a (Abstr.).
- Weiss, P. and B. Garber. 1952. Shape and movement of mesenchyme cells as a function of the physical structure of the medium. Contributions to a quantitative morphology. Proc. Natl. Acad. Sci. USA 38, 264-280.
- Weller, N. K. 1974. Visualization of concanavalin A-binding sites with scanning electron microscopy. J. Cell Biol. 63, 699-707.
- Westbrook, E., B. Wetzel, G. B. Cannon, and D. Berard. 1975. The impact of culture conditions on the surface morphology of cells *in vitro*. In Scanning Electron Microscopy/1975, O. Johari (Ed.), IIT Research Institute, Chicago, Ill. pp. 351-360.
- Wright, J. A. 1973. Evidence for pleiotropic changes in lines of Chinese hamster ovary cells resistant to concanavalin A and phytohemagglutinin-P. J. Cell Biol. 56, 666-675.

- Yahara, I. and G. M. Edelman. 1972. Restriction of the mobility of lymphocyte immunoglobulin receptors by concanavalin A. Proc. Natl. Acad. Sci. USA 69, 608-612.
- Yahara, I. and G. M. Edelman. 1973. The effects of concanavalin A on the mobility of lymphocyte surface receptors. Exp. Cell Res. 81, 143-155.
- Yahara, I. and G. M. Edelman. 1975. Modulation of lymphocyte receptor mobility by locally bound concanavalin A. Proc. Natl. Acad. Sci. USA 72, 1579-1583.

This report was done with support from the Department of Energy. Any conclusions or opinions expressed in this report represent solely those of the author(s) and not necessarily those of The Regents of the University of California, the Lawrence Berkeley Laboratory or the Department of Energy.

Reference to a company or product name does not imply approval or recommendation of the product by the University of California or the U.S. Department of Energy to the exclusion of others that may be suitable.

TECHNICAL INFORMATION DEPARTMENT
LAWRENCE BERKELEY LABORATORY
UNIVERSITY OF CALIFORNIA
BERKELEY, CALIFORNIA 94720